Organelles and Signals Controlling Vacuolar Sorting Receptor Trafficking in Plants

David C. Gershlick

Submitted in accordance with the requirements for

the degree of Doctor of Philosophy

The University of Leeds

Faculty of Biological Sciences

September 2013

The candidate confirms that the work submitted is his/her own, except where work which has formed part of jointly-authored publications has been included. The contribution of the candidate and the other authors to this work has been explicitly indicated below. The candidate confirms that appropriate credit has been given within the thesis where reference has been made to the work of others.

©2013 The University of Leeds and David Charles Gershlick

Publications

Foresti, O., Gershlick, D. C., Bottanelli, F., Hummel, E., Hawes, C., & Denecke, J. (2010). A recycling-defective vacuolar sorting receptor reveals an intermediate compartment situated between prevacuoles and vacuoles in tobacco. The Plant Cell, 22(12), 39924008. doi:10.1105/tpc.110.078436

Bottanelli, F., Gershlick, D. C., & Denecke, J. (2012). Evidence for sequential action of Rab5 and Rab7 GTPases in prevacuolar organelle partitioning. Traffic, 13(2), 338354. doi:10.1111/j.1600-0854.2011.01303.x

De Marcos Lousa, C., Gershlick, D. C., & Denecke, J. (2012). Mechanisms and concepts paving the way towards a complete transport cycle of plant vacuolar sorting receptors. The Plant Cell, 24(5), 17141732. doi:10.1105/tpc.112.095679

Gershlick, D. C., Foresti, O., Lee, A. J., daSilva, L. L. P., Bottanelli, F.,, De Marcos Lousa, C., & Denecke, J. (2013) Golgi-dependent transport of vacuolar sorting receptors is controlled by COPII, AP1 and AP4 protein complexes. Currently under review.

All figures from these publications used in this thesis have been produced by D. C. Gershlick. This work would not have been possible without the inclusion of unpublished genetic constructs and results obtained from past and present lab members as detailed below. Foresti, O. contributed by producing the long transmembrane domain mutants used to in Chapter 6. Lee, A. J. assisted with the experiments using the dual-fusion chimeric cargo, under my personal supervision, used in Chapter 5. daSilva, L. L. P. originally charactered the COPII inhibitors and some of the unpublished VSR point mutants (ASA mutant, and IMAA mutant) that cause mislocalisation of the VSR used in chapter 6. De Marcos Lousa, C. generated the RFP-RhaI construct used for a key experiment in Chapter 6.

"Curiosity demands that we ask questions, that we try to put things together and try to understand this multitude of aspects as perhaps resulting from the action of a relatively small number of elemental things and forces acting in an infinite variety of combinations"

Richard P. Feynman — The Feynman Lectures on Physics Vols 1-2

1964

ACKNOWLEDGEMENTS

Many people have helped me to complete this thesis, it would not have been possible without them. Unfortunately, there is not space to include them all here, however I will mention a subset to whom I am particularly grateful.

Firstly my family. I want to thank my mother, who taught me about honesty, integrity, loyalty and dedication – all of which have been invaluable throughout this PhD. I want to thank my father, who inspired my curiosity, intrigue, love of debate and work-ethic – my passion for science came from this. Also, my brother, Ben, not only one of the kindest and smartest people I know, but also a great friend.

Secondly I would like to thank my supervisor Jurgen Denecke. My PhD has been supported on all sides by Jurgen. The last four years have been some of my favourite, and that is thanks to Jurgen. Not only has Jurgen been a fantastic supervisor and boss, but also an inspiring and brilliant scientist and discussion partner. I can only aspire to be the scientist Jurgen is.

I would like to extend a special thanks to all my lab colleagues over the years. My undergraduate dissertation was supervised by Ombretta Foresti, who taught me the fundamental scientific techniques when I was an undergraduate, and was an inspiration to me as a postgraduate. I want to thank my current labmates, who have supported me in recent times, it has been a fantastic couple of years. Carine De Marcos Lousa, Jing An and Ibrahim Khalil Adam have made me feel part of a fun and intellectually stimulating team. Also, thanks to Francesca Bottanelli, her energy and work-ethic were an inspiration to me throughout my PhD.

Finally thanks to all my friends who have supported me in my free time over the years. My friends from school and travelling, in particular Tom – I have known you for 23 years now, I will be extremely disappointed if we are not friends for at least another 23. Pete, Dave and Charlie share great memories of Loughborough, Europe and Leeds with me. I also have great memories collected over the years with my great friends James and Will. My university friends have meant a very great deal to me, especially the resilience they showed over the years to support my many temporary hobbies and obsessions, in particular Nat, Jess and Alex– they all have supported me when I needed it. Finally, I will acknowledge my more recent friends who have put up with me during the latter years of my PhD. Matt and Laura, great house-mates and great friends- wherever we are in the world we will stay in contact. Mike has been my support within the department, we went through this PhD together and it would have been much more difficult without him. Lastly, great thanks Josh and Stu who have made this last year enjoyable over the course of countless weekends.

Funding for this project has come from the Biotechnology and Biological Sciences Research Council.

ABSTRACT

The maintenance of vacuoles/lysosomes is essential for the physiology of all eukaryotic life. In plants, sorting of soluble protein cargo to the lytic vacuoles/lysosomes is controlled by a family of type-I membrane spanning proteins, the Vacuolar Sorting Receptors (VSRs). Whilst the large lumenal domain mediates conditional ligand binding and release, the short cytosolic tail differentiates between anterograde and retrograde transport machinery in the cytosol.

In this thesis, experimental tools and techniques are developed and used to characterise the sorting cycle of plants. In contrast to previous studies, work presented here suggests that the different isoforms are not transported in an identical manner. In particular, one VSR member was characterised to have increased leakage to the vacuole, partitioning to the late-prevacuolar compartment rather than the prevacuolar compartment. Both the cytosolic C-terminus and the cargo interacting lumenal domain of this unique receptor were shown to interact differentially with partners when compared to the canonical receptor. In addition, the techniques developed here are used to characterise the sorting route of the canonical receptor. A region of the receptor important for export from the endoplasmic reticulum mediating its entry into COPII vesicles has been identified. Furthermore, this model receptor is also used to understand the general sorting of membrane spanning proteins within the secretory pathway, showing that the presence of a tyrosine motif within the C-terminus prevents default leakage towards the plasma membrane. Finally, it is shown here that the VSR does not traffic via the plasma membrane by default and thus probably traffics in clathrin coated vesicles from the Golgi apparatus/*trans*-Golgi network towards the late secretory pathway, despite containing a functional endocytic motif.

CONTENTS

LIST OF FIGURES

LIST OF TABLES

ABBREVIATIONS

Aleu ..... *Barley Aleurain Sorting Signal*

Amy ..... *α-Amylase*

Amy-spo ..... *α-Amylase fused to sporamine sorting signal*

AP ..... *Adaptor Protein Complex*

ATP ..... *Adenosine Triphosphate*

ATPase ..... *Adenosine Triphosphatase*

BiP ..... *Binding Protein*

BLAST ..... *Basic Local Alignment Search Tool*

BP80 ..... *Binding Protein 80*

BSA ..... *Bovine Serum Albumin*

CCV ..... *Clathrin Coated Vesicle*

CFP ..... *Cyan Fluorescent Protein*

CLSM ..... *Confocal Laser Scanning Microscopy*

COPI ..... *Coatomer Protein I Coated*

COPII ..... *Coatmer Protein II Coated*

CPY ..... *Carboxypeptidase Y*

DIC ..... *Differential Interference Contrast*

DNA ..... *Deoxyribonucleic Acid*

ER ..... *Endoplasmic Reticulum*

ERAD ..... *ER-Associated Degradation*

ESCRT ..... *Endosomal Sorting Complexes Required for Transport*

GAP ..... *GTPase-activating Protein*

GARP ..... *Golgi-Associated Retrograde Protein*

GEF ..... *Guanine Nucleotide Exchange Factors*

GET ..... *Guided Entry of Tail-anchored Proteins*

GFP ..... *Green Fluorescent Protein*

GTP ..... *Guanosine Triphosphate*

GTPase ..... *Guanosine Triphosphatase*

GUS ..... *Beta-Glucuronidase*

HRP ..... *Horseradish Peroxidase*

ILV ..... *IntraLumenal Vesicle*

LPVC ..... *Late Pre-Vacuolar Compartment*

MVB ..... *Multi-Vesicular Body*

NSF ..... *N-ethylmaleimide Sensitive Fusion Protein*

PAT ..... *Phosphinothricin Acetyl Transferase*

PCR ..... *Polymerase Chain Reaction*

PEG ..... *Polyethylene Glycol*

PH ..... *Pleckstrin Homology*

PM ..... *Plasma Membrane*

PVC ..... *Pre-vacuolar Compartment*

Rab ..... *Rat sarcoma-related in brain*

Ras ..... *Rat Sarcoma*

RFP ..... *Red Fluorescent Protein*

RNA ..... *Ribonucleic Acid*

RPM ..... *Revolutions Per Minute*

SDS-PAGE ..... *Sodium Dodecyl Sulphate Polyacrylamide Gel Electrophoresis*

SNAP ..... *Soluble NSF Attachment Protein*

SNARE ..... *SNAP Receptor*

SRP ..... *Signal Recognition Particle*

ST ..... *Sialyltransferase*

TA ..... *Tail-Anchored Protein Class*

TGN ..... *Trans-Golgi Network/Partially Coated Reticulum*

TRAPP ..... *Transport Protein Particle*

UPR ..... *Unfolded Protein Response*

VPS ..... *Vacuolar Protein Sorting*

VSR ..... *Vacuolar Sorting Receptor*

VSV-G ..... *Vesicular Stomatitis Virus Glycoprotein*

YFP ..... *Yellow Fluorescent Protein*

1 INTRODUCTION

1.1 NATURAL AND EXPERIMENTAL HISTORY OF PROTEIN TRAFFICKING

1.1.1 The Origin of Cells

Current theories suggest that between 3–4 billion years ago the first cell was formed. It is speculated to have been an auto-catalytic RNA molecule that was enclosed in a spontaneously generated fatty acid shell (Koch and Silver, 2005; Woese, 2002). This segregation would have allowed formation of the first mechanistic components that are common in all life today. Establishment of basic cellular constitution probably took place in these structures. There is good evidence to suggest that RNA complexes (rRNA/tRNA), elongation factors and rudimentary transcriptional activity were established before the divide of life into the five kingdoms (Langer et al., 1995; Woese, 2000, 2002; Woese et al., 2000).

Once these basic forms had been established, the discrete cellular systems independently developed. For example, bacteria evolved components such as the gram positive/negative cell wall, the bacterial flagellum and some specialised sub-compartments (e.g. the large carbon fixing carboxysomes). Archea are relatively similar to bacteria, but have evolved other independent structures such as ether-linked lipid based membranes and unique cell wall structures. Although the prokaryotic organisms do not contain separate internal membranes, the plasma membrane can be invaginated to form specialised substructures with a large surface area (Komeili et al., 2006). In contrast, the eukaryotic cell is much larger and more architecturally complex, with a wide variety of specialised compartments existing across all kingdoms. Internally the cells differ from prokaryotes with the membrane-bound compartments having physically

disconnected membranes. Compartmentalisation allowed for a heterogeneous distribution of proteins/lipids/organic molecules within the cell which allowed biochemical processes to occur in environments with high concentrations of the reagents, and in the absence of potential inhibitors.

1.1.2 The Discovery and the Characterisation of the Cell

Cells were originally discovered in the late 1600s by two scientists. Robert Hooke was the first to observe a dissected slice of cork as appearing "a little porous...much like a Honeycomb", he considered them reminiscent of cells in a monastery and thus referred to them as 'cells' (Hooke, 1667). Almost simultaneously in Holland, Antonie van Leeuwenhoek, a tradesman and amateur lens-maker, observed micro-organisms in scrapings from his teeth and pepper which had been cultured in water (Dobell, 1932; Singer, 1931). It took over a hundred years for the German scientists Schliden and Schwann to independently conclude that all life is made of cells, a fundamental tenet of 'cell theory' (Mazzarello, 1999). Thus, based on the observations of the first microscopists, the science of cell biology was born.

In every cell proteins are continuously crafted and assimilated. Protein synthesis is often accompanied soon after by specific transport of the newly synthesised proteins by a complex concert of cellular machinery. Surrounded by a liquid membrane, eukaryotic cells contain a molecular soup (the cytosol) and the membranous subcompartments (referred to as organelles) together forming the cytoplasm. The organelles of the cell can be broadly split into three classes, the endosymbiotic organelles, such as the mitochondria and the chloroplasts, the non-secretory organelles (eg. peroxisomes) and the secretory organelles– the subject of this

thesis. Cellular proteins fulfil functions within soluble contents of the organelles (the lumen), at the membranes, their periphery or in the cytosol.

1.1.3 Milestones in the Understanding of the Secretory Pathway

In the two hundred years after the establishment of cell theory the understanding of the inner workings were slowly elucidated using a combination of light microscopy, electron microscopy, confocal microscopy, biochemistry, *in vitro* reconstitution and genetics. The application of these techniques allowed a comprehensive understanding of the basic principles of cell biology. Early developments in electron microscopy allowed detailed analysis of the subcellular structure. In 1974 the Nobel laureate George Palade resolved the observed structures with particular functions. Palade's autoradiographic approach involved adding a radio-labelled leucine (^{3}H) pulse for 5 minutes, which was incorporated into nascent proteins, then checking the protein localisation by autoradiographed electron micrograph analysis at different time points (Palade, 1975). These observations were then coupled with cell fractionation studies confirming the introduction of the secretory pathway as a functional system of organelles with vectorial transport.

The next major discovery in the characterisation of protein targeting was the isolation and characterisation of the 'coated vesicle'. Vesicles are small spherical compartments which shuttle from one organelle to another, allowing for inter-compartmental transport yet preserving the heterogeneity of the compartments. Vesicles provide a mechanism for the transport of proteins, without having to cross a membrane. Vesicle budding/fusion events were characterised by *in vitro* reconstitution from isolated organelles (Banta et al., 1988; Kaiser and Schekman, 1990; Orci et al., 1986). In the following years, the major classes of

vesicles were characterised as COPI (Section 1.5.3, pg. 50), COPII (Section 1.4.2, pg. 41) or Clathrin (Section 1.8.1, pg. 59) based on the protein coat that forms them.

The initial characterisation of the proteins that maintain these processes was facilitated in the nineteen-seventies by yeast biologists. *Saccharomyces cerevisiae* was an ideal candidate model organism for this work, with a genome simpler than mammalian or plant genomes, but still maintaining the eukaryotic cellular architecture. These genetic studies into secretion of yeast led the way over the following 20 years with several key mutagenesis based screens (Deshaies and Schekman, 1987; Ferro-Novick et al., 1984; Orci et al., 1986). Although there was a degree of overlap between different screens, often new essential proteins were discovered. These methods identified a large array of key players, allowing the mechanisms of specific processes to be elucidated.

It was understood that if proteins need to reach a particular cellular destination, then they cannot do so passively and thus need to be concentrated in vesicles. Therefore some direction is necessary for proteins to fill the place reserved for them in the relevant vesicle or compartment. Thus, to differentiate proteins from one another, there are often protein or glycan 'sorting signals'. This allows for the fundamental distinction of 'cargo' (that is transported), from 'receptors' (that initiate transport steps). In a further layer of complexity, these receptors must bind to cytosolic components to mediate transport. They also continuously recycle to pick up another round of cargo; often receptors can pass through multiple compartments to deliver cargo.

The most recent studies have also taken advantage of the recent discovery of fluorescent proteins allowing for confocal laser scanning microscopy (CLSM)

localisation of specific proteins within the cell. Making fused chimeras, consisting of a protein of interest attached to a fluorescent protein has become commonplace. Fluorescent microscopy allows observation of the location of a protein within the context of a three-dimensional cellular environment of a living cell avoiding the requirement of tissue fixation and subsequent sectioning. Impressive recent advances allow single molecules to be observed, as well as the imaging of vesicles in living cells.

Eukaryotes are split into the four kingdoms: Protista, Plantae, Fungi, Animalia. Although there are conserved functions and analogous processes in the subcellular organisation between the kingdoms there are also differences. This variation could represent a biological divergence, or perhaps, semantic clashes between similar structures described in different fields. Despite this there are general functional categories that organelles can be divided into.

This introduction will describe protein sorting to the vacuole/lysosome in a biosynthetic manner. Beginning with protein synthesis in the cytosol and entry into the endoplasmic reticulum (ER) and resulting in delivery of proteins to the lytic compartments. Figure 1.1 shows an overview of the pathway. I will discuss the general function of the organelles of the cell across all kingdoms, but will pay extra attention to plant specific functions as they are the subject of this thesis.

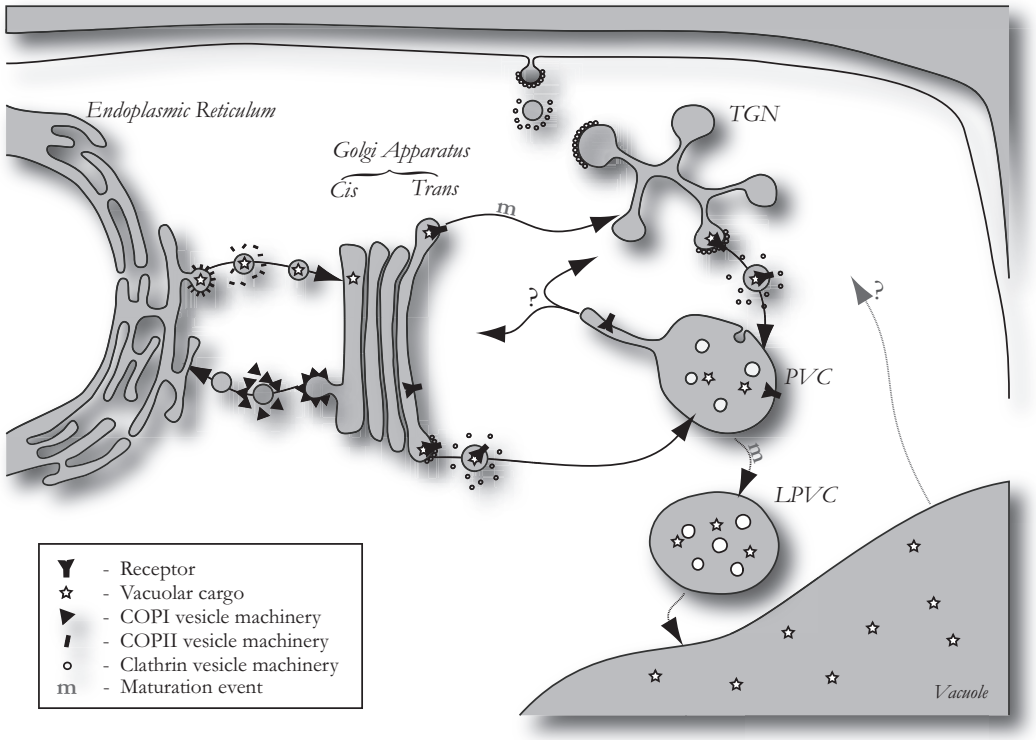

Figure 1.1: **A Model of Vacuolar Sorting in the Plant Secretory Pathway** A model showing the consensus route of selective VSR transport to the PVC. VSR transport to the PVC is a selective process that depends on the conserved Tyr residue present in all VSRs (DaSilva et al., 2006; Foresti et al., 2010; Kim et al., 2010; Saint-Jean et al., 2010; Sanderfoot et al., 1998). Moreover, this step is likely to occur by clathrin-mediated vesicle (CCV) budding for transport to the PVC (Happel et al., 2004; Jin et al., 2001; Kirsch et al., 1994; Sanderfoot et al., 1998). CCVs could either bud from the Golgi, the PCR/TGN, or both. The mechanism of Golgi-to-TGN transport is currently unknown but may occur by maturation (m). Selective recycling from the PVC is thought to be mediated by the VPS35/29/26 retromer core complex to prevent receptor degradation in the vacuole (Fuji et al., 2007; Jaillais et al., 2007; Oliviusson et al., 2006; Shimada et al., 2006; Yamazaki et al., 2008). This retrieval step also depends on sorting signals on the VSR tail (Foresti et al., 2010; Saint-Jean et al., 2010), leading to gradual PVC maturation (m) to form the LPVC (Foresti et al., 2010). Further transport of soluble cargo from the LPVC to the vacuole is dependent on the sequential action of Rab5 and Rab7 GTPases (Bottanelli et al., 2011, 2012), which are localised to the LPVC and vacuolar membrane, respectively. The destination organelle for the recycling routes from the PVC and the vacuole are unknown (indicated with a question mark).

1.2 GETTING INTO THE ER

In prokaryotes the processes of transcription and translation are coupled, and therefore the process of membrane crossing/insertion is post-translational. In eukaryotes however the processes are separated both spatially and mechanistically and thus it is possible to both post- and co-translationally insert into or cross the membrane. This results in a diversity in the insertion of proteins in the eukaryotic systems. Whilst protein secretion in prokaryotes occurs by translocation across the plasma membrane, eukaryotes use the membrane of the ER as the main platform for translocation to leave the cytosol (See figure 1.1). Entry into the ER is therefore functionally equivalent to protein export in eukaryotes.

1.2.1 Transcription in the Nucleus

All eukaryotic kingdoms contain a morphologically similar nucleus, with the surrounding membrane contiguous with the rough endoplasmic reticulum. Within is the cellular genomic DNA as well as the protein and RNA machinery that maintains the integrity of the genetic material. There are several different nucleus subdomains, the most characterised being the nucleolus— which is thought to be involved in ribosome assembly (Birnstiel et al., 1963). Inside the nucleus transcription as well as DNA replication takes place.

The membrane surrounding the nucleus is composed of two lipid bilayers (Figure 1.2). Macromolecules cannot diffuse through this nuclear envelope and thus the membrane is studded with protein channels called nuclear pores, which allow mRNA to exit the nucleus. DNA encoding for secretory pathway determinants is transcribed into mRNA in the canonical manner. The mRNA polymer is then

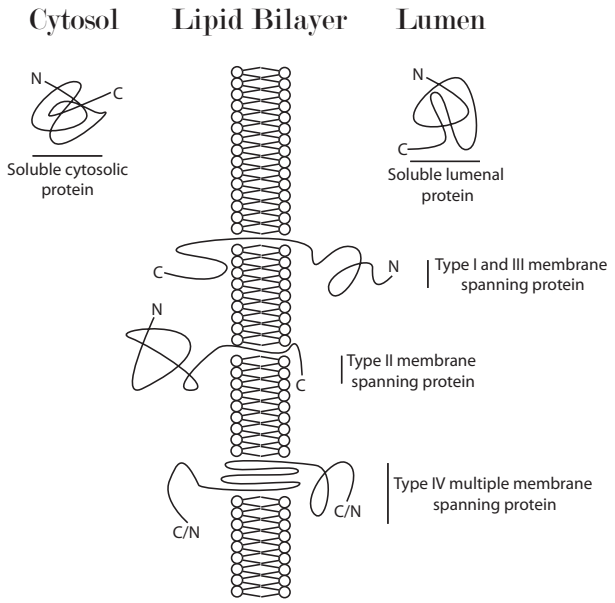

Figure 1.2: **The Topology of the Secretory Pathway** Within the secretory pathway proteins can be soluble either side of the membrane, or span across the membrane in both orientations. Type I membrane proteins span the lipid bilayer with the C-terminus (C) on the cytosolic side and the N-terminus (N) on the lumenal side, and type II are in the opposite orientation. Multiple membrane spanning proteins can also span in both directions.

both actively and passively transported into the cytosol via the nuclear pores that are embedded into the membrane of the nucleus (Cullen, 2000).

Once in the cytosol the mRNA molecule is recognised by the ribosome, initiating an interaction between the two and allowing translation to begin. It is during the very first stages of mRNA to protein translation that the proteins in the secretory pathway are segregated. This division is into three classes, which are functionally and mechanistically independent. These classes are lumenal, membrane-spanning and cytosolic proteins (Figure 1.2).

1.2.2 Synthesis and Translocation of Lumenal Proteins

Lumenal proteins are soluble proteins that reside within the delimiting membranes of the secretory network and are suspended in the aqueous lumenal fluid (See

Figure 1.1, grey sections and Figure 1.2). All organelles of the secretory pathway are composed of a single lipid bilayer which segregates the lumenal proteins from the cytosol (Figure 1.2). Typically proteins that are destined to enter the secretory pathway in this way are characterised by an N-terminal signal peptide, which is responsible for segregating the corresponding mRNA/protein complex to the secretory pathway via the ribosomes studding the rough ER (Blobel and Dobberstein, 1981; Palade, 1975; Vitale et al., 1993). These signal peptides are 20-30 amino acids long, and are hydrophobic by consensus (Heijne, 1985). After the signal peptide is completely synthesised and exposed on the surface of the ribosome (i.e. mid-translation) this protein motif is recognised by the hexapolypeptide-RNA complex known as the Signal-Recognition Particle (SRP), at which point translation stalls (Gilmore et al., 1982; Walter and Blobel, 1980). A guanosine triphosphate (GTP) dependent interaction is then initiated between the SRP-protein-ribosome complex and a membrane-spanning dimer referred to as the SRP receptor (Keenan et al., 2001). This interaction brings the nascent protein proximal to the translocation channel on the ER and causes dissociation of the SRP from the peptide, allowing translational activity to resume (Connolly and Gilmore, 1989). After protein insertion the SRP-SRP receptor complex is left bound to the membrane. The dissociation of this complex is mediated by a GTP hydrolysis event (Connolly et al., 1991). This, in turn allows the SRP to initiate a new round of binding and protein translocation (Miller et al., 1993).

As the protein is synthesised it is threaded through the aqueous core of a protein complex referred to as a 'translocation channel' or 'translocation pore' in a process known as co-translational insertion (Corsi and Schekman, 1996; Kalies et al., 1994), removing both the need for protein unfolding prior to membrane translocation and the direct need for ATP to drive translocation through the hydrophobic bilayer

(Cross et al., 2009). The translocation pore consists of the multiple membrane spanning heterotrimer Sec61 as a core, assisted by Sec62/63 (Deshaies et al., 1991). Sec61 contains three subunits, α, γ and β. The α subunit forms the inner cylinder of the channel (Mothes et al., 1994) which is in contact with the translocating protein and is otherwise aqueous (Simon and Blobel, 1991).

Originally, when inactive the channel was thought to be blocked by BiP on the lumenal side of the membrane (Hamman et al., 1998), however, more recent structural studies have identified the 'plug' domain of Sec61 (Junne et al., 2010). This protein domain resides on the lumenal side of the channel and folds back into the channel preventing passive transport through the unoccupied channel (Zimmer et al., 2008). During the first stages of insertion the signal peptide is inserted into the channel and folds back, effectively intercalating into the channel (Shaw et al., 1988). Simultaneously the lateral gate obstructing the channel and the plug are displaced (Zimmer et al., 2008). Once insertion is initiated and during synthesis the signal peptide remains stationary where it is partially degraded by the proteolytic enzyme signal peptidase, the remaining membrane bound peptide aggregates and exports into the cytosol (Lyko et al., 1995; Weihofen et al., 2002). Concurrently the elongating chain is extended into the membrane (Park and Rapoport, 2012).

As the synthesising nascent chain inserts through the membrane of the ER the hydrophobic residues of the unfolded protein interact within the ER with the chaperone Binding Protein (BiP) (Schneider et al., 1994). The bound BiP prevents the linear peptide from passively reverse translocating, as the BiP is bigger than the hydrophilic channel. Due to Brownian motion the peptide can further enter the ER, and is immediately bound to more BiP, and thus the protein is inserted progressively into the ER in a mechanism referred to as the 'Brownian ratchet'

(Matlack et al., 1999; Simon et al., 1992). The main role of BiP, however, is as a chaperone to stabilise the folding of proteins by binding exposed hydrophobic residues. Once bound, BiP hydrolyses ATP to thermodynamically encourage the folding of proteins and to destabilise misfolded intermediates (section 1.3.1). Once folded and assembled, chaperones such as BiP can no longer bind to the internal hydrophobic residues, and the protein is considered a soluble lumenal protein ready for export or functionality within the lumen of the ER (See Figure 1.2).

1.2.3 Synthesis and Translocation of Integral Membrane Proteins

Aside from the soluble lumenal proteins there are several other classes of proteins that encounter, either directly or peripherally, the secretory pathway. One such class is the membrane spanning proteins. Although there is no generally accepted classification system, for simplicity in this thesis a system based on previous classifications will be used (Chou and Elrod, 1999). In this nomenclature the membrane proteins are further subdivided into four classes: type I, II, III and IV (Figure 1.2). Type I membrane proteins have a single transmembrane domain (TMD) with the soluble N-terminus of the protein in the lumen of the ER. Type II are single pass with the C-terminus in the ER. Type III are single pass with the N-terminus in the lumen of the ER, but inserted into the membrane in a type II like manner. Type IV are multiple membrane spanning proteins, and can have any combination of the C/N termini on the cytosol/ER side of the membrane.

As in soluble lumenal proteins, type-I-membrane spanning proteins have an N-terminal signal peptide and therefore follow a comparable translocation process. When the hydrophobic TMD is being inserted into the Sec61 protein complex it stalls the protein in the translocation channel and is thus called the ‘stop-transfer’

sequence (Scott and Schekman, 2008). The channel splits open, and the protein exits the channel laterally allowing the 2-dimensional diffusion of the membrane protein into the lipid bilayer of the ER (Heinrich et al., 2000). This 'split' is mediated by the repositioning of 4 short transmembrane segments on one wall of the channel. There are two competing theories on the cause of the channel splitting open. The first states that there is a hydrophobic interaction between the lipid bilayer and the hydrophobic TMD, supported by the fact that regions with increased hydrophobicity insert with greater efficiency (Hessa et al., 2005; Junne et al., 2010). The second theory is based on the bacterial model and states that a positive kinetic force is required evidenced by the fact that addition of ATP increases the efficiency of insertion (Duong and Wickner, 1998). In reality the efficient translocation is probably a combination of both enzyme kinetics and hydrophobic interactions.

Type II membrane spanning proteins do not have an N-terminal signal peptide and thus cannot transfer via a type I mechanism. In this case the TMD has to act as a signal for membrane insertion. Depending on the length of the C-terminal section and the relative position of the TMD along the protein, there can only be insertion into the ER after a significant part of the protein has been translocated. This adds the additional complexity that nascent proteins might be partially folded prior to insertion. In a process that is similar to the co-translational mechanism, the SRP interacts firstly with the TMD of the protein, acting as a signal peptide (Kocik et al., 2012; Shao and Hegde, 2011). The canonical SRP-SRP receptor system then allows insertion into the membrane as well as translocation. One of the key differences between this pathway and the more traditional signal peptide mediated system is that the signal anchor sequence is not cleaved, but is integrated into the

membrane spanning domain of the protein. For this reason the TMD of a type-II membrane spanning is called a 'signal anchor' sequence.

There is a subset of type-II membrane spanning proteins, with a signal anchor/TMD proximal to the C-terminus. Therefore the ribosome completes translation before insertion in a post-translational mechanism. This tail-anchored (TA) protein class was first formally discussed in 1993 (Kutay et al.), and the model protein cytochrome b_5 was first noted for its ability it insert into microsomal vesicles under *in vitro* conditions (Strittmatter et al., 1972). The presence of a 'non-polar peptide segment' was observed by the partial quenching of the intrinsic tryptophan fluorescence when inserted into the membrane of either microsomal or preformed phosphatidylcholine (Fleming, 1978). It was even shown that the protein can freely transfer between vesicles, *in vitro*. The sequence required for membrane integration was labelled the 'insertion sequence' (Blobel et al., 1984) and was shown not to compete for insertion at the translocation channel or require SRP or any membrane spanning receptor (Anderson et al., 1983; Bendzko et al., 1982). After these fundamental experiments, it was shown that cytochrome b_5 represented a class of topologically similar proteins (Kutay et al., 1993) that notably include the SNARE (SNAP Receptor) protein family discussed below (Section 1.4.6, pg. 46). TA protein insertion mechanism is Sec61 protein complex independent (Borgese et al., 2003; Walter et al., 2001; Yabal et al., 2003). Instead the GET (guided entry of TA proteins) targeting/insertion system is used. The Sgt2 chaperone protein complex comprising Get4 and Get5 binds to the newly synthesised TA proteins (Chang et al., 2010; Wang et al., 2010). This complex then interacts with the ATPase Get3 (Wang et al., 2011), which mediates delivery to the membrane via interaction with Get1 and Get2 which are associated with the membrane (Auld et al., 2006; Jonikas et al., 2009; Schuldiner et al., 2008).

The insertion of the proteins into the membrane is dependent on both Get3 and ATP (Bozkurt et al., 2009; Favaloro et al., 2009; Stefanovic and Hegde, 2007). A consequence of the post-translational insertion and the Sec61 independence is that this protein class could conceptually insert into membranes, other than the ER, within the cell.

Type III protein insertion occurs in a similar way to the signal-anchor based type II mechanism. There appear to be three general rules that determine the topology of the insertion of the protein (Junne et al., 2010; Park and Rapoport, 2012; Rapoport et al., 2004). Firstly, if there are any stably folded protein intermediates either before or after the TMD, they can obstruct the insertion in either orientation (Denzer et al., 1995). Secondly the 'positive inside rule' where the topology is defined by an increased presence of positive residues of the first TMD, which is thus inserted with these positive residues in the cytosol (Hartmann et al., 1989; Heijne and Gavel, 1988). Finally the length of the hydrophobic span within the TMD; longer TMDs are more often orientated with the C-terminus in the cytosol (Sakaguchi et al., 1992; Wahlberg and Spiess, 1997).

1.2.4 The Cytosolic Side of the Membrane

Aside the from membrane spanning proteins and the lumenal proteins the final class of proteins associated with the secretory pathway is a subset of the cytosolic proteins. These proteins are not fully integrated into the membranes of the cell but may interact by either harbouring lipid anchors such as prenylation and myristoylation (Haucke and Paolo, 2007; Sorek et al., 2009), or by associating peripherally with the exposed cytosolic domain of true membrane spanning proteins – these specific interactions are by-definition impossible to predict without direct

experimental evidence. The synthesis of cytosolic proteins is less complex than the synthesis of the membrane spanning proteins and lumenal proteins, as they are synthesised in the cytosol by free ribosomes and remain in the aqueous soluble environment (Palade, 1975). However, due to the various post-translational mechanisms further layers of flexibility can be exploited. Firstly, these proteins can directly insert or associate with the membranes of the secretory pathway at a later stage than the ER. Secondly, they can differentially interact in a signal mediated manner, associating and dissociating depending on the physiological status of the cell providing localised functionality. As such these proteins can maintain transient processes such as membrane curvature via a mechanistic bending of the membrane from the outer leaflet though either insertion, crowding, scaffolding or shaping the outer membrane (Kirchhausen, 2012). Furthermore, as discussed below (Section 1.4.5, pg. 44) the lipid anchored RabGTPases and tail anchored SNARES often allow for either the separation or fusion of organelle membranes (Bonifacino and Glick, 2004).

1.3 EVENTS IN THE ER

Upon entry into the ER the integral-membrane proteins diffuse in the 2-dimensional space across the lipid bilayer of the ER, and the lumenal proteins diffuse into the soluble space within the lumen of the ER. Both the rough and smooth ER share the same lumenal space, but have different functions. The rough ER is studded by ribosomes and mainly associated with protein translocation, protein folding/oligomerisation and ER associated degradation (ERAD) discussed below. The smooth ER is associated with lipid metabolism, detoxification of the ER network and calcium influx/eflux from the lumen of the ER (Black et al., 2005). As a whole the ER is a tubular and cisternal network like structure that has a large

volume and surface area, the shape of which is highly variable dependent on the cell physiology. This tubular-like structure is maintained by the 'wedged' shaped reticulons (Yang and Strittmatter, 2007). Although the ER is often depicted as being directly proximal to the nucleus, the vast network permeates throughout the cytosol (Shibata et al., 2010). In plants there is also a distinct cortical ER network that is functionally differentiated and tethered to the plasma membrane (Hepler et al., 1990; Sparkes et al., 2009b; Zhang et al., 2012). A number of sub-structures also exist on the ER, such as the ER export sites, from which the vesicles destined for the Golgi apparatus bud (DaSilva et al., 2004). There are also sub-structures formed by the 'contact zones' as the ER is transiently fused to another organelle to facilitate lipid transfer between the two (Levine, 2004).

1.3.1 Folding in the Endoplasmic Reticulum

The insertion of lumenal proteins into the ER via the Sec61 translocation channel is only the first stage of several protein sorting pathways available in the secretory pathway. When entering the ER, proteins are bound to BiP via their hydrophobic residues, preventing the formation of stable but undesirable folding intermediates (Snowden et al., 2007). These dynamic intermediates in the folding process need to be protected to avoid side-reactions and misfolded polypeptides. The hydrolysis of the adenosine triphosphate (ATP) on BiP to ADP allows the release of BiP and simultaneously allows the folding protein to interact with different BiP molecules which are in the active (ATP bound) state. Any exposed hydrophobic region can bind to BiP or an analogous chaperone that increase thermodynamic probability of a coherently folded protein, this is reffered to as 'unfoldase' activity (Goloubinoff et al., 1999; Slepenkov and Witt, 2002). Chaperones in eukaryotic cells act in the ER, but have been found in all compartments where folding is known to take place

(Hartl and Martin, 1995). The ER lumen, however, is thought to have the highest concentration of folding intermediates and chaperone-interactions are particularly well studied in this organelle.

1.3.2 Protein Modifications in the Endoplasmic Reticulum

The maturation of a protein from a two dimensional peptide sequence to a three dimensional, functional protein often requires further post-translational modifications after the completion of folding. Within the ER there are a variety of these processes that facilitate the final stages of protein processing. One such process is glycosylation— the covalent attachment of a small oligosaccharide to the surface of a protein. The most characterised type of glycosylation is the addition of an N-acetylglucosamine to the exposed nitrogen on the asparagine residue within the consensus 'Asn–X–Ser/Thr' (where X is any amino acid other than proline), termed 'N–linked glycosylation' (Dempski and Imperiali, 2002; Hart et al., 1979; Vitale et al., 1993). This process is facilitated by a lipid glycan donor synthesised on the cytosolic side of the ER with an exposed glucose$_3$–mannose$_9$–*N*–acetylglucosamine, which is transferred to the lumen in an ATP dependent, membrane inversion event by the enzyme flippase Rft1p (Helenius et al., 2002). The terminal *N*–acetylglucosamine can then be transferred from the lipid to the protein in one step by a membrane spanning oligosaccharyltransferase complex (Dempski and Imperiali, 2002).

Supplementary to to N–linked glycosylation in the ER proteins also form cysteine-cysteine covalent disulphide bonds that are stable in the oxidising environment of the ER. As well as allowing for stable tertiary structures of single proteins the formation of these bonds also allows for fully folded

proteins to form multimeric structures post-translationally. Although these bonds were originally shown to form spontaneously (Anfinsen, 1973), *in vivo* the 'protein disulphide-isomerase' family catalyses their formation (Frand et al., 2000; Freedman et al., 1994). In addition, the presence of oxidized glutathione in the ER provides the oxidising equivalents and is expected to participate in a thioldisulphide exchange (Frand et al., 2000).

Despite these strategies to fold and stabilise proteins it is still possible under certain conditions to induce a build-up of stable misfolded proteins. This build up of unfolded proteins in the ER can cause titration of chaperones or high molecular weight conglomerates that can perturb ER function and result in mammalian diseases (Corrigall et al., 2001) as well as phenotypic abnormalities in yeast (Rose et al., 1989). In order to combat these effects a protein cascade called the unfolded protein response (UPR) can be activated that induces the expression of chaperones and causes degradation of misfolded proteins (Ron and Walter, 2007).

1.3.3 The Unfolded Protein Response

There are three known proteins that induce the UPR transcriptional response cascade, inositol-requiring protein-1 (IRE1) (Cox et al., 1993), protein kinase RNA (PKR)-like ER kinase (PERK) (Harding et al., 1999; Shi et al., 1998) and activating transcription factor-6 (ATF6) (Haze et al., 1999). The induction of a gene expression based cascade from protein stress in the ER has two main conceptual issues to overcome, (1) the signal needs to cross the membrane of the ER and (2) the protein based mechanism needs to interact with genomic material. Each of the three known UPR sensors (IRE1, PERK and ATF6) have a unique mechanism for inducing the stress response. The classical mechanism

is based on the titration of BiP by the unfolded protein intermediates that reversibly prevent BiP from binding to IRE1 inducing homo-oligomerisation of IRE1 (Bertolotti et al., 2000; Okamura et al., 2000). This interaction between IRE1 allows for *trans*-autophosphorylation of the cytosolic domain of the IRE1 activating the endonuclease activity causing the specific, differential splicing of the XBP1 mRNA (Sidrauski and Walter, 1997). The IRE1 spliced XBP1 mRNA encodes a transcription factor that induces UPR related gene expression (Yoshida et al., 2003).

The activity of PERK is topologically analogous, with a similar oligomerisation under stressed conditions (Bertolotti et al., 2000). However, the kinase activity of the cytosolic domain has two known effects. Firstly *trans*-autophosphorylation of the cytosolic domain causes a conformational change allowing for the recruitment of eIF2α. The eIF2α can then also be phosphorylated by PERK (Marciniak et al., 2006). This in turn lowers the GDP to GTP auto-GAP activity of the eIF2 protein complex which decreases protein translation unilaterally (Harding et al., 1999). In plants, however, there is evidence to suggest that ER stress selectively reduces secretory but not cytosolic protein expression, perhaps due to a compounded effect of translocation pore competition and mRNA stability (Leborgne-castel et al., 1999; Snowden et al., 2007).

The final UPR activating pathway is initiated by the protein ATF6 (Haze et al., 1999). ATF6 is also activated by the titration of BiP due to unfolded proteins (Shen et al., 2002), which in turn allows for the trafficking of the ATF6 from the ER to the Golgi apparatus. At the Golgi apparatus the protein is cleaved by a combination of proteases that release the cytosolic domain of the protein into the cytosol as a soluble fragment (Ye et al., 2000). However the direct targets and mechanism of the soluble fragment of ATF6 are not known.

1.3.4 ER Associated Degradation

Aside from a general decrease in mRNA levels due to PERK related suppression, the activation of the UPR results in transcriptional up-regulation of various gene classes (Schröder and Kaufman, 2005). The study for the identification of UPR targets used mRNA preparations of artificially ER stressed yeast to compare the expression profiles with unstressed cells using oligonucleotide arrays (Travers et al., 2000), an experiment that was confirmed with similar findings in mammalian cell lines (Okada et al., 2002), as well as plants (Martínez and Chrispeels, 2003). The genes discovered fall into several categories including, translocation, glycosylation, protein folding (i.e. chaperones), vesicle trafficking, lipid metabolism and finally vacuolar protein sorting. Taken as a whole, it seems that there are four basic strategies for recovering from ER stress the first of which is stopping the increasing buildup of misfolded proteins, this is achieved by the general decrease in mRNA levels and the enhanced folding of the proteins by chaperone production. The second seems to be to clear the ER of misfolded proteins, perhaps explaining the general increase in vesicular trafficking, removing ER residents for either secretion or vacuolar sorting. The third strategy is remodeling the ER by the induced lipid metabolism, which has been observed in multiple studies. The final strategy is the protein degradation pathway, including the ER Associated Degradation (ERAD) pathway which helps to clear the ER and jammed translocation pores of terminally misfolded intermediates (Meusser et al., 2005).

ERAD allows for the selective degradation of soluble and membrane spanning ER lumenal proteins, avoiding unwanted degradation of the contents of the ER (Bonifacino and Lippincott-Schwartz, 1991; Lippincott-Schwartz et al., 1988; Meusser et al., 2005; Wiertz et al., 1996). The basic principle involves the recognition of misfolded proteins, retrotranslocation *back* thorough the Sec61

translocon, ubiquitination and subsequent degradation by the proteasome protein degradation complex. Although there are multiple theories of substrate recognition, the most prevalent is the idea that the BiP-unfolded protein complex interacts with a Sec61p allowing for proximity induced retrotranslocation (Nishikawa et al., 2001). The retrotranslocation event itself occurs by the protein being threaded back through the Sec61 translocation pore, perhaps with accessory proteins forming part of the pore complex (Kalies et al., 2005; Scott and Schekman, 2008). The ubiquitination and subsequent polyubiquitination of ERAD targets is mediated by a series of E1/E2/E3 ubiquitin ligases (Vembar and Brodsky, 2008) that allow for interaction with Rpn13, a proteasome subunit (Husnjak et al., 2008). This process allows for the turnover of terminally unfolded protein and the recovery of ER function under stress conditions. Successfully folded proteins are now free to traffic to their destination compartment.

1.4 POST-ER TRANSPORT IN THE EARLY SECRETORY PATHWAY

In addition to the ER export route, trafficking between the organelles of the secretory pathway is based on discrete vesicular trafficking steps, all of which are controlled by protein-protein interactions that shape membranes. Although the protein machinery differs between the individual transport steps the general principle is remarkably conserved as outlined below (See Figure 1.3).

1.4.1 Principle of Vesicular Trafficking

Vesicles bud essentially from a 'donor' compartment ('vesicle budding', Figure 1.3, a and b) (Bonifacino and Lippincott-schwartz, 2003; Kirchhausen, 2000b). In this budding process, coat proteins aggregate forming patches on the cytosolic

side of donor compartment membrane, bending it to the extent that it deforms leaving only a thin 'neck'. Protein-protein interactions between the membrane bound coat proteins and vesicle contents allow for selective recruitment and loading of soluble cargo as well as membrane proteins in budding vesicles. Various GTPases provide the energy that finally detaches the vesicle, allowing membrane dissociation (Kirchhausen, 2000b) (Figure 1.3, c and d). The uncoating of the vesicle also requires the activity of a GTPase, providing the energy to remove the soluble protein coat from the vesicle. The vesicles then traffic in a ATP dependent way tethered to the cellular cytoskeleton (Hehnly and Stamnes, 2007) before fusing via vesicle-target recognition ('vesicle targeting') to the target membrane ('vesicle fusion') (Bonifacino and Glick, 2004) (Figure 1.3, e and f).

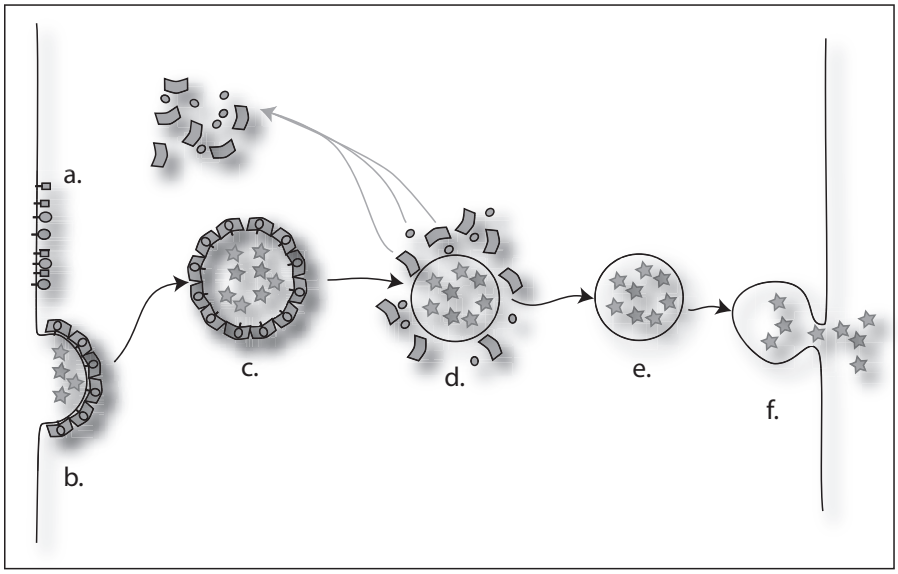

Figure 1.3: **Vesicular Transport** The basic principle of vesicular trafficking is conserved across all eukaryotic kingdoms. It can be broken down into six individual steps; protein aggregation (a), membrane deformation (b), budding (c), uncoating (d), motility (e) and fusion (f).

Although the ER export selection for membrane spanning proteins and soluble cargo from the ER is different, the vesicular route is the same. The mechanisms and principles of transport in the early secretory pathway can be considered analogous for the various trafficking routes, for example the principle of vesicular

trafficking described below is relevant to the COPII (Section 1.4.2) vesicles that leave the ER, as well as the COPI vesicles (Section 1.5.3) that return to it and the clathrin machinery of the late secretory pathway (Section 1.8.1)

1.4.2 COPII Vesicle Formation and Budding

Of the various vesicular trafficking routes in the cell, the first that a protein in the secretory pathway will encounter is the Coatmer Protein II Coated (COPII) route, from the ER to the Golgi apparatus (Barlowe et al., 1994) (See Figure 1.1). The budding of COPII vesicles is initiated by a small GTP binding protein, SarIp (Lee et al., 2005). The cytosolic GTPase is recruited to the ER membrane by an N-terminal hydrophobic domain which is exposed when SarIp is conjugated to GTP (Huang et al., 2001). Similar to other molecular switches, SarIp can either be GTP or GDP bound and GDP to GTP exchange initiates membrane insertion, and is catalysed by the guanine nucleotide exchange factor (GEF), Sec12. This is a type II membrane protein which is permanently membrane bound but excluded from the nascent transport vesicle (Sato and Nakano, 2005). The association of SarIp to the membrane recruits the two heterodimers Sec23/Sec24 (Hicke et al., 1992) and Sec13/Sec31 (Salama et al., 1993) sequentially from pools in the cytosol (Antonny and Schekman, 2001; Barlowe et al., 1994; Hughes and Stephens, 2008). The resulting hetero-tetramer complex induces membrane curvature (Gürkan et al., 2006; Zanetti et al., 2012). The multimer propagates on the ER surface eventually forming a strong lattice that induces membrane curvature and enhances stability of the protein-vesicle complex. When the curvature is complete the GAP activity of Sec23 (Yoshihisa et al., 1993) promotes the hydrolysis of SarIp-GTP to form SarIp-GDP, providing the energy for complex dissociation. *In vitro*, COPII vesicles can be stabilised by using GTPγS, a non-hydolysable GTP analogue. *In vivo*,

inhibition of GTP hydrolysis causes a more complex sequence of events, perhaps preventing vesicle uncoating (Bielli et al., 2005). Both soluble and membrane spanning proteins can be included in COPII vesicles.

1.4.3 ER Export and the Bulk Flow Hypothesis

All soluble secretory proteins that are not targeted by ERAD are thought to be competent for entry into COPII vesicles destined to the Golgi apparatus (See Figure 1.1). The current accepted model suggests that they are sorted without a sorting signal via passive diffusion or 'bulk flow'. This hypothesis was first presented in 1987 (Wieland et al.), based on the efficient export of radiolabelled oligosaccharide tagged proteins. Although in the publication both the bulk flow mechanism and the ER retention mechanism (see section 1.5.2) were correctly predicted in this manuscript, the authors extended their conclusions to membrane proteins.

Initially bulk flow of the soluble cargo was cast into doubt by immunogold localisation electron microscopy with antibodies against the soluble protein serum albumin, which showed enrichment in the vesicular export sites on the ER suggesting that there was a selection mechanism (Mizuno and Singer, 1993), but has since been criticised as being non quantitative and using an antibody labelling protocol prone to non-specific signal amplification (Griffiths et al., 1995). The bulk flow of soluble proteins has since been convincingly demonstrated. By forcing heterologous soluble cytosolic proteins to enter the ER lumen of plants after fusion to signal peptides secretion was effectively demonstrated (Denecke et al., 1990). Deletion of an ER retention signal ('HDEL') from the normally ER localised Calreticulin, resulted in its secretion (Crofts et al., 1999). ER export

inhibitors in the same system prevented secretion (Phillipson et al., 2001). Finally, using a similar approach in the CHO mammalian cell system these results were shown to be conserved in other kingdoms (Thor et al., 2009). There is also evidence that fusion of the proregion section of the yeast protein alpha-factor to soluble proteins can induce ER export to non-exported soluble proteins- although this could also be due to the masking of a retention signal (Herrmann et al., 1999; Schwientek and Ernst, 1994).

The theory of bulk flow, as originally presented does not hold true for membrane proteins. Using an electron microscopy immunolocalisation against an overexpressed heterologous membrane spanning protein 'vesicular stomatitis virus glycoprotein' (VSV-G), the relative amount of protein was compared in vesicles and on the ER of Normal Rat Kidney Epithelial Cells (Balch et al., 1994). Convincingly, an enrichment of the protein was found in the vesicles indicating that there is some selective mechanism. The VSV-G became a model protein for the understanding of the signal mediated export of the ER export mechanism, and the discovery of the first 'ER export motifs'.

1.4.4 ER Export Motifs of Membrane Spanning Proteins

The evidence that the ER export of a protein is dependent on residues in the cytosolic terminus first came from deletion experiments with VSV-G (Doms et al., 1988). These experiments show that the C-terminus is necessary for protein transport and the findings quickly related to other model proteins (Guan et al., 1988). A diacidic *'DXE'* motif ((D/E)(X)(D/E) [X=any amino acid]) in the cytosolic C-terminus of VSV-G was shown to be required for the efficient ER export (Nishimura and Balch, 1997), a model that was later shown to be overly

simplistic (Sevier et al., 2000). Sevier and colleagues suggest that the ER export motif has a tyrosine residue -2aa from the first acidic residue and is part of a complex region of ER export. Similar observations were made on a DXE motif in a mammalian potassium channel. It was first shown that when both acidic residues were alanine substituted anterograde trafficking was abolished (Ma et al., 2001). Interestingly, the ER export could be restored to both the AXA mutant receptor and a different potassium channel isoform when the motif in its original context (FCY**E**N**E**) was fused to the C-terminus, indicating that FCYENE is not only necessary, but sufficient for ER export. In addition **A**C**A**ENE and FCY**A**N**A** did not restore ER export indicating, once again the necessity of a tyrosine as part of the ER export motif. Similar di-acidic motifs have also been identified in yeast (Malkus et al., 2002; Votsmeier and Gallwitz, 2001) and plant proteins (Hanton et al., 2005; Jung et al., 2011).

In addition to the diacidic motif there is also an 'FF' motif that has been implicated as an ER export motif (Barlowe, 2003). This motif for ER export was first observed in the p24 protein family (Dominguez et al., 1998; Fiedler et al., 1996) and also seen in the ERGIC53, ER/Golgi interface protein (Kappeler et al., 1997) and the plant p24 homologues (Contreras et al., 2004). The inclusion of both the FF and diacidic type proteins in ER export vesicles seems to be mediated by interaction with SarIGTP (Aridor et al., 2001), although there is also evidence for an interaction with the whole coat protein complex (Dominguez et al., 1998).

1.4.5 Rab Proteins

Upon cargo loading into the COPII vesicles, budding from the ER and subsequent uncoating, the vesicles need to approach, recognise and fuse with the correct

target compartment. In the case of COPII vesicles the target organelle is the Golgi apparatus (Hughes and Stephens, 2008). As mentioned previously, other known vesicular target recognition and fusion mechanisms follow the same general principle (Kirchhausen, 2000b) and the COPII model will serve as an example in this introduction.

The first step of the vesicular fusion process is the tethering mechanism controlled by a subgroup of the low molecular weight Rat sarcoma (Ras)-related in brain (Rab) GTPases (Rutherford and Moore, 2002; Stenmark, 2009), a hypothesis first proposed based on a secretion defective yeast mutant (Salminen and Novick, 1987). As other G proteins, the low molecular weight Rab GTPases exist in two conformational states, one active and the other inactive. When 'inactive' the protein is bound to GDP; GDP can be exchanged for GTP facilitated by a guanine nucleotide exchange factor (GEF) which activates the molecular switch (Delprato et al., 2004). To close the cycle Rab GTP hydrolysis is activated by a GTP activating protein (GAP) (Haas et al., 2007a). The Rabs are often soluble and cytosolic when in the GDP form, and membrane associated when in the GTP form. A Rab GDP dissociation inhibitor (GDI) stabilises the Rab when soluble, shielding the exposed hydrophobic lipid anchor from the soluble environment (Matsui et al., 1990). Although RabGTPases have been implicated in a multitude of processes their roles as regulators of membrane identity though active protein recruitment and vesicle trafficking is well established (Pfefffer, 2013; Stenmark, 2009). There are thought to be up to 60 members in the mammalian kingdom (Haas et al., 2007a; Stenmark, 2009) and 57 in the *A. thaliana* genome (Vernoud et al., 2003). These RabGTPases are involved in processes across the whole cell and as such are associated with the majority of organelles (Chavrier et al., 1990).

The RabGTPase involved with the tethering of the COPII vesicles to the Golgi in mammalian cells is hypothesised to be Rab1 (Plutner et al., 1990; Schmitt et al., 1986; Tisdale and Bourne, 1992), with a similar finding for the plant Rab1 homologue (Batoko et al., 2000). Rab1 is the most characterised of the RabGTPases, and can serve as a model. In the case of COPII vesicular fusion there is a cascade of interactions that facilitate the action of the RabGTPase. Initially the Sec23 in the vesicular coat binds the protein mBet3p in the 7 protein TRAPPI complex (Sacher et al., 2001; Yu et al., 2006). This complex acts as both the Rab1 binding site and as the Rab1 GEF (Wang et al., 2000). Activation of the Rab1 by TRAPPI causes homodimerisation of the Rab1, which in turn recruits a tethering factor dimer of p115/Uso1p and GM130 (Allan et al., 2000; Moyer et al., 2001; Sapperstein et al., 1995; Weide et al., 2001). Once the large multimeric complex is bound the hydrolysis of the GTP on the Rab brings the membranes closer together facilitating the subsequent fusion event. Although the Rabs can mediate the tethering of vesicles to organelles, they are not directly involved with the membrane fusion event which is regulated by the SNARE family.

1.4.6 SNARE Proteins

The final stage of a vesicular trafficking event is the membrane fusion of the vesicle with the target compartment. The result of which is the correct delivery of both soluble and membrane proteins whilst maintaining topology. This membrane fusion is mediated by SNARE (SNAP [Soluble NSF Attachment Protein] Receptor) proteins (Jahn and Scheller, 2006), which overcome the high repulsive forces that exist between two lipid bilayers when in close proximity (1-2 nm) (Jahn and Südhof, 1999).

SNAREs form tetrameric complexes (*trans*-SNARE complex or SNAREpin), with one on the vesicle and three on the target membrane. Accordingly, SNAREs are divided into two classes based on the presence of a arginine (R) or glutamine (Q) in the zero-ionic layer of the assembled SNARE tetramer (Fasshauer et al., 1998). Generally, R SNAREs are on the vesicle and Q SNAREs are on the target compartment. Q SNAREs are further subdivided into Qa, Qb and Qc classes based on their 'coiled-coiled' domain representing their structural role in the trans-SNARE tetrameric complex (Bock et al., 2001). This SNARE class system is conserved across all eukaryotic kingdoms. The formation of this tetrameric complex allows fusion of the two proximal membranes, with the outer leaflets of the lipid bilayer fusing first, generating a transient 'stalk' structure (Markin et al., 1984), which spreads allowing for the inner leaflets to contact in a structure called the hemifusion state (Jahn and Scheller, 2006). Finally the inner leaflets fuse forming a pore releasing the contents of the vesicle into the target compartment and allowing diffusion of the membrane protein cargo into the target organelle membrane (Chernomordik and Zimmerberg, 1995). After the membranes have fused the soluble ATPase NSF and its co-factor α-SNAP are required for dissociation of the SNARE complex and re-cycling of SNAREs (Söllner et al., 1993), in a ATP dependent manner. The dissociated SNARE proteins are now competent for a new round of interaction and membrane fusion.

After the fusion event and the breaking of the SNARE complex, the SNAREs remain embedded on the membrane of the target organelle. Although it is not known whether these SNAREs recycle, it seems probable. If so, it is also not known if they recycle to the site of synthesis (the ER) or to the membrane of their action.

With regards to the COPII SNAREs, upon the fusion of COPII vesicles with the Golgi apparatus, the Golgi releases the soluble bulk flow cargo which diffuses into the lumenal space. The selectively exported membrane spanning proteins can laterally diffuse into the membrane of the donor compartment, and thus the budding-movement-fusion cycle of a vesicle is complete.

1.5 THE GOLGI APPARATUS

The organelles of the secretory pathway can be broadly divided into the early and late secretory pathway. The Golgi apparatus is situated between both. It is the second organelle that proteins encounter on the biosynthetic route and can be regarded as the last organelle in the early secretory pathway (See Figure 1.1). The Golgi can be seen as a branching point for protein trafficking. There are three destinations that proteins can reach from the Golgi; (1) the ER, for soluble cargo retained in the ER, (2) the plasma membrane (PM) for secreted cargo and (3) the route to the vacuoles/lysosomes .

1.5.1 Discovery and Morphology of the Golgi Apparatus

The Golgi was the first cellular organelle discovered, being described in the late 1900s by the Italian biologist Camillo Golgi (Fabene and Bentivoglio, 1998). It is composed of 'stacks', which are pancake like flat cisternae with the lumenal contents fully stratified across the Golgi stack. In animals these stacks are laterally connected in a large reticulated network and in yeast the network is completely dispersed, however in plants the Golgi stacks exist as discrete cisternal stacks forming mobile units (Sparkes et al., 2009a). Generally, there are 5–7 cisternae per stack, however there can be as few as 3 or as many as 20 cisternae per single

Golgi stack. The cisternae that receive the contents from the ER are referred to as the cis-Golgi, in the middle are the medial-Golgi stacks and the most distal cisternae are referred to as the trans-Golgi. There is evidence to suggest that these cisternae mature from one another directly, as well as being connected via vesicular trafficking routes (Pelham and Rothman, 2000). In plants individual Golgi bodies also seem to be attached to the ER network, connected by actin filaments (Boevink et al., 1998; DaSilva et al., 2004; Nebenführ et al., 1999). The link with the cytoskeleton facilitates active motility of individual Golgi stacks, but the biological function of the Golgi motion in plants remains unknown.

1.5.2 Sorting of ER Retained Proteins

Due to the non-selective bulk flow nature of ER export discussed above (Section 1.4.3), proteins that need to accumulate in the ER have to be trafficked in a retrograde manner from the Golgi apparatus (Rothman and Wieland, 1996).

A mechanism for this process was proposed when it was shown that a conserved sequence of 4aa's (KDEL) exposed at the C-terminus of several ER resident soluble proteins was both necessary and sufficient for effective ER retention of soluble, ER localised proteins (Munro and Pelham, 1987). This finding was later extended with a thorough analysis in plants, increasing the array of known ER retention signals (Denecke et al., 1992). Based on cargo modification assays using cathepsin D as a reporter for Golgi mediated glycan modifications it was shown that KDEL mediated ER retained cargo passed through the Golgi (Pelham, 1988).

The receptor of this recycling step was shown to be Erd2p, a seven TMD protein identified in a genetic screen for defective ER retention (Lewis et al., 1990), and shown to mediate both capacity and specificity of ER retention (Lewis and

Pelham, 1992). This retrograde sorting pathway is a vesicular route, which, although following similar mechanistic principles to COPII vesicles (Section 1.4.2), uses a different set of regulatory proteins and cytosolic coat components.

1.5.3 COPI Vesicular Trafficking

Other than the COP vesicle complex already described (Section 1.4.2), eukaryotic cells also contain a second COP complex. The COPI complex shapes vesicles that bud at the Golgi apparatus to be trafficked to the ER (Bonifacino and Glick, 2004; Waters et al., 1991). COPI vesicles are shaped at the Golgi with the 7-subunit 'coatamer' protein complex (α, β, β', γ, δ, ϵ and ζ) (Malhotra et al., 1989), and have been shown to be essential for retrograde Golgi→ER transport (Letourneur et al., 1994). The vesicle is nucleated by the interaction between the β subunit and the small GTPase ADP-ribosylation factor (ARF) (Donaldson et al., 1992; Peyroche et al., 1996; Zhao et al., 1997). Unlike the previously described vesicle budding related GTPase Sar1p, ARF is bound to the membrane by N-terminal myristoylation (Antonny et al., 1997). The membrane insertion mechanism is, however, analogous to Sar1p as when in the GDP bound form ARF masks the myristoylation site, preventing membrane binding (Goldberg, 1999). The presence of ArfGTPase in the vesicle coat allows for further binding of vesicle associated proteins (Gillingham and Munro, 2007). As with Sar1p in COPII vesicles the hydrolysis of ARF causes vesicle uncoating (Kirchhausen, 2000b). This GTP→GDP 'activation' is catalysed by the ArfGAP protein family (Scheffzek et al., 1998), and GTP hydrolysis is possible, but slow without the presence of a GAP (Kahn and Gilman, 1986). The COPI vesicles are subsequently tethered to the ER membrane by a three subunit (Dsl1p, Dsl3p, and Tip20p) protein complex (Zink et al., 2009). After successful tethering membrane fusion

can commence under control of the Ufe1p/Syn18, Sec20 and UseI Qabc SNARE complex (Kraynack et al., 2005), a fusion event perhaps under control of different SNARE proteins in plants (Lerich et al., 2012).

1.6 THE LATE SECRETORY PATHWAY: TWO DISTINCT TARGETS

Proteins without signals for recycling back to the ER can be considered competent for export from the Golgi apparatus, in the anterograde direction. These proteins can then be directed to two major end locations, either secretion to the plasma membrane or transported to the vacuoles (See Figure 1.1). For this reason, the two pathways are considered late with regards to the overall system. It should also be understood that the endocytic pathway starts at the plasma membrane and can either lead to vacuoles or the ER. The following subheading describes processes from a biosynthetic perspective (from ER to the PM or vacuole).

1.6.1 The Morphology of the Plasma Membrane

Soluble proteins that are directed for secretion are targeted to the outside of the cell, generally referred to as the extracellular matrix. In plant cells, this is also termed the apoplastic space (See Figure 1.1), the compartment that exists within the plant cell wall, and outside of the membrane. The PM has a multitude of membrane proteins embedded within it. These proteins allow the outside of the cell to communicate with the inside and include G protein coupled receptors, ion channels, aquaporins and cell type specific receptors. In addition membrane proteins can span across the bilayer allowing the structural proteins to indirectly connect the inside and the outside of the cell. The current accepted model of the micro-structure of the plasma membrane is the 'fluid-mosaic model' (Edidin,

2003). The 'fluid' refers to the liquid membrane and the 'mosaic' refers to the embedded proteins that passively diffuse in the 2-dimensional plane throughout the membrane.

Any molecular import from the extracellular environment needs to either occur via protein pores in the PM or be mediated by endocytosis in vesicular structures, thus making the membrane selectively permeable. There is a dynamic system with early electron microscopy studies predicting that there is a total turnover of 50% of the cell surface PM of fibroblast cells in one hour (Steinman et al., 1983), a number that is likely cell type dependent.

In addition to the mosaic of proteins embedded in the membrane there is the macromolecular crowding of protein-lipid complexes called 'lipid rafts'. Although lipid rafts are thought to exist throughout the cellular membranes (such as at vesicular formation sites on the Golgi apparatus) they were initially characterised using the PM as a model. Indeed some PMs are thought to derive their structure from lipid raft mediated transport (Simons and Ikonen, 1997). Lipid rafts are part of a fluid-mosaic membrane structure model of the PM and other membranes (Simons and Ikonen, 1997; Singer and Nicolson, 1972), and were first formally demonstrated in 1992 (Brown and Rose) despite initially being posited four years prior (Simons and Meers, 1988). The role of lipid rafts has remained controversial with some claiming that the resistance to solubilisation by detergents is consistently interpreted by experimenters with a positive bias towards finding their protein of interest in a lipid raft (Edidin, 2003; Munro, 2003). Nevertheless, the existence of the lipid rafts seems likely, but their transient or stable nature and biological function has yet to be shown.

1.6.2 Targeting to the Plasma Membrane

Transport of soluble proteins through the Golgi apparatus to the plasma membrane was first tracked by pulse-chase auto-radiography of newly synthesised proteins (Palade, 1975). This was later backed up with studies showing that the addition of a signal peptide to heterologous cargo is sufficient to cause secretion (Denecke et al., 1990). Futhermore secreted cargo was observed in the Golgi apparatus (Mizuno and Singer, 1993) and evenly distributed across the stacks, unlike cargo with an ER retention signal which is progressively depleted *cis* to *trans* (Phillipson et al., 2001).

For membrane spanning proteins the secretion to the PM is more complex. Studies on the yeast integral membrane protein dipeptidyl aminopeptidases suggest that the sorting is signal-mediated, as the deletion of the C-terminus prevents PM localisation (Roberts et al., 1992). Early work in plants suggested that a single TMD and 18 residues in the C-terminus of a tonoplast localised protein were enough to target a chimeric reporter to the cell surface (Höfte and Chrispeels, 1992). Later studies suggested that entry into this route might be mediated by the size of the membrane spanning domain (Brandizzi et al., 2002), and this is supported by the ability of some proteins to efficiently localise to the Golgi apparatus (Hanton et al., 2005; Wee et al., 1998). It should be noted here that it is technically challenging to know whether the export route to the PM is via a secondary organelle or direct, a concept further explored below (Section 1.8.4, pg.64).

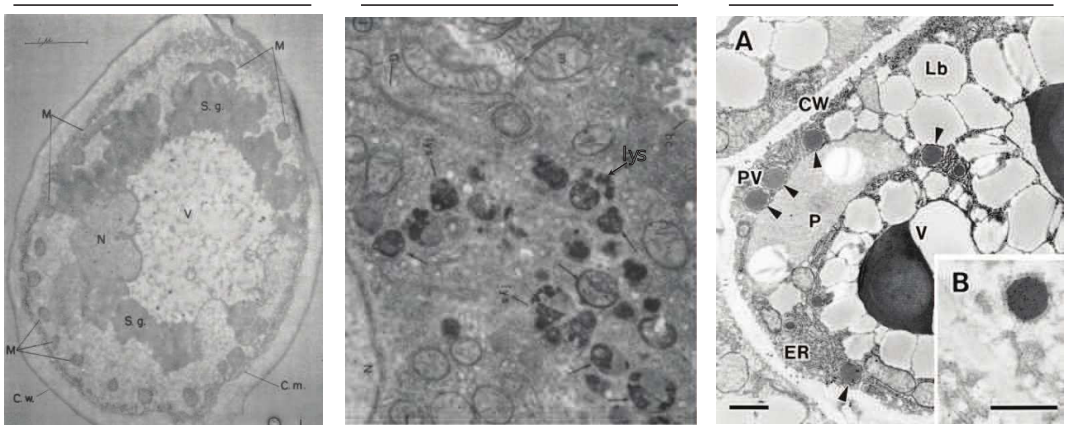

Figure 1.4: **The Different Eukaryotic Lytic Compartments** The three lytic compartments within the three eukaryotic kingdoms as seen in the electron microscope. On the far left is the large *S. cerevisiae* vacuole (V) a representative from the fungal kingdom (Agar and Douglas, 1956). In the centre is a mammalian representative, the lysosome can be seen (lys) as notably smaller than the yeast/plant counterparts (Ashford and Porter, 1962). On the far right the plant storage vacuole (v) can be seen from an *Arabidopsis thaliana* seed tissue section (Hara-Nishimura et al., 1998). The marker in the plant section is 500nm and all the three images are to approximately the same scale.

1.6.3 The Vacuole

Aside from the plasma membrane, proteins that leave the Golgi may reach the vacuole/lysosome either as lumenal, soluble proteins or as membrane proteins of the vacuolar membrane, also termed the tonoplast (See Figure 1.1 for an overview). The primary role of the vacuole is to degrade proteins and lipids to allow for a stable level of component homoeostasis and within the cell and maintain protein turnover. Each of the three eukaryotic kingdoms has a similar compartment, however it is called the lysosome in mammalian systems (see Figure 1.4). Vacuoles fulfil multiple functions dependent on the tissue, for example in plant cells the vacuoles can provide turgor pressure (Marty, 1999), and in mammalian skin tissue are adapted to melanosomes for skin pigmentation (Futter and Ramalho, 2004). There are also plant vacuoles that have very specialised roles such as the protein storage vacuoles which are present in some plant tissues. Protein storage vacuoles have been a controversial topic with suggestions that the vacuoles co-existed in

leaf epidermal cells (Paris et al., 1996). This was later refuted with convincing evidence that the defining markers of the storage/vacuolar organelles, members of the aquaporin family, co-localised in the leaf epidermal tissue (Hunter et al., 2007). Nevertheless, the presence of the storage vacuole in seed tissue is uncontested and can be considered a unique adaptation to the lytic compartment of the vacuole. Post-Golgi transport in eukaryotic cells is a process that relies heavily on active sorting motifs and sorting receptors.

Due to the involvement of multiple organelles, the protein transport pathways to the vacuole are complex and controversial. This is more-so in the plant model system where there are contrasting views on the role of the *trans*-Golgi network, and the proposed presence of multiple vacuoles. As a result there are several pertinent questions on this topic. A selection of these questions are addressed in this thesis and therefore the various models of vacuolar protein sorting are explored in detail below.

1.7 VACUOLAR SORTING SIGNALS AND RECEPTORS

To divert proteins from the default pathway to the cell surface, specific sorting signals are needed to interact with a membrane spanning receptor, analogous to ERD2 described above. This indirectly allows the soluble cargo to interact with the vesicle coat protein apparatus that is in the cytosol. Vacuolar sorting motifs on the soluble cargo are comprised of protein surface structures in yeasts and plants. In plants, there are C, N and internal sorting sequences characterised for a variety of cargo molecules (Matsuoka and Neuhaus, 1999). In yeast there are at least two different consensus cargo sorting signals; one type present in carboxypeptidase Y (CPY) and vacuolar aspartyl protease proteinase A and another present in vacuolar

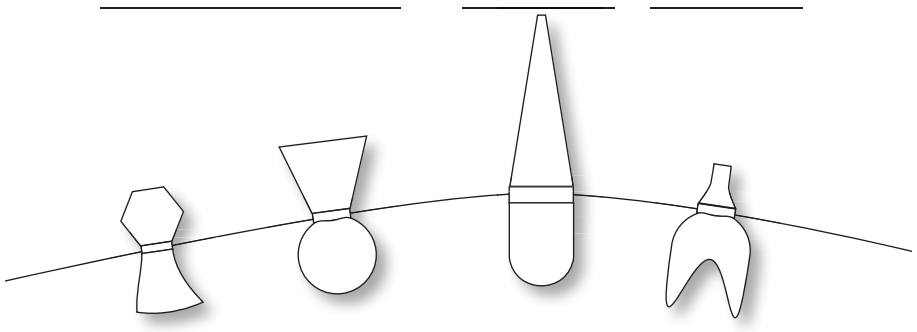

Figure 1.5: **The Cross-Kingdom Lysosomal Sorting Determinants**

aspartyl protease proteinase B (Robinson et al., 1988). Finally, in mammalian cells there are also at least two different types, one protein motif and a unique phosphomannyl post-translational motif (Braulke and Bonifacino, 2009; Kornfeld, 1992).

There are a number of characterised receptor molecules for vacuolar sorting which all share common topology of a type-I-membrane protein (Figure 1.5). It is possible that many vacuolar sorting receptors share a common ancestral form. The focus for this thesis is the model plant Vacuolar Sorting Receptor (VSR), described below (Section 1.7.3), however there are analogous receptors in other systems that have contributed to the understanding of receptor-mediated sorting in general which will be also described in detail.

1.7.1 The Mammalian Sorting Receptors

The first identified and characterised lysosomal sorting receptor was the mammalian mannose-6-phosphate receptor (M6PR) which has been shown to have a direct role in lysosomal sorting as well as endocytosis (Kornfeld, 1992). The M6PR was shown to bind to phosphomannosyl residues which are conjugated to

proteins in the Golgi apparatus (Kaplan et al., 1977), allowing for entry into CCVs (Campbell and Rome, 1983). The original observations identified the M6PR as an endocytic determinant, however, it was quickly realised that an anterograde sorting step would involve the M6PR and clathrin during biosynthesis of the receptor (Pearse and Bretscher, 1981; Rothman and Fine, 1980). This hypothesis was confirmed when it was shown that the M6PR is concentrated in the Golgi apparatus (Brown and Farquhar, 1984). It was also shown that there are two types of M6PR, one, a small 'cation-independent' (CDM6PR or MPR46) and the other much larger 'cation-dependent' receptor (CIM6PR or MPR300) (Hoflack and Kornfeld, 1985).

The mannose-6-phosphate receptors represent a unique lysosomal sorting system as they do not recognise cargo by a protein-protein interaction, but by a phosphomannosyl residue covalently attached to proteins post-translationally. Other mammalian sorting receptors use protein-protein interactions to mediate sorting, for example sortilin (Nielsen et al., 2001). Sortilin is a type I membrane spanning receptor with a short C-terminus that indirectly interacts with the clathrin protein coat. The lumenal domain of sortilin interacts with and traffics sphingolipid activator proteins, a family of molecules essential for glycosphingolipid catabolism in the lysosome (Lefrancois et al., 2003).

1.7.2 The Fungal Vps10p

In yeast, the best characterised sorting receptor is the sortilin homologue Vps10p. Vps10p was originally proposed to be involved with vacuolar protein sorting (*vps*) when a *vps10* mutant was highlighted in a genetic screen for mutant yeast strains that secreted the vacuolar model cargo carboxypeptidase Y (CPY) (Raymond

et al., 1992; Robinson et al., 1988). Chemical cross-linking of Vps10p and its ligand indicated that Vps10p was the sorting receptor for the vacuolar hydrolase CPY (Marcusson et al., 1994). The stoichiometry of this interaction was shown to be approximately 1:1 (Cooper and Stevens, 1996). CPY is proteolytically processed when it arrives at the vacuole, which abolishes the interaction with Vps10p and serves a routine tool to monitor CPY anterograde transport in sorting assays and mutant screens (Cooper and Stevens, 1996).

1.7.3 The Plant Vacuolar Sorting Receptor

The model receptor used in this thesis is the plant vacuolar sorting receptor (VSR). There are 7 VSRs in *A. thaliana*, two of which are highly homologous direct repeats (De Marcos Lousa et al., 2012; Hadlington and Denecke, 2000). Using a biochemical approach the VSR family of proteins was originally identified in 1994 (Kirsch et al., 1994). In this landmark study, the plant vacuolar sorting receptor was shown to interact with peptide motifs of the vacuolar sorted protein aleurain. Subsequently, it was shown that VSRs have a large lumenal domain, which mediates interaction with the cargo, and a short cytosolic C-terminus that mediates interaction with the cytosolic apparatus (De Marcos Lousa et al., 2012). The lumenal domain has been studied with respect to ligand binding, and a variety of cargo molecules have been identified that interact with the receptor for their delivery into the vacuole. Specific binding of a recombinant VSR, lacking its TM domain and cytosolic tail showed that a monomeric lumenal domain alone can interact with the cargo (Cao et al., 2000; Sanderfoot et al., 1998). Surface plasmon resonance using purified lumenal VSR domains expressed in insect cells confirmed this (Watanabe et al., 2002) and was further supported by secreted soluble VSR domains purified from the culture medium of tobacco Bright Yellow 2 (BY2)

suspension cells (Suen et al., 2010). Experimental evidence for the requirement of specific disulfide bonds or N-linked glycans in the lumenal domain remains to be obtained. Interaction with the cargo has been shown to be dependent on both the calcium concentration as well as the pH of the compartment as recently reviewed (De Marcos Lousa et al., 2012).

1.8 VACUOLAR SORTING MACHINERY AND PATHWAYS

The role of the M6PR, VPS10p and VSR is obviously highly analogous. These receptors all seem to bind to cargo in the Golgi/ER and traffic from the Golgi to the vacuolar branch of the secretory pathway. At this juncture, the theories in the fields of the three model systems diverge, particularly with regards to the sorting routes and organelles. This difference could be a semantic nomenclature issue, or could be functional divergence. All the receptors described above have, however, been associated with the clathrin vesicle coat machinery.

1.8.1 Clathrin Mediated Trafficking

The first characterised vesicle coat was the clathrin protein machinery based on early studies that coupled cell fractionation and electron microscopy. (See Figure 1.1). This pathway is mediated cross-kingdom by the clathrin protein coat, generating clathrin-coated vesicles (CCVs) (Kirchhausen, 2000a; Pearse, 1976). These can either bud from the plasma membrane for endocytosis or from the *trans*-Golgi stack/network for biosynthetic anterograde trafficking. Generally, the lysosomal/vacuolar sorting clathrin coat complex consists of a soluble, lumenal cargo molecule bound to a membrane spanning receptor which is in turn bound to a clathrin adaptor protein complex (Kirchhausen et al., 1997). The adaptor

complex is subsequently bound to the clathrin heavy/light chain, allowing for the formation of a scaffold which shapes the membrane (Xing et al., 2010). The clathrin heavy chain has a three pronged 'triskelion' that tessellates into a lattice-like structure (hence the name *clathrin* from 'clathrate' - the ability to form a lattice) (Kirchhausen and Harrison, 1984), each 'arm' of the heavy chain has one associated clathrin light chain protein (Harrison and Kirchhausen, 1983).

The protein machinery that allows for the association of the membrane spanning protein to the clathrin complex is the adaptor (AP) complex. There are four currently characterised AP complexes (Boehm and Bonifacino, 2001; Robinson and Bonifacino, 2001) and one more recent putative AP complex (Hirst et al., 2011). AP1 and AP2 are clathrin dependent, whereas AP3, AP4 and AP5 seem to be clathrin independent. All the complexes however have a similar composition. Each complex contains one μ adaptin, one small σ adaptin, a large β adaptin and one other large subunit, either a γ, α, δ or ϵ large subunit (Boehm and Bonifacino, 2001). This general composition ($\mu/\sigma/\beta$/large) remains regardless of which AP complex (1-4) with various subunits are substituted (e.g. AP1 contains μ1 subunit). There have been broadly defined roles of each AP complex, with AP1 associated with Golgi export, AP2 with PM endocytosis, AP3 with Golgi export and the AP4 associated with perinuclear trafficking (ER/Golgi) (Nakatsu and Ohno, 2003). These definitions are broad and perhaps too simplistic, with conflicting examples of each, and perhaps diverged roles in mammalia/fungi/plants. In addition to the AP complexes other proteins have been associated with the interaction between the membrane spanning protein and the clathrin complex, such as the GGA protein family (Dell'Angelica et al., 2000; Kirchhausen, 2002).

The formation of a CCV begins with the weak association of the adaptor protein complex with the lipid species on the membrane (e.g. PI-4,5-P_2). The clathrin coat

does not have a high affinity for a single adaptor complex, but instead is stabilised to the membrane when bound to two or more adaptor complexes (Cocucci et al., 2012). This clathrin-adaptor complex causes the binding pocket in the adaptor to 'open' allowing for association with the exposed cytosolic tail of the membrane spanning protein (Rapoport et al., 1997). Upon interaction with the cytosolic tail, the CCV is considered committed and the coat begins to aggregate. This model of 'stochastic initiation' is a novel idea that replaces the previously accepted concept of 'heterologous initiation' (i.e. the nucleation of a CCV from a protein-protein interaction (Ehrlich et al., 2004)).

Experiments in *in vitro* systems show that the fundamental mechanism for clathrin membrane deformation is the positive curvature induced by the clathrin lattice itself (Dannhauser and Ungewickell, 2012). There are several other mechanisms that decrease the entropy of the curvature, the non-symmetrical disposition of large polar head/small polar head lipid groups between the leaflets of the lipid-bilayer (Zimmerberg and Kozlov, 2006), the presence of the lipid binding Epsin protein in the clathrin complex (Ford et al., 2002) and finally macromolecular crowding on the membrane surface (Stachowiak et al., 2012). Upon further curvature the membrane is deformed into an 'O' shaped pit, however the final dissociation of the vesicle from the membrane requires more energy than the membrane deformation can provide.

Vesicle detachment requires the small GTPase dynamin (Hummon and Costello, 1992; Robinson, 1994). The use of both GTPγs and dominant negative dynamin mutant traps aborted CCVs at the 'O shaped pit' stage (Bliek et al., 1993; Takei et al., 1995). The dynamin is thought to associate with the lipid species present in the neck of the clathrin pit via the pleckstrin homology (PH) domain (Lee et al.,

1999), although the number of turns of dynamin dimers needed to allow scission is currently unknown.

Once budded the CCV uncoating is mediated by two proteins. The co-chaperone auxillin is the first to associate to the clathrin heavy chain, at the center of each triskelion of a CCV; this in turn allows for association of the Hsc70 ATPase with the J-domain of auxillin (Böcking et al., 2011). The ATP hydrolysis of Hsc70 causes the triskelion to laterally rotate and 'unlock' from the lattice (Böcking et al., 2011). Recent theories have also suggested that biosynthetic CCVs use an ARF GTPase to provide the energy to uncoat vesicles that specifically bud from the Golgi apparatus and *trans*-Golgi network — perhaps to allow differential regulation between the biosynthetic and endocytic pathways (Natsume et al., 2006; Sauer et al., 2013; Tanabe and Torii, 2005). Once uncoated, the naked CCV is fusion competent.

1.8.2 Sorting Signals in Receptor Tails

The previous section illustrates that protein sorting receptors do not just bind to ligands with their lumenal domains but need to contain protein motifs within the cytosolic termini to interact with cytosolic sorting machinery. The C-terminus of the MPR46 was shown to interact with the clathrin adaptor complexes 1, 2 and 3 (AP1/2/3) (Höning and Sosa, 1997; Storch and Braulke, 2001) through a dileucine motif present in the C-terminus of the receptor (Hofmann et al., 1999). In addition the MPR46 has also been shown to interact with the GGA protein family (Doray et al., 2002). This family of proteins interacts with the γ subunits of the adaptor complexes. The cytosolic tail of the other characterised mammalian protein sorting determinant, sortilin, interacts with the clathrin adaptors GGA2

(Nielsen et al., 2001) and the μ subunit of AP1 complex (Canuel et al., 2008) to allow for inclusion into CCVs. The AP1 interaction is dependent on a YXXϕ motif present in the receptor tail (ϕ is any hydrophobic residue).

The trafficking of Vps10p is also dependent on a conserved YXXϕ motif (Cereghino et al., 1995; Cooper and Stevens, 1996). Immunoprecipitation of clathrin-coated vesicle extracts showed that Vps10p is found in clathrin-coated vesicles (Deloche et al., 2001). Cell lines expressing VPS10 with the C-termini removed resulted in lower Vps10p stability and vacuolar cargo missorting (Cereghino et al., 1995). Taken as a whole, there are two routes towards the yeast vacuole, both in CCVs. One of these routes seems to be signal mediated and allows for cargo sorting and the other is independent of the cytosolic tail and does not allow for cargo sorting.

1.8.3 Sorting Signals of Plant VSRs

As with the VPS10p, the C-terminus of the VSR has been shown to be essential for trafficking with a deletion mutant missing the cytosolic tail (DaSilva et al., 2005). In order for the receptor to traffic in a specific manner, there are multiple domains within the C-terminus of the receptor that allow for the collection and release of the cargo in the correct organelles. The two motifs that have been most characterised are the YXXϕ and the ExxxIM motifs. A conserved tyrosine residue (Y612) in the YXXϕ motif was shown to mediate interaction with the μ subunits of the clathrin adaptor complex of both AP1 and AP2 (Happel et al., 2004; Sanderfoot et al., 1998), (in detail below 1.8.1). There is also evidence that the ExxxIM motif acts as an additional anterograde sorting mechanism. Expression of a dominant-negative dynamin mutant known to interfere with clathrin-coated vesicle budding lead to accumulation of a fluorescent vacuolar cargo (sporamin-GFP) in the Golgi stacks

as indicated by a strong colocalisation with the Golgi marker ST-RFP (Jin et al., 2001). In the same study, the authors also localised the wild-type dynamin to the Golgi, which corresponds to the Golgi localisation of the plant AP2 type μ adaptin (Happel et al., 2004). Evidence for biochemical interactions between Epsin1, clathrin, AP-1 and VSR1, as well as a vacuolar sorting defect in an Epsin1 T-DNA insertion line, strongly suggests that vacuolar sorting in plants is initiated by Golgi-mediated clathrin-coated vesicle budding (Song et al., 2006). In addition, recently, the VSR was shown to be enriched in purified CCVs (Sauer et al., 2013) - confirming earlier studies (Hinz et al., 1999; Kirsch et al., 1994).

Despite this abundance of evidence it has been proposed that clathrin is not essential for the anterograde sorting pathways of the VSR, with some suggestions going as far to suggest a route bypassing the Golgi from the ER (Niemes et al., 2010a,b). By expressing a fluorescent GFP-VSR chimera in a background of overexpressed full length VSR, redistribution of GFP-VSR from the late secretory pathway to the ER is observed, which is in contrast to other membrane proteins that seem to maintain normal localisation. The authors theorise that the VSR is competing at the level of the ER for entry into an uncharacterised vesicle to reach the TGN directly. Whilst there is no substantial evidence ruling out receptor binding to nascent cargo in the ER, and despite the lack of direct evidence, a totally novel ER export route that gives priority to the VSR is a tempting hypothesis.

1.8.4 The Plant Trans-Golgi Network/Partially Coated Reticulum

Although mammalian and yeast studies generally agree that CCVs involved with anterograde trafficking to the lysosome/vacuole bud from the Golgi apparatus and

bind to the multi-vesicular body (MVB), this issue is a central point of controversy in the plant field (De Marcos Lousa et al., 2012). Originally observed as the partially-coated reticulum, and named due to the appearance of a protein coat around the organelle (Pesacreta and Lucas, 1984; Tanchak et al., 1988) it was later renamed the TGN (Dettmer et al., 2006; Staehelin and Moore, 1995). The TGN appears in electron micrographs as extended tubules which connect budding vesicles which are coated with a clathrin like coat (see figure 1.6). Occasionally attached to the Golgi apparatus, the trans-Golgi network (TGN) is still observed as an independent organelle that can be several μm from the nearest Golgi stack (Foresti and Denecke, 2008). This organelle has been proposed to be analogous to mammalian early endosome (Lam et al., 2007), alternatively it could be the equivalent of the recycling endosome (De Marcos Lousa et al., 2012).

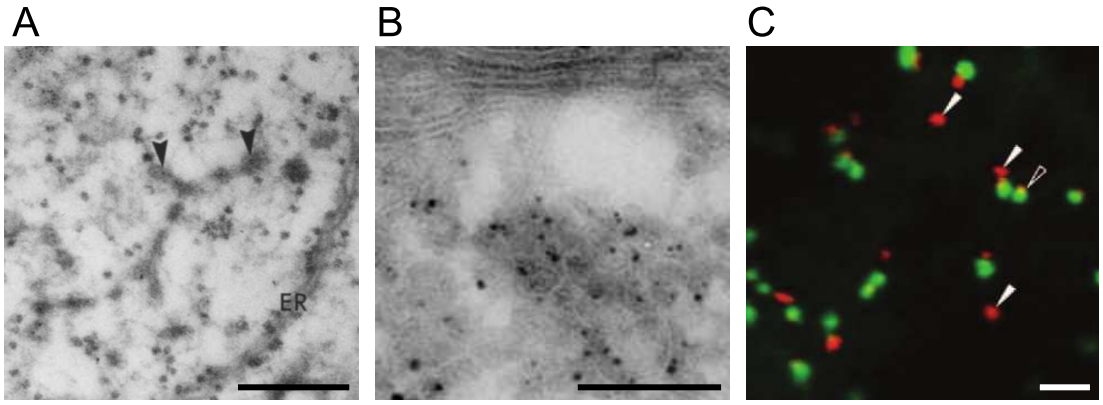

Figure 1.6: **Possible Models for the Role of the Plant Trans-Golgi Network**
A. Images of the originally characterised Partially-Coated Reticulum or Trans-Golgi Network. The arrows point to the putative clathrin coat around the edges of the organelle (Tanchak et al., 1988). Marker = 300nm.
B. Immunogold labelling of electron micrographs using antibodies against a biosynthetic TGN marker showing the suggested proximity to the Golgi apparatus (Dettmer et al., 2006). Marker = 250nm.
C. Live-cell fluorescent microscopy in tobacco cells showing the lack of co-localisation of the Golgi and TGN markers, thus establishing the TGN as an independent organelle (Foresti and Denecke, 2008) Marker = approx 5μm.

It should be noted here that the term TGN is easily confused with the trans-Golgi cisternae. Indeed, numerous articles have referred to the term TGN when

using markers of the trans-Golgi stack, such as the well established fluorescent sialyl-transferase fusions (i.e., ST-XFP), and in the mammalian and yeast fields the *trans*-Golgi stack is commonly referred to as the *trans*-Golgi network. The origin of the new nomenclature has emerged from the use of the SNAREs SYP61 and SYP41 as markers in plants, the yeast equivalents of which (TLG1 and 2) are termed late Golgi markers, but there is no colocalisation of the trans-Golgi cisternae marker ST-CFP with YFP-SYP61, suggesting that the organelles are spatially independent (Foresti and Denecke, 2008). This perhaps represents a true difference between the kingdoms, as, the RabGTPase termed Rab11 also localizes to the plant SYP61/41 compartment (Chow et al., 2008); in mammals, however, Rab11 is a marker for the recycling endosome, which is clearly distinct from the mammalian TGN (Grant and Donaldson, 2011; Ijzendoorn, 2006; Maxfield and McGraw, 2004). The post Golgi structure of plants labeled by SYP61/41 is currently referred to as the TGN, but should be considered independently from the mammalian and yeast literature. It is currently unknown if VSRs traffic via the TGN or directly from the *trans*-Golgi cisternae.

1.8.5 Multi-Vesicular Body/Pre-vacuolar Compartment

Another post-Golgi organelle, called the prevacuolar compartment (PVC) or multi-vesicular body (MVB) was discovered in electron microscopy of mammalian cells (Palade, 1955). Later studies in yeast observed a similar organelle (Hornick et al., 1985), which was also reported in plants (Tse et al., 2004) and referred to as the pre-vacuolar compartment (PVC) (Sanderfoot et al., 1998) (See Figure 1.1). Morphologically, the PVC (MVB) is a spherical organelle that contains multiple vesicles called 'intralumenal vesicles' (ILVs) suspended within.

The PVC fulfills several biological functions, and can be considered an important sorting station of the vacuolar route in the late secretory pathway. There are two classes of proteins that converge in this organelle. The first class are targeted to the vacuole for degradation, and are often ubiquitinated. The second class are proteins containing vacuolar sorting signals that are targeted via receptors from the early secretory pathway; this class of protein is not to be degraded, but has a function in the vacuole (e.g. the lytic hydrolases).

The PVC receives vesicles containing receptor-ligand complexes from the early secretory pathway (ER-Golgi). In addition, endocytosed vesicles from the plasma membrane may fuse to the PVC, containing membrane spanning receptors that have been targeted for degradation. The 'endosomal sorting complexes required for transport' (ESCRT) complex causes membranes and proteins to be internalised into the organelle for degradation. The results of this process are the characteristic 'intralumenal vesicles' (ILVs) of the organelle. ILVs are delivered into the vacuole/lysosome thus allowing for turnover of cytosol (within the ILVs) and membrane spanning proteins, which would otherwise not be exposed to the lytic compartment.

The ESCRT pathway is initiated by the ESCRT-0 complex, a dimer that binds to the membrane (Henne et al., 2011), of which there is no homologue in plants. Membrane spanning proteins are marked for inclusion into the complex, and thus degradation by the addition of ubiquituin, an 80aa protein, to lysine residues. Unlike soluble protein degradation (above, section 1.3.4, pg. 38), this is not a poly-ubiquitination event but a mono-ubiquitination. These proteins are sequestered by the ESCRT-I complex which interacts with both the ESCRT-0 and the ubiquitinated protein. This complex also induces the membrane invagination which is mediated by the further recruitment of the ESCRT-II complex, which

also strengthens the association with the endosomal membrane. At the later stages of the invagination the membrane proteins can be considered as isolated from the MVB membrane and are deubiquitinated. The final stage of the process is completed by the ESCRT-III complex, which mediates scission and the release of the ILV into the soluble lumen of the MVB. These processes have been reconstituted *in vitro*, although the mechanism by which the membrane invagination and scission happens is unknown, and topologically distinct from classical vesicular formation pathways.

1.9 RECEPTOR RECYCLING

In order for receptors, such as the VSR, to avoid degradation within the PVC the best supported models suggest that receptor and cargo complexes dissociate within the lumen of the PVC due to a combination of calcium and pH dependence (De Marcos Lousa et al., 2012). Reports have shown that VSR-cargo binding is optimal at pH 6 to 7, while release occurs in more acidic pH environments (Cao et al., 2000; Kirsch et al., 1994). VSR-ligand interactions were also shown to be promoted by high (millimolar) Ca levels (Suen et al., 2010; Watanabe et al., 2002; Watanabe et al., 2004); and indeed, 1 mM $CaCl_2$ was included in the original purification binding of the VSR to column-bound aleurain (Kirsch et al., 1994). This dissociation event allows the receptor to recycle back to the early secretory pathway, for a new round of cargo binding- this process is mediated by the retromer protein complex.

1.9.1 The Retromer Complex

The recycling of sorting receptors as exemplified by the ERD2 system described above is a key feature to explain the high efficiency of sorting reactions. The recycling mechanism is thought to be mediated by the retromer sorting complex (Seaman et al., 2012). The retromer complex is conserved in all eukaryotes. This pentameric complex consists of Vps35, Vps29 and Vps26 in one large subunit bound to the sorting nexins, Vps17 and Vps5 (also known as sorting nexin 1 and 2)(Seaman et al., 1997, 1998). The Vps35 subunit binds to the exposed cytosolic tail (Nothwehr et al., 2000) of the membrane spanning protein, as well as the Vps29 and Vps26 subunits (Horazdovsky et al., 1997). The sorting nexins bind to the 35/26/29 trimer, as well as lipid species in the membrane acting as membrane curvature sensors causing further deformation and abstraction of the lipid bilayer (Collins, 2008; Seaman et al., 2012). It is important that this interaction only takes place in the organelle where the VSRs release their cargo. This suggests that the receptor tail might be masked up to this point, perhaps by members of the clathrin complex.

Using a combination of immunoprecipitation and mutant yeast strains the retromer complex was originally shown to mediate the recycling of VPS10p (Seaman et al., 1998). Additionally, both the cation-dependent and the independent M6PR have been implicated in retromer mediated recycling (Seaman, 2005); as has the mammalian Vps10p homologue, sortilin, which was shown to be mislocalised in retromer component knock-downs (Canuel et al., 2008). In plants there are homologues of all 5 major components (Jaillais et al., 2006, 2007; Niemes et al., 2010a; Oliviusson et al., 2006; Yamazaki et al., 2008).

1.9.2 Retromer in Plants

There are three Vps35 paralogues in *A. thaliana* Vps35a, b and c (also known as B, A and C respectively), which are physiologically redundant (Yamazaki et al., 2008). Other than the characterisation of a sorting nexin studied in regards to the sorting of a tyrosine kinase (Vanoosthuyse et al., 2003), the first retromer component studied in plants was the VPS35/29/26 complex (Oliviusson et al., 2006). The authors could show that the complex is a stable trimer, and the highly conserved VPS35 subunit coimmunoprecipitated with VSRs and labeled the PVC together with antibodies to the syntaxin Pep12. This interaction is thought to be dependent on a hydrophobic residue present in the YXXϕ motif, as mutation of the ϕ (leucine) into an alanine resulted in the VSR being unable to recycle back to the early secretory pathway (Foresti et al., 2010). The membranes of multivesicular bodies were consistently labeled with antibodies to all three subunits of the VPS35/29/26 complex, providing a strong case for their action at the PVC membrane. However, other studies have localised sorting nexins and proposed that the point of plant retromer sorting is the TGN (Niemes et al., 2010a).

Evidence for the role of retromer in VSR recycling arose from an elegant genetic screen for vacuolar mis-sorting in Arabidopsis seeds and provided convincing genetic evidence for a role of VPS29 in vacuolar sorting in Arabidopsis seeds and possible interactions between VPS29 and VPS35 (Fuji et al., 2007; Shimada et al., 2006). The role of retromer in vacuolar sorting was later corroborated by a reverse genetic approach using combinations of knockouts in the three Arabidopsis VPS35 genes (Yamazaki et al., 2008). Although, yeast retromer mutants show increased vacuolar degradation of VPS10p, retromer mutants in plants did not show such a clear-cut effect on VSR stability, as individual lines

showing either increased or reduced degradation were found (Yamazaki et al., 2008). Moreover, interference with the sorting machinery itself does not only have the potential to prevent VSRs from recycling but also other essential components required for anterograde transport. Precedence for this principle is the well-known inhibition of COPI-mediated recycling by Brefeldin A, which does not increase secretion of HDEL proteins, but instead causes retention of secretory proteins in the ER, accompanied by fusion of ER and Golgi membranes (Boevink et al., 1998; Nebenführ, 2002).

While the role of the trimeric retromer core complex in vacuolar sorting is supported by convincing evidence from multiple research groups, the exact role of the sorting nexin dimer is less established. Evidence for a possible role of the accessory sorting nexin 1/2 dimer in plant membrane trafficking arose from the identification of a putative SNX1 homolog (Vanoosthuyse et al., 2003) and subsequent gene knockout in Arabidopsis leading to pleiotropic developmental defects and aberrant sorting of the auxin influx carrier PIN2, but not PIN1 (Jaillais et al., 2006). Moreover, Arabidopsis SNX1 was colocalised with fluorescent fusions of the canonical form of plant Rab5 (ARA7, RabF2b) and VPS29 (Jaillais et al., 2007). The Arabidopsis genome contains two other closely related sorting nexins SNX2a and SNX2b (Vanoosthuyse et al., 2003), the second of which was shown to bind directly to phosphatidylinositol 3-phosphate and caused vacuolar trafficking defects when overexpressed (Phan et al., 2008). Although SNX2 was shown to localise to the PCR/TGN (Niemes et al., 2010b), other reports localise the three sorting nexins to punctate structures that colocalise with markers of the PVC (Jaillais et al., 2006, 2007; Phan et al., 2008; Pourcher et al., 2010). The observation that sorting nexins appear to be dispensable for VSR-mediated sorting (Pourcher et al., 2010) illustrates that the discrepancy between the localization of the VPS35/29/26

retromer core complex and that of the sorting nexins may not be a contradiction per se. A snx1-2 snx2a-2 snx2b-1 triple mutant showed normal localization and function of VPS29. Although the VPS29 mutant shows defects in the sorting and processing of both 12S globulin and 2S albumin, the sorting nexin triple mutant only showed defects in the processing of 12S globulin, whereas sorting of the VSR ligand 2S albumin was unaffected (Pourcher et al., 2010). This would explain why a dominant-negative SNX2a mutant lacking the coiled-coil domain for membrane deformation had no effect on the sorting of the VSR model ligand amy-spo (Niemes et al., 2010b). In general, negative data should be interpreted with care.

The retromer complex is not thought to yield a vesicle, but a tubule (Seaman et al., 2012). Recent evidence suggests that the scission of this tubule is mediated by the ATPase 'spastin' (Allison et al., 2013), however there is no obvious spastin homologue in the *A. thaliana* genome. The membrane still needs to fuse with the target organelle and thus there are some SNAREs associated with this event. There have been none identified in the plant and yeast literature, however there are a number of candidate SNAREs from the mammalian field. Based on studies of the trafficking of shiga toxin the Q SNAREs Vti1a, syntaxin 16 and syntaxin 6 as well as the R-SNARE VAMP3 and/or VAMP4 have been highlighted as potential retromer SNAREs, which have homologues both in yeast and plants, although the plant homologues show relativity low similarity (∼50-60%) (Attar and Cullen, 2010). In addition, this event is proposed to be mediated by the Golgi-associated retrograde protein (GARP) complex. The GARP complex was originally characterised in *S. cerevisiae* as a tetramer consiting of Vps51, Vps52, Vps53 and Vps54 (Conibear and Stevens, 2000; Conibear et al., 2003; Siniossoglou and Pelham, 2001, 2002). In mammalian systems, the complex has been reported

to associate with both the trans-Golgi face as well as endosomes (Ho et al., 2006; Liewen et al., 2005; Perez-Victoria et al., 2008; Perez-Victoria et al., 2010) and RNAi depletion resulted in vacuolar/lysosomal mis-sorting (Perez-Victoria et al., 2008; Perez-Victoria et al., 2010). In plants, the complex is known to be required for pollen tube growth, localises to endosomal compartments and is embryo-lethal when knocked-out (Guermonprez et al., 2008; Twell and Pelletier, 2004), although no direct protein sorting studies have been reported on to-date.

1.10 THE DELIVERY OF CARGO TO THE VACUOLE/LYSOSOME

After receptor recycling and the biogenesis of the PVC by ESCRT mediated protein turnover, the final step in the vacuolar sorting pathway is the delivery of the cargo to the vacuole/lysosome. In plants this is facilitated by the maturation of the MVB/PVC into the late-prevacuolar compartment (LPVC). The maturation of the endosomal compartment and the final fusion event to the lysosome are intrinsically linked, requiring the role of the four protein complexes in the process: the Retromer complex, the ESCRT complex, the CORVET complex and the HOPS complex. Although in the literature these processes are often depicted as happening independently they are all sequentially and perhaps causally related to each other, allowing a nascently biosynthesised MVB to fuse to the lysosome.

1.10.1 Late-Prevacuolar Compartment

The Late-Prevacuolar Compartment (LPVC) is the most recently discovered organelle within the secretory system (Contento and Bassham, 2012; De Marcos Lousa et al., 2012) (See Figure 1.1). It was originally identified in 2010 using a recycling defective member of the VSR protein family (Foresti et al., 2010).

It was thus identified as one of the 'last' organelles of the secretory pathway before the vacuole. As a recently discovered organelle, the properties are still relatively unknown; it is however, rich with vacuolar cargo and is fusion competent with the vacuole (Bottanelli et al., 2012; Craddock et al., 2008; Foresti et al., 2010), with the fusion observed in electron micrographs (Scheuring et al., 2011). Morphologically, it is similar to the PVC shown by immunogold labelling electron microscopy using antibodies against residents of the LPVC (Haas et al., 2007b). The other likely properties are that it is more acidic than the early secretory pathway, possibly approaching the acidity of the vacuole. This notion is supported by the localisation of the AAA-ATPase Vps4 to the PVC/LPVC (Haas et al., 2007b; Shahriari et al., 2010) which is suggested to acidify the compartment as it matures. This could be potentially due to the presence of a yet unidentified proton transporter. It is also likely to have different membrane properties than the organelles of the early secretory pathway that allow it to become fusion competent with the vacuole, as has been described in the mammalian systems (Huotari and Helenius, 2011).

1.10.2 The Final Maturation of the Endsosome and the Fusion to the Vacuole/Lysosome

The PVC→LPVC maturation event can be considered in some ways a vacuolation of the PVC (See Fig 1.7). In yeast and mammals the process of endosomal fusion is fairly well characterised (Epp et al., 2011). There seems to be a multi-step protein cascade based around the RabGTPases Rab5 and Rab7 as controllers of the process (Rink et al., 2005; Rojas et al., 2008). Both Rab7 and Rab5 have been implicated in binding the HOPS (homotypic vacuolar fusion and protein sorting)/CORVET (class C core vacuole/endosome tethering) protein complexes

(Ostrowicz et al., 2010; Peplowska et al., 2007). HOPS and CORVET are two related multi-protein, endosome associated units (Solinger and Spang, 2013). Both HOPS and CORVET share the Vps11/16/18/33 tetramer, which interacts with Vps39 and Vps41 in the HOPS complex and Vps8 and Vps3 in the CORVET complex (Epp et al., 2011).

Current theories suggest that the CORVET complex is involved at an earlier stage of endosome maturation/fusion as mutants show abnormal endosome morphology lacking ILVs (Peplowska et al., 2007). The CORVET complex has also been shown to interact with the Rab5GTPase, as part of the maturation process. Whereas the Rab5/CORVET complex is thought of as essential for endosome maturation, the Rab7/HOPS complex has been implicated in the fusion process (Stroupe et al., 2009).

Some reports suggest that the loss of Rab5 from the endosome is coupled by the accumulation of Rab7. This CORVET to HOPS cascade seems to be mediated by Rab7 GEF Mon1-Ccz1, that is recruited by the CORVET complex and in turn recruits Rab7. During this transition there also seems to be simultaneous recruitment of the retromer complex by the Rab7 (Balderhaar et al., 2010). The Mon1-Ccz1 negotiated binding and nucleotide exchange of Rab7 causes Vps8 and Vps3 to dissociate from the CORVET complex allowing its transition into the HOPS complex by recruitment of Vps39 and Vps41.

Work with homotypic fusion in yeast has comprehensively described the events that allow membrane fusion to the vacuole (Wickner, 2010). Interestingly, homotypic fusion seems to be the same as endosomal fusion from a molecular perspective, further supporting the idea that endosome maturation is analogous to vacuolation. In a process that has been completely reconstituted *in vitro*, the fusion event itself

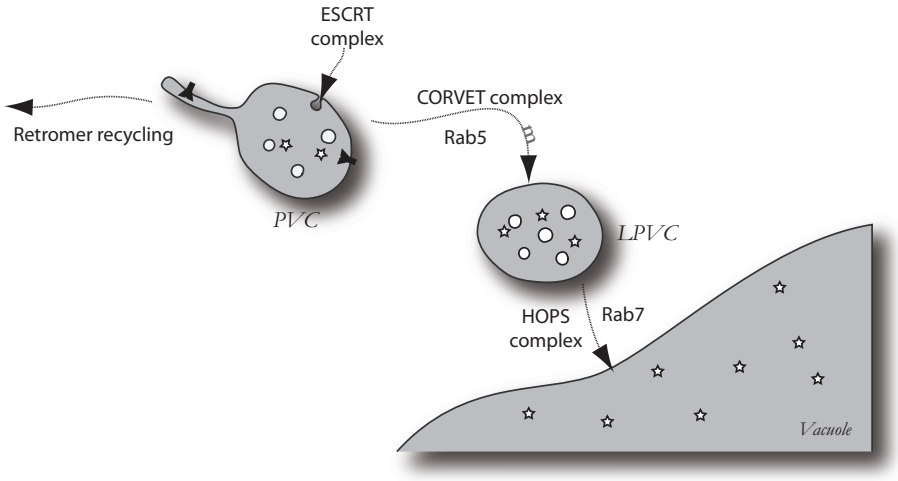

Figure 1.7: **Maturation of the Endosomes**

is very similar to a SNARE arbitrated fusion event, which is supplemented by the action of Rab7 and the HOPS complex. There are two SNARE complexes implicated in the process; the first complex consists of the three Q-SNAREs Vam3, Vam7 and Vti1 which can interact with the second complex containing the R-SNARE Nyv1 or the R-SNARE Ykt6 (Mima et al., 2008; Thorngren et al., 2004). The tethering of the vacuolar SNARE complex to the endosome seems to be through interaction with the HOPS complex, assisted by Rab7. Through an unknown mechanism, perhaps the hydrolysis of the Rab7 followed by the canonical SNARE activity, the endosome is brought into close contact with the vacuole coupled with membrane fusion.

A similar process has been partially documented in plants. Rab7 has been shown to partition to the vacuole, and Rab5 to the LPVC (i.e. late endosome) (Bottanelli et al., 2012; Foresti et al., 2010). Furthermore, dominant negative (asparagine to isoleucine, NI) mutants of both Rab5 and Rab7 prevented the fusion of the LPVC to the vacuole (Bottanelli et al., 2012). Finally, it was observed that the Rab5NI seemed to stop the maturation of the LPVC, as both PVC markers and LPVC markers colocalised. This is in contrast to the Rab7NI that seemed to preserve

the PVC/LPVC differentiation, but prevent fusion of the LPVC to the vacuole, demonstrated by an increase in LPVC organelle numbers (Bottanelli et al., 2012). In addition, homologues of three of the four members of the HOPS complex have been shown to form an interaction complex (Rojo et al., 2003) and *A. thaliana* with a mutant of the plant Vps16 homologue cannot form vacuoles (Rojo et al., 2001). There has been no homologue, however, of the HOPS/CORVET core subunit VPS18 identified in plants (the most similar from a BLAST search of the protein sequence shares only 18% identity), and only weak homology of putative Vps41 and 39 homologues was found.

The fusion of the late endosome/LPVC to the vacuole is the final event in the delivery of cargo to the vacuole. The soluble proteins involved in the process are released into the cytosol in an ATP dependent manner, and are reused for the next binding event. Upon fusion the ILVs are released into the vacuole for degradation.

1.11 OPEN QUESTIONS AND AIMS

Although great leaps in understanding specific steps in vesicle trafficking have been made by a combination of genetic, biochemical and imaging approaches, many questions related to understanding the complex pathways remain. From the point of view of this thesis project, the first of these questions is; at which point do vacuolar and secreted soluble cargo segregate? They are both synthesised at and translocated across the ER membrane, however, they could either segregate at the ER, the Golgi apparatus or the *trans*-Golgi network. The second question is regarding the active lipid dynamics; in short, from where do organelles generate and how is the membrane of the organelles recycled? All models predict a final

fusion event as the last step in vacuolar sorting (see section 1.10.2), however this would result in a gradual loss of organelle membrane and a constant expansion of the vacuole. It follows that there must be an either uncharacterised recycling mechanism of membrane from the vacuole allowing for organelle biogenesis, or a turnover of the lipid bilayer within the vacuole. A third question related to both of the former two questions addresses the recycling pathway of protein-sorting receptors. There is not a single transport route in which the complete circle of events has been fully described with direct evidence. In the case of VSRs it is not known if the receptor passes through the TGN or to where it recycles.

As described above, the VSR protein family plays a primary role in protein sorting in plants. Some of the individual steps of this process are fairly well characterised and unanimously accepted. For example, it is accepted that the receptor traffics in clathrin-coated vesicles (CCVs) at least once per trafficking cycle- a step dependent on the conserved Yxxϕ motif within the receptor terminus. It is also accepted that the receptor recycles from the late to early secretory pathway. Finally, it is clear that the receptor differentially interacts with ligands allowing for association/dissociation in the appropriate compartments. As such, the VSR is one of the most understood receptors from the perspective of cell biology across all kingdoms. The VSR, therefore, represents one of the choice model proteins for addressing questions regarding protein sorting. The general aim of this PhD is to refine the model of VSR targeting and recycling in a direct manner by critically assessing both the poorly understood and controversial elements of the trafficking pathways of the receptor, in turn these findings can contribute to the general questions on protein targeting postulated above.

In order to complete the transport cycle of the receptor a series of specific open questions need to be addressed. They can be split into three broad questions: 1)

What are the initial trafficking steps of the VSR? 2) How does the VSR traffic in an anterograde manner, and does it pass via the plasma membrane? and 3) to where does the VSR recycle? The first of these questions pertains to the ER export route of the VSR. The VSR co-translationally inserts into the ER, but the initial trafficking step is in dispute. The assumed model had always been that there was a trafficking route in COPII vesicles (See Figure 1.1), however a recent publication suggested a novel route, in an uncharacterised vesicle that potentially bypasses the Golgi apparatus (Niemes et al., 2010b)- this is an exciting possibility that lacks direct supporting evidence, and thus needs to be assessed. The second question regarding the anterograde trafficking of the VSR is also controversial, as stated above, the VSR is known to traffic in CCVs, however if this is between the Golgi and PVC, or the PM and TGN/PVC - is unknown. The final question is related to the first, as a pair the question could be reworded to: where do VSRs interact with their ligands?

To address these questions the initial aim of this thesis was to establish a controlled biochemical methodology to test the effect of an untagged effector protein on protein sorting quantitatively and to permit assays to compare different effectors with each other. The second goal of this thesis was to use the natural variation present in the different and less characterised isoforms of the *A. thaliana* VSR protein family to try and understand the anterograde/retrograde recycling pathways, contributing to a biological understanding of the role of VSRs and their role in maintaining physiological homeostasis of the cell. The final goals are to utilise the unique tools developed to directly address two fundamental questions of VSR trafficking, regarding the ER export of the receptor and whether the VSR traffics via the plasma membrane. The mechanisms that govern both of these questions allude to the broader questions in cell biology namely the segregation of

soluble and secreted cargo and the nature of receptor recycling. By combining direct experimental data with the published evidence, it should be ultimately possible to generate a near-complete model of receptor trafficking.

2 THE GENERATION OF A β-GLUCURONIDASE BASED QUANTITATIVE PROTOPLAST EXPRESSION REPORTER SYSTEM

2.1 INTRODUCTION

The generation of individual plant cells from established plant tissue originated with the explicit goal to observe the growth of a single cell into a mature plant (Bergmann, 1960; Gill et al., 1978). The first stage of this process requires the release of plant cells from the tissue. In order to achieve this, the plant cell walls were digested using a combination of purified fungal enzymes. The resulting spheroplast-like culture cells are referred to as protoplasts, and have been widely used in plant biology for studies on electro-physiology (Elzenga et al., 1991), protein trafficking (Denecke et al., 2012), protein localisation (Sheen et al., 1995), hormone characterisation (Delbarre et al., 1994) and protein-protein interactions (Walter et al., 2004).

Although the use of protoplasts started with the focus on whole-plant regeneration, the technique was quickly adapted with the maturation of molecular biology to allow for genetic transformation of the protoplasts. There were various methods developed for this purpose including *A. tumefaciens* mediated transformation (Krens et al., 1982; Paszkowski et al., 1984), naked DNA and polyethylene glycol (PEG) incubation (Negrutiu et al., 1987) and direct incubation of the protoplasts with the naked DNA alone (Hain et al., 1985). Simultaneously the technique of transformation by electroporation in plants was adapted from lymphocyte transformation methods in mammalian systems (Potter et al., 1984), to protoplast cells in plant systems (Fromm et al., 1985). The use of electroporation to transform

the protoplasts avoided the variance endemic in the viral/bacterial vector based and the PEG based methodologies which depend on manual mixing and diluting. The tobacco protoplast system was rapidly adapted to provide reliable and quantitative transient assays to study protein secretion to the culture medium, permitting the study of cell biology and secretory systems (Bednarek et al., 1990; Denecke et al., 1990, 2012; Holwerda et al., 1992).

The strength of transport assays by transient expression in protoplasts is two-fold. Firstly, the use of a homogeneous population of ∼2 million cells and the individual recovery and separation of both the cells and the culture medium for up to 48 hours after electroporation allows for high amounts of reproducibility. Secondly, the extraction of 100% of the cellular proteins allows samples to be treated volumetrically allowing for robust sample manipulations with minimal experimental error. Thus the secretion of a particular protein can be assayed in both the cell and medium fractions and the resulting medium:cells ratio (a.k.a. secretion index) can be compared across samples, quantifying protein secretion. As a consequence, tobacco protoplasts have been used extensively in protein trafficking studies in the last twenty years and there have been a number of key findings in plant cell biology that have used this system. Advances made include the discovery that the default soluble protein pathway is secretion (Denecke et al., 1990) and that it is dependent on COPII mediated trafficking (Phillipson et al., 2001), that various sorting signals confer protein retention and organelle localisation (Bednarek et al., 1990; Denecke et al., 1992; Matsuoka and Nakamura, 1991; Neuhaus et al., 1991) and that expression of a GFP tagged plant Vacuolar Sorting Receptor (VSR) titrates the system inducing secretion of its cargo (DaSilva et al., 2005).

Often, protoplast studies observe the action of one protein (the 'effector') on another (the 'cargo') (DaSilva et al., 2006; Foresti et al., 2006; Scheuring et al., 2011; Shahriari et al., 2010). When these interactions are compared, the cargo is usually monitored. Despite the clear strengths of this method, there are limitations. Although the variability between different transient expression experiments is low, the variability between the quality of individual DNA preparations and obtained transient expression is high. Indeed, different large-scale DNA preparations of the same plasmid prepared on different days might have up to 20-25% expression variability, despite the same amount of DNA being electroporated (Prof. Denecke, personal communication). The reasons for this variability could be a multitude of factors including the presence of trace amounts of contaminants such as salt and RNA in the preparation. This complication is compounded due to the effector usually being an untagged protein in order to avoid any steric or protein mis-folding artifacts. Therefore, unless there is an antibody specific to the protein of interest, there is no practical way to assay the expression of the effectors. The routine use of antibodies against effectors is impractical as one experiment may require a multitude of different effectors, for example one experiment might use a receptor and an array of deletion/point mutants of the receptor (see DaSilva et al. 2006)—each reporter variant would need a unique antibody to be generated.

In order to monitor and control for the expression of untagged effector genes, a double vector system has been previously established in which the untagged effector is paired on a plasmid with a second effector encoding a standard marker, originally using β-Glucuronidase (GUS) as the normalising factor (Denecke et al., 1992) and rejuvenated recently using 'ST-RFP' as the internal marker (Bottanelli et al., 2011).

Using the system developed by Bottanelli et. al. (2011) the expression of the gene-of-interest can then be monitored by SDS-PAGE followed by immunblot assay using antibodies against RFP and thus effector expression between samples can be qualitatively compared. Although this system is a vast improvement on previous blind systems, it suffers from several limitations. The system is limited by the relatively poor sensitivity and labour-intensity of immunoblot assays, especially if there is a large range of expression within the same experiment. In addition, the system suffers as it is purely qualitative, using immunoblot intensities to compare samples visually. The final limitation is the lack of comparability between different experiments due to variations in gel to membrane transfer, gel run times, antibody binding and incubation times in both the antibody binding stages and the visualisation techniques.

In order to generate a more quantitative normalisation system, I have utilised β-Glucuronidase (GUS) as an internal marker as opposed to ST-RFP, similar to the system generated originally in 1992 (Denecke et al.). This system allows for direct expression comparisons, quantitative normalisation between experiments and highly sensitive expression read-outs. The vector generated to be used for the novel GUS system has been specifically engineered to include a polylinker for the subcloning of a range of effectors, and any superfluous and unique restriction sites have been removed from the rest of the plasmid. I have used this normalisation system to compare the proteolytic pattern of the Vacuolar Sorting Receptor protein family in *A. thaliana*.

2.2 RESULTS

2.2.1 Immunoblot Comparison of the Plant Vacuolar Sorting Receptors

Plant vacuolar sorting is initiated and controlled by the Vacuolar Sorting Receptor VSR protein family in *A. thaliana* (De Marcos Lousa et al., 2012). There are 7 VSRs in *A. thaliana*, two of which are direct repeats that share high identity and can be considered analogous. There are three protein domains, the lumenal domain for ligand binding, the membrane spanning domain and the cytosolic C-terminus. It was shown previously that the cytosolic tail can mediate VSR trafficking even if the lumenal domain of the receptor is removed and replaced with GFP or another fluorophore. Indeed this type of fusion has proven useful not only for localisation studies, but also for monitoring vacuolar delivery. When GFP-VSR fusions are delivered to the vacuole GFP is proteolytically cleaved yielding a soluble 'GFP core', a processing intermediate that can be monitored by immunoblot assay with polyclonal antibodies against GFP.

In order to compare the different VSR isoforms with each other, and perhaps identify functional differences between them, GFP fusions of the six different VSRs were generated. Constructs encoding each of these GFP-VSR fusions were then electroporated into tobacco mesophyll protoplasts and expressed for 24 hours and total protein extracted from the cellular fraction. The proteolytic processing was then compared by SDS-PAGE immunoblot assay using polyclonal antibodies against GFP (Fig. 2.1). Two different volumes of each DNA preparation were electroporated, to allow for a comparison of the proteolytic patterns.

As can be seen in Figure 2.1, the VSRs do indeed show a different proteolytic degradation pattern, in particular VSR5, which seems to have both a shift in the

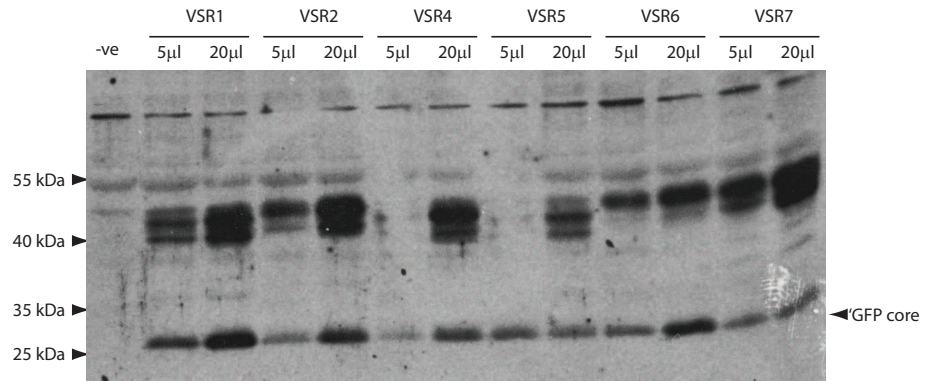

Figure 2.1: **Immunoblot comparison of the plant Vacuolar Sorting Receptors** Large-scale DNA preparations of the VSR-GFP fusions in the pUC19 vector were generated. 5μl and 20μl of each was electroporated into tobacco mesophyll protoplasts. After 40 hours expression cell pellets were extracted in 'protein extraction buffer', and electrophoretically separated by size using SDS-PAGE. Once transferred to a membrane, α-GFP antibody was used. '-ve' indicates a mock electroporation and the size ladder is annotated to the left of the blot. The ~27 kDa vacuolar processed 'GFP core' is indicated right of the blot.

GFP precursor:core ratio, as well as one of the higher molecular weight bands. In addition, there seems to be less of the total protein present on the blot. This could indicate two possibilities, either there is a higher level of protein turnover of the VSR5, or there is less of the VSR5 fusion protein synthesised, perhaps due to lower plasmid transfection efficiency. Due to the lack of a quantitative internal marker it is impossible to distinguish between these possibilities.

2.2.2 Assembling the Double Vector

In order to generate a plasmid that reports plasmid transfection efficiency via the expression of an untagged effector a double vector system needed to be designed with an internal reporter. Although there were several different candidate reported proteins, including luciferase, chloramphenicol acetyl transferase and green fluorescent protein, I selected β-glucuronidase (GUS) for routine assays in tobacco protoplasts. This approach was used in a similar system by Denecke et al. 1992, and this protein assay reporter system has been shown to be stable,

sensitive and quantitative. In addition to these attributes, the vector needed to be adaptable enough to be able to subclone any of the desired effector regions in a practical manner. For this purpose the internal GUS reporter gene was constructed in a manner that excluded restriction sites at the junction. Moreover, a polylinker was designed that allowed for the common effector-flanking restriction sites to be effectively used (see Figure 2.2 c.).

A multistep PCR assembly would be typically used to generate the desired vector. This would require a minimum of 3 steps, followed by subcloning of the 3500bp fragment into the vector backbone. An assembly PCR strategy would be effective, but not desirable as the repeated PCR steps would increase the chance of a polymerase induced mutagenesis event. In order to avoid these limitations a 'Gibson assembly' strategy was used. The Gibson assembly technique was devised in 2009 (Gibson et al., 2009). In the simultaneous multi-fragment assembly each of the fragments is individually PCR amplified with overlapping primers. The assembly-reaction then involves an incubation at 50°C for 1 hour with 5'-3' exonuclease, a polymerase and a DNA ligase. The exonuclease exposes the 3' ends of the fragments, and is denatured after ∼10 minutes. The exposed 3' ends have homology due to the overlapping DNA and will therefore anneal. The overlap acts as a 'primer' for the polymerase which elongates to the point where the exonuclease reached. The final missing phosphodiester bond is formed by the DNA ligase. The Gibson assembly can be used for fragments of up to 1Mb in size and up to 12 fragments simultaneously.

The generation of a GUS reporter vector using the Gibson strategy required 5 fragments, with overlapping ends including the polylinker (see Figure 2.2 A, B, and D). All fragments were amplified by PCR, aside from the vector backbone that was isolated using restriction digestion followed by gel isolation (Figure 2.2 e.).

After the isothermal assembly, transformation into *E. coli*, and plasmid isolation from twenty of the resulting colonies a diagnostic restriction digest was used to identify the positive clones (Figure 2.2 f., $*$ indicate the putative positives.). A further digest was undertaken to show that 4 of the 5 identified clones were true positives (Figure 2.2 g. 1, 8, 9 and 16). These clones were sent for DNA sequencing and used for further analysis.

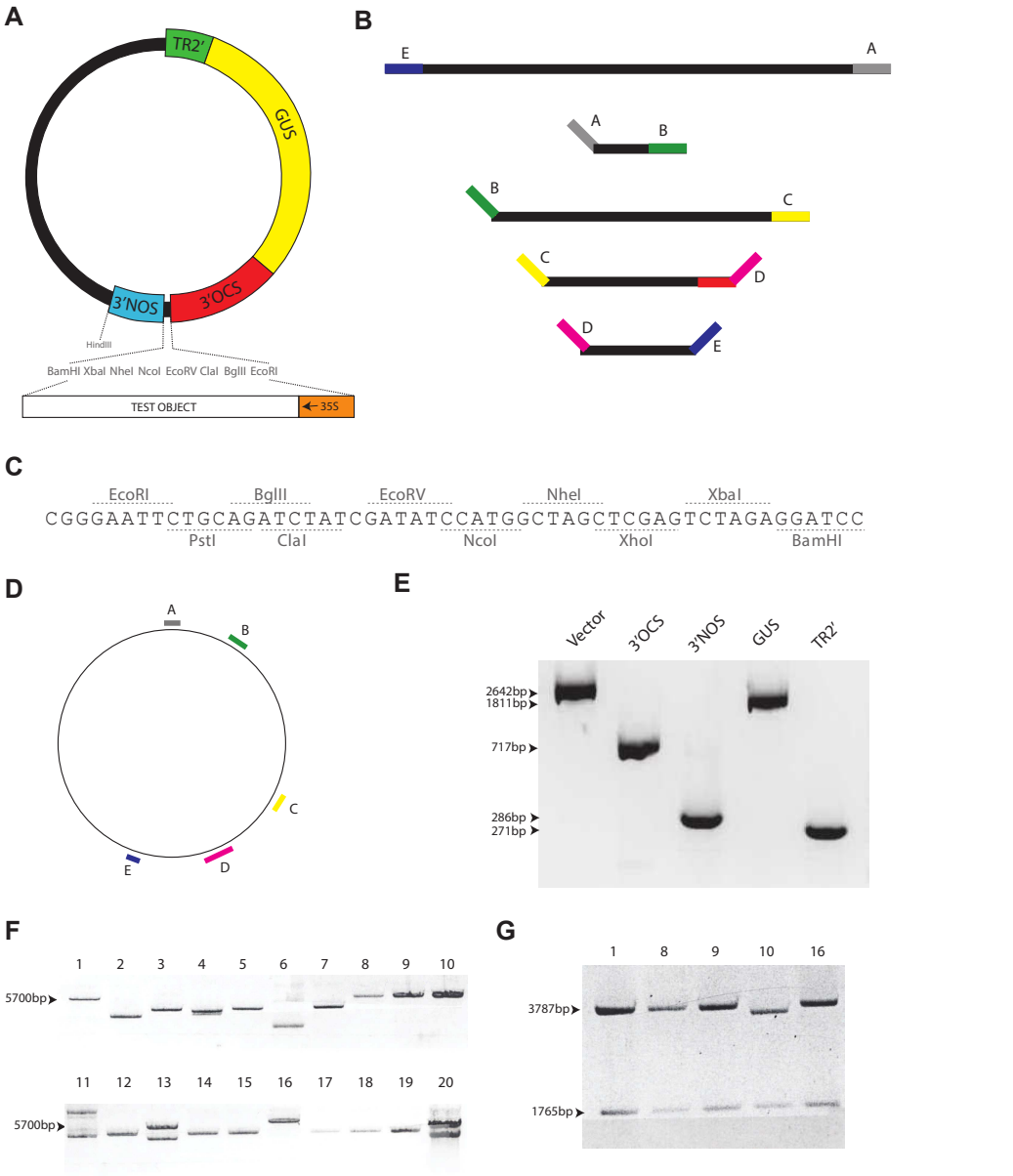

Figure 2.2: **Generation of a GUS Double Vector**
A. Vector map of the planned construct, including the polylinker designed to easily subclone any relevant test construct.
B. The various fragments used in the Gibson Assembly with their overlap colour coded, which correlates to the map (**D.**).
C. The sequence for the polylinker encoded by the primers for the assembly.
E. The various fragments from section B, prepared and loaded onto an agarose gel.
F. EcoRI restriction endonuclease digest on small scale DNA preparations from twenty *E. coli* colonies generated from the isothermal assembly with the putative positives being clones 1, 8, 9, 10 and 16, with a size of 5700bp.
G. The putative positive DNA preparations digested by the restriction endonuclease EcoRV showing the four positives (3787bp, 1765bp and 231bp (not visible on gel). Notice that clone 10 is shown to be negative, further digestion (not shown) demonstrated that the clone was lacking the 3'nos fragment.

2.2.3 Electrotransformed Beta-Glucuronidase Gives Quantifiable Activity in Tobacco Protoplasts

After the vector was built and sequenced it was necessary to confirm that the assay works under the standard experimental constraints used for protein trafficking. For this purpose, a relatively high concentration ($\sim 1\mu g/\mu l$) DNA preparation was generated. Isolated protoplasts were then electrotransformed with and without $5\mu g$ of the DNA. After $\sim$24 hours expression the protoplasts were harvested.

Usually trafficking assays rely on co-transfection of a plasmid encoding for the enzyme α-Amylase or a derivative as a trafficking cargo. Amylase, however, is not stable in β-Glucuronidase extraction buffer or vice-versa. Therefore, to allow for both Amylase assays and GUS assays to be performed on the same sample, only $500\mu l$ of the protoplasts suspension was used for the GUS assay, allowing the remaining 2ml to be used for Amylase assays. The sample to be used for GUS assays ($500\mu l$) was mixed with GUS extraction buffer, sonicated and centrifuged. The supernatant was then used for GUS assays as by Denecke et al. (1992). There is background absorbance from a protoplast extract at $\lambda 405$, which means that data from different experiments cannot be compared unless we include a 'zero stop' (i.e. instantly stopped assay) to permit the comparison of δ O.D. between experiments. The assay gave significantly different values (two-tailed Mann-Whitney test, p=0.0009) with at least a ten fold difference after a one hour assay (Figure 2.3). This showed that the generated vector and experimental conditions could be used for future analysis.

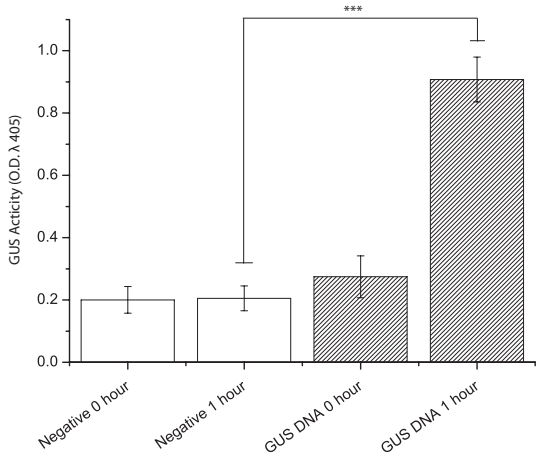

Figure 2.3: **Gene Expression can be Monitored in Tobacco Mesophyll Protoplasts** The empty 'GUS vector' (Section 2.2) was transfected via electroporation into Tobacco mesophyll protoplasts. After 24 hours the cell pellet was extracted in GUS extraction buffer and assayed as described in the materials and methods section (Section 8.4.2. After stopping the O.D. was measured at λ 405 in a spectrophotometer. The control mock electroporation has no activity (white bars). In addition a 0 stop assay was included to take account of background λ 405 absorbance from the chlorophyll in the sample. A two-tailed Mann-Whitney test was performed showing the activity difference significant to three decimal places (p=0.0009).

2.2.4 The Absorbance Values from the Beta-Glucuronidase Assay are not Directly Proportional to the GUS Concentration

Although the assay in Figure 2.3 shows that it is possible to monitor GUS expression activity, the specific constraints of the assay under the particular conditions used (e.g. protoplast suspension, 280μl total volume) needed to be tested. The assay is likely to suffer from saturation due to substrate limitation and colorimetric saturation of the sample O.D. reader. In order to test the linearity of the assay and the effect of the various saturation points a series of assays were done on a concentration series generated from a saturating sample and a mock electroporation being mixed in different ratios (Figure 2.4).

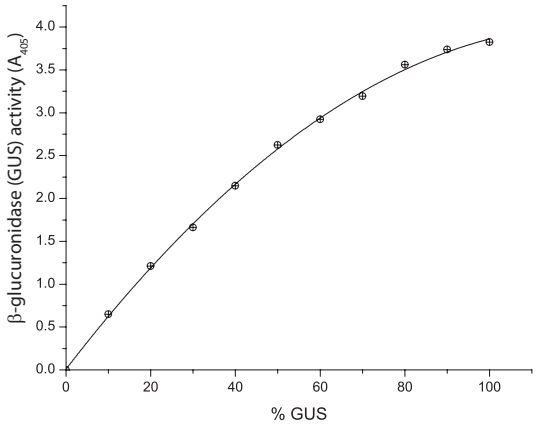

Figure 2.4: **Enzymatic Activities of a Beta-Glucuronidase Dilution Series**
A dilution series of beta-Glucuronidase containing sample showing the activity curve after a two hour assay. Notice the linearity of the assay to ∼2/2.5.

Fig. 2.4 shows that the relationship between the ΔO.D. and GUS concentration is essentially non-linear, although it could be argued that the assay appears linear between the concentration of GUS and the O.D. up to O.D. ∼2.5. The assay seems to suffer from a substrate limitation. Figure 2.4 shows that even between the linear range (O.D. 0-2.5) the assay is not directly proportional. For this reason the calibration curve was calculated from the curvature of the activity curve as follows:

$$y = -0.0003x^2 + 0.0643x + 0.0085$$
$$x = \textit{normalised value } y = \textit{O.D.}$$

The above equation can be routinely used to adjust a given O.D. into a normalised '%' value that represents a GUS value allowing for proportional comparison between samples. For all future GUS readouts, this normalisation was used. Due to the fact that the curve flattens above O.D.=3, any measurements above this point are considered inaccurate and were repeated under different assay conditions.

2.2.5 The Activity of the Beta-Glucuronidase Assay is Linear Over Time

In order to avoid the saturating assays, it is practical to avoid readouts (O.D.>2.5) by performing shorter assays. However, in order for the assays to be comparable over time, the linearity over time needed to be tested. In order to test this the protein extract of several electroporations was pooled and a dilution series was made proportional to the time of each assay. For example, the sample used for the 1 hour assay was undiluted, but the sample for the two hour assay was diluted to 50% and the four hour assay to 25%. As can be seen in Figure 2.5 the assay is reproducible over time with the differences in the samples being less than the expected experimental variations from pipetting (Figure 2.5). Therefore, it can be concluded that the substrate and the enzyme are extremely stable making it possible to compare assays performed over different times on different days with one another.

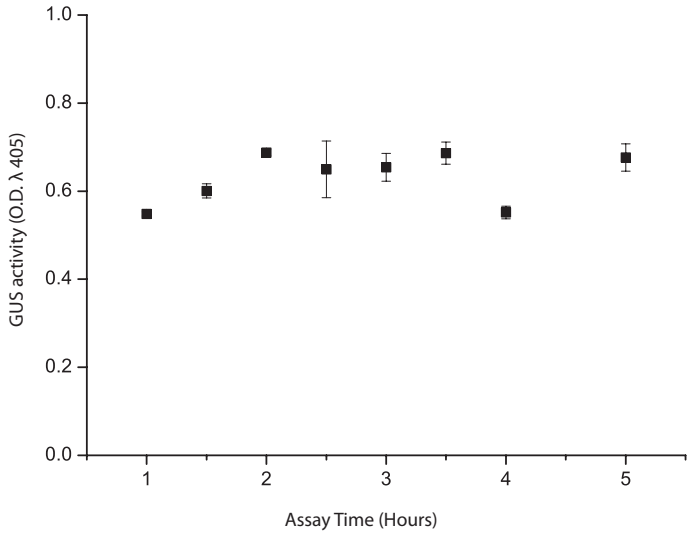

Figure 2.5: **A Time Series of Beta-Glucuronidase Activity**
A standard sample of GUS was diluted 8 times (1x, 1.5x, 2x, 2.5x, 3x, 3.5x, 4x and 5x). Each sample was then assayed as a proportion of the dilution (i.e. 1x for 1 hour, 2x for 2 hours etc.), with three repetitions. Error bars represent standard error over three repetitions.

2.2.6 Protein Levels of Reporter and Test Object are not Linear at High Expression Levels

The use of this expression system is dependent on an understanding of the relationship of the test object and the correlating factor over various conditions. For this purpose, the α-Amylase gene under control of the 35S promoter was subcloned into the polylinker of the GUS normalisation vector (subcloning by Mr. I. K. Adam). A dilution series of the plasmid was electroporated into tobacco epidermal protoplasts. After 24 hours expression, as before, a GUS assay was performed on 500μl of the cell suspension. Additionally, 500μl of the cell suspension was sonicated and the α-Amylase activity determined. The activity of the two different enzymes can then be compared as a ratio (Figure 2.6).

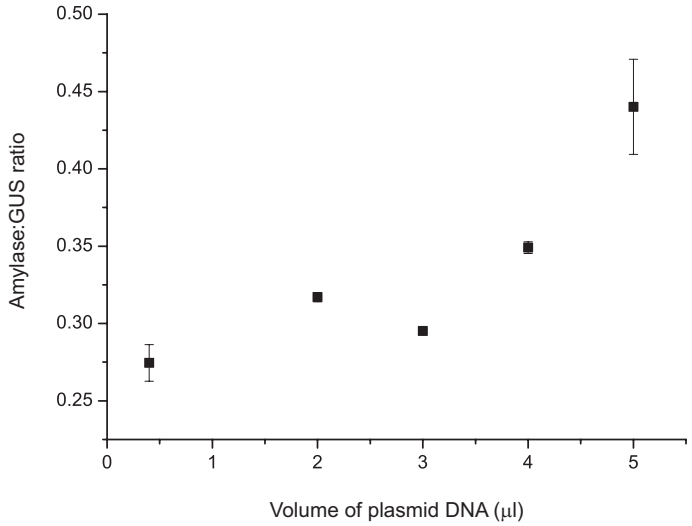

Figure 2.6: **Expression Correlation of Two Different Enzymes on the Same Plasmid** A double vector encoding Amylase and Beta-Glucuronidase (pIKA9, I. K. Adam) was transfected into Tobacco protoplasts. Total activity of each was assayed and the ratio between the two calculated. Error bars = Standard Deviation of multiple repeats].

As can be seen in Figure 2.6 the GUS and Amylase activity correlate well at lower expression levels. However, at higher expression levels the Amylase seems to exhibit a great increase in activity compared to GUS. Therefore the use of the

system should be restricted to analysis of the expression of similar effectors, with similar GUS activity in a comparative manner, rather than in an isolated manner.

2.2.7 The Use of GUS Normalised GFP-VSRs Highlights The Unique Processing of VSR5

The establishment of this assay system allows for the re-evaluation of the question posited in section 2.2.1; namely, do the VSRs have unique processing? To address this the individual GFP-VSRs needed to be subcloned into the vector generated in section 2.2.2, the presence of the polylinker allowed for all the fragments to be subcloned using the restriction endonucleases EcoRI and HindIII. Large scale DNA preparations could then be generated. After electroporation into tobacco mesophyll protoplasts at two different concentrations each and expression for 24 hours the relative GUS activity was compared – allowing for quality and yield of the DNA preparations to be assessed (data not shown). There was a large amount of variation in activity between samples ($\sim$ 25%), and in order to reduce this variation the DNA was diluted according to the GUS activity. The experiment was repeated with the relative dilutions used and the GUS assays performed to ensure a lack of variation between expression. The remaining protoplast suspension was then used to generate a protein extract with the total extraction volume equalised by GUS activity for immunoblot assay. In addition, the membrane bound and proteolytically digested GFP-VSR core could be separated as the core can be extracted before the membrane bound pellet is extracted.

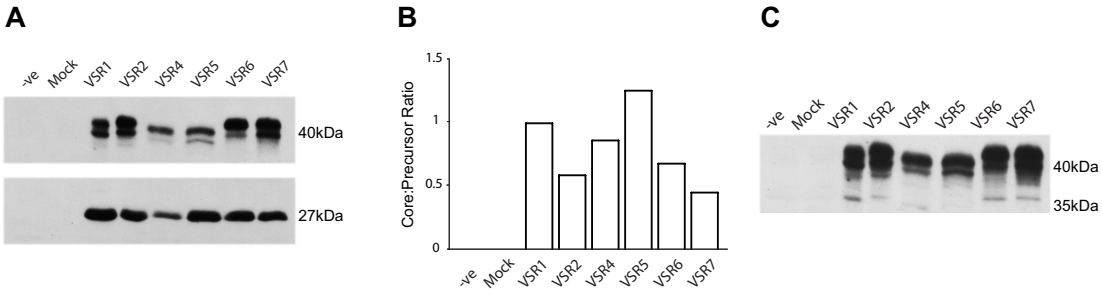

Figure 2.7: **Immunoblot Assay of Expression Normalised VSR Protein Family**
A. Immunoblot assay of volumetrically normalised protein samples extracted from the membrane pellet (upper) and the soluble vacuolar fraction (lower) using α–GFP antibodies. The membrane bound fraction represents the full length GFP-VSR isoforms, whereas the soluble fraction represents the vacuolar proteolytically processed core form.
B. *in silico* comparison of the core:precursor ratio from A. The mean intensity reading was taken for equal areas of each immunoblot assay using ImageJ, the average of the negative readings (which were identical) were then taken from the readings, which were then used to make a core:full length ratio. Notice that GFP-VSR5 has the highest value.
C. A longer exposure of the upper immunoblot assay in panel A, which better demonstrated the differential proteolytic processing of trafficking intermediates. In particular notice the lack of the 37kDa intermediate from the GFP-VSR5.

As can be seen in Fig. 2.7 the the proteolytic pattern and total protein levels vary among the VSRs in a biologically relevant manner, as it is known that equal expression amounts were loaded by GUS activity. The quantitative comparison by numerical comparison of the ratio of the average intensities of the immunoblot assay (2.7, B.) shows the variation in the ability of the various VSRs to reach the vacuole/recycle from the late secretory pathway. In addition, a longer exposure of the immunoblot assay highlights differences in trafficking/degradation intermediates (2.7, C.). Taking both sets of results into account the main difference between the VSRs can be seen by GFP-VSR5 which seems to have a higher core:precursor ratio, and a unique proteolytic pattern.

2.3 DISCUSSION

2.3.1 Limitations of the GUS Expression System

The use of GUS normalisation has allowed for the direct expression, and direct comparison of effectors. To date, over 30 effectors have been subcloned into the GUS normalisation vector, to allow for controlled expression. Although the strengths are clear there are a number of limitations to be aware of. The primary limitation is the assumption that the GUS expression is directly proportional to the expression of the effector, regardless of the size of the genetic element. In reality, this is not likely to always be the case- as demonstrated by Figure 2.6. Although, the expression of the two proteins is likely to be highly correlated, there can be issues of differential mRNA stability, translocation pore competition and mRNA silencing that could affect the relative protein levels. These effects would also become more pronounced at higher expression levels. With that in mind, the GUS expression normalisation is more suited to comparing the expression of related proteins that would be affected by these confounding factors in the same way.

2.3.2 The Use of the GUS Expression System

In addition the use of the GUS system has allowed the comparative analysis of different members of the GFP-VSR protein family fusions. The GUS system is particularly suited to this problem as the VSRs are all homologous with comparable sizes. The VSRs are difficult to compare visually without normalisation as any shift in the recycling from the late secretory pathway will result in an increase in protein turnover. Thus it is difficult to distinguish between poor expression

and higher protein turnover without the presence of the GUS normalisation. As shown in figure 2.7, even when normalised there is a relatively large amount of variation between the samples, which can now be attributed to properties of the VSR fusions themselves and not quality differences between DNA preparations and associated differences in transfection rates.

2.3.3 Differences Between the VSR Protein Family

Evidence from *A. thaliana* knock-outs and comparative genetic crosses has previously suggested that VSR5 and VSR6 are not involved in the vacuolar sorting of Aleurain sorting cargo (Zouhar et al., 2010), in the same study it was shown that the VSR1 and VSR2 are redundantly required to sort the Aleurain cargo. This was further supported in a later study, which also showed that 'phaseolin' cargo was trafficked with similar dependencies (Lee et al., 2013). In addition both VSR1, VSR2 and VSR3 were shown to be necessary for the sorting of the 'VAC2' protein (Zouhar et al., 2010), that has been implicated in the protein storage vacuoles in seed tissue.

In this study, the comparison of the degradation of different GFP-VSR chimeras by immunoblot assays (Figure 2.7) also suggests that VSRs fall into three classes. GPF-VSR1, 4 and 6 all seem to have comparable abilities to recycle, and thus similar amounts reach the vacuole, as shown by the core:precursor ratio. GFP-VSR2 and 7 are also comparable with each other, with the best recycling ability, and thus lowest core:precursor ratio. GFP-VSR5 is the worst recycler, thus leaking most to the vacuole and having the highest core:precursor ratio. The VSR5 also stands out as having unique processing intermediates, that can be seen in Figure 2.7C. In particular there is a ∼35kDa intermediate uniquely not present

in the GFP-VSR5 lane. Perhaps this indicates a different trafficking route. In addition GFP-VSR4 seems to have less total protein than the other GFP-VSRs, despite being equally transfected and thus having equal GUS activity. VSR4 also has a unique processing pattern. There has been no suggested biological function that explains the consistent divergence in the VSR protein family function, a concept explored in the next chapter.

3 THE LOCALISATION AND CHARACTERISATION OF VSR5: A UNIQUE PLANT VACUOLAR SORTING RECEPTOR

3.1 INTRODUCTION

In the previous chapter a quantitative expresssion system was developed. This system was used to compare the proteolytic processing of the VSR protein family. The VSRs showed divergence in not only their leakage to the vacuole, but also in the proteolytic processing intermediates.

The study and understanding of Vacuolar Sorting Receptors was started in 1994 when the *Pisum sativum* vacuolar sorting receptor was identified through a column affinity approach as binding to the vacuolar cargo 'Aleurain' (Aleu). Soon after this, the *A. thaliana* homologue was identified and characterised in a number of publications. There are seven homologues in *A. thaliana* and as discussed (Section 2.3) there are multiple lines of evidence to suggest a divergent function. Understanding the trafficking of VSRs is one of the key aims of this thesis, and thus any functional differences need to be fully characterised.

The 'Aleurain' protein was the first identified VSR ligand and the first identified vacuolar cargo in plants. Attempts to identify mistargeting mutants in knock-out studies have been difficult due to the redundancy between the seven VSR isoforms. Despite the lack of obvious developmental phenotypes in *vsr1* knockout lines, storage proteins are partially mistargeted as precursor forms to the extracellular matrix (Shimada et al., 2003). In contrast, *A. thaliana* aleurain (ALEU), at the time classified as a typical lytic vacuolar cargo protein, did not show evidence for mistargeting in the *vsr1* knockouts. This led to the proposal that VSR1 may be responsible for storage, but not lytic vacuolar transport. However, after

germination of seeds, the mistargeted storage protein precursors were degraded normally, suggesting that some lytic proteases were likely to be secreted as well but may have remained below the detection limit of immunocytochemistry (Shimada et al., 2003). In order to overcome the issues with the genetic approaches, heterologous cargoes were used in a *vsr1* knockdown background (Craddock et al., 2008). Under these conditions both the storage and lytic type cargoes had altered proteolytic processing and partial secretion in a *vsr1* mutant background. Thus, earlier binding studies suggesting a broad specificity of VSR-ligand interactions were confirmed (Jolliffe et al., 2004; Kirsch et al., 1996; Miller et al., 1999; Suen et al., 2010).

Accession	C-Terminus	Neuhaus and Paris (2005), Foresti et al. (2010)	Hadlington and Denecke (2000), Paris et al. (2002)	Miao et al. (2006), Zouhar et al. (2010), Saint-Jean et al.(2010)	Laval et al. (1999)
AT3G52850	SGHHMI	VSR1;1	Atbp80b	VSR1	AtELP1
AT2G30290	SSQLEL	VSR1;2	Atbp80c	VSR2	AtELP4
AT2G14720	TNDERA	VSR2;1/2	Atbp80a'	VSR4	AtELP2a
AT2G14740	VNDERA	VSR2;2	Atbp80a	VSR3	AtELP2b
AT4G20110	AEPFTL	VSR3;1	Atbp80f	VSR7	AtELP3
AT2G34940	NQDSFK	VSR3;2	Atbp80e	VSR5	AtELP5
AT1G30900	RLTSAA	VSR3;3	Atbp80d	VSR6	-

Table 3.1: **Nomenclature of the VSR Protein Family**
A table comparing the various VSR nomenclatures used in the last 15 years. To avoid future confusion, the second column refers to the last six terminal residues that act as a fingerprint helping to differentiate quickly between the different isoforms. Within this thesis VSR3;2 and VSR5 are used interchangeably whilst VSR2 refers to the TNDERA isoform.

There are 7 VSR paralogues in the *A. thaliana* genome, with two being highly homologous direct repeats. Table 3.1 shows a comparison between the different VSRs with the nomenclature used in various publications. These paralogues were compared in a comprehensive knock-down analysis (Zouhar et al., 2010). In this study members of VSR1 and VSR2 groups (Table 3.1, column 3) were shown to contribute to the sorting of both storage and lytic vacuolar cargo. It should

be noted that induced secretion of typical lytic vacuolar cargo Aleu-GFP was only detectable in a double VSR knockout covering members of the first two VSR families (Zouhar et al., 2010), which explained why in the earlier study Aleu mis-sorting was not observed in the single VSR1 knockout (Shimada et al., 2003). Even in a double knockout, secreted Aleu represented only a minor fraction, and most of the lytic cargo was still transported to the vacuole (Zouhar et al., 2010). One interpretation is that Aleu may contain two different vacuolar sorting signals, only one of which is VSR specific. Alternatively, it could be that Aleu is simply a stronger ligand that binds with higher affinity to the same VSR. Interestingly, knockout mutants of the six remaining *A. thaliana* VSR isoforms other than VSR1 do not accumulate storage proteins in the extracellular matrix (Shimada et al., 2003; Zouhar et al., 2010). This is expected for those isoforms that are not expressed in seeds but unexpected for VSR2 group isoforms that are also highly transcribed in seeds (Laval et al., 2003). However, mRNA levels are not always correlated with protein levels, and it is possible that VSR1 would be the major protein isoform expressed in developing seeds. Although data are available for mRNA expression (Laval et al., 2003), no independent protein expression data are available for the various VSR isoforms. This hypothesis is supported by the fact that, if we assume that the anti-VSR1 antibody has identical affinity for all VSRs due to the high sequence homology of the lumenal domain, only the *vsr1* knockout line exhibited a detectable reduction in VSR protein levels (Zouhar et al., 2010), and it will be interesting to verify protein levels also in developing seeds. Another important finding is that the VSR3 group appeared to play no detectable role in vacuolar transport(Zouhar et al., 2010).

In the previous chapter an immunoblot assay of a series of expression normalised GFP–VSR fusions using an anti-GFP polyclonal antibody identified differential

turnover and hydrolytic processing of the various VSR paralogues (Fig. 2.7). Here, the VSRs are compared in a phylogenetic analysis and the standout VSR (VSR5 aka 3;2 - NQDSFK, Table 3.1) is selected for further analysis. VSR5 is shown not to interact with VSR2 ligands in a novel *in vivo* binding assay and not to co-localise with the canonical VSR2. Further localisation of VSR5 to known markers of the plant secretory pathway shows that the VSR localises to an uncharacterised compartment, possibly a late prevacuolar compartment. This theme is further explored in the next chapter.

3.2 RESULTS

3.2.1 A Cross Kingdom Phylogeny Suggests a Specialised Class of VSRs in Vascular Plants

The normalised immunoblot assay comparison of the *A. thaliana* VSRs indicates that a GFP fusion of the VSR analogues in the VSR3 class have different proteolytic processing when compared to the other VSRs (Fig. 2.7). In order to understand the relationship that the different *A. thaliana* VSRs have with one another a phylogenetic tree was constructed using the complete sequence, not just the cytosolic C-terminus as has been done before.

All receptor protein sequences were obtained using publicly available data (www.ncbi.nlm.nih.gov/). The VSR sequences analysed strictly show a predicted type 1 single membrane spanning topology with an N-terminal signal peptide, a large lumenal domain of remarkably similar size between the different organisms, and a transmembrane (TM) domain followed by a highly conserved sequence of 23 amino acids. These full-length vacuolar sorting receptor protein sequences were then aligned using the BLOSUM62 algorithm with the ClustalW alignment tool (www.ebi.ac.uk/Tools/msa/clustalw2/). The resulting alignment was subsequently manually adjusted, in particular the position of the TM domain of the *C. reinhardtii* VSR was corrected to be aligned with the other VSRs.

The aligned sequences were assembled into a phylogenetic tree using the boot-strapped neighbor-joining algorithm (Saitou and Nei, 1987) and the Jones, Taylor, and Thornton amino acid substitution model (Jones et al., 1992) in MEGA 5.05 with 1000 trials (http://www.megasoftware.net/). Included in this analysis were VSR sequences of *A. thaliana, G. max, O. sativa, P. patens, O.*

tauri, P. sitchensis, C. reinhardtii, Micromonas strain RCC299, P. infestans and *P. tricornutum*. Due to the recent genome duplication in soybean (Shoemaker et al., 1996) leading to five pairs of almost identical VSR orthologs, only one representative of each was used to avoid unnecessary complexity. The *P. patens* class has been labelled here as VSR12 to indicate the ancestral relationship with both *A. thaliana* class 1 and 2. *P. patens* XP_001759820 (VSR12;2) has a very close homologue, XP_001759928 (VSR2;3), which has been omitted in the analysis due to a small gap in the sequence contig preventing accurate gene modelling and sequence alignment. In parallel, the phylogenetic tree was also resolved using a boot-strapped maximum likelihood algorithm, resulting in a comparable topology and the same three angiosperm VSR classes (data not shown).

As can be seen in Fig. 3.1 the sequences can be broadly divided into five clades, with the VSR sequences from angiosperms consistently falling into the same three categories as described earlier (Avila et al., 2008; Neuhaus and Paris, 2005) and shown in Table 3.1. Spruce appears to contain only class 2 and 3 VSRs, while the moss Physcomitrella appears to form a separate clade of VSRs seemingly ancestral to classes 1 and 2 of vascular plants. Green algae, diatoms, and oomycetes appear to represent a VSR ancestral clade. Class 3 of vascular plants appears to be due to an early segregation, prior to the class 1 and 2 divide. The GFP–VSR fusions shown to exhibit altered processing (above, Fig. 2.7) fall into this class. It is plausible that this indicates a specialised role of class 3 unique to to vascular plants. Indeed, recent experimental data suggests that VSR5 may not play a canonical role in vacuolar cargo sorting (Lee et al., 2013).

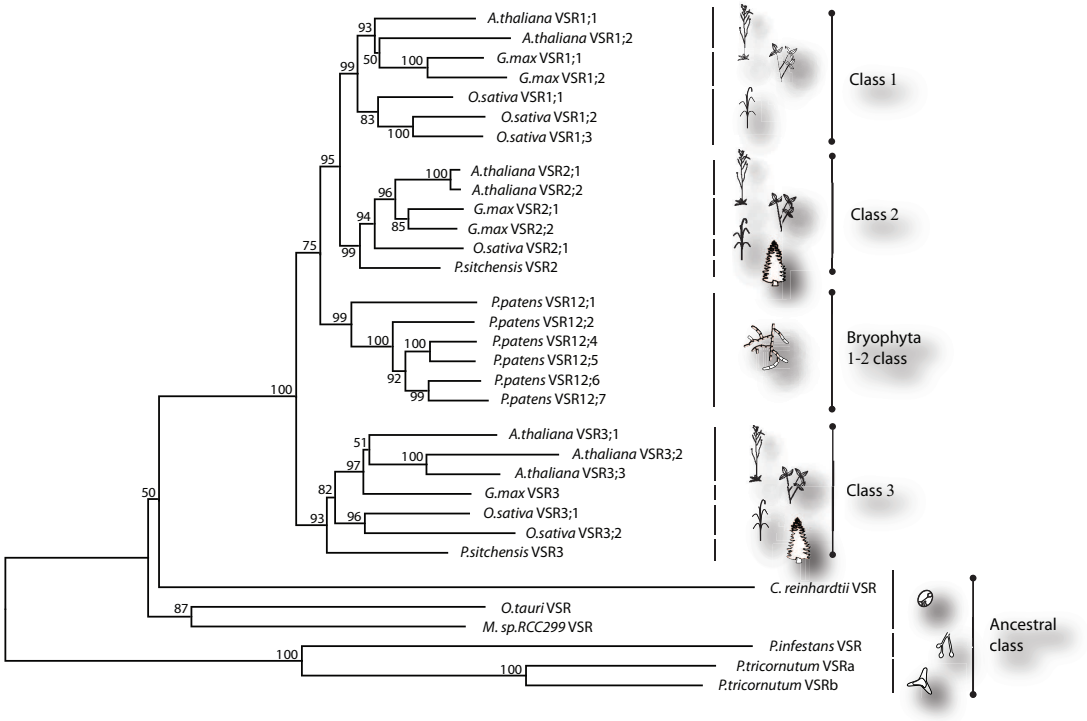

Figure 3.1: **Cross-species Phylogenetic Analysis of Plant VSRs**
A phylogeny showing a Jones, Taylor, and Thornton amino acid substitution algorithm comparison with 1000 trials. Organisms compared are *A. thaliana, G. max, O. sativa, P. patens, O. tauri, P. sitchensis, C. reinhardtii, Micromonas strain RCC299, P. infestans* and *P. tricornutum*. The classification of the VSRs can be seen to the right of the phylogeny and the representative organisms from each protein sequence aligned is shown by the images next to each alignment. Bootstrap values from 1000 trials are indicated as percentages of the 1000 trials at their respective node.

3.2.2 VSR5 and VSR1 Do not Co-localise with Canonical VSRs

The variation in the proteolytic processing combined with the divergent phylogeny supported the hypothesis that the VSRs have divergent functionality. These results justify a re-evaluation of earlier data suggesting that all VSR isoforms co-localise (Miao et al., 2006). The subcellular localisation of GFP–VSR2 is well established, and is treated as one of the defining markers of the multivesicular prevacuolar compartment (PVC). Thus the localisation of RFP-VSR2 (Foresti et al., 2010) was used as a common denominator to compare the localisation of all the various GFP-VSR fusions used in Fig. 2.7. Plasmid vectors harbouring the relevant

chimeras were used to transform *A. tumefaciens* to allow infiltration mediated transient expression. For co-localisation the *A. tumefaciens* cultures were mixed 50:50 prior to infiltration. After 24-48 hours expression a 1cm^2 leaf section was excised and mounted on a microscopy slide. For each co-localisation data set images were collated from at least two independent microscopy sessions. The compiled image collection (∼20-30 images or 200-400 organelles per co-localisation) was subjected to a statistical analysis as described previously (Foresti et al., 2010). The result of the analysis is shown in a scatterplot that allows for a qualitative visual appraisal of the results, in addition a quantitative Spearman's rank correlation coefficient value ranging from -1 to +1 was calculated (3.2).

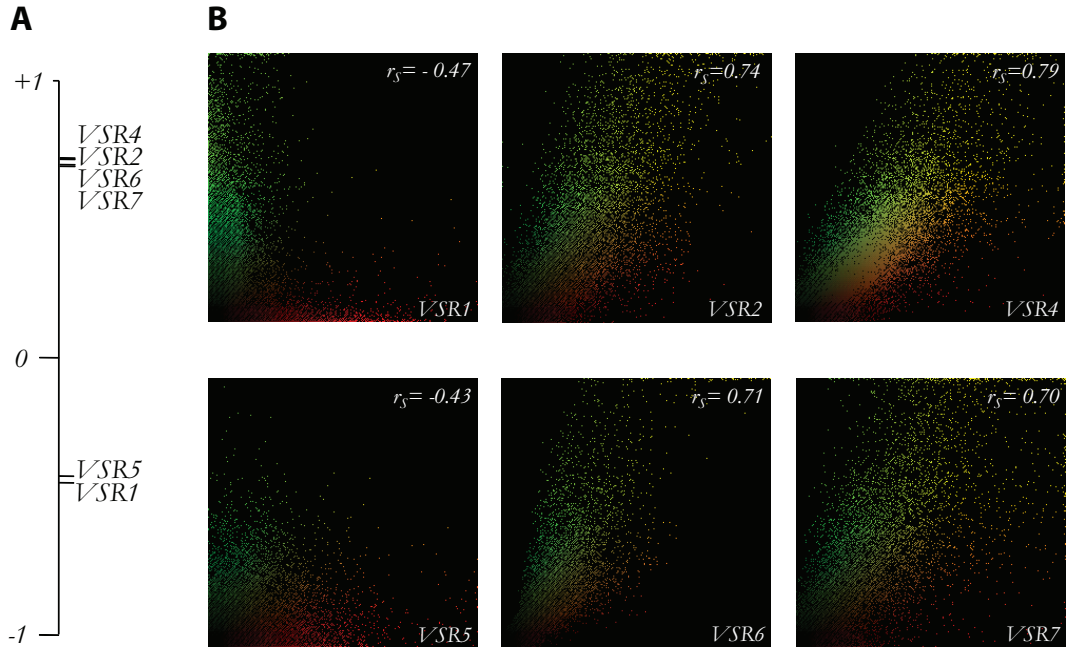

Figure 3.2: **A Localisation Screen of the VSR Protein Family**
Agrobacterium strains encoding for N-terminal GFP fusions of the various *A. thaliana* VSR orthologues were co-infiltrated in tobacco epidermal tissue with the N-terminal RFP fusion of VSR2, a common denominator. After sufficient data recovery from the CLSM, a statistical analysis was undertaken.
A. The resulting Spearman's rank correlation coefficient (between -1 & +1) displayed to scale on a number-line graph.
B. A scatterplot of each co-localisation

As can be seen in Fig. 3.2 the control GFP-VSR2 shows a diagonal yellow pattern in the scatterplot and a high Spearman's correlation coefficient ($r_s = 0.74$) indicating a colocalisation with RFP-VSR2, as expected. This pattern is similar to the GFP-VSR4 ($r_s = 0.79$), GFP-VSR6 ($r_s = 0.71$) and GFP-VSR7 ($r_s = 0.70$), which localise to the PVC. In contrast, both GFP-VSR1 and GFP-VSR5 seem to have a a split population in the scatterplot and a sub-zero Spearman's correlation coefficient ($r_s = -0.47$ and $r_s = -0.43$ respectively). This indicated that these two isoforms localise to other structures than the PVC and may have specialised biological functions.

3.2.3 Comparison of the Ability of VSRs to Compete for Vacuolar Sorting Machinery

To probe the variation in the VSR trafficking even further, the ability of the various receptor isoforms' C-termini was tested for the ability to interact with cytosolic machinery. This can be experimentally interrogated using a 'competition assay'. Expression of VSR2, with the cargo interacting lumenal domain replaced with GFP, causes VSR-interacting vacuolar cargo to be missorted and secreted (DaSilva et al., 2006). This is due to the exposed C-terminus of the GFP-receptor chimera interacting with cytosolic machinery, titrating the machinery away from the endogenous receptors. This, in turn, prevents the endogenous receptor from correctly sorting the VSR cargo. In addition, it seemed that the cytosolic recycling machinery was titrated first, as addition of full-length VSR alleviated the effect.

The generation of the quantitative GUS expression system in this thesis allows for the 'competition effect' of the various GFP-VSR isoforms to be quantitatively compared. Therefore each of the GFP-VSR fusions in the GUS normalisation vector was expressed in tobacco protoplasts with a constant amount of the VSR

cargo Amylase-Sporamine (Amy-Spo). The presence of the GFP-VSR isoforms in the GUS normalisation vector allows for the ability of each to cause the induced secretion to be calculated as a factor of the expression of the receptors, deduced from the GUS activity.

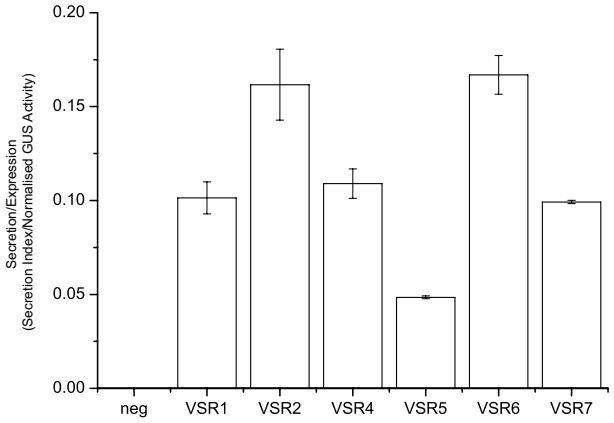

Figure 3.3: **A Screen of the Competition Effect of the Competition Ability of GFP-VSR Fusions**
The GFP-VSR fusions within the GUS normalisation expression vector were standardised in a trial experiment (data not shown) and electroporated into Tobacco mesophyll protoplasts. The GUS activity, as well as the secretion index was measured from each sample, and the secretion plotted as a factor of the deduced expression i.e. the GUS activity. The experiment was repeated multiple (at least 3 for each sample) times showing the same trend. Error bars represent the standard deviation multiple experimental readings of both the SI and the GUS activity.

Figure 3.3 shows that there is differential ability of the VSRs to cause the 'competition effect' described above. In particular GFP-VSR2 and 6 cause this effect the most, and noticeably VSR5 has the lowest level of competition. This assay, once again, highlights the difference of VSR5 from the other VSRs.

3.2.4 The C-terminus of VSR5 Shows Reduced Ability to Compete for Cytosolic Transport Factors

The *A. thaliana* VSR5 seems to not only have differential interaction with canonical cargo (Lee et al., 2013), but also when compared to the other VSRs, different proteolytic processing (Fig. 2.7), leakage to the vacuole (Fig. 2.7), localisation

(Fig. 3.2), ability to interact with endogenous cytosolic machinery and finally seems to belong to a vascular plants specific sub-class of the VSR protein family (Fig. 3.1). In order to further explore the differences between VSR5 and the canonical VSR2 in a physiological context; an experiment was designed to assess the ability of VSR5 to interact with endogenous machinery. It has been shown that co-expression of the GFP–VSR2 fusion used above (Fig. 2.7) with vacuolar cargo (Amylase-Sporamine [amy-spo]) causes induced secretion of the amy-spo in a dose-dependent manner. This effect is recoverable by expression of the full-length receptor. This indicates that the GFP–VSR2, that cannot interact with cargo due to the lack of a lumenal domain, is causing a titration of cytosolic components due to the functional and exposed C-terminus. VSR5 C-terminus has high homology to the VSR2 C-terminus, although there are several divergent residues, that are conserved in the remaining 6 VSRs. To identify if there is any biological consequence of this divergence VSR5 was assessed for its ability to cause the competition induced secretion of amy-spo. Dilution series of both VSR2 and VSR5 were electroporated into tobacco mesophyll protoplasts with a constant amount of amy-spo.

As can be seen in Fig. 3.4 VSR5 seems not to cause competition induced secretion to the same extent as the VSR2. However this experiment suffers from the same limitation as in Fig. 2.1, in that there is no way to tell whether the effect was due to a biological lack of titration in the case of the GFP–VSR5 or alternately due to less expression of VSR5 expression series. Thus this needed to be explored using the more quantitative GUS normalisation system.

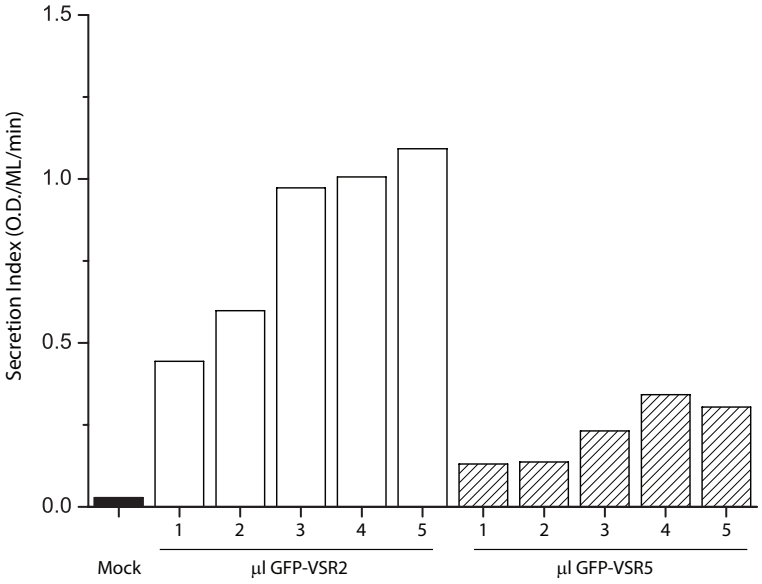

Figure 3.4: **The C-terminus of VSR5 has Reduced Induced Competition Mediated Secretion when Compared to VSR2**
Dose series of 1-5μl of DNA preparations of GFP–VSR2 and GFP–VSR5 were electroporated into Tobacco mesophyll protoplasts with a constant amount of Amy-spo. After 24 hours the cells and medium were independently tested for amylase activity and the ratio (medium:cells) presented as secretion index. The experiment was repeated to confirm the result (data not shown).

3.2.5 GUS Can be Used to Quantify Delivery Induced Secretion

In order to understand the nature of this dose response relationship the GUS expression system introduced above needed to be utilised (Section 2). Thus VSR2 and VSR5 GFP fusions were subcloned into the polylinker of the GUS expression vector allowing for the quantitative expression of the GFP–VSR2 and GFP–VSR5 when co-expressed with the vacuolar cargo. After DNA preparation and a preliminary experiment to normalise the GUS activity, the experiment was repeated, normalised as discussed in the previous chapter and the induced secretion plotted against the expression as deduced by the GUS activity.

As can be seen in Figure 3.5 the induction of secretion is comparatively higher in the VSR2 than VSR5. This can be better visualised by comparing the gradient of the slope (3.5, right panel)- the gradient of the slope (induced secretion/expression)

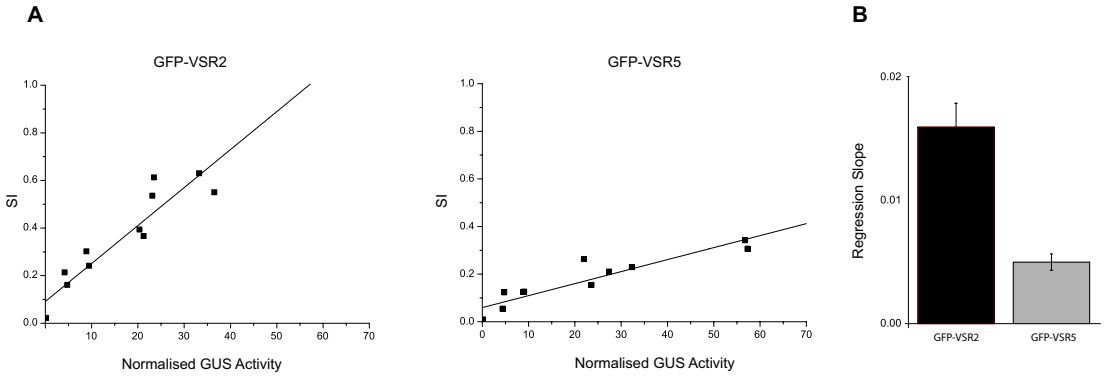

Figure 3.5: **The C-terminus of VSR5 has Reduced Induced Competition Mediated Secretion when Compared to VSR2**
A. The dose-dependent ability of GFP-VSR2 and GFP-VSR5 to induce the secretion of vacuolar cargo, as plotted against the normalised activity of beta-Glucuronidase.
B. A comparison between the slope (SI/GUS) of the regressions from panel A displayed on a histogram. The error bar represents the average distance of the data points from the linear regressions.

of the GFP-VSR5 is $\sim$ one third that of GFP-VSR2. This indicates that the C-terminus of VSR5 does not interact with the same cytosolic machinery as endogenous VSR2.

3.2.6 Development of a Quantitative *in vivo* Protein-Protein Interaction Assay

The presence of the third class of sorting receptor shown by the VSR phylogeny (Fig. 3.1) combined with the divergent localisation of VSR5 (Fig. 3.2), and the differential interaction with the cytosolic machinery (Fig. 3.5) warranted further investigation. In order to explore this question in an *in vivo* situation a biochemical assay was required that would report on ligand binding in a live cell system. In order to achieve this a biochemical assay was developed that employs the ability of full length receptors to co-secrete vacuolar cargo when mistargeted to the plasma membrane (DaSilva et al., 2005; Foresti et al., 2010). This effect, referred to here as the 'drag & drop' effect, is explained by the binding of the lumenal domain of the mutant receptor to the cargo in the early secretory pathway, followed by

misdirection ('drag') and release at the cell surface ('drop'). It is postulated that the cell surface pH conditions in the protoplast buffer cause dissociation of the cargo from the receptor, effectively delivering the cargo from a cell into the medium. Misdirecting the receptor to the cell surface is achieved by imposing the Y612A mutation on the full length region of VSR2. Results from this published assay (DaSilva et al., 2006) however, could not be analysed comparatively due to difference in transfection ability (discussed above in Section 2). Thus we took advantage of the GUS dual expression system developed in Section 2. This allows for normalisation of the various induced expression levels based on the relative GUS activity levels. The Y612A full-length receptor (FL-VSR2(Y612A)) and the wild-type control (FL(VSR2)) were thus subcloned into the polylinker of the GUS vector developed in Fig. 2.2. After DNA preparation and a preliminary experiment to normalise the GUS activity, the experiment was repeated with a concentration series of the adjusted volumes of DNA and a constant amount of the amy-spo encoding plasmid. After at least 3 repetitions of the experiment the results were compiled and the secretion index of amy-spo plotted against each of the GUS activities showing the dose response of each of the effectors (Fig. 3.6).

As expected the VSR2(Y612A) (Fig. 3.6, panel A) gives rise to a secretory dose response with a higher slope than the wild-type VSR2 (Fig. 3.6, panel B). It should also be noted that a slight induction of secretion can be observed with the wild-type receptor. This could be due to saturation of the vacuolar transport route, but is minimal compared to the Y612A mutant and can be regarded as the base level.

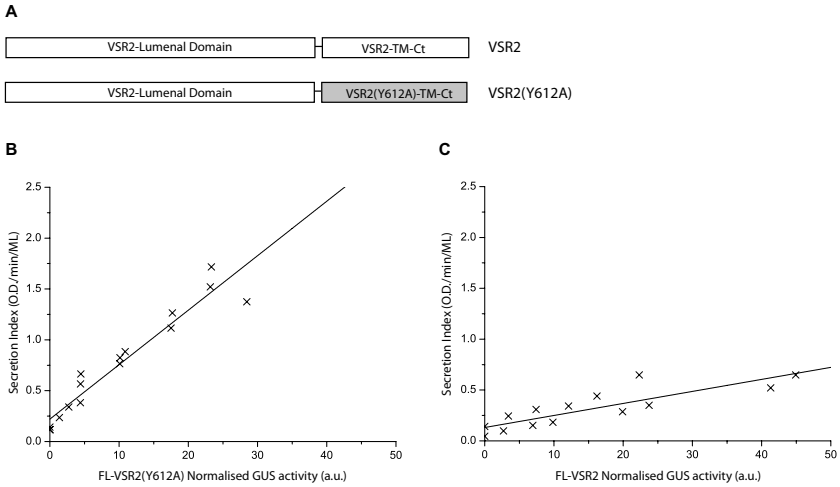

Figure 3.6: **The VSR2(Y612A) Point-Mutant Induces Secretion in a Directly Quantifiable Dose-Dependent Manner**
A. Diagram of the constructs used in this experiment.
B. DNA of double vectors containing the full-length VSR2 and the full-length VSR2(Y612A) point mutant were prepared. A serial dilution was electroporated normalised to the activity of a preliminary experiment with a constant amount of the cargo molecule (Amy-spo). After 24 hours the cells and medium were split and the activity in each one analysed, and expressed as a medium:cells ratio (Secretion Index). After several repetitions the results could be pooled and each secretion index plotted according the GUS activity. Notice the induced secretion of the cargo due to the VSR2(Y612A) in comparison to the wild-type VSR.

3.2.7 The Lumenal Domain of VSR5 Does not Cause Induced Secretion of Canonical VSR Cargo

The delivery of the cargo to the medium in the 'drag & drop' assay developed above (3.2.6) is dependent on an interaction between the lumenal domain of the receptor (VSR2) and the cargo (amy-spo) in the early secretory pathway. This assay could therefore be adapted to directly experimentally assay, *in vivo*, the ability of the lumenal domain of VSR5 to interact with the canonical VSR cargo, amy-spo. The VSR2 lumenal domain in the VSR2(Y612A)-GUS dual expression vector was replaced by the lumenal domain of VSR5, yielding a VSR5-2(Y612A) chimeric protein with the lumenal domain of VSR5 and the C-terminus of the VSR2 Y612A mutant. The 'drag & drop' assay was performed as before; a

DNA preparation was made, normalised and repeated experiments performed and plotted according to their respective GUS activity (Fig. 3.7).

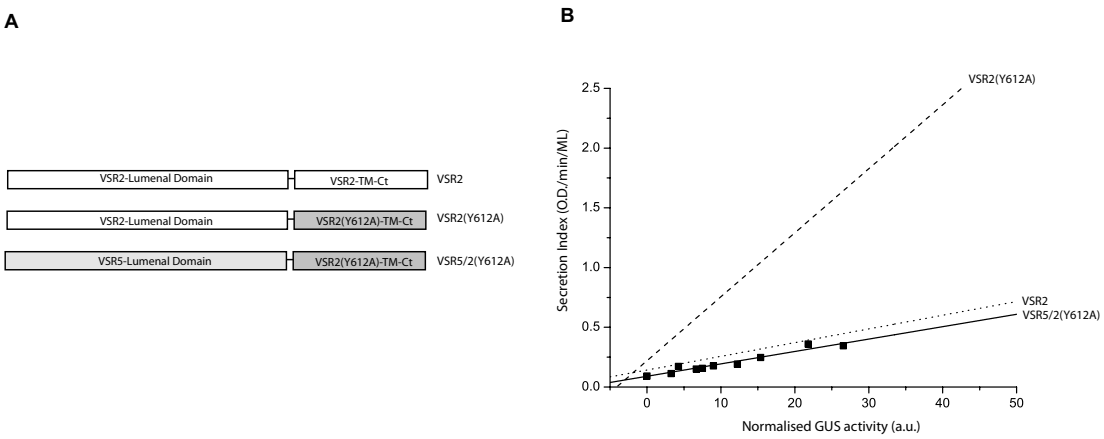

Figure 3.7: **The Lumenal Domain of VSR5 does not Induce the Interaction Mediated Secretion of Canonical VSR2 Cargo**
A. The effectors used in this experiment.
B. Similar to figure 3.6 a DNA preparation of VSR2(Y612A) with the lumenal cargo interaction domain was generated, normalised and expressed as a dilution series in tobacco mesophyll protoplasts with a constant amount of Amy-spo cargo. The graph shows the positive control of the VSR2(Y612A) [dashed line], the negative control of the wild-type full length VSR2 [dotted line] and the chimeric test object VSR5/2(Y612A) [black boxes and solid line]. VSR5/2(Y612A) is more comparable to the negative control rather than the positive suggesting that the lumenal domain of VSR5 does not interact with Amy-spo.

Figure 3.7 strongly suggests that the lumenal domain of VSR5 does not interact with the sporamine protein sorting signal. There seems to be some residual induced secretion that could be due to either a weak interaction between the amy-spo and the lumenal domain of VSR5 , or due to the weak competition effect that the VSR2(Y612A) has, causing mild induced secretion due to titration of endogenous machinery. Regardless VSR5 seems to have a different physiological function, that is specific for vascular plants.

3.2.8 VSR5 Potentially Localises to a Late-Endosomal Compartment

Several lines of evidence point to a divergent function in VSR5 *A. thaliana* VSR homologue. In order to understand the functionality of the protein, it was decided

to further test the localisation. The GFP–VSR5 was co-expressed with organelle markers for the Golgi apparatus, the TGN and compared to the PVC localisation above. As previously described *A. tumefaciens* harbouring the relevant markers were mixed, inoculated and incubated and the plant cells expressing the fluorescent proteins imaged. Also as above (Fig. 3.7), a statistical analysis was performed on the datasets giving both the scatterplots and Spearman's rank correlation coefficient value.

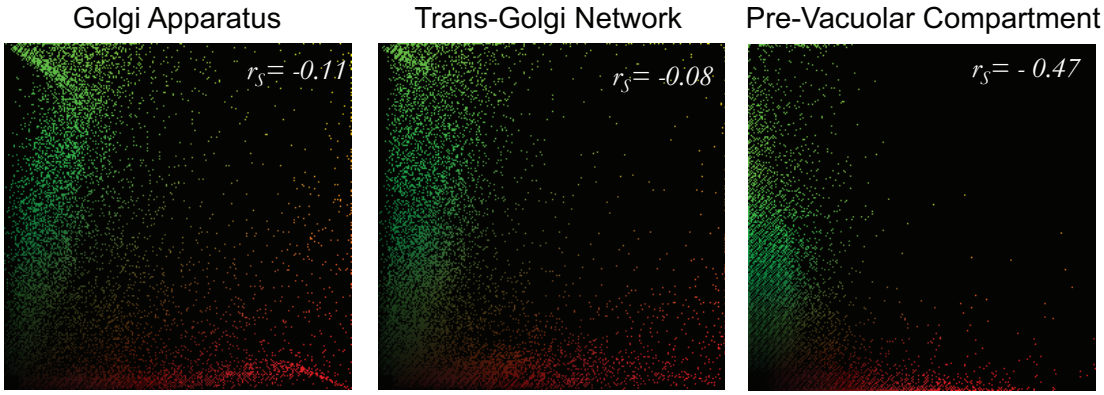

Figure 3.8: **The Localisation of VSR5**
Agrobacterium strains encoding for GFP–VSR5 and characterised markers of the secretory pathway (ST–YFP – Golgi apparatus, SYP61–RFP – TGN, RFP–VSR2 – PVC) were co-infiltrated in tobacco leaf epidermis.

As can be seen in Fig. 3.8 there is a surprising lack of co-localisation in any of the three images. This indicates that either VSR5 is causing an identity shift in the PVC or that VSR5 localises to a different organelle. In order to test which of these hypothesis is correct it was decided to examine the colocalisation of VSR5 with another marker of the PVC. However, there are no characterised markers other than the VSR2 of the PVC, and thus in order to complete this analysis several additional markers of the late endosomal pathways would be needed. This will be explored further in Chapter 4.

3.3 DISCUSSION

3.3.1 VSR5 and VSR2 Have Different Functions

There are several lines of evidence that corroborate the results from the genetic analysis of VSRs that suggests that the canonical receptor and VSR5 have different roles (Lee et al., 2013). In the initial immunoblot screen described in the previous chapter there are several observable differences between the various VSRs with VSR5 showing a higher core:precursor ratio indicating that VSR5 seems to traffic differently than some of the other VSRs. In addition a phylogenetic analysis indicates that this VSR belongs to a vascular plant specific clade, in agreement with other analyses of the VSR C-terminus. In order to understand the ligand binding capabilities an *in planta* binding assay was developed and utilised. The 'drag & drop' assay utilises the cargo mis-sorting activity of a C-terminal mutant of the receptor that traffics via the plasma membrane. Due to the intrinsic binding capabilities of the VSR2 lumenal domain ligand binding is initiated in the early secretory pathway and dissociation is induced upon exposure to the protoplast medium at the plasma membrane. Thus the receptor effectively delivers cargo to the cell surface.

In order to understand the cargo binding capabilities of VSR5 a chimeric protein was made consisting of the lumenal domain of VSR5 fused to the C-terminus of the Y612A mutant. The transmembrane domain and mutated cytosolic tail are shown to be sufficient to target GFP to the plasma membrane (DaSilva et al., 2006; Foresti et al., 2010). As opposed to the control construct, a VSR5 fusion does not cause the 'drag & drop' effect. There are three interpretations of this result. The first, and most likely is that VSR5 does not bind to the same cargo as VSR2, and therefore cannot 'drag & drop'. The second explanation would

be that VSR5 binds to the cargo, but has a different dissociation constant and thus does not 'drop' the ligand at the plasma membrane. The third possibility is that having a different lumenal domain stops interaction of the receptor with the exocytic machinery perhaps by preventing dimerisation of the receptors. This last hypothesis is particularly weak as the GFP-fusions of VSRs are known to traffic to the same compartment as the endogenous receptor.

The role of the C-terminus of the VSR is to mediate interaction with cytosolic apparatus, in turn allowing for indirect association with vesicle coat apparatus (DaSilva et al., 2006; De Marcos Lousa et al., 2012; Sanderfoot et al., 1998). The ability of the C-terminus of the various receptor isoforms to interact with the cytosolic machinery was tested with a 'competition assay' (DaSilva et al., 2006). Overexpression of a GFP fusion in which the lumenal domain of the endogenous receptor is replaced with the fluorophore causes induced secretion of a co-expressed VSR cargo. This is thought to be due to the GFP-fusion competing with endogenous receptors by titrating the soluble recycling machinery thus causing receptor depletion at the ER-Golgi (DaSilva et al., 2005). Thus, the ability of a receptor to cause competition induced secretion indicates whether it interacts with the same cytosolic machinery as the endogenous receptor.

In this case, GUS could be used to normalise the expression of VSRs, which indicated that VSR5 seems not to interact with the same cytosolic machinery as VSR2. This is unexpected as the YXXϕ motif in the C-terminus of VSR2 which mediates interaction with cytosolic clathrin adaptor protein is present in VSR5. The only difference between the two is the second residue which is a methionine in VSR2 and Isoleucine in VSR5. The presence of this in the X position of the motif would not be abnormal under usual situations, however perhaps explains

the lack of competition, indeed cross-kingdom VSR5 is the only VSR with this point mutation.

3.3.2 VSR5 Localises to an Uncharacterised Compartment

A localisation analysis of the VSR protein family indicated that two of the VSRs (1 and 5) did not colocalise with the canonical VSR2. Taking into account the evidence that VSR5 interacts with different cargo and does not compete, the localisation of this GFP fusion was further analysed. The GFP-fusion of VSR5 was colocalised with various organelle markers of the plant secretory pathway. There was no co-localisation with any of the punctate structures, characterised by a low Spearman's correlation value and a split scatterplot. This lack of co-localisation is in contrast to other published findings (Lee et al., 2013; Miao et al., 2006). One possible explanation for this difference could be that other studies have used either the protoplast system or cell cultures which suffered from overexpression, whereas, in this study short expression times are used in a tobacco leaf epidermal expression system.

There are a series of open questions regarding the subcellular localisation of VSR5. The first being, to which organelle does VSR5 localise? This question is broadly addressed in the next chapter, however there are certain pieces of evidence available above. The presence of the increased core/precursor ratio in the immunoblot screen described previously (Fig. 2.7) indicates that the receptor leaks at least as much, and probably more, to the lytic vacuole. It would be fair to conclude, based on this, that the receptor localises to the recently discovered late PVC (LPVC, Foresti et al., 2010), an organelle that is placed distal to the PVC, at a later stage of the pathway in a biosynthetic sense.

A final open question relates to the function of VSR5. There are two potential theories that would explain the differences between the canonical receptor and VSR5. One explanation would be that it was a gene duplication or pseudogene that has been mutated via genetic drift and thus holds limited biological relevance, other than as a naturally occurring mutant to observe the lumenal/cytosolic binding dependences. The second possibility is that VSR5 is a specialised receptor, that perhaps is functionally relevant in a particular physiological context. The second of the hypotheses seems to carry more weight as there are differences in both the C-terminus and the lumen that seem to have specific effects on the functionality of both domains. In addition, publicly available expression data indicate that VSR5 is specifically upregulated in maturing leaves, the root meristem and roots and is highly co-regulated ($r^2 \sim 0.5$) with a number of genetic elements that seem to all be involved in cellular signalling pathways. This level of co-regulation is important as it implies active transcriptional control of the protein levels, by way of comparison the highest VSR2 co-regulating factor r^2 is approximately half that (~ 0.25) of VSR5. This would also allow us to speculate upon the function of the receptor, however there are a number of missing pieces of information, namely the ligand and the localisation of the receptor. The focus for the next chapter is in the understanding of the compartmental localisation of VSR5 in the vacuolar branch of the pathway and VSR5 in particular.

4 IDENTIFYING RESIDENTS OF THE LATE ENDOSOMAL SYSTEM IN PLANTS

4.1 INTRODUCTION

As discussed in detail in the previous chapters the secretory system is a complex network of organelles which interconnect to form a network. In *A. thaliana* the transport of soluble proteins to the vacuole is mediated by membrane spanning receptors (VSRs) that shuttle back and forth in the secretory system. Using a combination of techniques presented in the earlier chapters a VSR paralogue (VSR5) was shown not to co-localise with VSR2 at the MVB/PVC (Figure 3.2) and to have unique binding properties in both the lumenal and cytosolic domains (Figures 3.7, 3.5). When the VSR was localised, it did not localise to any of the characterised compartments of the secretory pathway (Figure 3.8), and was thus hypothesised to localise to the Late-Prevacuole (LPVC), a notion supported by the increased amount of 'GFP core' of VSR5. This could not be tested experimentally, as there are no characterised markers of the newly identified organelle.

The existence of this multi-vesicular body was first proposed from electron microscopy in mammalian systems (Palade, 1955) and later also observed in yeast (Hornick et al., 1985). This organelle was also observed in plant systems (Tse et al., 2004) and referred to as the pre-vacuolar compartment (PVC). Cross-kingdom, the MVBs have a similar structure. The organelle is spherical and contains internal vesicular like structures referred to as 'intralumenal vesicles' (ILVs).

Electron microscopy in plants identified two characterised markers of the PVC. The SNARE Pep12/Syp21 was shown to localise to a post-Golgi/pre-vacuolar compartment that was later shown to be the PVC. In addition the membrane

spanning VSR2 localises to the PVC. In addition both of these proteins can be fused to fluorophores and visualised using confocal microscopy. Pep12 can be N-terminally fused to a fluorophore. Likewise the receptor VSR2 can have the cargo binding lumenal domain replaced with a fluorophore to allow for CLSM visualisation.

However, although characterised as markers of the secretory pathway there are undesired pleiotropic side effects of using both chimeras in CLSM. Overexpression of Pep12 has been shown to interfere with the secretory pathway, inducing secretion of vacuolar sorted proteins (Foresti et al., 2006). There are two major observable effects of this interference, the induction of secretion of vacuolar cargo and the formation of large vacuolated organelles. Both of these effects are thought to be due to the excess of the Pep12 causing loss of membrane identity possibly due to titration of other interaction SNARE complex components. This loss of organelle identity and the formation of enlarged vacuolated organelles undermines its use as a marker for co–localisation studies. Aside from the effects of the Pep12, the GFP-VSR fusion also causes an undesirable effect on the cell. Overexpression of this chimeric protein in tobacco mesophyll protoplasts was shown to induce the secretion of vacuolar cargo (DaSilva et al., 2006; Foresti et al., 2010). This was explained by a titration effect as it was recoverable by the addition of the full-length VSR2 (DaSilva et al., 2005).

The complications due to the lack of any neutral markers of the late secretory pathway is has been increased by the recently discovery of the late prevacuolar compartment (LPVC). The LPVC was initially passively observed as the punctate structures that are visible in addition to the diffuse vacuolar fluorescence when visualising fluorophore fused vacuolar cargo. This organelle was established by a leucine to alanine point mutant in a YXXϕ of VSR2 (Foresti et al., 2010). This

compartment was also shown to be 'closer' to the vacuole in a biosynthetic sense as VSR(L-A) had increased degradation. The LPVC has the same micro-morphology as the MVB/PVC but it is enriched in the vacuolar cargo. This compartment is probably characterised by a depletion of wild type VSRs as they are recycled from the earlier PVC. The LPVC is finally expected to fuse to the vacuole to deliver its contents, which includes proteins targeted for degradation in ILVs as well as soluble vacuolar hydrolases targeted to the vacuole.

As discussed in the previous chapter, VSR5, has similar properties to the VSR2(L-A) mutant, showing a lack of co-localisation at the PVC and an increase in vacuolar delivery. Therefore it is proposed that the VSR5 localises to this compartment. However, in order to address this there need to be more markers established that will allow for neutral co-expression and localisation. In this chapter a number of protein-fluorophore fusions are co-localised with known markers in order to try and identify markers of either the PVC or LPVC and allow for further characterisation of these organelles.

4.2 RESULTS

4.2.1 N-terminally Fused VPS35 Can Not be Observed Recruited to Endosomes

One of the processes expected to occur as the PVC matures into in LPVC is the retrieval of the VSR back to the early secretory pathway. This signal-mediated retrieval mechanism has been linked to the retromer protein complex (Attar and Cullen, 2010; Seaman et al., 2012). The retromer complex is a pentameric complex consisting of two sub-complexes. The protein-binding sub-complex is a trimer made from VPS35, VPS26 and VPS29 (Seaman et al., 1997). The second sub-complex consists of a dimer of BAR domain containing sorting nexins that mediate the membrane curvature (Seaman et al., 1998). The keystone of the retromer complex is VPS35, as it binds directly to the cargo, and has been shown to bind to the VSR (Oliviusson et al., 2006). There are three VPS35 paralogs in *Arabidopsis thaliana* a, b and c (AT1G75850, AT2G17790 and AT3G51310 respectively) (Table 4.1). Publicly available *in silico* co-regulation microarray data shows that expression of *A. thaliana* VPS35a is highly regulated with that of a vacuolar sorting receptor (ELP1/VSR1). There are also homologous members in plants for all members of the complex (Table 4.1).

In order to try and localise the retromer protein complex using CLSM in plant epidermal tissue and to try and identify a novel marker of the late endosomes VPS35a was fused N-terminally to YFP. The expression cassette was subcloned into an *A. tumefaciens* expression vector which was used to transform *A. tumefaciens*. This strain was infiltrated into Tobacco leaf epidermal tissue. After 24-48 hours expression a 1cm^2 leaf section was excised and imaged by CLSM (Fig. 4.1). The layer of cytosol above the vacuole and beneath the plasma membrane in a

Accession	Arabidopsis	Yeast Homologue	Mammalian Homologue
AT2G17790	VPS35a	VPS35	VPS35
AT1G75850	VPS35b	VPS35	VPS35
AT3G51310	VPS35c	VPS35	VPS35
AT5G53530	VPS26a	Pep8p/VPS26	VPS26a
AT4G27690	VPS26b	Pep8p/VPS26	VPS26a
AT3G47810	VPS29	VPS29	VPS29
AT5G58440	SNX2a	VPS5p	SNX2
AT5G07120	SNX2b	VPS5p	SNX2
AT5G06140	SNX1	Snx4p	SNX2

Table 4.1: **Retromer Homologues in Plants**
A table comparing the various *A. thaliana* retromer homologues with the Yeast and Mammalian counterparts. Based on primary data from the BLAST protein database (Altschul et al., 1990) and published findings (Fuji et al., 2007; Jaillais et al., 2007; Oliviusson et al., 2006; Shimada et al., 2006; Yamazaki et al., 2008).

region of the cell referred to as the 'cortex' in particular was imaged to observe punctate structures. There were no detectable punctate structures observed. All cells displayed strictly cytosolic fluorescence distinguishable by a diffuse, uneven pattern with negative 'shadows' from organelle occupied space.

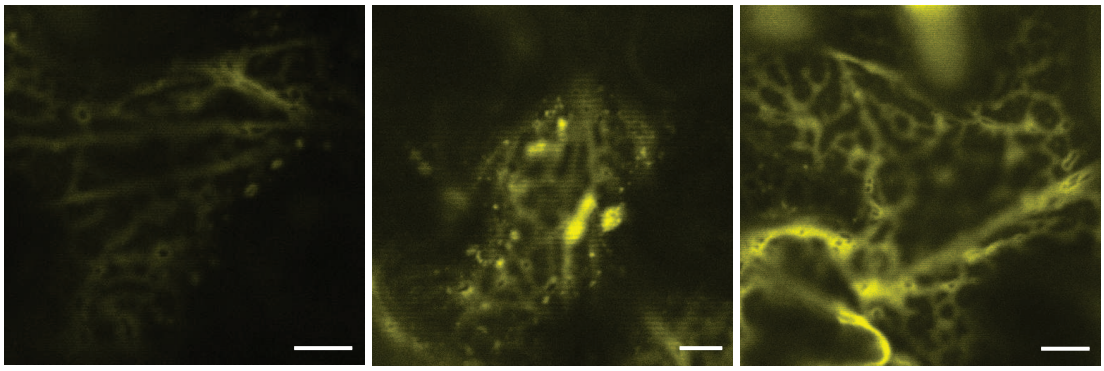

Figure 4.1: **An N-terminal YFP fusion is cytosolic**
Agrobacterium strains encoding for an N-terminal YFP fusion of VPS35a in tobacco epidermal tissue was imaged using CLSM of the cell cortex. Notice the blurred reticulate like structure of the cytosol, as well as the negative 'shadows' of the non-labelled organelles suspended within the cytosol. Marker = $5\mu m$.

In order to try and promote organelle recruitment the VPS35 was expressed over longer times and co-expressed with full length VSR, however neither condition induced membrane recruitment (data not shown). One possible explanation is

that the VPS35 recruitment to the membrane is dependent on the concentration of other soluble factors. It is also possible that the VPS35 isoforms work in redundancy in some tissues and not others, or the YFP-fusion is non-functional or over-expressed.

4.2.2 VPS29

In order to further observe the retromer protein complex a different component of the core-subcomplex was selected. VPS29 has only one paralogue in *A. thaliana* (Table 4.1), and is therefore more likely to be ubiquitously involved in plant retromer. VPS29 is a component of the core trimer of the retromer complex and has a catalytically inactive metallophosphoesterase fold that allows for interaction with two metal ions and in turn the interaction with VPS35 (Collins et al., 2005; Hierro et al., 2007). To identify the localisation of the retromer complex in *A. thaliana* VPS29 was C-terminally fused to both RFP and GFP, a strategy that proved successful in mammalian cell lines (Rojas et al., 2008). The fusion chimera was subcloned into an *A. tumefaciens* expression vector, and used to transform *A. tumefaciens*, infiltrated into Tobacco leaf epidermal tissue, expressed as above and imaged accordingly (Figure 4.2).

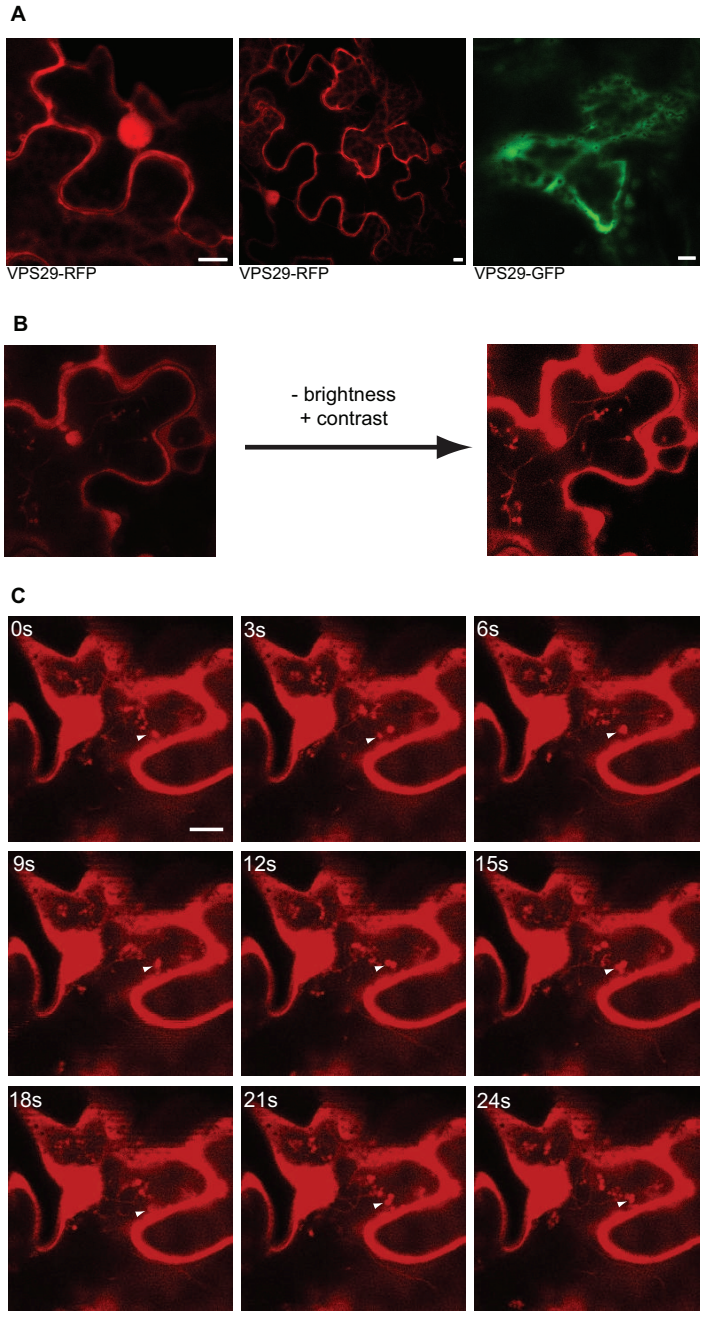

Figure 4.2: **VPS29-RFP and VPS29-GFP is Mostly Cytosolic as well as Being Recruited to Tendril-like Structures**
A. Agrobacterium strains encoding C-terminal GFP and RFP fusions of VPS29 were used to infiltrate tobacco epidermal tissue, which was imaged using CLSM of the cell cortex region. Notice the blurred reticulate like structure of the cytosol, as well as the negative 'shadows' of the non-labeled organelles suspended within the cytosol. In addition the nucleus in the left panel indicates a soluble cytosolic protein. in Marker = $5\mu m$.
B. The image adjustments made in ImageJ (*http://imagej.nih.gov/ij/*) to better observe the structures.
C. A time series of adjusted images showing the movement of the 'tendrils'. The white arrowhead points to an uncharacterised motile structure. The time point is indicated in the top left of each micrograph.

Upon initial analysis it appeared as if the fusion proteins are cytosolic similar to the VPS35, as shown by the diffuse fluorescence throughout the cytosolic cortex, nuclear pattern and the negative organelle punctae (Figure 4.2, A). Further imaging showed unusual structures in a subset of cells expressing either the VPS29-GFP or the VPS29-RFP (Figure 4.2, C). These structures can be better observed when the brightness is decreased and the contrast increased due to the brightness of the cytosolic background (Figure 4.2, B). They are most observable within the centre of the cell, perhaps as they pass through intervacuolar strands. They are highly motile and could be described as organelle like structures connected by tendrils. No such structures have previously been reported in the literature. Although attempts were made to further characterise the observed punctae, the compounded experimental effects of the high background:signal ratio and the fact that they were present in a small subset of cells ($< 10\%$) made any meaningful statistical localisation impractical. However, it cannot be ruled out that the tendrils represent retromer tubules (Rojas et al., 2008) as they would be infrequent and short lived.

4.2.3 FYVE Protein

Due to the difficulties described above with recruiting retromer to the membrane in the Tobacco leaf epidermal system a different approach was attempted. The mammalian protein Early Endosome Antigen 1 (EEA1) localises to the early endosomes of mammalian cells, via its FYVE domain (Lawe et al., 2000). The FYVE domain was named after four proteins (Fab1p, YOTB, Vac1p and EEA1) that contain this motif (Stenmark et al., 1996). Biologically this protein domain binds to phosphatidylinositol-3-phosphate (PI3P), an amphiphile that integrates into lipid bilayers. Indeed, a chimeric protein containing two tandem FYVE domains and a fluorophore can be used as a 'biosensor' for the endosome enriched

PI3P both in mammalian cells and plants (Gillooly et al., 2000; Vermeer et al., 2006). In order to try and find more markers of the late endosomal system in plant cells an *in silico* 'BLAST' protein homology analysis (Altschul et al., 1990) was undertaken with the FYVE domain of human EEA1 against the genome of *A. thaliana* (Table 4.2).

Accession	Annotation	Homology
AT3G43230	zinc finger (FYVE type) family	67
AT1G29800	phosphoinositide binding	64
AT1G20110	zinc finger (FYVE type) family	62
AT5G12350	Ran GTPase binding	62
AT5G42140	zinc finger protein	62

Table 4.2: **FYVE Domain Containing Proteins in *A. thaliana***
A table comparing the various FYVE domain containing proteins found annotated in the *A. thaliana* database, found from a BLAST search of the FYVE domain from EEA1 (Altschul et al., 1990). Also shown is the annotation of each sequence as well as the homology (% similarity) found.

This study was in agreement with a similar *in silico* analysis, which found 27 FYVE domain proteins in plants (Wywial and Singh, 2010). The gene with the most homology, AT3G43230, named here as *At*FYVE1, is noted to contain a Domain of Unknown Function in addition to the FYVE domain. The gene expression is highly correlated with a number of other genes with secretory pathway like functions, of note are a RAB5A like protein and a exocyst complex component-related protein. The gene was cloned from an *A. thaliana* cDNA library and fused C-terminally to RFP as the FYVE domain is closer to the N-terminus. Subcloning, expression and imaging was as in previous experiments (Figure 4.3).

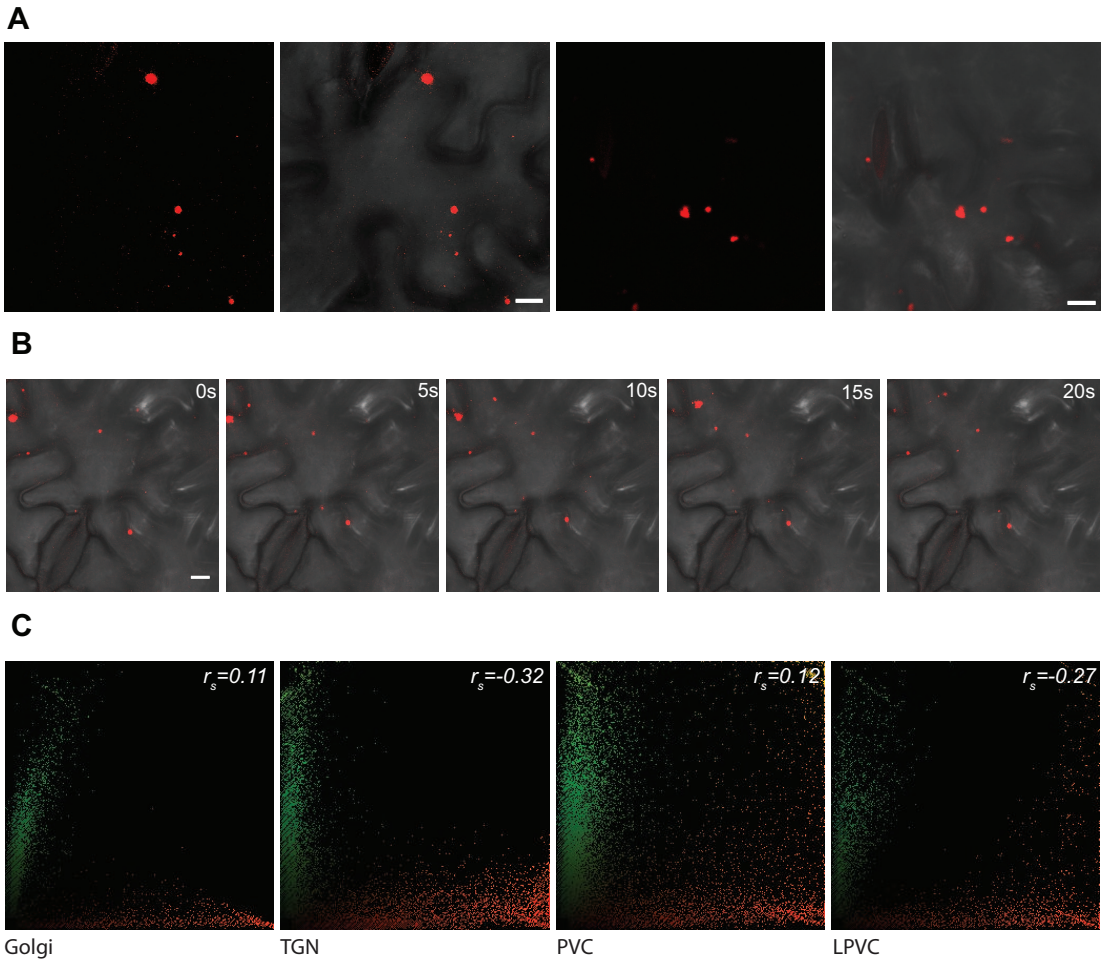

Figure 4.3: **An *A. thaliana* FYVE Domain Containing Protein, *At*FYVE1, is Recruited to an Undefined Organelle when Fused to RFP**
A. Agrobacterium strains containing plasmids encoding for C-terminal RFP fusions of *At*FYVE1 were infiltrated into tobacco epidermal leaves and the tobacco cells imaged. Two images with corresponding DIC are shown in the panel. Notice the variability in the size of the structures. Marker = $5\mu m$.
B. A time series with overlayed DIC showing the motility of the FYVE organelles.
C. A statistical analysis of *At*FYVE1 fusion protein colocalised with markers of the secretory pathway. Golgi marker = St, TGN marker = SYP61, PVC marker = VSR2, putative LPVC marker = Aleurain. The Spearman's rank correlation value can be seen in the top right of the image.

*At*FYVE1-RFP localises to large organelle like structures within the cytosol of Tobacco leaf epidermal cells (Figure 4.3, A). These structures varied in size and are unlike previously characterised organelles or endosymbionts of the plant cell. In order to test if these were protein aggregates, the motility of the structures was monitored over time (Figure 4.3, B), showing that they have motility as observed

with other organelles. To analyse whether these were either 1) aggregations of a known organelle or 2) a novel structure a full co-localisation series was performed (using GFP-VSR2 as a marker for the PVC and the cargo Aleu-GFP as a marker for the LPVC), a statistical analysis was performed to see an overview of the findings (Figure 4.3, C). There was no general co-localisation observed to any one particular organelle. There is a second protein (accession:AT1G20110, here: *At*FYVE2) that contains a similar DUF/FYVE domain structure that was observed in the *in silico* analysis presented here (Table 4.2) and by Wywial and Singh (2010).

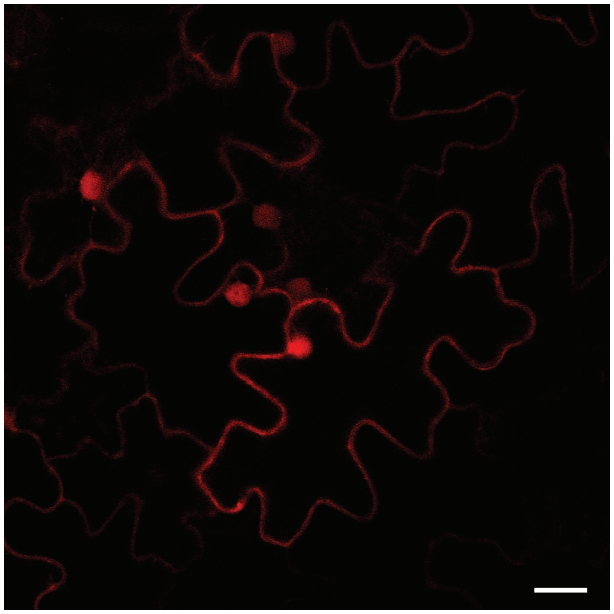

Figure 4.4: **An *A. thaliana* FYVE Domain Containing Protein, *At*FYVE2, is Cytosolic when Fused to RFP**
Agrobacterium strains containing plasmids encoding for C-terminal RFP fusion of *At*FYVE2 in tobacco epidermal tissue was imaged using CLSM of the cell. Notice the nucleus of multiple cells and the smooth cell outlines indicating a soluble cytosolic protein. Marker = $10\mu m$.

*At*FYVE2 was subjected to a similar analysis as *At*FYVE1, and did not localise to these organelles, but instead appeared to have a cytosolic fluorescence pattern (Figure 4.4). Thus, the role of *A. thaliana* FYVE domain proteins remains uncharacterised, and warrants further investigation, which is outside the scope

of this chapter. The work so far did not result in the identification of a reliable novel marker for the late endosomal pathway, and thus other strategies to identify one needed to be attempted.

4.2.4 VAMP727

There are a number of SNARES that localise to the late endosomal system, one being the original marker for the PVC, Syp21/Pep12. Syp21, however, causes pleiotropic effects to secretion when overexpressed (Foresti and Denecke, 2008) and does not localise as efficiently to the PVC when expressed under control of a weaker promoter (Personal communication from Dr. De Marcos Lousa, University of Leeds). Therefore Syp21 was ruled out as a marker. Within most tetrameric SNARE complexes there are three Q SNAREs and an R SNARE, Syp21 is a Q SNARE in a complex that also contains the R SNARE VAMP727. VAMP727 has been shown to localise to the PVC and to the tonoplast when under control of the constitutive CaMV35S promoter (Ebine et al., 2011; Ueda et al., 2004). This construct, however, has also been shown to induce the secretion of vacuolar cargo and cause similar vacuolation effects as Syp21/Pep12 (Denecke Lab, unpublished data). The ORF and 3'NOS terminator was subcloned into an *A. tumefaciens* expression vector under control of the TR2' promoter that has been shown to have weaker expression than the CaMV35S promoter, to limit the overexpression effects. The colocalisation analysis was performed with the standard markers of the organelles, as well as the Aleurain cargo, a putative marker of the LPVC, that was shown not to co-localise with VSR2 (Foresti et al., 2010).

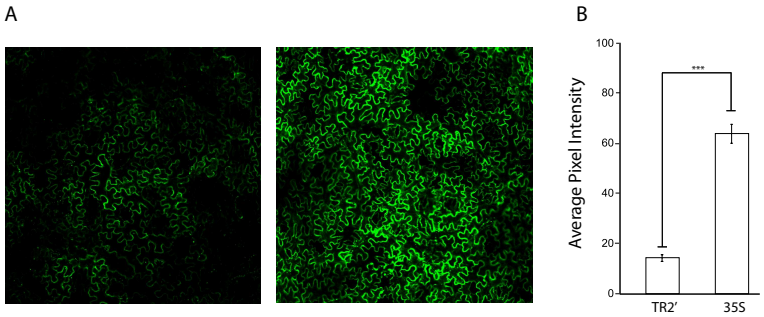

Figure 4.5: **The TR2' Promoter is Weaker than the CaMV35S Promoter in Tobacco Leaf Epidermal Cells**
A. Two widefield images showing VAMP727 under control of the TR2' promoter (left) and the CaMV35S promoter (right). Notice the appreciable difference in the intensities of the images. **B.** Multiple images from the dataset shown in panel A. were sampled with a fixed area. The mean pixel intensity was sampled for ~ 10 per image across 4/5 images. These mean intensities were compiled and averaged. The average of the mean intensities can be seen on the Y-axis with the standard error of the mean intensities of each dataset shown by the error bar. A Mann-Whitney test showed the difference significant to three decimal places (Mann-Whitney U = 400, n1 = n2 = 20, P <0.0001, two-tailed).

Figure 4.5 shows that the TR2' promoter causes lower levels of fluorescence than the CaMV35S in infiltrated Tobacco leaves. In order to see if the weaker expressed TR2' promoter localises to the endosomal system a statistical co-localisation series was generated. The TR2' VAMP727 was co-localised with markers for the secretory pathway and a PSC statistical analysis undertaken (Foresti et al., 2010; French et al., 2008).

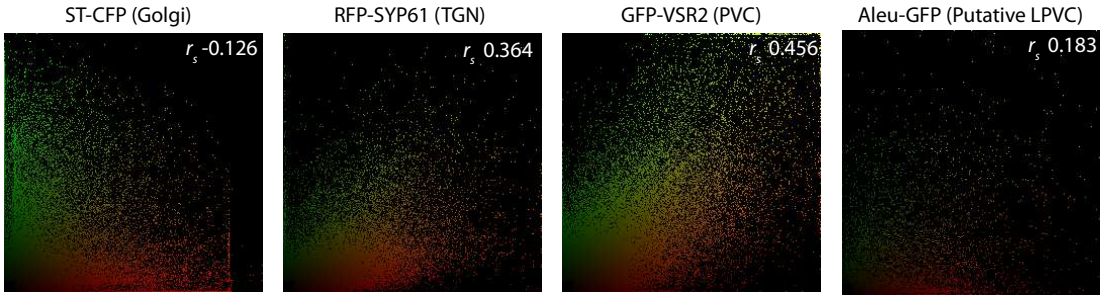

Figure 4.6: **A Statistical Analysis Indicating that TR2' VAMP727 Localises to the Late Secretory Pathway**
A. A statistical analysis was undertaken on datasets comprising of TR2'–VAMP727 with common markers of the secretory pathway. The Spearman's rank correlation value can be seen in the top right of each scatterplot.

As can be seen in Figure 4.6 the VAMP727 localises to the TGN/PVC/LPVC, but not the Golgi apparatus. The localisation to these late-pathway organelles appears to be mainly to the PVC, which has a high PSC correlation value (0.456), however there is also a high level of correlation with the TGN marker SYP61 (0.364). There appears to be a population of organelles that only contain red pixels (SYP61). This observation represents complex co-localisation due to the protein being in multiple compartments and thus is difficult to interpret in its current format.

4.2.5 Development of Population Distribution Analyser

The localisation analysis with VAMP727 was an example of a complex localisation analysis. These are difficult to appreciate due to the number of situations that can arise (For examples, see Fig. 4.7, A). There can be co-localisations arising from situations where a protein localises either to a number of compartments, partially overlapping with a marker in two classes or where a protein localises to a subset of a particular compartment. These situations are biologically relevant but often overlooked due to the difficulty in discerning the complexity of the localisations using traditional techniques. The scatterplots (as exemplified in Fig. 4.7, A) display this information as they are a complete representation of every pixel in all the images in this study, with the relative frequency of a certain red:green ratio represented by the intensity on the plot. The data are still difficult to comprehend visually as there can be situations where a particular population is spread across a variety of intensities or is focused on a smaller section of the plot. These data are better presented in a histogram where the relative red:green ratios can be qualitatively compared.

In order to better present these data a macro was generated for ImageJ (*http://imagej.nih.gov/ij/*) that groups the pixels from a single scatterplot into 16 different categories with increasing red/green ratios. The first 'bin' indicates all pixels that have a red/green ratio between 0 and 6.25 % red, the second bin includes ratios from 6.25 to 12.5% red and so on until the 16th and final bin which includes 93.75100% red. In each 'bin' the mean red intensity, the mean green and the mean total is collected. These data can then be visually compared on a histogram plot to display complex co-localisations in an appreciable manner.

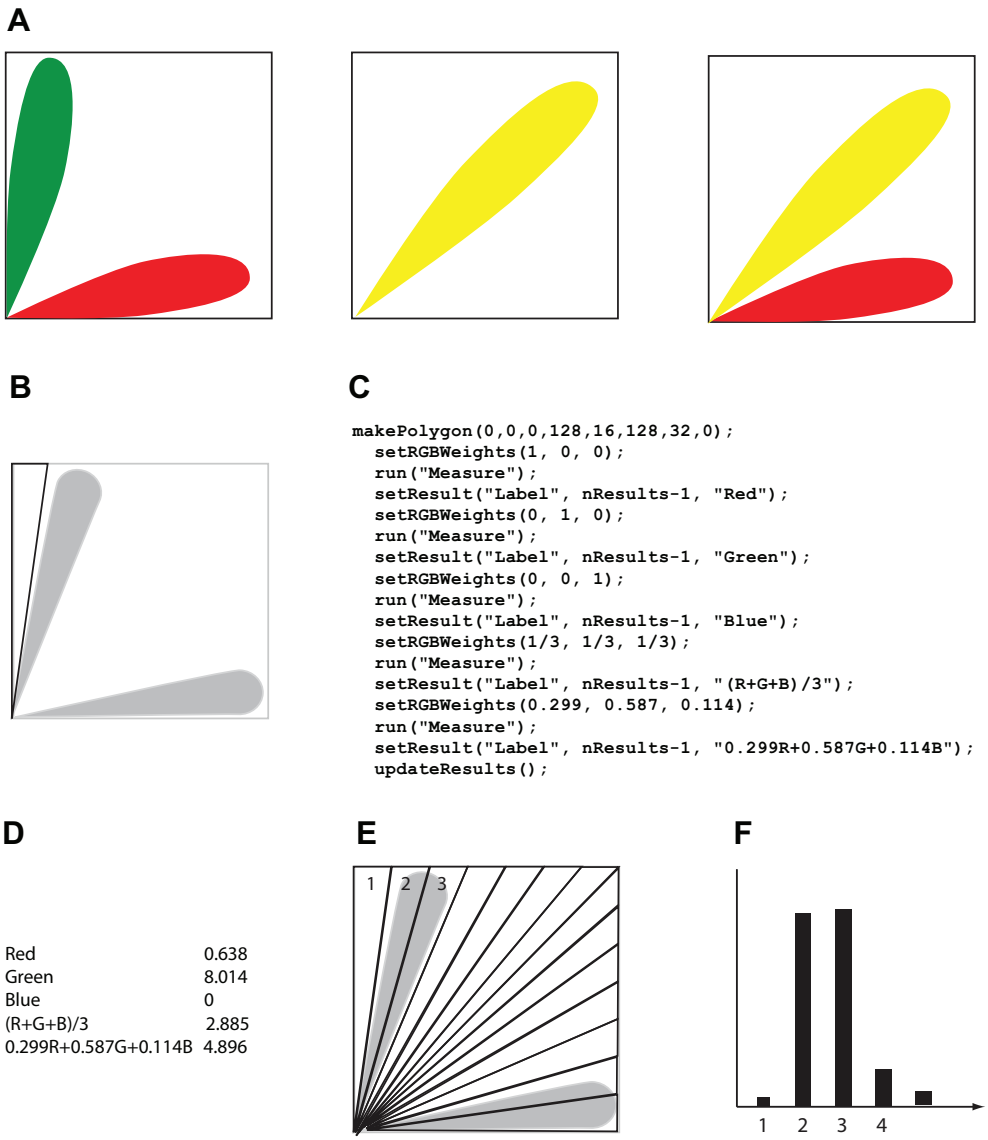

Figure 4.7: **Qualitative Appreciation of Complex Localisation Scatterplots**
A. Representative images of scatterplots showing a non co-localisation on the left, a co–localisation in the center and a complex localisation on the right.
B. An image showing the sampling method used to split the image up into 'pie–like' slices.
C. A sample of the macro used to make the slice seen in panel B. 'makePolygon' defines the shape. The entire macro is a repetition of this sample, with different polygons to define each slice, of equal pixel area.
D. An example of the output for one section. The 'red' and 'green' headings define the mean intensity of the red and green channels. The remaining outputs were discarded.
E. An image showing a scatterplot split up into segments. The sampling output shown in D. was gathered for each segment.
F. An example of the expected output of the analysis of the scatterplot of panel E shown on a histogram.

Figure 4.7 shows how a scatterplot can be converted into a histogram to compare different co–localisations. In order to better compare the co–localisation data for the VAMP727, this technique was applied to this dataset. Each scatterplot from Figure 4.6 was subjected to the 'population distribution analysis' macro in ImageJ.

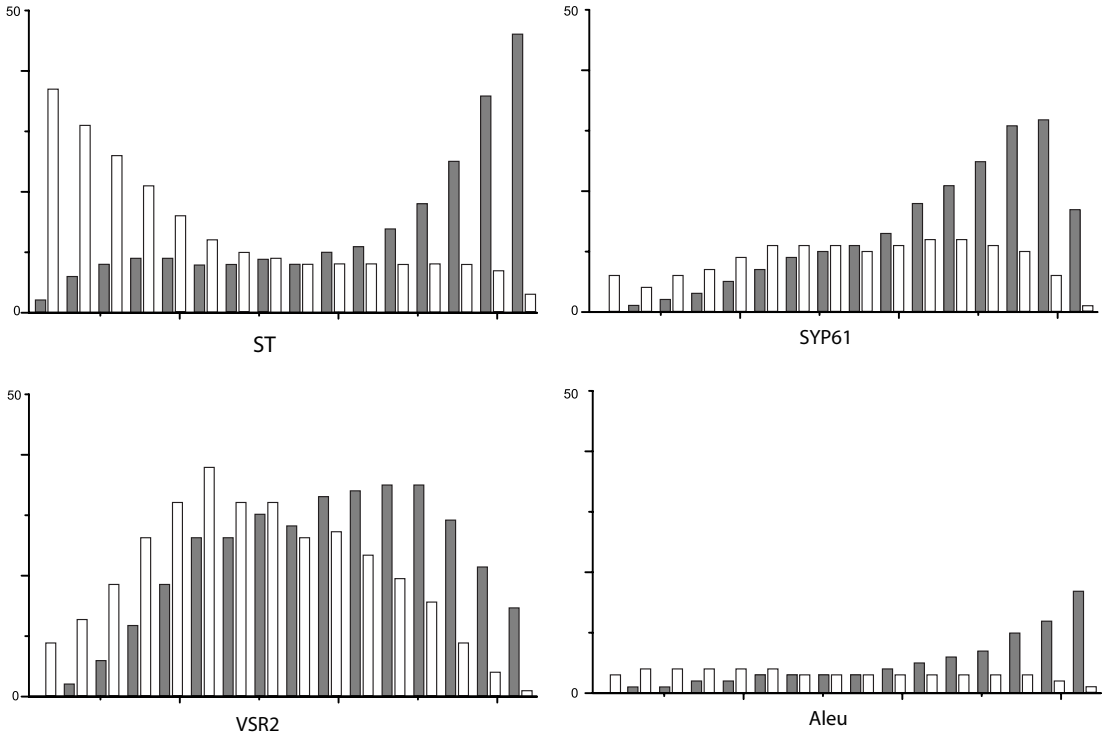

Figure 4.8: **A Population Distribution Analysis Indicates that VAMP727 Localises to the Late Secretory Pathway**
The 'population distribution analysis' described in Figure 4.7 was performed on the scatterplots in Figure 4.6. The VAMP727 intensity is represented by the grey bars and the corresponding markers are represented by the white bars. The furthermost left bars represent the red/green ratio between 0 and 6.25 % red and progress to a red/green ratio between 93.75 and 100 % red. The Y-axis represents the mean pixel intensity for each colour (max=255).

As can be seen in Figure 4.8 the localisation data is much clearer using the 'population distribution analysis' and histogram display. The Golgi marker ST-CFP shows very little or no co–localisation with the VAMP727 which can be observed by the two non co-localising populations either the ST marker (white bars) or the test object, VAMP727 (grey bars). The TGN marker, RFP-SYP61

has more of a complex co–localisation, with a co-localising population and a non co-localising population to the right of the histogram. There is a clear increase in the amount of co–localisation with the PVC marker, VSR2 – it appears as if the VAMP727 primarily localises to the PVC. The final co–localisation with the putative marker of the LPVC, Aleurain, shows a situation similar to the SYP61, however there is also a small amount of VAMP727 alone organelles (green bars on left of graph). Although these results strongly implicate VAMP727 as a marker of the PVC, it is also clear that the VAMP727 localises to multiple organelles, even when weakly expressed. It is due to this that the VAMP727 is not suitable as a standard marker of the PVC.

Despite VAMP727 partially localising to the PVC, even under low expression conditions it seems to also localise to other organelles, potentially implying that it is having effects on organelle identity and conclusively ruling it out as a useful and practical endosomal marker.

4.2.6 Low Expression of RabGTPases

The last potential marker of the PVC/LPVC system available is the RabGTPase family. The characterised RabGTPases that have roles in late secretory pathway are the Rab7 family and the Rab5 family. The Rab7 family mediates the fusion of the late endosome/LPVC to the vacuole and localises to the tonoplast in plants. There are three Rab5 paralogues in *A. thaliana*, all thought to be functionally involved in the biogenesis/maturation of the PVC family that localise to the PVC, however, they also affect vacuolar sorting, inducing secretion of vacuolar cargo when overexpressed. In order to avoid these effects and obtain a non-disrupting marker of the PVC one of the *A. thaliana* Rab5 (RhaI) paralogues, fused to the YFP

analogue Venus, was subcloned to be under control of the TR2' promoter, as above. This effector region was further subcloned into an *A. tumefaciens* expression vector that was used to transform *A. tumefaciens*. Tobacco leaf epidermal cells were infiltrated with the *A. tumefaciens* strain harbouring TR2'-Venus:RhaI-3'NOS and an array of markers for the secretory pathway. After 24-32 (low expression) hours expression a leaf disk was imaged by CLSM from each sample (4.9).

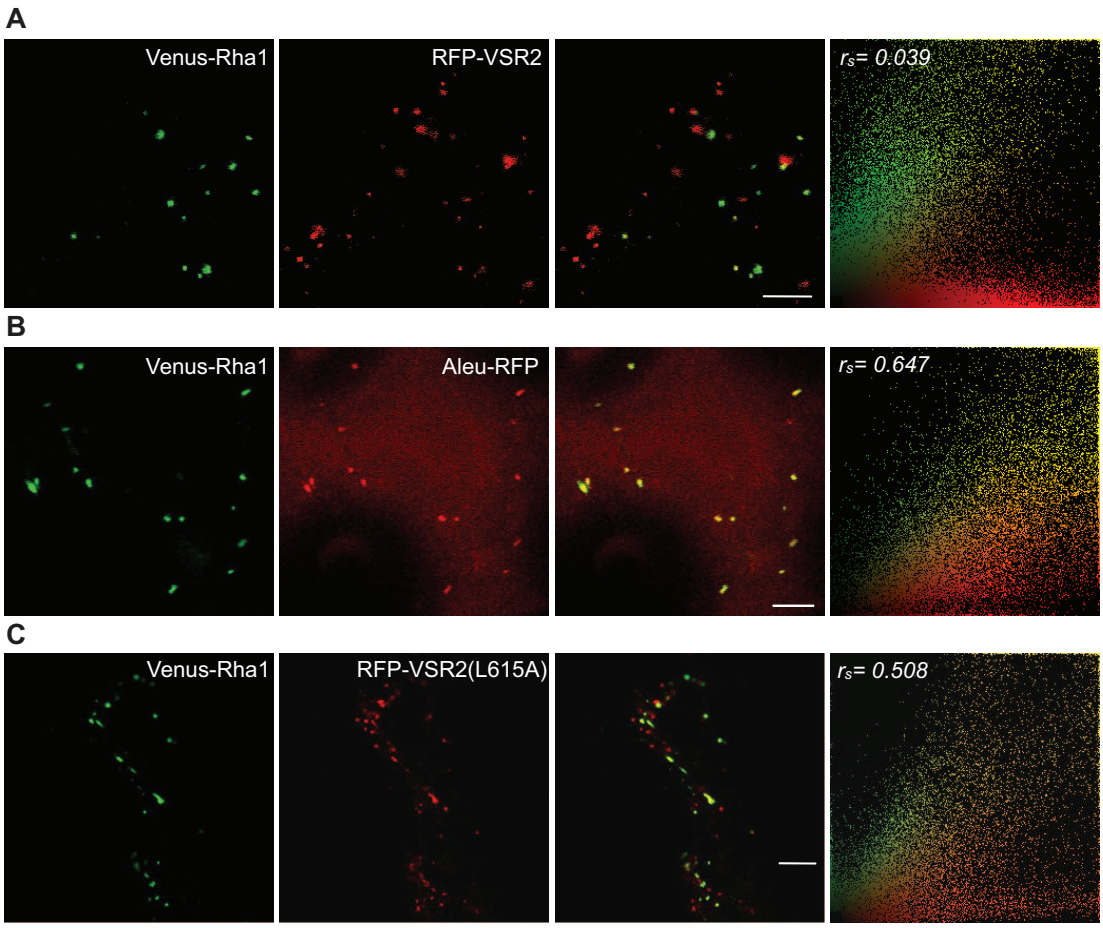

Figure 4.9: **Weak Expression of RhaI-YFP Localises to the LPVC**
In situ coexpression experiment in tobacco leaf epidermis cells using Venus-Rha1 (green) as test object. Marker = 10 μm.
A. Coexpression with wild-type RFP-VSR2 as a PVC marker
B. Coexpression with the soluble vacuolar cargo Aleu-RFP as a putative LPVC marker.
C. Coexpression defective RFP-VSR2(L615A) as a secondary putative LPVC marker.
Notice that both Aleu-RFP and RFP-VSR2(L615A) show much higher correlation coefficients when coexpressed with Venus-Rha1 compared with the wild-type RFP-VSR2.

After extended statistical analysis it appears as if the RhaI under control of the TR2' promoter does not localise to the PVC demonstrated by the two-population scatterplot and the low/negligible Pearson and Spearman's correlation value. Instead, the RhaI co-localises to the LPVC demonstrated by the single population of the scatterplots and high Pearson and Spearman's correlation value with both the cargo and the recycling deficient mutant. This additional marker reaffirms the organelle as a biologically relevant compartment and not an artifact. In addition, these data demonstrate clearly that the Aleurain localisation represents an accumulation of cargo on the vacuolar route. Finally, the RhaI is topologically distinct providing a relevant addition to the portfolio of markers. A number of studies have observed a difference between the Rab5 paralogues RhaI and Ara6, so the localisation of a weakly expressed Ara6 was also analysed to screen for a potential difference between the two Rab5s when under weaker promotion.

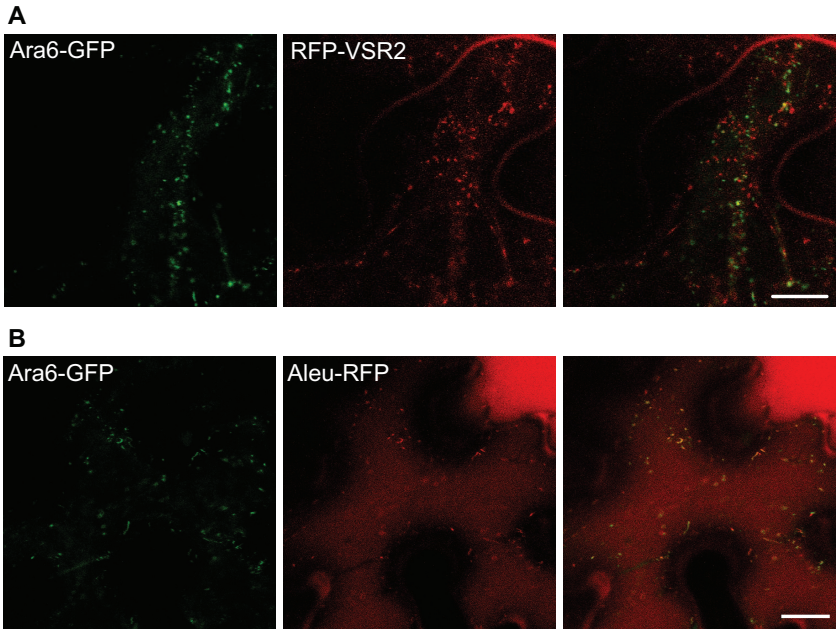

Figure 4.10: **TR2' Ara6-GFP Localises to the LPVC**
A. Co–expression of TR2'–Ara6-GFP with the PVC marker RFP–VSR2. Notice the lack of co–localising organelles. Marker = 10μm.
B. Co–expression of TR2'–Ara6-GFP with the LPVC marker Aleurain–RFP. Notice the co–localising punctate structures. Marker = 10μm.

A non-statistical microscopy screen also showed that the Rab5 paralogue Ara6 localises to the LPVC as well as the RhaI, establishing both the Rab5 proteins as markers for the LPVC and allowing the AleuRFP to be considered an acceptable marker for the organelle, as the punctae showed good co–localisation with the Rab5 markers.

4.2.7 VSR5 Localises to the LPVC

The final question to be addressed here is the question initially posited at the end of the previous chapter and later in the introduction of this chapter, namely: 'does VSR5 localise to the LPVC?'. Above, the use of the Rab5 paralogues Ara6 and RhaI as well as the soluble cargo (AleuRFP) have all been justified as markers of the LPVC. This allows the use of a marker that has been tested as a GFP, YFP and RFP fusion. Previously, VSR5 has been analysed as a GFP fusion and in order to remain consistent a co–localisation was performed with the RFP marker of the LPVC, AleuRFP as well as the novel marker, RhaI - under control of the weak pNOS promoter.

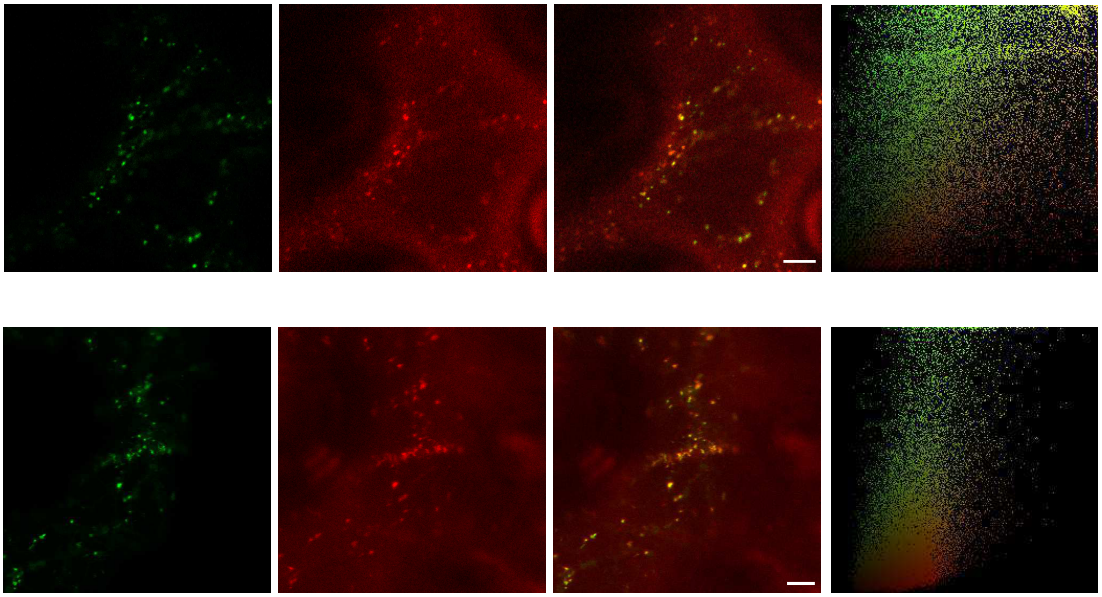

Figure 4.11: **GFP-VSR5 Localises to the LPVC**
A. Co–expression of GFP-VSR5 with the LPVC marker Aleu-RFP.
B. Co–expression of GFP-VSR5 with the LPVC marker RFP-Rha1.
Notice the co–localisation of the organelles in both datasets. Marker = 5μm. The right panel shows the statistical data from a large dataset (15-20 images).

The two *A. tumefaciens* strains harbouring the coding regions of AleuRFP and GFP-VSR5 were co-infiltrated into the leaf epidermis and imaged by CLSM (Figure 4.11). The images coupled with a co–localisation analysis show clearly that there is a high co–localisation between the VSR5 and the soluble cargo in the LPVC. There is a single population in the scatterplot and a high Spearman's correlation value, which is in contrast to the lack of co–localisation with any of the remaining markers of the secretory pathway organelle (see Fig. 3.8) indicating that the VSR5 localises to the LPVC. This means that unlike other VSRs which recycle slowly from the PVC and show the highest steady state levels in this compartment, VSR5 is targeted beyond the PVC and reaches the LPVC. This could either be due to lack of recycling from the PVC or enhanced anterograde transport towards the LPVC due to a new active transport mechanism.

4.3 DISCUSSION

4.3.1 The Localisation of Plant Retromer

In this study fluorophore fusions of the retromer components VPS35 and VPS29 were primarily localised to the cytosol of Tobacco leaf epidermal cells. Previous immunofluorescent localisation has localised the endogenous VPS35 to the PVC (Oliviusson et al., 2006), whilst the endogenous VPS29 has been localised to the TGN (Niemes et al., 2010a). The sorting nexins have been expressed as fusion proteins and have been localised to the TGN (Niemes et al., 2010a). The lack of the recruitment of the ectopically expressed VPS35/VPS29 in this present study perhaps hints that the activation of the retromer complex is concentration and/or situation specific.

Tendril like structures were seen in a subset of the cells expressing VPS29-RFP and GFP. These structures are undefined in the literature and appear unlike any other known organelles. Attempts to colocalise them were unsuccessful due to their low frequency of occurrence and their position in the cell. One potential explanation is that, when highly expressed, the VPS29 induces the formation of large scale retromer mediated tubulation of the membrane. Another possible explanation would be that these retromer tubules represent *in vivo* transport, happening not as a gradual retrieval of the VSR from the PVC, but in defined abrupt steps when a critical mass of retrograde cargo has accumulated. This would explain their infrequent appearance and short lived existence. There have been tubular-like structures previously observed in electron micrographs of plant MVBs (Scheuring et al., 2011). This model could explain the abundance of the VSR in the PVC and the lack of the VSR in the LPVC.

4.3.2 The FYVE Domain Protein Family

Phosphotidlyinositiol-3-phosphate (PI3P) is a lipid enriched in the late endosomal system. The retromer sorting complex has affinity for PI3P as do proteins containing the FYVE domain. The FYVE domain protein family in plants has 15 members (Wywial and Singh, 2010). Two of these members, named here as *At*FYVE1 and *At*FYVE2 share a similar domain structure, with a FYVE domain on the C-terminal side of the center of the protein and an N-terminal 'Domain of Unknown Function'. When C-terminally fused to a fluorescent protein, *At*FYVE1 was recruited to a unknown cellular structure and *At*FYVE2 was cytosolic. *At*FYVE1 containing structures were motile, indicating that they were not just protein/lipid aggregates and showed no major co–localisation with any secretory organelles, although there was occasional co–localisation with the PVC and LPVC. There were also notably few per cell (1-3 per slice, perhaps 10-15 per cell) and they also varied in size and shape, from diffraction limiting to some approaching 500μm. The cytosolic nature of *At*FYVE2 suggests that although the two proteins are homologous they have functional divergence. It also suggests that *At*FYVE1 might be associating to the membrane by more than just the FYVE domain. The function of both of these proteins remains unknown and it would be interesting to investigate the function of these proteins and the *At*FYVE1 organelle further.

4.3.3 VAMP727 Localises to Multiple Organelles

Expressing the SNARE VAMP727 with a weaker promoter in Tobacco leaf epidermal cells reduced the obvious vacuolation caused by overexpression. The localisation analysis also showed that the VAMP727 did localise to the PVC,

however a major fraction of the protein also localised to the plasma membrane and a subsection to the TGN. The influence that VAMP727 has on constitutive secretion and vacuolar sorting has never been formally directly compared with other inhibitors, however the multiple localisations could hint at inhibitory effects despite weak expression of the fusion protein. Alternatively, there is evidence that VAMP727 localises to the plasma membrane using total internal reflection fluorescence microscopy, and that it interacts with effectors at the membrane (Ebine et al., 2011), perhaps, therefore the VAMP727 plays a role in multiple SNARE complexes at multiple locations. It is also for these reasons that VAMP727 would be a poor organelle marker.

4.3.4 The Plant Rab5s Localise to the LPVC

Weak expression coupled with statistical localisation data showed that the Rab5 GTPases Rha1 and Ara6 are independent markers for the LPVC , showing that LPVC structures are not an artifact caused by expression of an aberrant receptor molecule. This localisation allows earlier results on the localisation of this class of GTPase to be further refined (Bolte et al., 2004; Haas et al., 2007b; Kotzer et al., 2004; Lee et al., 2004; Sohn et al., 2003; Ueda et al., 2001, 2004). In addition, we can speculate about the nature of the LPVC because it has been shown that the three Arabidopsis Rab5 GTPases are found to localize to multivesicular bodies using immunogold electron microscopy (Haas et al., 2007b). For this reason, it is very likely that both PVC and LPVC exhibit a multivesicular morphology. Internal vesicles are destined for vacuolar degradation and should not be affected by the process of receptor retrieval from the delimiting membrane. The differences between PVC and LPVC are thus likely to be restricted to the exact lipid and

protein composition of the delimiting membrane, although the heterogeneity of the lipid distribution is unknown.

4.3.5 VSR5 Localises to the LPVC

The localisation of the Rab5s at the LPVC and their co–localisation with Aleu-RFP justified the use of Aleu-RFP as a marker of the organelle. Due to the increased amount of vacuolar core, it had been hypothesised that the VSR5 was a non-recycling VSR and thus would have a high steady state level at the LPVC, similar to non-recycling mutants of the canonical receptor (Foresti et al., 2010). Therefore, the localisation of VSR5 was tested using Aleu-RFP as a marker of the LPVC. VSR5 seemed to significantly localise to the LPVC, especially when comparing the result to the lack of localisation seen with VSR2 in the previous chapter. A hydrophobic leucine within the YXXϕ motif of the VSR2 C-terminus has been shown to be responsible for the recycling of the receptor from the PVC to the early secretory pathway (Foresti et al., 2010). Interestingly, the apparently recycling deficient VSR5 contains this motif including the leucine essential for recycling. The motif is not identical, VSR2 contains a YMPL, whereas VSR5 contains a YIPL – a potential explanation for the lack of recycling. Alternatively there are other differences between the two C-termini that could possibly explain this difference as explored in the previous chapter.

5 EXPORT OF PLANT VACUOLAR SORTING RECEPTORS FROM THE ENDOPLASMIC RETICULUM TO THE GOLGI APPARATUS IS MEDIATED BY THE COPII MACHINERY

5.1 INTRODUCTION

The development of novel techniques and screens in the previous chapters identified VSR5 as a unique vacuolar sorting receptor. In addition, markers of the late endosomal system were characterised. These findings raise questions on the route of the canonical trafficking of the VSR receptors. In particular, we can attempt to address some of the questions outlined at the start of this thesis: '1) What are the initial trafficking steps of the VSR? 2) How does the VSR traffic in an anterograde manner, and does it pass via the plasma membrane? and 3) to where does the VSR recycle?'.

Arabidopsis thaliana Vacuolar Sorting Receptors (VSRs) are membrane spanning proteins that specifically traffic 'cargo' proteins towards the vacuole. Of the 7 VSR paralogues VSR2 is the most characterised. The receptor binds cargo in the early secretory pathway and traffics to the late secretory pathway where it dissociates from the cargo and recycles back to the early secretory pathway for a new round of binding. The steady-state localisation of VSR2 is at the Pre-Vacuolar Compartment (see Figure 1.1), which is where it is thought to dissociate from the cargo (DaSilva et al., 2005; Tse et al., 2004). The trafficking of the receptor is dependent on multiple domains within the C-terminus of the receptor (DaSilva et al., 2006). This short C-terminus has been extensively dissected in order to characterise the trafficking mechanisms that take place between the receptor and cytosolic components. Anterograde trafficking of VSRs is dependent on a canonical

conserved tyrosine residue (Y612) that is part of a YXXϕ motif that mediates interaction with a clathrin adaptor complex, for clathrin mediated transport (Happel et al., 2004; Sanderfoot et al., 1998). Alanine substitution of this residue has been shown to prevent arrival of the receptor at the PVC (Foresti et al., 2010). There is also evidence that an ExxxIM motif present in the exposed terminus acts as an anterograde sorting mechanism. In addition to both motifs playing a role in anterograde sorting, the YXXϕ plays is also involved in recycling as the ϕ residue (L615) has been shown to be essential for receptor recycling from the late secretory pathway. Similarly, the IM in the ExxxIM motif has been shown to be recycling deficient when alanine-substituted (Saint-Jean et al., 2010).

Although these data suggest that clathrin-coated vesicles mediate anterograde VSR transport from the Golgi/TGN to the PVC, this notion has recently been contested (Scheuring et al., 2011). In addition, VSR recycling via retromer is suggested to occur either from the PVC (Oliviusson et al., 2006) or the TGN (Niemes et al., 2010a). For example, although there is no debate that the receptor is co–translationally inserted into the ER, the COPII dependent export of the receptor *from* the ER has recently also been contested (Niemes et al., 2010b). By expressing a fluorescent GFP-VSR2 chimera in a background of overexpressed, full-length VSR2 redistribution from the late secretory pathway to the ER was observed, whereas other membrane-spanning proteins seem to maintain normal trafficking. The interpretation presented is that the VSR is competing at the level of the ER for entry into an uncharacterised vesicle bypassing the Golgi. This is in contrast, however with other evidence which suggests that the soluble vacuolar cargo traffics in a COPII dependent manner, for example the inhibition of COPII trafficking via Sec12-overexpression has been shown to retain a vacuolar targeted RFP VSR ligand in the ER (Bottanelli et al., 2011). Since this cargo depends on

VSRs it could thus be argued that VSRs are COPII dependent as well. However, none of the previous studies directly tested the COPII-dependence of VSR export from the ER.

To dissect the signals controlling anterograde VSR transport from the ER towards its final point of retrieval, in this chapter the ER export and further anterograde VSR transport has been systematically studied using a variety of techniques. With the help of dual-signal cargo it has been shown that both the VSR and the HDEL receptor ERD2 can compete for interaction with the same cargo, providing strong evidence against VSRs bypassing the Golgi. In addition, interference with the COPII-dependent transport leads to ER retention of both VSR and its cargo in the ER. Moreover, a series of deletion mutations that create consecutive truncations of the C-terminus of the VSR demonstrate that the VSR-C-terminus contains a conserved stretch of amino acids necessary for efficient ER export but that does not appear to be of the canonical di-acidic nature.

5.2 RESULTS

5.2.1 Soluble Vacuolar Proteins Pass Through the Golgi Apparatus in an Anterograde Manner.

It has previously been shown that ER retention of soluble proteins occurs mainly from the cis-Golgi via C-terminal tetrapeptides HDEL or closely related derivatives, because their density is highest at the cis-Golgi and rapidly declines towards the trans-face (Phillipson et al., 2001). Vacuolar sorting receptors (VSRs) show the opposite polarity and are enriched at the trans-face of the Golgi stack (Hillmer et al., 2001). The barley aleurain N-terminal sorting signal is the first described VSR-interacting motif (Kirsch et al., 1994) and can direct secreted fluorescent proteins and barley α-amylase (Amy) to the central lytic vacuole (Foresti et al., 2010). To test if such vacuolar proteins pass through the Golgi, or reach the TGN in a Golgi-independent manner (Niemes et al., 2010b), dual-signal cargo molecules exhibiting both the N-terminal Aleurain sorting signal and a C-terminal HDEL signal were constructed. If the Aleurain signal causes the cargo to bypass the Golgi stack, HDEL-mediated retrieval is not expected to function. However, if vacuolar sorting occurs from the Golgi cisternae, then the HDEL-receptor ERD2 may intercept the fusion protein and sequester it back to the ER. Therefore, a secretory red fluorescent protein (RFP) was used as cargo to compare the dual-signal cargo (Aleu-RFP-HDEL) with secreted RFP (secRFP), vacuolar RFP (Aleu-RFP) and ER retained RFP (RFP-HDEL) by fluorescence microscopy in leaf epidermis cells (Figure 5.2).

To test if Aleu-RFP can be localised to the ER upon addition of the HDEL tetrapeptide a fusion construct was used to transform *A. tumefaciens* in order to mediate transient expression. *In situ* analysis of tobacco leaf epidermis cells

transformed by infiltration with *Agrobacterium tumefaciens* was undertaken on Aleu-RFP, Aleu-RFP-HDEL and RFP-HDEL.

Figure 5.1 B, C shows that secRFP is found exclusively in the apoplast, and was undetectable in the vacuolar lumen or when in transit through the ER. Addition of the C-terminal HDEL signal prevented apoplastic deposition and caused efficient ER retention under these experimental conditions (RFP-HDEL). As expected from previous findings, the vacuolar fusion Aleu-RFP segregates efficiently from the default secretory route to the vacuole, and is found in small punctate structures (5.1B) corresponding to LPVC compartments (Foresti et al., 2010) as well as the central vacuole lumen where it produces homogeneous fluorescence (5.1B,C). Interestingly, the dual signal cargo Aleu-RFP-HDEL was strongly redistributed to the ER, suggesting an efficient retrieval from the Golgi apparatus. Therefore, the Aleu-signal for vacuolar sorting does not mediate bypassing of the Golgi apparatus.

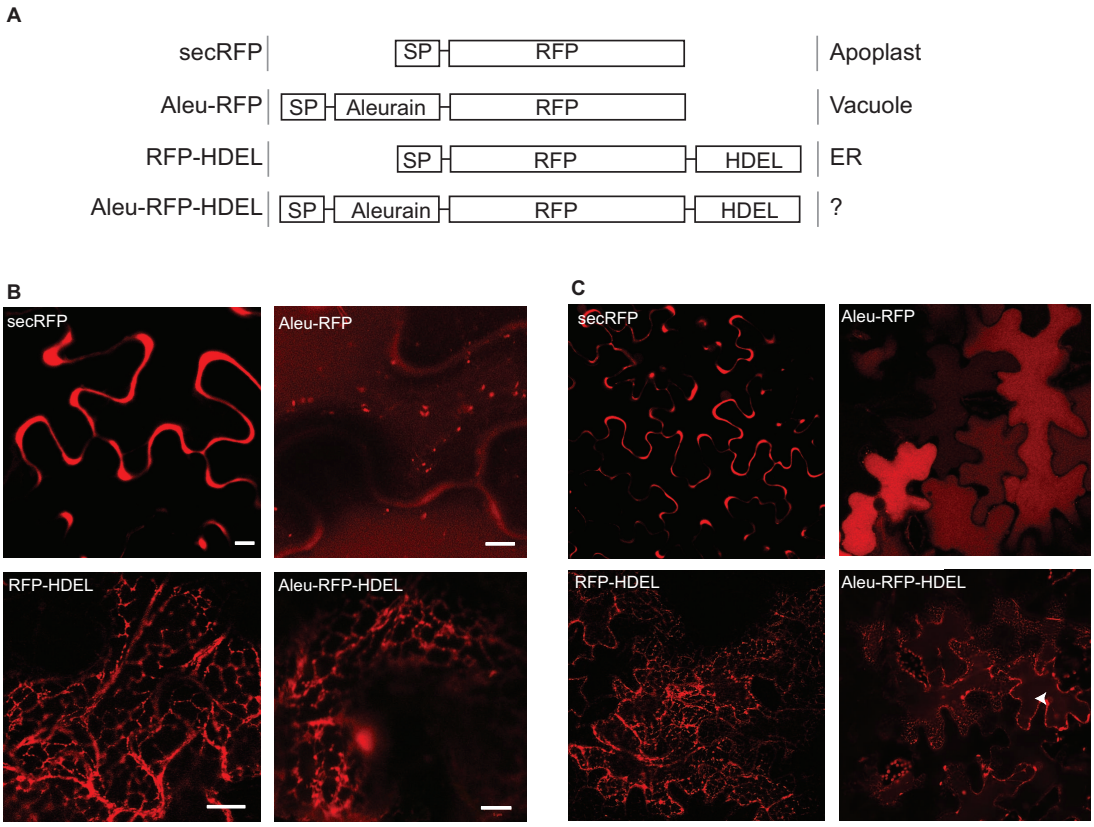

Figure 5.1: **The majority of the soluble cargo Aleu-RFP-HDEL is retained in the ER**
A. The chimeras used in this experiment, 'Aleurain' refers to the sorting signal from barley aleurain, RFP the Red Fluorescent Protein and HDEL is a 4 amino acid C-terminal fusion.
B. A near-field confocal laser scanning image from *N. tabacum* lower epidermal leaf cells. Notice the retention of the Aleu-RFP-HDEL in the ER, comparable to RFP-HDEL rather than Aleu-RFP. Marker = 5μm.
C. A wide field image showing a cross-section of multiple cells. Notice the faint vacuolar fluorescence (white arrow), not visible in the near field image — representing soluble cargo that has reached the vacuole. Images $\sim$100μmx100μm.
The SecRFP images in the top left of panels B. and C. courtesy of F. Bottanelli.

5.2.2 VSRs and ERD2 Compete for Interaction with Aleu-amy-HDEL

Aside from the clear fluorescence of the dual cargo Aleu-RFP-HDEL in the ER, weak homogeneous fluorescence in the central vacuolar lumen was also seen consistently, and best appreciated at low magnification for cells with the focal plane including vacuolar lumen Fig. 5.1). It was shown previously that HDEL-mediated ER retention can be leaky, possibly via saturation of the sorting receptor ERD2

(Crofts et al., 1999; Pimpl et al., 2006). However, leakage of RFP-HDEL to the apoplast was not detected, suggesting efficient retention of HDEL-ligands under these experimental conditions. The weak fluorescence of Aleu-RFP-HDEL in the vacuole is therefore unexpected because it would be harder to detect in the large lytic vacuole compared to the less lytic and more confined volume of the apoplast.

To test if a vacuolar sorting signal could interfere with ER retention of the dual signal cargo, the experiment was repeated using the more quantitative barley alpha amylase (Amy) reporter system in tobacco leaf protoplasts (Phillipson et al., 2001), which is more suitable for monitoring secretion. Thus vacuolar Aleu-Amy (Bottanelli et al., 2011) was compared with ER retained Amy-HDEL (Phillipson et al., 2001) and the test cargo Aleu-Amy-HDEL (Fig. 5.2). Figure 5.2 B shows that under control conditions, secretion of Aleu-Amy is detected at very low levels, well below the slow secretion of the ER retained Amy-HDEL and the fast secretion of the control (Amy). This suggests that vacuolar sorting is less leaky compared to ER retention. The dual-signal cargo Aleu-Amy-HDEL is essentially undetectable in the medium, probably due to the cooperative action of two sorting signals that mediate segregation from the secretory default route.

To quantify how much of the cargo is exported from the ER and delivered to vacuoles, the drug Wortmannin was used to specifically redirect vacuolar cargo to the cell surface, without affecting the early secretory pathway or constitutive secretion (Pimpl et al., 2003)- it was shown that the drug prevents VSR-recycling, leading to secretion of VSR cargo without affecting constitutive secretion (DaSilva et al., 2005). Transfected protoplast suspensions were therefore divided into two equal portions, one to be incubated without the drug giving rise to data described above (first 3 lanes of figure 5.2B), the other to be supplemented with Wortmannin to generate data in the last 3 lanes of figure 5.2B. The results confirm that the

drug did not affect the behaviour of the control cargo (ER-retained Amy-HDEL). However, secretion to the medium was strongly induced for Aleu-Amy and Aleu-Amy-HDEL (Fig. 5.2B). The wortmannin-induced proportion in the medium is representative of the amount that escaped the ER and would normally have been targeted to the vacuoles in the absence of the drug.

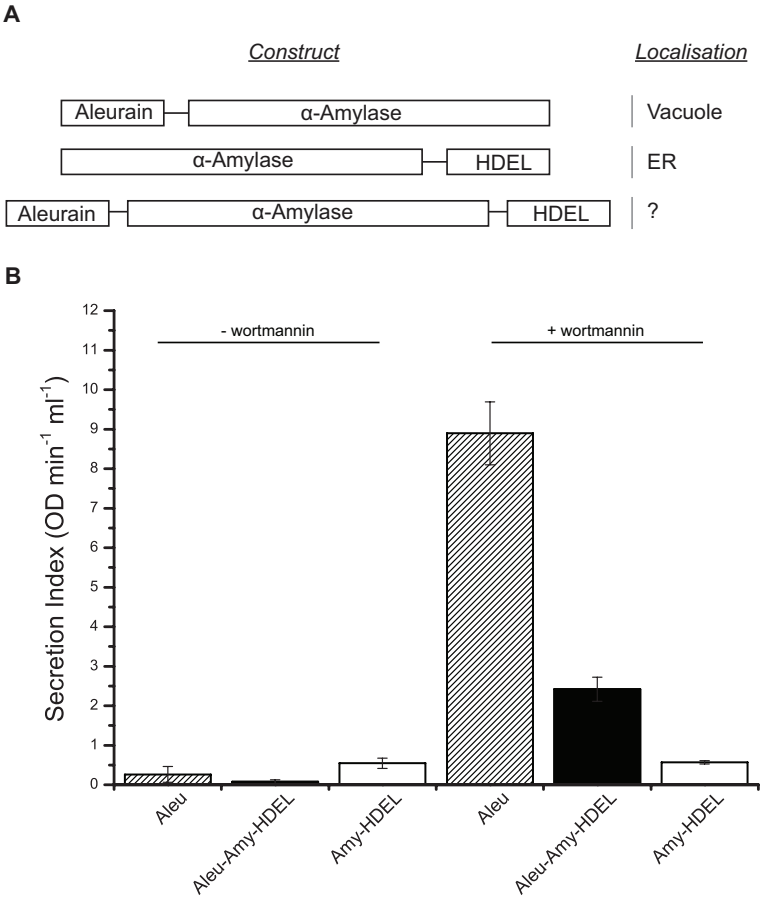

Figure 5.2: **VSRs and ERD2 can compete for interaction with the soluble chimeric cargo Aleu-Amy-HDEL**
A. The chimeras used in this experiment, 'Aleurain' refers to the sorting signal from barley aleurain and HDEL is a 4 amino acid C-terminal fusion.
B. Tobacco protoplasts were electroporated with a constant amount (10μg) of DNA encoding the various soluble cargoes. The left three bars of the graph represent the secretion index of the cargoes in normal conditions, and the right three bars of the graph are in 33μM wortmannin. Whilst there is no clear differentiation in the left three bars, when in the presence of wortmannin the Aleu-amy shows considerable secretion (crossed bar), the Amy-HDEL shows a low secretion index (clear bar) and Aleu-amy-HDEL shows the intermediate.

The quantitative assays confirm that HDEL effectively causes retention of Aleu-Amy-HDEL compared to Aleu-Amy, ruling out that the Aleurain signal causes bypassing of the Golgi. However, in the presence of wortmannin Aleu-Amy-HDEL shows significantly more secretion compared to Amy-HDEL, suggesting either that the efficiency of ER retention has been reduced or folding of the HDEL signal has been reduced/contextually altered by the presence of the Aleurain signal. A direct effect on the display or folding of the HDEL signal is unlikely as Aleurain and HDEL are fused to opposing termini of the protein. However, the effect could be explained if VSRs and ERD2 bind to the dual signal cargo in a mutually exclusive manner. Since HDEL cargo is not bound to its receptor in the ER (Ceriotti et al., 1998; Pelham, 1988; Pelham et al., 1988), competition by the two receptor types is likely to take place on even terms in the Golgi apparatus.

5.2.3 ER Export of Soluble VSR Cargo is COPII Mediated

Although the previous experiments suggest that the vacuolar cargo transits the Golgi stack, it remains to be shown which carrier mediates VSR export from the ER. The canonical ER export mechanism is via the COPII protein machinery, consisting of Sec23,24,13,31, the GTPase SarI and its GEF Sec12. There are two known experimental methods to specifically inhibit COPII transport, (1) overexpression of Sec12 inhibits COPII traffic by titrating Sar1 (Phillipson et al., 2001) and (2) expression of a dominant-negative SarI(H→L) point mutant that stops COPII vesicular budding (Aridor et al., 1995; Takeuchi et al., 2000). It is already known that overexpression of Sec12 inhibits the ER export of the cargo (Bottanelli et al., 2012), but the experiment did not include the VSR fusion directly to study the trafficking.

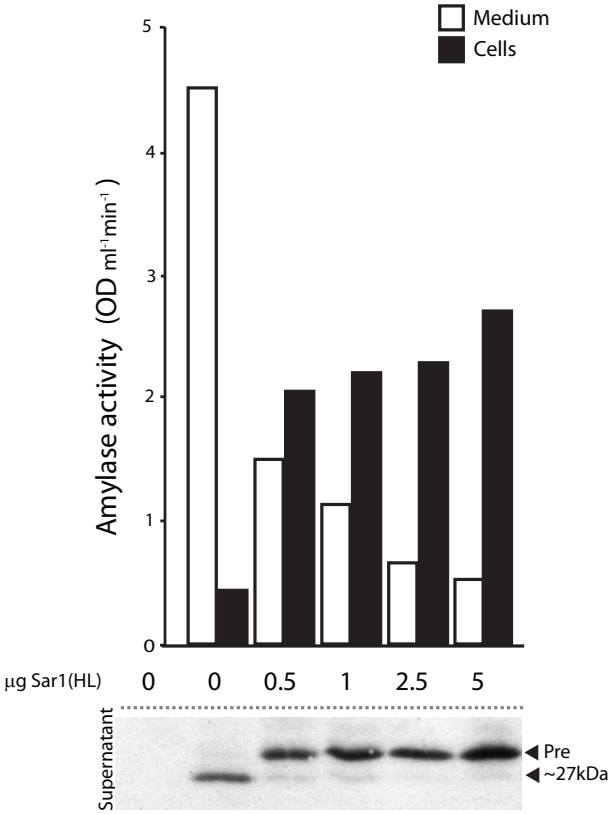

Figure 5.3: **Expression of a Dominant-negative SarI(HL) Inhibits ER Export of VSR Ligands in Tobacco Mesophyll Protoplasts**
Tobacco Mesophyll Protoplasts were electroporated with constant amounts of DNA encoding Aleurain-GFP and α-amylase, and varying amounts of of plasmid encoding SarI(HL) (0, 0.5, 1, 2.5 and 5μg). After 24 hours incubation the medium and cells were split into two fractions and the α-amylase activity assayed on both. The cell sample was also analysed by an SDS-PAGE immunoblot assay using anti-GFP primary antibodies to probe the membrane. As can be seen that there is a dramatic shift from the vacuolar processed form to the heavier weight precursor, even with approx 0.5μg of the COPII inhibitor SarI(HL)

When GFP-VSR fusions reach the vacuole, they are processed into a lower molecular weight fragment (GFP-core) through the activity of hydrolytic enzymes (DaSilva et al., 2005). I wanted to test if the GFP-core formation can also be used for the VSR ligand. By monitoring the ratio of this core to the non-proteolytically processed form on an immunoblot assay the transport of the VSR ligand Aleu-GFP towards the vacuole can be ascertained. The activity of the SarI(HL) can be monitored by co-expressing a constant amount of the secreted COPII dependent α-amylase (Amy). To increase the number of tools, the effect of the SarI(HL) was tested on the vacuolar cargo Aleu-GFP. An immunoblot assay was performed on protoplasts electroporated with constant amounts of the VSR ligand Aleu-GFP and a dilution series of the COPII inhibitor SarI(HL).

Figure 5.3 shows increasing the dose of SarI(HL) causes a reciprocal increase in amy activity in the cells whilst the amy activity in the medium decreases. The immunoblot assay displayed below, monitoring the processing of the co-transfected VSR ligand Aleu-GFP shows that at very low amounts of SarI(HL) the ratio of precursor to a vacuolar-processed form dramatically shifts. This shows that also soluble Aleu-GFP is proteolytically trimmed to a low molecular weight form and that this step can be inhibited by SarI(HL).

5.2.4 ER Export of VSR is Sensitive to Overexpression of Sec12

Although the results of Figure 5.3 demonstrate that the ER Export of the VSR cargo is COPII dependent, the receptor could still export in an independent export vesicle and reach the Golgi apparatus in a different manner. This would allow the receptor to traffic at a higher efficiency than the bulk flow mechanism of the soluble cargo. Therefore, COPII inhibitors Sec12 and SarI(HL) were tested on

GFP-VSR rather than the cargo. Firstly, using a microscopy approach it was determined if *in situ* overexpression of Sec12 has an effect on trafficking of VSR.

Confocal-laser scanning microscopy (CLSM) was performed using *N. tabacum* epidermal leaves transiently transformed by leaf infiltration with *A. tumefaciens* strains containing the relevant T-DNA inserts. The test object was the GFP-VSR2, fusion protein, in which the lumenal domain of the receptor was replaced with the fluorophore GFP. Although GFP-VSR2 cannot interact with cargo, it can still traffic in the endogenous manner due to the C-terminal sorting signals (DaSilva et al., 2006). GFP-VSR2 was co-infiltrated with a dual-expression vector encoding (1) untagged Sec12 and (2) Golgi marker ST-YFP. The use of dual-vector constructs allowed cells expressing the untagged Sec12 to be differentiated from untransformed cells through visualisation of the YFP reporter, whilst avoiding affecting the activity of the effector by fusing it to a fluorescent protein. As a control a dual-vector encoding ST-YFP and the untagged non-effector phosphinothricin acetyl transferase (PAT) were also included, and are shown in comparison. Figure 5.4 shows representative images demonstrating that upon Sec12 overexpression the GFP-VSR2 is redistributed to a an ER-like reticulated organelle in the ST-YFP expressing cells. Also the Golgi-marker ST-YFP is redistributed by Sec12 overexpression. This is in contrast to the normal punctate PVC and Golgi structures observed with the mock effector.

In order to further support this evidence an immunoblot assay was performed. The use of electroporated protoplasts allows for a more quantitative assay to be performed as the result is the outcome from $\sim$2 million cells, as opposed to the 500-1000 analysed at the microscope. When the GFP-VSR2 reaches the vacuole, it degrades due to the presence of hydrolytic enzymes, resulting in a stable GFP core (DaSilva et al., 2005), and an apparent disappearance of the full-length receptor

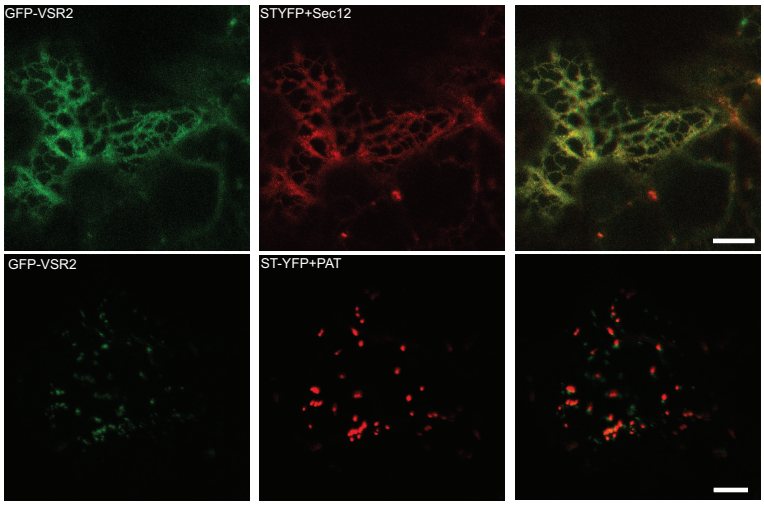

Figure 5.4: **Overexpression of Sec12 inhibits the ER Export of GFP-VSR2 in infiltrated tobacco leaf epidermal cells**
The lower row shows the expression of the GFP-VSR2 when co-expressed with a double vector encoding ST-YFP and an untagged protein, PAT— which has no effect on vacuolar sorting. In the upper row the GFP-VSR2 is co-expressed with a double vector encoding ST-YFP and the untagged COPII inhibitor, Sec12. As can be seen there is a redistribution of both the GFP-VSR2 and ST-YFP into the reticulated ER. Marker = 10μm.

when visualised using GFP antibodies. The difference in molecular weight between prevacuolar and GFP core is greater than for Aleu-GFP (Fig. 5.3) and can easily be assessed by western blotting. In order to see if the transport of VSR2 can be perturbed using Sec12, a constant amount of plasmid DNA encoding GFP-VSR2 and two concentrations of untagged Sec12 encoding plasmid were electroporated in *N. tabacum* mesophyll protoplasts. The protein extracts were then separated using an SDS-PAGE approach and visualised in an immunoblot assay with anti-GFP antibodies.

Figure 5.4 shows that an increase in the dosage of the Sec12 causes a shift in the precursor:core ratio. This indicates that inhibition of COPII trafficking prevents the proper trafficking and processing of the GFP-VSR, thus further supporting the hypothesis that VSRs traffic in a COPII dependent manner.

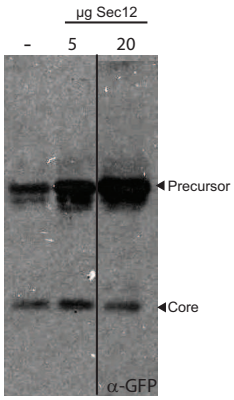

Figure 5.5: **Overexpression of the COPII component Sec12 Inhibits Trafficking of GFP-VSR2 in Tobacco Mesophyll Protoplasts**
A constant amount of plasmid encoding GFP-VSR2 was electroporated with different amounts of plasmid encoding Sec12 (0, 5, 20μg). After expression for 24 hours the cells were pelleted, proteins extracted and used for an SDS PAGE-Immunoblot assay. The dose-dependent shift in the amount of precursor to the core form indicates that the Sec12 inhibits trafficking of the GFP-VSR2

5.2.5 ER Export of VSR is Sensitive to Expression of SarI(HL)

In order to further reconfirm the conclusions made above, the SarI dominant-negative effect was used as described earlier (Figure 5.3). Tobacco protoplasts were electroporated with a constant amount of plasmid encoding secreted α-amylase together with a dilution series of plasmid encoding GFP-VSR2 and an increasing amount of SarI(HL). The effect of the SarI was tracked by monitoring the redistribution of the amy from the extracellular medium to the cellular fraction, thus controlling for the activity of the untagged SarI(HL). The processing ratio of the GFP-VSR2 protein was visualised by analysing cell extract from the same protoplast suspension in an immunoblot assay.

Figure 5.6 clearly demonstrates that constitutive secretion is gradually inhibited by the SarI mutant in a dose-dependent manner. In addition, there is a clear shift in the precursor:core processing ratio that is both sensitive and dose dependent to the SarI(HL). Compared to the secretory marker Amy, this dose-response appears to be more sensitive as observed for the cargo Aleu-GFP in Figure 5.3. Multiple

lines of evidence strongly suggest that both the VSR and its cargo traffic to the Golgi apparatus in the canonical COPII vesicular sorting route and can possibly interact upon synthesis in the ER.

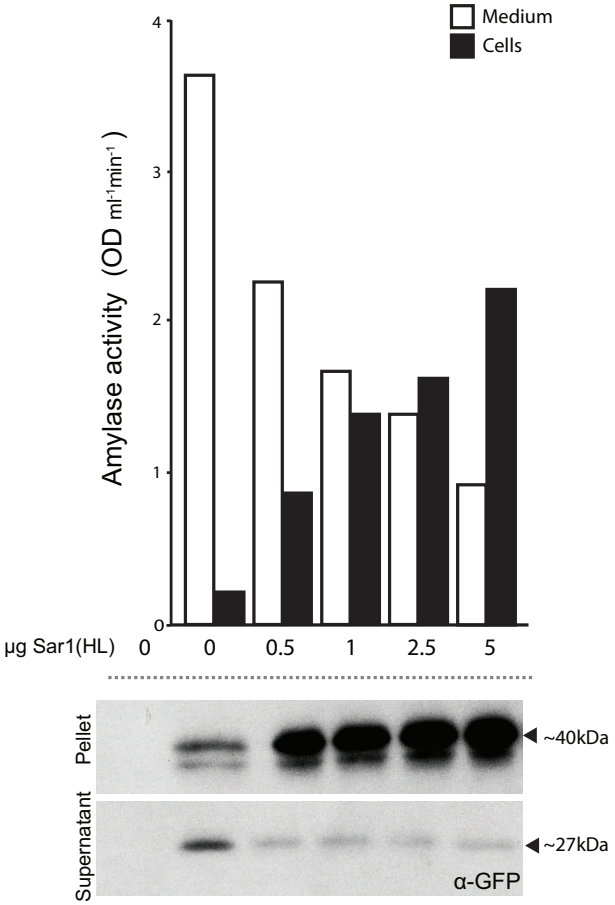

Figure 5.6: **Expression of a Dominant-negative SarI(HL) Inhibits ER Export of GFP-VSR2 in Tobacco Mesophyll Protoplasts**
Tobacco Mesophyll Protoplasts were electroporated with constant amounts of plasmid encoding GFP-VSR2 and α-amylase, and varying amounts of of plasmid encoding SarI(HL) (0, 0.5, 1, 2.5 and 5μg). After 24 hours expression the medium and cells were split into two fractions and the α-amylase activity assayed on both. The cell sample [supernatant], and the re-suspended cell pellet (after sonication) [pellet] were also analysed by an SDS-PAGE immunoblot assays using anti-GFP primary antibodies to probe the membrane. As can be seen there is a dramatic shift from the vacuolar processed form to the heavier weight precursor, even with approx 0.5μg of the COPII inhibitor SarI(HL)

5.2.6 The Membrane Proximal Region of the Cytosolic Tail of VSRs is Responsible for Efficient ER Export

Previous work on the GFP-VSR2 fusion established that deletion of the cytosolic tail downstream of the positive amino acid cluster near the transmembrane domain (GFP-VSR2ΔCT) led to partial retention in the ER and abolished *in vivo* competition with endogenous VSRs (DaSilva et al., 2006), suggesting a severe anterograde transport defect. In order to test the requirements for VSR ER-export and post Golgi trafficking, it was decided to compare this deletion construct with a series of shorter deletions up to and including the YMPL motif (Figure 5.7A). Furthermore, previous work was carried out in protoplasts that are known to suffer from overexpression issues, and thus previous localisations were worth revisiting.

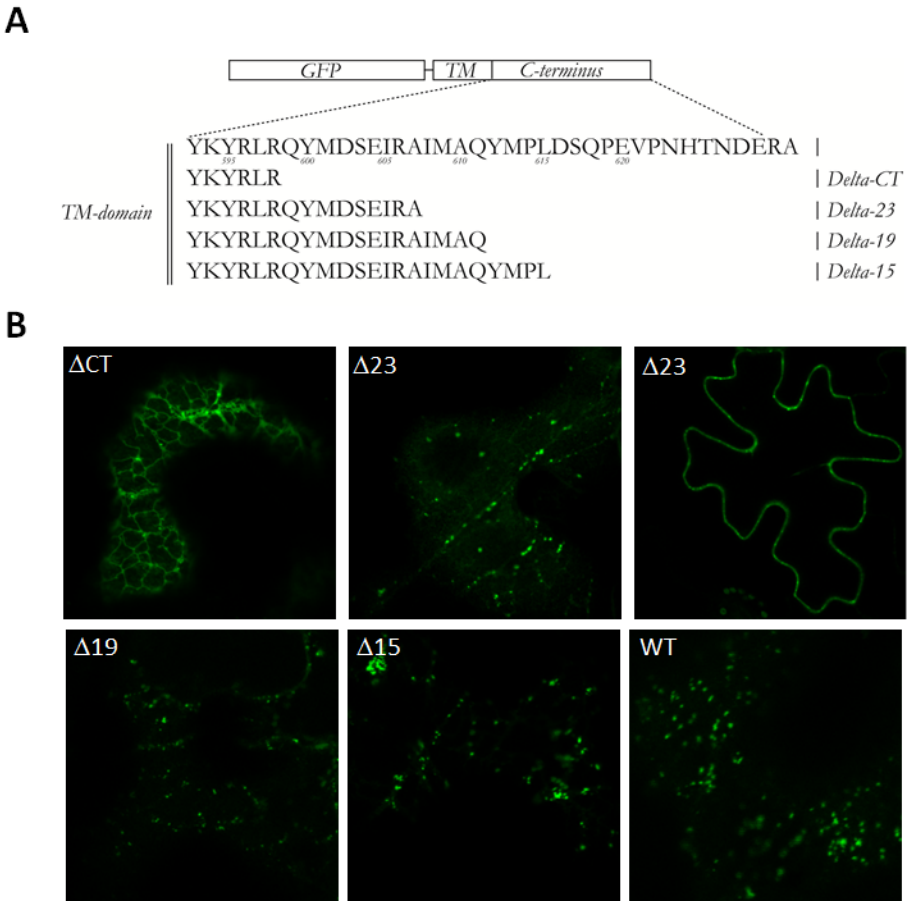

Figure 5.7: **Localisation Screen of VSR2 Deletion Mutants**
Confocal laser scanning micrographs of Agrobacterium infiltrated tobacco leaf epidermis cells expressing four deletion mutants of the fluorescent receptor model cargo GFP-VSR2. Shown is the cortex of a cell expressing either the deletions ΔCT, Δ23, Δ19, or Δ15. To appreciate the partial plasma membrane partitioning of the Δ23 mutant, an additional image with the focal plane in the centre of the cell is shown.

Figure 5.7B shows that the longest deletion (GFP-VSR2ΔCT) expressed in tobacco leaf epidermis is mostly present in a typical ER network, in line with earlier observations with the same construct in protoplasts (DaSilva et al., 2006). In addition to the ER labelling, mobile punctate structures were also observed, suggesting that a minor portion is exported from the ER. Lengthening the C-terminus by nine amino acids (Δ23) completely abolished ER retention. Instead, the fusion protein was found in punctate structures and the plasma membrane, indicating that the fusion contained active information for ER export that has

been deleted in GFP-VSR2ΔCT. The two shortest deletions (Δ19 and Δ15) yielded mainly punctate structures, showing that further sorting information prevented accumulation at the plasma membrane, either by decreased transport to- or accelerated endocytosis from the cell surface.

5.2.7 VSR Export is not Mediated by a Typical DXE Motif

The results from Figure 5.7 are consistent with the presence of an ER export motif contained within the nine amino acids (QYMDSEIRA) constituting the membrane proximal region of the VSR cytosolic tail. This region contains the sequence DSE, a typical di-acidic peptide sequence motif (DXE) that has been implicated in the selective ER export of the vesicular stomatitis virus (VSV) G-protein in animal cells (Nishimura and Balch, 1997) as well as the associated cargo concentration (Nishimura et al., 1999). Similar DXE signals were also shown to mediate efficient ER export of membrane proteins in plants (Hanton et al., 2005). Curiously, single point-mutations of the two acidic residues in VSR2 had little effect on in vivo competition by GFP-VSR2 (DaSilva et al., 2006). Moreover, mutating the second acidic residue (E604A) was shown to cause Golgi/TGN retention of the receptor (Saint-Jean et al., 2010). Neither of these observations support a role in ER export.

To test a role of the DXE motif in VSR2 export from the ER directly, a double point-mutation was generated (D602A + E604A, hereafter referred to as ASA) within the context of the full-length VSR-tail and the subcellular fluorescence pattern of the GFP-VSR2(ASA) transformants was compared with wild-type GFP-VSR2 and GFP-VSR2ΔCT.

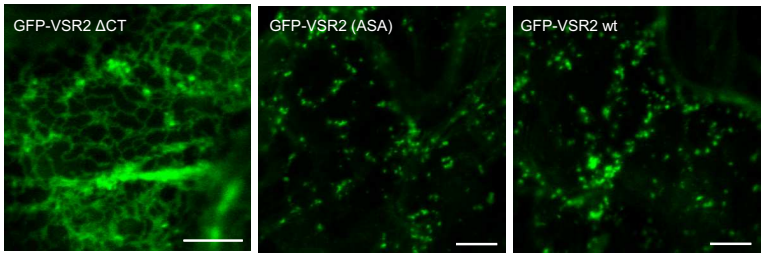

Figure 5.8: **Localisation Screen of VSR2 Deletion Mutants**
Confocal laser scanning micrographs of Agrobacterium infiltrated tobacco leaf epidermis cells expressing either GFP-VSR2ΔCT, wild type GFP-VSR2 (wt), or the point mutant (ASA).

Figure 5.8A shows that the ASA mutant is exclusively found in punctate structures, similar to the pattern of the wild type fusion. There was no evidence for an extensive ER network, suggesting that the ASA mutant is fully ER export competent. The results show that VSR-export is mediated by an unusual signal that does not match the best characterised di-acidic type, but seems to be contained within the sequence QYMDSEIRA. The results are consistent with the fact that plants are known to use less related di-acidic signals (i.e. EXXD) for accelerated ER export (Chatre et al., 2009). Also in mammalian cells, reports suggest that the popular DXE motif is not always supported by clear-cut data (Sevier et al., 2000), calling for a more complex motif for ER export signaling.

5.3 DISCUSSION

The purpose of this study was to directly test experimentally whether a COPII independent export pathway of plant VSRs exists and leads to vacuolar sorting independent of the Golgi. Here this hypothesis has been tested on both the cargo and the receptor using a combination of experimental approaches.

5.3.1 VSR-mediated Sorting of Soluble Cargo does not bypass the Golgi Apparatus

Although VSRs have been shown to traffic through the Golgi apparatus, based on glycan modification studies (DaSilva et al., 2006; Kim et al., 2010) and immunocytochemistry (Hinz et al., 1999), these studies cannot distinguish between arrival at the Golgi in an anterograde or retrograde manner. Using a dual signal cargo bearing a vacuolar sorting signal (Aleu) as well as an ER retention signal (HDEL), Golgi-mediated anterograde cargo transport was studied. The results presented here show that vacuolar cargo does not bypass the Golgi as cis-Golgi mediated retrieval of the cargo was observed.

The results suggest that vacuolar and ER sorting machinery compete for the dual signal cargo at the Golgi apparatus, possibly starting at the cis-Golgi from which the majority of HDEL-proteins is retrieved in plants (Phillipson et al., 2001). There are two arguments for this model. It was shown that ER retention does not involve receptor-ligand interactions in the ER but occurs via receptor-mediated capture at the Golgi, followed by recycling to the ER and subsequent ligand release (Ceriotti et al., 1998; Pelham, 1988). If the majority of VSR-ligand interactions would occur in the ER lumen, this would take precedence and obstruct the later ERD2-ligand interaction in the *cis*-Golgi. Likewise, VSR-ligand interactions

cannot be restricted to the late Golgi cisternae or the dissociated TGN, because in that case the HDEL signal would be dominant as it is retrieved mainly from the *cis*-Golgi. The fact that the dual-signal cargo assumes an intermediate behaviour suggests that there is equal competition.

It should be pointed out that it is highly unlikely that both receptor types can bind to the dual signal cargo at the same time. If this would happen, it is likely that the resulting ternary complex would be trapped in the Golgi apparatus, but any significant Golgi fluorescence mediated by the Aleu-RFP-HDEL fusion was undetectable (Fig. 5.1). Therefore, it is reasonable to assume that interactions of dual signal cargo with VSRs or ERD2 are mutually exclusive.

Whilst ERD2 recycles to the ER upon ligand binding, causing rapid depletion of ER residents from cis to trans Golgi cisternae in plants (Phillipson et al., 2001), VSR and its ligands continue by cisternal progression together with secretory bulk flow. A second signal-mediated mechanism must mediate segregation of VSR-ligand complexes from secretory bulk flow.

5.3.2 VSRs are actively exported from the ER to the Golgi via the COPII-pathway

Transit through the Golgi stack does not rule out per-se that VSRs may leave the ER in a novel COPII-independent manner (Niemes et al., 2010b). Only a direct COPII inhibition assay could demonstrate this however this was not tested experimentally. To obtain evidence in favour of this hypothesis, inhibitors of the COPII-mediated pathway that have been previously characterised were used (Phillipson et al., 2001; Takeuchi et al., 2000). The results here failed to indicate any evidence for COPII-independent trafficking of VSRs. Instead,

the data support the notion that VSRs leave the ER in a canonical fashion, using COPII-coated membrane carriers, to reach the Golgi apparatus. Both Sec12-overexpression as well as Sar1(H74L) co-expression inhibited GFP-VSR2 transport along the pathway. Evidence for COPII-independent trafficking would have required insensitivity or at least reduced sensitivity to COPII-transport inhibition compared to typical COPII cargo. Instead, VSR processing to post-ER forms was observed to be more sensitive to Sar1(H74L)-dosage than the secretion of α-amylase. Therefore, no evidence was obtained supporting the suggestion that VSRs may use a novel pathway from the ER. Moreover, the results re-inforce the notion that the Golgi apparatus is the next step in the anterograde VSR-transport because COPII-mediated transport leads to the cis-Golgi in plants (Brandizzi and Barlowe, 2013).

5.3.3 VSRs Contain a Signal for COPII Entry

Whilst soluble proteins do not require export signals to leave the ER, membrane spanning proteins may have to be actively incorporated into COPII carriers because they are confined to the limited space in the membranes, and need to intercalate with essential machinery for vesicle budding, transport and fusion. Indeed, membrane spanning proteins have been widely shown to contain active signals for ER export (Hanton et al., 2005; Nishimura, 1999; Nishimura and Balch, 1997; Sevier et al., 2000; Votsmeier and Gallwitz, 2001). Here it is demonstrated that VSRs contain a discrete stretch of amino acids that can be implicated in active transport out of the ER. Comparison of two GFP-VSR2 deletion mutants (ΔCT and Δ23) implicated the sequence QYMDSEIRA in ER export. Although it appears to contain a DXE sequence earlier shown to act as ER export signal in plants (Hanton et al., 2005), the VSR sequence is more complex because

point-mutation of the two acidic residues did not stop ER export of the receptor (Figure 5.8). This is reminiscent of VSV-G protein which contains a conserved DXE like motif but as part of a more complex signal (YTDIEM) with a tyrosine in the -2 position of the aspartic acid as does the plant VSR sequence. Individual mutation of the comparable tyrosine residue and other single amino acids in the identified VSR region do not affect trafficking and *in vivo* competition with endogenous receptors (DaSilva et al., 2006). Also in the case of the VSV-G protein, all six residues had to be replaced by alanine to obtain a clear ER export defect (Sevier et al., 2000). Nevertheless, the results suggest that VSRs are not exported from the ER by passive bulk flow, but do so actively, and in a COPII mediated manner. Alternatively, this region could be allowing for the receptor to enter into the COPII vesicles passively (i.e. not by protein-protein interactions), further experiments are needed to distinguish between these two possibilities.

6 VSRS DO NOT TRAFFIC VIA THE PLASMA MEMBRANE DUE TO A DOMINANT YXXϕ MOTIF

6.1 INTRODUCTION

In the previous chapter multiple approaches have suggested that the primary anterograde trafficking route for the VSR from the ER leads to the Golgi in COPII vesicles. The deviation from the default pathway to the plasma membrane (Denecke et al., 1990) is therefore a post-ER event but the exact position of the branch points in the pathway remain to be found (De Marcos Lousa et al., 2012). Results from the previous chapters suggest that this segregation is highly effective and takes place, at least in plants, at the Golgi cisternae, the *trans* cisternae of the Golgi apparatus (*trans*-Golgi) or the physically separated "partially coated reticulum" (Tanchak et al., 1988). The latter is also called *trans*-Golgi network (TGN) (Dettmer et al., 2006), not to be confused with the *trans*-cisternae of the Golgi stack. At one or both of these locations, specific vacuolar sorting receptors (VSRs) are thought to recruit vacuolar but not secreted proteins into clathrin-coated vesicles (CCVs) destined for fusion with the prevacuolar compartment (PVC), at which receptors are thought to release their ligands (De Marcos Lousa et al., 2012).

Unlike the cargo which contains signals for vacuolar transport only, the receptor contains signals for active anterograde transport as well as selective recycling within the short cytosolic VSR C-terminus (Foresti et al., 2010). Anterograde VSR transport critically depends on the conserved tyrosine residue within the conserved YMPL motif that mediates interaction with clathrin adaptor complex AP1 (Happel et al., 2004; Sanderfoot et al., 1998). Substituting this tyrosine with

alanine (Y612A) causes partial receptor mistargeting to the plasma membrane (PM) (DaSilva et al., 2006) accompanied by partial accumulation at the TGN (Foresti et al., 2010). Mutagenesis of the leucine (L615A) causes defective receptor recycling from the PVC and leakage to a rab5-labeled late PVC (LPVC) and the vacuole where it is more rapidly degraded (Foresti et al., 2010).

There is also evidence to suggest that the conserved ExxxIM motif present in the exposed terminus plays an important role in receptor transport (Saint-Jean et al., 2010). In addition, in the previous chapter the localisation of a deletion mutant not containing the IM of the ExxxIM motif localised to the plasma membrane whereas a mutant including the IM was localised to punctate structure. Finally, there is strong evidence for a role of the cytosolic retromer core complex in receptor salvage from the PVC to prevent degradation in the vacuole (Kang et al., 2012; Kleine-Vehn et al., 2008).

The role of the plasma membrane (PM) in the anterograde transport of the VSR is unclear. Studies using point mutations have suggested that the VSR passes via the PM during the canonical trafficking pathway (Saint-Jean et al., 2010). Other studies have suggested that the VSR passes through the secretory pathway towards the vacuole in a clathrin-independent manner. These studies explain the presence of the VSR in clathrin-coated vesicles by inducing a clathrin dependent *trans*-Golgi Network to PM route, as part of the normal sorting pathway of the VSR. However, the plasma membrane faces an acidic apoplast that could lead VSRs to release their ligands.

In the previous chapter a deletion series was generated to attempt to address the signal mediated ER export of the receptor. Here, the same deletion series is used to understand a potential role of the ExxxIM motif. A combination of

biochemical 'Drag & Drop' assays with CLSM shows that the conserved tyrosine motif YMPL takes precedence over passive bulk flow to the plasma membrane and actively prevents cargo mis-sorting to the cell surface. However, in the absence of the YMPL motif, VSRs can still reach the PVC/LPVC via the plasma membrane. A conserved IM motif mediates endocytosis and targeting to the PVC but is insufficient for recycling from the PVC. In addition the results demonstrate that this route is not suitable for biosynthetic vacuolar sorting as ligands dissociate and secrete before the receptor reaches the PVC. The 'detour' via the plasma membrane may act as back-up mechanism to rescue mis-targeted receptors from the plasma membrane when they fail to enter the signal-mediated PVC targeting route from the Golgi/TGN.

6.2 RESULTS

Previously a series of deletion mutants identified a region of the C-terminus of the VSR that was essential for ER export. The initial screen also identified a deletion mutant (Δ23) that was relocalised to the PM. The remaining deletions were localised to punctate structures. Whilst ER and plasma membrane can be identified morphologically, analysing the identity of these punctate organelles required systematic co-expression of the four GFP-VSR2 fusions with either the Golgi marker ST-RFP, the TGN-marker RFP-SYP61, or the PVC marker RFP-VSR2. In contrast to wild type VSR2 and the well-defined YMPL mutants (Foresti et al., 2010), none of the new deletions shows a clear co-localisation with just one of the organelle markers. Instead, co-localisation was partial at best, although clear trends could be established after extensive correlation analysis from large datasets using the PSC co-localisation plug-in for ImageJ (French et al., 2008) to calculate Spearman correlation coefficients and red-green scatterplots (Figure 6.1). The results for the analysis of at least 400 punctate structures for each combination and associated scatterplots reveal that steady state levels of the four deletion constructs are distributed differentially between the three organelle types.

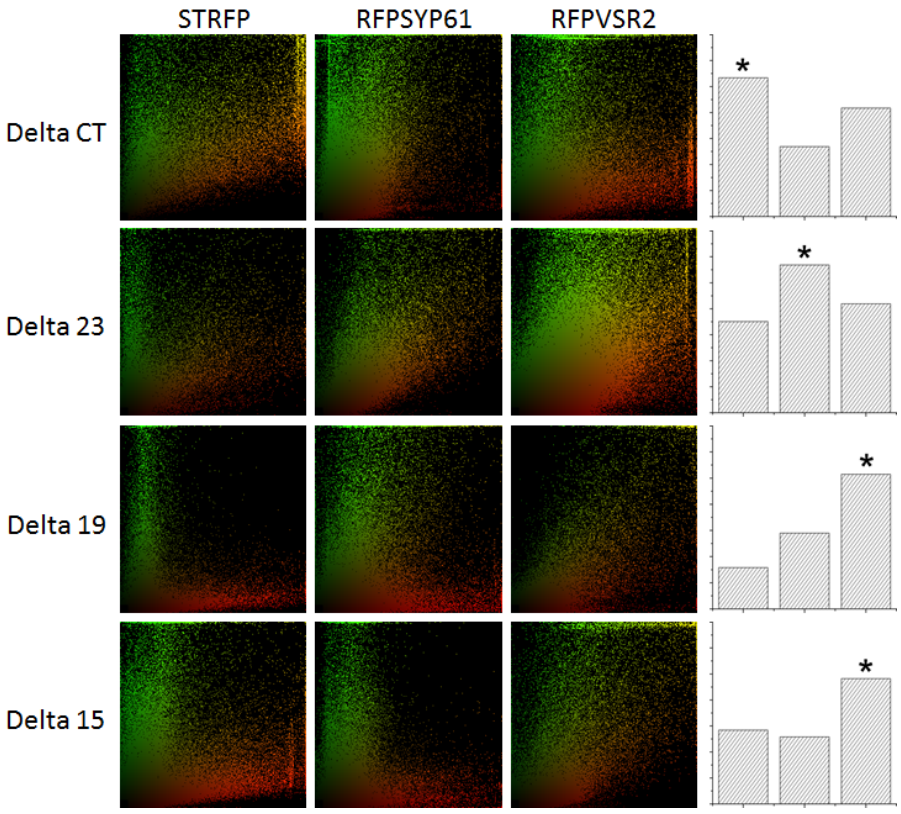

Figure 6.1: **Localisation Screen of VSR2 Deletion Mutants**
Statistical correlation analysis of GFP-VSR2 ΔCT, Δ23, Δ19, or Δ15 with the Golgi marker ST-RFP, the TGN-marker RFP-SYP61, or the PVC marker RFP-VSR2. The scatterplots are representative of at least 400 punctate structures, comprising a minimum of 50,000 pixels. On the right, the spearman correlation coefficients are shown (Golgi=left, TGN=centre, PVC=right) for each deletion construct. The highest correlation is indicated by a star.

The post-ER signals observed for GFP-VSR2-ΔCT were best correlated with the Golgi bodies, followed by the PVC and only a very weak correlation with the TGN. Taken together with the results of Figure 5.7B, the distribution-trend of ΔCT was thus ER→ Golgi→ PVC→ TGN. The next shortest deletion (GFP-VSR2Δ23) resides predominantly in the plasma membrane rather than the ER and shows a clear shift towards the TGN as the main punctate organelle of residence. This gives rise to a totally different steady state distribution for Δ23: PM→ TGN→ PVC→ Golgi. Finally, the two shortest deletions (Δ19 & Δ15) were mainly found at the PVC and with little in transit through the two earlier compartments and

no labelling of the ER and the plasma membrane. Therefore, in addition to ER export information, the membrane proximal region of VSR contains an alternative PVC targeting signal as the Δ19 deletion does not comprise the YMPL motif.

6.2.1 Evidence for Yxxϕ-independent VSR Targeting to the PVC

The presence of GFP-VSR2Δ23 at both the TGN and the plasma membrane matches well with the earlier observation that the YMPL motif is crucial for anterograde transport to the PVC, and that mutation of the tyrosine motif (Y612A) causes the same pattern of accumulation. Unexpectedly, addition of just 4 further amino acids to the tail provides information for targeting of GFP-VSR2 Δ19 to the PVC, yet the YMPL motif is still absent. The region that differentiates Δ23 and Δ19 contains a highly conserved IM motif in all plant VSRs (De Marcos Lousa et al., 2012), previously implicated in endocytosis from the plasma membrane and recycling from the PVC (Saint-Jean et al., 2010). To test this construct within our model system, the point mutations I608A and M609A on the standard VSR fusion were generated changing the region from IMAQ to AAAQ, here termed GFP-VSR2(IMAA), and tested for vacuolar leakage after expression in tobacco leaf epidermis cells.

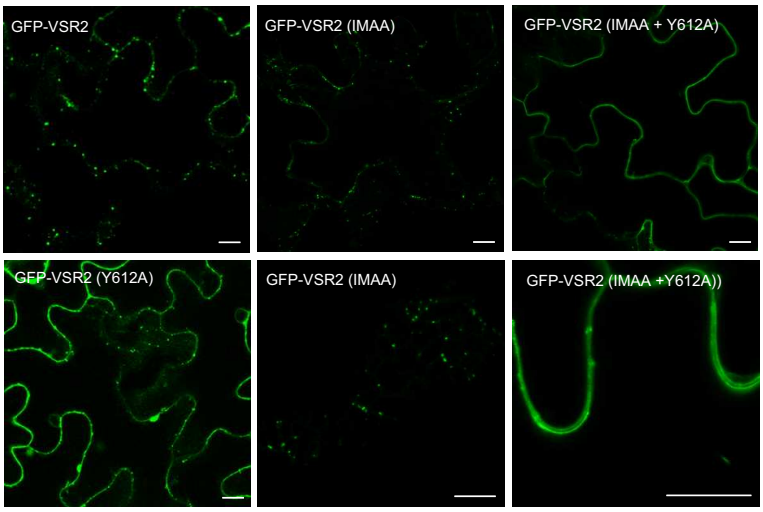

Figure 6.2: **Subcellular localisation of VSR2 point mutations**
Confocal laser scanning micrographs showing tobacco leaf epidermis cells infiltrated with Agrobacterium strains harbouring either GFP–VSR2(wt), GFP–VSR2(Y612A), GFP–VSR2(IMAA) or GFP–VSR2(IMAA+Y612A).

Figure 6.2 shows that the dramatic re-localisation to the vacuolar lumen previously reported was not detectable under the experimental conditions used here (Saint-Jean et al., 2010). GFP-VSR2(IMAA) is found in punctate structures at the cell periphery similar to wild-type GFP-VSR2, giving rise to crisp punctate structures when imaged at high magnification at the cell cortex. The results correspond well with the earlier observation that single point mutations I608A and M609A had only minor effects on *in vivo* competition (DaSilva et al., 2006).

For this reason, the triple mutant which combines IMAA with Y612A (IMAA+Y) was tested as a GFP fusion. Figure 6.2 shows that GFP-VSR2(IMAA+Y) is almost completely redistributed to the plasma membrane compared to the Y612A mutant which shows numerous bright punctate structures, earlier identified as TGN (Foresti et al., 2010). Infrequent punctate signals can be found occasionally for the double mutant (IMAA+Y) but these are exceptions. The results are in strong agreement with the data reported by Saint-Jean and colleagues (2010), despite the differences in the fusion protein. Therefore, current results attribute a

crucial role to the IM motif in preventing plasma membrane accumulation when the YMPL motif is absent (compare Δ23 with Δ19 in Figure 5.7 or mutated Y612A, Figure 6.2), but do not support a role in the recycling from the PVC.

The main difference between deletions Δ19 and Δ15 was that inclusion of the YMPL motif in the latter was accompanied with a higher correlation of Δ15 at the Golgi compared to Δ19 (Figure 6.1), accompanied with lower correlations with TGN and PVC. In line with the role of the hydrophobic leucine residue of the YMPL signal in recycling (Foresti et al., 2010), the introduction of the YMPL signal could increase the recycling efficiency from the PVC. Higher levels of Δ15 at the Golgi-stack would be consistent with a model in which receptor-recycling from the PVC would lead to the Golgi-stack rather than the TGN. To test if the Δ19 deletion is indeed recycling-deficient, leakage to the LPVC was monitored. Rab5 GTPases such as Rha1 accumulate at the LPVC rather than the PVC when expressed at low levels, as shown in chapter 1.10.1 and (Bottanelli et al., 2012). To avoid Rab5-overexpression-mediated merging of PVC and LPVC markers, RFP-Rha1 was expressed under the transcriptional control of the weak pNOS promoter (Teeri et al., 1989) and co-expressed with either GFP-VSR2Δ19 or GFP-VSR2Δ15. Analysis was carried out 36 hours after infiltration to avoid overexpression-induced leakage of VSR fusions to the LPVC.

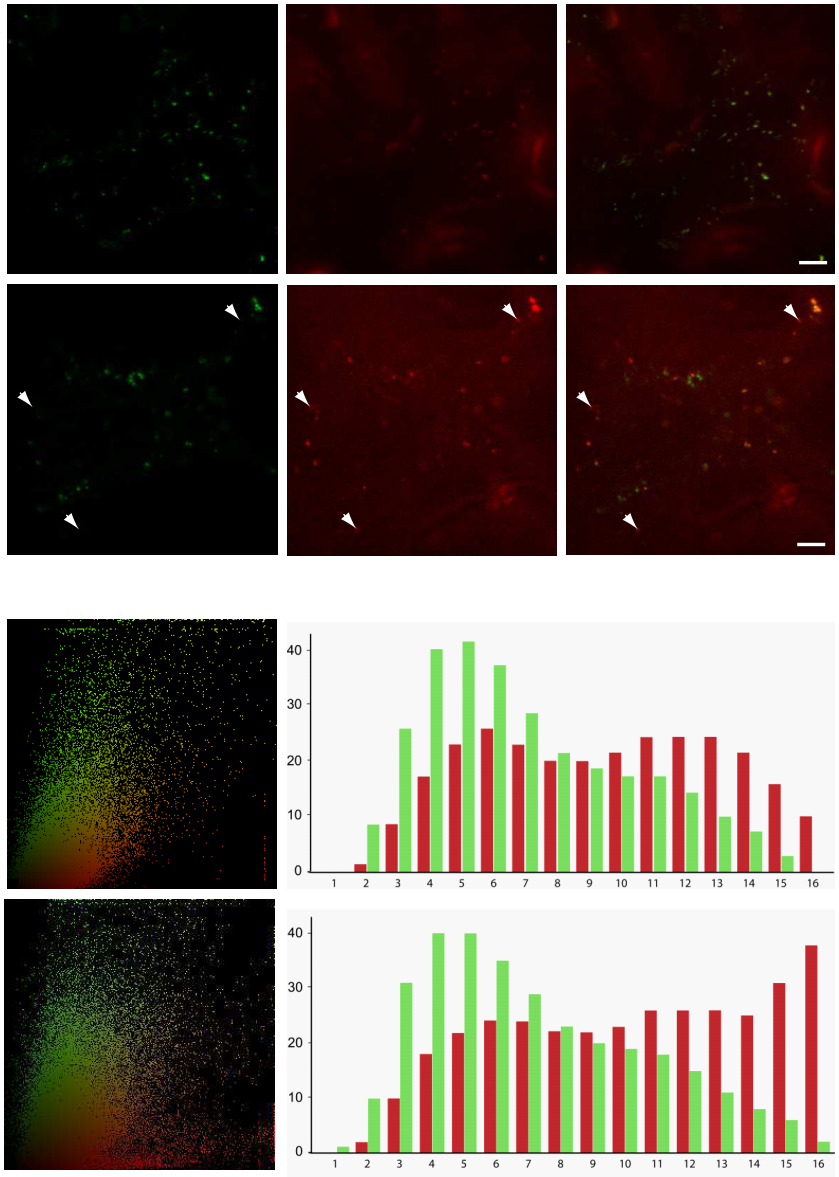

Figure 6.3: **GFP–VSR2Δ19 and GFP–VSR2Δ15 Differentially Localise to the PVC-LPVC**
A. Confocal laser scanning micrographs of Agrobacterium infiltrated tobacco leaf epidermis cells expressing either GFP-VSR2Δ19 or GFP-VSR2Δ15 with RFP-Rha1 expressed from the weak pNOS promoter. The cells are imaged at the cell cortex and shown in three channel mode (green, red, merged in yellow). White arrow heads in the GFP-VSR2Δ15 panel indicate red-only LPVCs labelled with RFP-Rha1. Markers = $\sim$5μm
B. Statistical correlation analysis of either GFP-VSR2Δ19 (top) or GFP-VSR2Δ15 (bottom) with the LPVC marker RFP-Rha1. Bar-charts on the left hand side show the results of the segmented population analysis in which the sum of green and red signals is shown in bar charts in each of the 16 bins. Notice the sharp increase in red signals in bins 15 and 16 of Δ15 compared to Δ19, accompanied by a reduction in the Spearman correlation coefficient (r).

Figure 6.3 A shows a typical example of the microscopy data obtained for either GFP-VSR2Δ19 or GFP-VSR2Δ15 when co-expressed with RFP-Rha1. The Δ19 construct shows a much better co-localisation with RFP-Rha1 compared to the Δ15 construct which contains the YMPL motif. No distinct red-only LPVC structures could be discerned, suggesting that the Δ19 mutant is recycling-defective and proceeds to the LPVC. In contrast, the GFP-VSR2Δ15 panel contains specific red-only LPVC punctae that represent segregating LPVCs (white arrow heads). In order to obtain statistically meaningful data, a correlation analysis was performed for a segmented population analysis of scatterplots to document partial population shifts in co-localisation experiments (Bottanelli et al., 2012). Scatterplots were subdivided into 16 slices of equal surface, representing data-bins of 16 different categories with progressively increasing red/green ratios (from left to right).

Figure 6.3 B illustrates that GFP-VSR2Δ19 shows a degree of co-localisation similar to or slightly higher than what was reported for the recycling-defective GFP-VSR2(L615A) mutant (Foresti et al., 2010). In contrast, GFP-VSR2Δ15 segregates from the LPVC marker as seen by a sharp increase of the red bars on the right hand side of the bar charts compared to the GFP-VSR2Δ19 chart. The segregation of GFP-VSR2Δ15 is not as clear cut as reported for the wild type GFP-VSR2-fusion (Foresti et al., 2010) which could show that the context at the C-terminus of the tail may be required for optimal functioning of the YMPL motif, in particular the L615 residue crucial for recycling (Foresti et al., 2010). The combined results suggest that the Δ19 mutant reaches the PVC via an alternative Yxxϕ-independent transport pathway and is unable to recycle. This confirms that the IM motif can play a role in endocytosis from the plasma membrane and further transport to the PVC, but does not have a function in recycling from the PVC.

6.2.2 The IM and YMPL Motifs Mediate Targeting to the PVC via Different Pathways

To understand the role of the IM-motif in endocytic recycling and transport to the PVC, the 'drag & drop' assay introduced in chapter 3 was used. Since the microscopy only shows the steady state levels at a given moment in time, it is not possible from these data to conclude if GFP-VSR2Δ19 reaches the PVC via the plasma membrane or directly from the Golgi or possibly via the TGN. However, since the deletion mutant lacks the YMPL motif, it could follow a different path, in addition to its inability to recycle. Likewise, the previously reported mis-targeting of GFP-VSR2(Y612A) to the TGN and plasma membrane (Foresti et al., 2010) is insufficient as evidence to propose that wild type receptors normally use the TGN as the main hub for signal-mediated VSR trafficking to the PVC (De Marcos Lousa et al., 2012).

To interrogate potential receptor arrival at- or transit via- the plasma membrane in a quantitative manner, I used the ability of full length VSR to co-secrete its ligands when it is mistargeted to the plasma membrane (DaSilva et al., 2006; Foresti et al., 2010). This was effectively demonstrated by imposing the Y612A mutation on the full length coding region of VSR2, hereafter termed flVSR2(Y612A). This mutant is capable of ligand binding in the early secretory pathway but releases the ligands for delivery to the cell surface rather than the PVC, leading to secretion of vacuolar cargo to the culture medium in protoplasts and the apoplast in plants. The effect is dosage-dependent as increasing numbers of mistargeted receptors effectively 'drag' cargo away from endogenous receptors by competition, and 'drop' it off for secretion instead. Here the 4 deletion constructs have been used within the remit of the full-length receptor containing the complete lumenal ligand binding domain

to test which of the resulting mutants are capable of this 'drag & drop' activity to cause co-secretion of vacuolar cargo amy-spo.

To carry out the comparison in a quantitative manner, the four flVSR2 deletion mutants were inserted into a dual expression plasmid carrying a gene for cytosolic beta glucuronidase (GUS) as internal reference for transfection efficiency (Figure Figure 2.2). Similar dual expression vectors were created for flVSR2 wild-type and its dominant-negative flVSR2(Y612A) mutant as negative and positive controls respectively. Experiments were first carried out to normalise all transfections via the GUS reporter. After establishing the conditions for comparable transfection efficiencies, the dual expression plasmids were used for dose-response assays and co-transfected at increasing levels with a constant amount of vacuolar cargo amy-spo encoding plasmid. Following gene-transfer and incubation, GUS was measured again in all samples to establish the dose, as well as the amylase activity in the medium and in the cells to monitor the response. The resulting amy-spo secretion index (ratio activity medium/cells) was then plotted as a function of internal GUS standards to correct for minor differences in effector co-expression. This resulted in a very robust dose-response analysis shown in Figure 6.4.

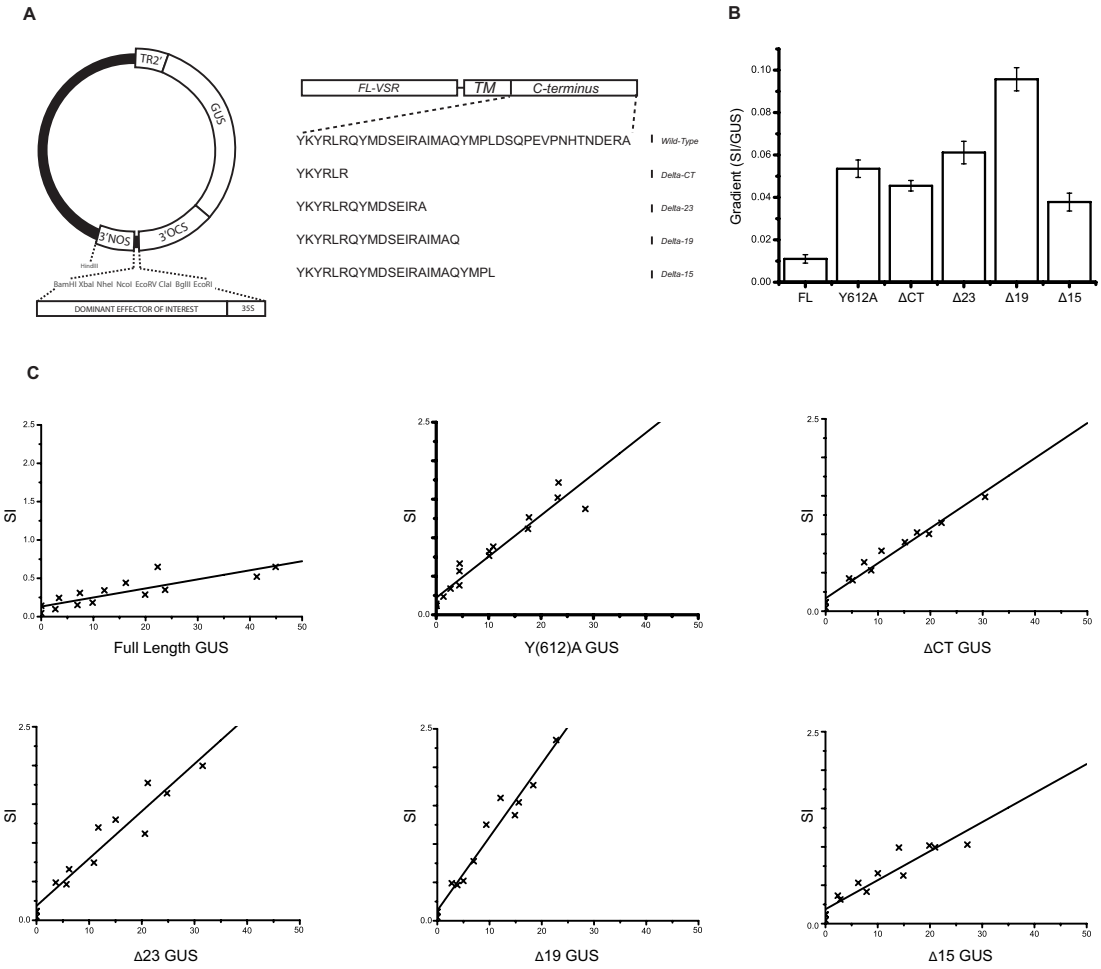

Figure 6.4: **Biochemical 'Drag & Drop' Assay to Monitor VSR Transit via the Plasma Membrane**
A. Schematic of the dual expression vector containing the internal marker GUS for normalisation of transfection efficiencies and the polylinker, as well as the sequences of the individual deletion constructs used in this study.
B. Overview of the observed gradients as a function of the internal GUS reference with the error bar representing the standard error of the distance of all data points from the calculated slope.
C. Individual X/Y scatter graphs illustrating individual secretion index (SI) data points (x) plotted as a function of internal GUS reference activity and linear regression lines.

As shown previously (Figure 3.6) flVSR2(Y612A) causes induced secretion of vacuolar cargo in a dose-dependent manner consistent with earlier reports (DaSilva et al., 2006; Foresti et al., 2010). Overexpressed flVSR2 wild type shows only minor effects on the cargo and serves as base-line for the experiments. Interestingly, complete deletion of the cytosolic tail (flVSR2ΔCT) results in a receptor molecule

that causes significant mis-targeting of amy-spo to the cell surface, as indicated by a 4-fold increased secretion compared to the wild type baseline. This supports the finding that the deletion mutant is not trapping significant quantities of cargo in the ER which would prevent its arrival in the culture medium. Arrival of the ΔCT construct at the plasma membrane or transit via the plasma membrane may have been below the detection limit of fluorescence microscopy (Figure 5.7) but the strongly induced amy-spo secretion suggests that even small numbers of flVSR2ΔCT that escape the ER reach a location from which cargo can be released to the culture medium. flVSR2ΔCT does not seem to trap amy-spo intracellularly, despite its predominant presence in the ER followed by the Golgi. Together with the observed competition between ERD2 and VSRs for dual signal cargo, the results suggest that any VSR-ligand interactions in the ER must be infrequent, whilst VSRs probably start binding cargo efficiently as early as the cis-Golgi.

Addition of the sequence QYMDSEIRA (flVSR2Δ23) shows a further increase in vacuolar cargo secretion compared to flVSR2ΔCT, exhibiting a slightly steeper dose-response compared to the positive control flVSR2(Y612A) (Figure 6.4). The Δ23 mutant is able to exit the ER more efficiently compared to the ΔCT mutant, and partitions to the plasma membrane and the TGN. Interestingly, further inclusion of the tetrapeptide IMAQ (Δ19) results in a receptor molecule that mediates the strongest induction of amy-spo secretion, showing the steepest dose-response compared to the positive control flVSR2(Y612A) and flVSR2Δ23 (Figure 6.4). In contrast to the Y612A mutant and the Δ23 deletion mutant, Δ19 did not show detectable steady state levels at the plasma membrane (Figure 5.7), confirming that plasma membrane retention is not required to mediate efficient mis-targeting of vacuolar cargo. In contrast, accelerated endocytosis may boost the mis-targeting efficiency of the mutant receptor.

Finally, inclusion of the YMPL motif in the shortest deletion (Δ15) drastically reduces the dose-dependent cargo secretion. Partial functionality of the YMPL without the spatial context of the complete tail can explain weak amy-spo secretion compared to wild type flVSR2 (compare fl and Δ15 in Figure 6.4). However, the dose-response of the Δ15 is the lowest of all the deletion constructs, even lower than the complete deletion of the tail (ΔCT). The obtained results provide strong evidence that the YMPL is dominant over the alternative IM signal, and prevents mis-targeting of vacuolar cargo by the wild type receptor.

6.2.3 The YMPL Motif is Dominant and Prevents Ligand-loss to the Apoplast

Figure 6.4 provided evidence suggesting that the YMPL signal prevents receptor-cycling via the plasma membrane but may be dependent on the spatial context of the entire VSR tail. To test the importance of this motif in its native context in preventing cargo-mistargeting to the cell surface, a different assay tested if YMPL-mediated transport to the PVC is dominant over signals that promote plasma membrane partitioning. Previous observations demonstrated that the length of the transmembrane domain played a role in mediating targeting of single span type I membrane proteins to the plasma membrane (Brandizzi et al., 2002). The work showed that long transmembrane domains of 23 amino acids and more promoted detection of fluorescent type 1 membrane spanning cargo at the plasma membrane. In order to see if a long transmembrane domain mediated a similar pathway two further receptor mutants were created by elongating the VSR2 transmembrane domain by 4 hydrophobic amino acids, either followed by a wild type cytosolic tail, or the Y612A transport mutant.

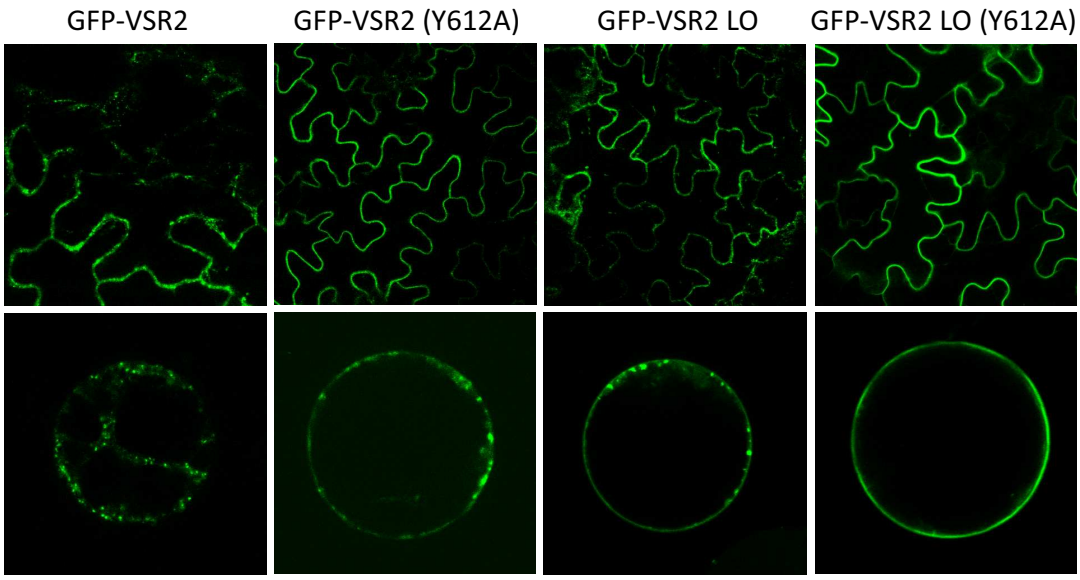

Figure 6.5: **Plasma Membrane Localisation of IM, Y and LoTM VSR2 Mutants** Confocal laser scanning micrographs of Agrobacterium infiltrated tobacco leaf epidermis cells expressing the four GFP-VSR2 fusions (upper panels) and protoplasts generated from stable transformed plants (lower panels) . Individual constructs are indicated above each lane. Top row images are approx 100μm across, and bottom row are approx 60μm.

Figure 6.5 shows the subcellular location of the two long transmembrane domain (LoTM) constructs GFP-VSR2LoTM and GFP-VSR2LoTM(Y612A) in comparison with GFP-VSR2 and GFP-VSR2(Y612A). Expression in epidermis leaves (upper row) reveals that lengthening of the transmembrane domain alone can lead to a similar partial plasma membrane partitioning as previously observed by introducing the Y612A point mutation. Combining the two modifications resulted in an almost exclusive localisation of GFP-VSR2LoTM(Y612A) to the plasma membrane. This is best appreciated by imaging protoplasts prepared from transformed leaf epidermis cells and imaged at the centre of the cell so that the plasma membrane forms a sharp uninterrupted smooth circle around the cell (Figure 6.5, lower row).

Using this information on plasma membrane partitioning, the 'drag & drop' assay was repeated by creating combinations of long transmembrane domains (LoTM)

with or without the Y612A substitution within the context of the full length receptor, yielding the constructs flVSR2LoTM and flVSR2LoTM(Y612A). These were subject to the same GUS-normalised dose-response assays to monitor induced amy-spo secretion as in Figure 6.4.

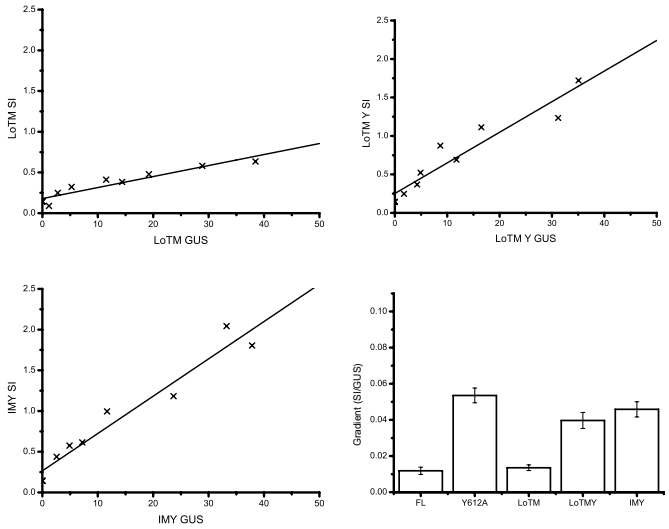

Figure 6.6: **Influence of plasma membrane partitioning on 'Drag & Drop' activity** Individual X/Y scatter graphs illustrating individual secretion index (SI) data points (x) plotted as a function of internal GUS reference activity and linear regression lines as well as the overview of observed gradients as a function of the internal GUS reference with the error bar representing the standard error of the distance of all data points from the calculated slope.

Figure 6.6 shows that lengthening the transmembrane domain alone yielded little or no effect on amy-spo secretion compared to the wild type construct. This confirms that the presence of a fully functional YMPL motif effectively prevents the 'drag & drop' effect, and that increased plasma membrane localisation of GFP-VSR2LoTM may be due to recycling from the PVC back to the plasma membrane. If flVSR2LoTM reaches the PVC first and dissociates from amy-spo, recycling to the plasma membrane will not cause further amy-spo secretion. The two constructs harbouring the Y612A mutation, however, yielded a strong dose-dependent amy-spo secretion, regardless of the size of the transmembrane domain. Therefore, the absence of a functional YMPL motif enables the 'drag &

drop' effect, whilst further re-partitioning from the TGN to the plasma membrane in the double mutant (LoTM + Y612A) did not exacerbate induced amy-spo secretion; on the contrary it seems to diminish compared to Y612A alone.

The combination of the long transmembrane domain with the Y612A mutant (Fig. 6.5) almost completely redistributes the protein to the PM. Therefore, to further probe the relationship between PM localisation and the YXXϕ motif an equivalent full length receptor mutant flVSR2(IMY) was created and a GUS-normalised dose-response analysis was carried out. Figure 6.6 shows that this construct also co-secreted amy-spo, albeit not more strongly than protoplasts transformed with the control construct flVSR2(Y612A). It is possible that both the IMAA mutation and lengthening the transmembrane domain inhibit endocytosis from the plasma membrane, rather than promote targeting to the cell surface. In mammalian cells it has been suggested that exclusion of membrane proteins with long transmembrane domains from clathrin-coated pits explains higher steady state levels at the plasma membrane (Mercanti et al., 2010). If the rate of exocytosis is unaffected, it would explain why the proteins maintain a higher steady state level at the plasma membrane without mediating a more pronounced cargo mis-sorting effect.

6.3 DISCUSSION

6.3.1 Where is the Default Location for Type-1-Membrane Spanning Proteins?

In the previous chapter it was established that VSR trafficking to the Golgi is via active selection into COPII carriers, the question remains how VSRs specifically segregate to the vacuolar transport route. Since VSRs also carry hydrolases that should not be mis-sorted to the cell surface, it is essential that this segregation is highly efficient. Type 1 membrane proteins have been proposed to reach different default locations depending on the length of the transmembrane domain (TMD). Short TMDs of 17 amino acids are thought to mediate accumulation in the ER membranes (Brandizzi et al., 2002), but it is not yet established if this is due to poor export competence or efficient segregation into COPI coated structures for retrieval. In contrast, proteins with intermediate sized TMDs (20 amino acids) accumulate at the Golgi stack whilst those with long TMDs (23 amino acids and more) partition to the plasma membrane without further signals (Brandizzi et al., 2002).

Deletion of a KKXX type-1 membrane protein ER retention signal has indeed resulted in plasma membrane re-partitioning (Benghezal et al., 2000) and would support this idea. However, an earlier report suggests that type I membrane proteins can progress by default to the tonoplast (Barrieu and Chrispeels, 1999). This seems to correspond to the situation in yeast where deletion of the vacuolar sorting receptor (VPS10) C-terminus results in accelerated degradation in the vacuole, suggesting that at least this type of membrane protein can reach the vacuole by default (Cereghino et al., 1995; Cooper and Stevens, 1996). The YXXϕ

motif of VPS10 has therefore been proposed to mediate receptor recycling from the PVC to the Golgi in yeast, using a retromer-dependent pathway.

In plants, the equivalent YXXϕ motif was shown to be important for both anterograde and retrograde transport, as shown by the anterograde transport mutant Y612A and the recycling mutant L615A (Foresti et al., 2010). Deletion of the VSR C-terminus results in a more severe anterograde transport defect compared to Y612A, causing partial ER retention and reduced vacuolar degradation of the resulting GFP-VSR fusion (DaSilva et al., 2006). Although this seems to be in contrast to results obtained with truncated VPS10, it should be noted that GFP-VSR2ΔCT showed residual processing to the vacuolar core-fragment. Therefore, type I membrane spanning proteins with intermediate sized TMDs can reach the tonoplast, but when this occurs at low rates it is difficult to see through microscopy due to degradation of the lumenal fluorophore. A critical appraisal of the existing data suggests that identification of the highest steady state levels in fluorescence microscopy is insufficient to distinguish between different transport events or to rule out rapid transit through an organelle. Some membrane proteins may thus reach multiple locations, other than those showing detectable steady state levels.

6.3.2 The 'Drag & Drop' Assay Reveals Receptor Transit via the Plasma Membrane in the Absence of YXXϕ-Mediated Targeting

To increase the number of tools for receptor trafficking analysis, post-Golgi trafficking of VSRs has been studied via a combination of microscopy and a sensitive biochemical transport assay that actively explores the ligand-binding and release properties of the VSR lumenal domain. The biochemical assay takes advantage of the fact that VSRs release their ligands in the acidic extracellular medium when

mistargeted to the plasma membrane (DaSilva et al., 2006), here termed the 'drag & drop' assay. The power of this complementary approach was shown earlier using the Y612A mutant. Imposed on the GFP-VSR2 fusion, the mutation strongly inhibits the competition with endogenous receptors, showing that its transport route has changed dramatically. This is confirmed by a redistribution from the PVC to the plasma membrane and TGN (DaSilva et al., 2006; Foresti et al., 2010). When imposed onto the full-length receptor, it transforms a neutral receptor molecule to a receptor that snatches ligands away from endogenous receptors and drops them off at the cell surface, thus revealing an alternative pathway.

When this dual approach is applied to the deletion of the cytosolic tail (ΔCT), new quantifiable observations allowed me to obtain evidence for transit through compartments despite low steady state levels. When imaging GFP-VSR2ΔCT in transformed leaf epidermis cells, a typical ER network that comprises the majority of the fluorescence is revealed, although a variety of post-ER compartments are labeled as well (Figure 6.1). The most significant of the post ER compartments was the Golgi apparatus, as shown before (Brandizzi et al., 2002). This confirms that removal of the tail predominantly results in an anterograde transport defect to the vacuolar route. However, partial localisation at post-Golgi compartments such as the TGN and the PVC (Figure 6.1) also confirmed that the deletion mutant can slowly enter the route to the lytic vacuole (DaSilva et al., 2006). Although plasma membrane localisation of GFP-VSR2ΔCT was not observed by fluorescence microscopy, evidence for transit via the plasma membrane arose from the more sensitive 'drag & drop' assay. Figure 6.4 shows that deletion of the cytosolic tail of full length VSR2 (flVSR2ΔCT) results in a dominant mutant that induces the secretion of vacuolar cargo despite the presence of endogenous wild type receptors. The effect is almost as strong as reported for the Y612A

mutant of the full length receptor (flVSR2(Y612A)) and illustrates that only small quantities of cell surface VSR display are required for co-secretion of vacuolar cargo. The results also show that VSR-ligand interactions in the ER are not likely to be significant because flVSR2ΔCT would have had to cause ER retention of vacuolar cargo instead of induced secretion.

Putting these results together suggests that bulk flow of a type I membrane spanning protein such as VSR leads to high steady state levels in the ER and the Golgi, but it also reaches the plasma membrane, the TGN, the PVC and the vacuole, in agreement with all previous reports (Barrieu and Chrispeels, 1999; Benghezal et al., 2000; Brandizzi et al., 2002; DaSilva et al., 2006). Introduction of the sequence QYMDSEIRA in the Δ23 deletion mutant abolished ER retention of the GFP-fusion, and increased the 'drag & drop' activity of flVSR2Δ23 compared to the ΔCT construct (Figure 6.4). Interestingly, the partial Golgi-localisation observed for GFP-VSR2ΔCT was also reduced and instead there was a more prominent plasma membrane and TGN localisation. A plausible explanation for this shift in steady state levels is that increased ER export simply reveals arrival at the plasma membrane that was below the detection limit of fluorescence microscopy for the ΔCT construct. Another hypothesis is that there is a second transport motif that promotes Golgi export to the plasma membrane and/or the TGN. It can also not be excluded that increased levels at the plasma membrane and TGN are the result of rate-limiting endocytosis and export from the TGN, both of which may not be detectable for the ΔCT construct. However, both proteins still partially reach the PVC, which suggests that there is no simple default location for membrane spanning proteins in the secretory pathway, and proteins may reach the plasma membrane, but will also slowly partition to the vacuole for degradation.

6.3.3 Biosynthetic VSR Targeting to the PVC is not by Bulk Flow and Avoids Transit via the Plasma Membrane

One of the key-observations of this work is the evidence for at least two completely separate routes to the PVC in plants. Dissection of the VSR C-terminus via the combination of microscopy and the 'drag & drop' assay reveals that one of the main functions of the YMPL motif is to prevent arrival of receptors at the plasma membrane to avoid vacuolar cargo mis-sorting. Figures 6.4 and 6.6 show that the presence of a functional YMPL motif within its natural context not only acts for selective anterograde transport to the PVC and subsequent recycling from this compartment, but that it targets the receptor-ligand complex in such a manner that mistargeting via the cell surface is effectively avoided. Only constructs encoding a deleted or mutant (Figure 6.4, Y612A) YMPL motif elicit strong 'drag & drop' activity. However, vacuolar cargo mis-sorting is not correlated with plasma membrane localisation alone, suggesting that cargo-dissociation occurs rapidly even if endocytosis is efficient.

The observed difference between the Δ23 and Δ19 mutants with respect to localisation suggest that the IM motif plays a secondary role at the plasma membrane to mediate VSR endocytosis, in agreement with earlier observations (Saint-Jean et al., 2010). VSR-endocytosis may not occur frequently for wild type receptors that use the YMPL-mediated route to the PVC. Under normal physiological conditions, VSRs may reach the plasma membrane only by accidental bulk flow leakage, but even under overexpression conditions as in our experimental system, induced amy-spo secretion is minimal for wild type VSR. This illustrates the high efficiency of the YMPL-mediated anterograde VSR transport to the PVC, which cannot be explained by unspecific bulk flow. In short, the data presented here and in the previous chapter is consistent with a model in which the VSR

traffics from the Golgi stack towards the vacuole in a YXXϕ dominant manner to the vacuole, in clathrin-coated vesicles, avoiding the plasma membrane.

7 GENERAL DISCUSSION

As the detailed explanations of the results have been discussed individually in each chapter, this section will be reserved for discussions on the interrelated data within the thesis. Aside from the scientific questions addressed in this work, this thesis introduces new methodologies the benefits of which are experimentally exploited. In addition, I will highlight areas in the field where there are open questions, either not addressed in the thesis or based on results gathered in this work. Finally, I will present a model based on all data on the trafficking route of the *A. thaliana* VSR.

7.1 KEY FINDINGS

7.1.1 The Introduction of Novel Approaches Allows for Greater Quantification and Qualitative Appreciation

Internal markers were used to (1) distinguish active secretion from unspecific leakage from cell mortality (default secretion versus cytoplasmic marker (Denecke et al., 1990)), (2) differentiate the effect of the unfolded response on secretory versus cytosolic proteins (Leborgne-castel et al., 1999) and (3) to identify individual cells by fluorescence microscopy in which untagged and potentially cytosolic mutants were expressed together with the specific reporter (Bottanelli et al., 2011). Although the principle of dual-expression was clearly established, its potential for quantitative analysis remained unexplored. In Chapter 2 a GUS internal control expression system that included a polylinker for practical subcloning was generated.

One of the main problems of transient expression technology is the uncertainty regarding expression levels. In protoplast electroporation this is dependent on the quality of the plasmid preparation and the copy number of transfected plasmids in different cells. In leaf infiltrations with *A. tumefaciens* the timing of DNA transfer to individual cells after infiltration is highly variable and accounts for large differences in gene expression at the time of analysis. Quantification of expression, however, is crucial for the establishment of dose-responses. In addition, protein transport and processing can be influenced by expression levels alone. In this thesis, a GUS expression system was used initially to monitor the expression of GFP-VSR fusion proteins to control for protoplast expression and the turnover of the fusion protein. Due to the simplicity of the assay and the ease of subcloning into the expression vector the assay was used for several additional experiments in this thesis.

In Chapter 3 the GUS normalisation system was used as part of an *in planta* protein-protein interaction assay that demonstrated that the lumenal domain of VSR5 compromises its interaction with the canonical VSR2 cargo (See Figure 3.7). This assay relied on the 'drag & drop' effect that was also utilised in Chapter 6 and discussed below. The GUS internal marker in this assay allowed for the magnitude of the secretion effect for both the sample and the control to be plotted against respective gene expression. The results still depend on the assumption that two different proteins are synthesised at comparable rates to a reference marker on the same plasmid. Since VSR2 and VSR5 are similar proteins, this assumption was justifiable, but care has to be taken when comparing totally different genes. As an extension of this work this assay could be used as an *in planta* protein-protein binding assay in a more general sense, for example, to confirm results of a Yeast-two hybrid screen. A candidate receptor would be

fused in place of the lumenal domain in the VSR(Y612A) construct and the potential ligand would be fused to a signal peptide N-terminally and a peptide tag (e.g. His tag) C-terminally. If the proteins interact then the receptor will deliver the protein to the cell surface in a 'drag & drop' like manner. Immunodot or SDS-PAGE immunoblot assays could then be used to assess secretion and thus the presence/absence of an interaction. The only caveat with this approach would be that it not only requires selective binding in the ER-Golgi system, but also selective dissociation at the cell surface.

This 'drag & drop' approach was also used as part of an experimental dissection of the VSR2 cytosolic C-terminus (see Figures 6.4 and 6.6 in Chapter 6). This approach utilised a similar concept to the lumenal domain swap experiment described above, but instead was monitoring the ability of various C-terminal mutants to 'visit' the plasma membrane, and thus induce the 'drag & drop' effect. Once again the secretion induction was plotted against the expression of the GUS internal control and thus the comparative effect was comparable from the magnitude of the slope. This metric was particularly useful in this case as it allowed for multiple gradients to be qualitatively appreciated (e.g. Figure 6.4, panel B). In this case, the comparison of genes with minor modifications (i.e. point mutations, short deletions) was unlikely to induce differences in protein synthesis and it is probable that GUS levels adequately reflected the expression of the test genes. In conclusion, the internal marker assay would be appropriate to compare the effect of point-mutations on a specific gene, for instance a GTPase, but it may not be best to compare a GTP-trapped GTPase with an overexpressed exchange factor, and any results should be regarded as qualitative.

An additional qualitative comparison tool was introduced in Chapter 4 (see Figure 4.7). This *in silico* ImageJ (*http://imagej.nih.gov/ij/*) macro allows

for histogram visualisation of PSC scatterplots and thus easier visualisation of complex co-localisations, this technique was used recently to compare the effects of various Rab mutants on vacuolar sorting (Bottanelli et al., 2012) see Figure 6, the histogram overview allowed for the observation of the fusion of two organelles under specific conditions. Although this approach is unnecessary for simple co-localisations in which you either have a non co-localising population of organelles or a perfectly co-localising population, in reality, there are often more complex situations where a protein is trafficking through a series of organelles, or has a steady state level at one organelle only. In these situations, the histogram visualisation allows for easier interpretation.

7.1.2 VSR5 is a Unique *A. thaliana* Vacuolar Sorting Receptor

One of the key findings in this thesis relates to the role of the *A. thaliana* Vacuolar Sorting Receptor paralogue, VSR5. Multiple lines of evidence indicate that VSR5 plays a unique role in a physiological context. In this study it has been demonstrated that the VSR5 has increased protein turnover, does not interact with canonical VSR2 cargo and finally localises to the LPVC rather than the PVC (Figures 2.7, 3.7 and 4.11 respectively). Other groups have used a genetic approach to show that VSR5 was unable to rescue a VSR1/2 double mutant (Lee et al., 2013; Zouhar et al., 2010).

The role of the VSR5 has yet to be directly experimentally addressed. One approach that might get to the true function of VSR5 would be to use the lumenal domain to 'fish' for an interacting partner, either by immunoprecipitation or a column bound approach. These approaches, however, make the assumption that the role of VSR5 is in protein sorting. There is a possibility that VSR5 interacts

with a glycan conjugated to a protein, similar to the Mannose-6 Phosphate Receptor, or alternatively it could sort oligosaccharides to/from the cell wall. Unlike mammalian cells, plant cells contain a polysaccharide-rich extracellular matrix the maintenance and synthesis of which may involve endocytic recycling rather then *de novo* synthesis. A speculative model could be that VSR5 recycles cell wall components during cell growth, perhaps expressed in certain tissues.

It would also be interesting to see if VSR5 interacts with different cytosolic sorting determinants. In the anterograde sorting route it could be possible that VSRs interact with the same sorting apparatus in an anterograde direction, but not in the retrograde direction. GFP-VSR2 causes a 'competition effect' when ectopically expressed, this is due to the titration of endogenous cytosolic machinery and results in the secretion of vacuolar cargo. In Chapter 3 a similar experiment with VSR5 showed that this effect does not occur with GFP-VSR5. When the competition effect was originally demonstrated it was proposed to cause a recycling defect, rather than an anterograde transport defect, as overexpressed full-length VSR2 recovered vacuolar sorting (DaSilva et al., 2006). Therefore, we can conclude that VSR5 interacts with different transport machinery that prevents recycling via YMPL machinery, experimentally supported by the fact that VSR5 localises to the LPVC, a compartment only reached by the recycling defective mutants of VSR2. Therefore, either VSR5 interacts with different retrograde recycling machinery than VSR2 or it does not recycle. There is the possibility that one of the retromer VPS35 subunit paralogues (See table 4.1) does not interact with the VSR5, a concept discussed previously (Lee et al., 2013). Alternately, if VSR5 is completely recycling deficient as in the immunoblot assay (Fig. 2.7) increased leakage of the receptor towards the vacuole could be observed. Possibly VSR5 gets included into ILVs within the MVB/PVC preventing interaction with retromer.

7.1.3 The LPVC is a Physiologically Relevant Organelle

The existence of an organelle beyond the PVC, but before the vacuole, was originally demonstrated using a VSR point mutant (L615A) (Foresti et al., 2010). However, the primary experimental evidence was co-localisation data, and it could not be ruled out that the L615A mutation of the receptor induced the formation of the LPVC as an artifact of expression of an aberrant receptor. The presence of the wild-type fusion Venus-RhaI, Ara6-GFP and GFP-VSR5 at this compartment, therefore, validate the existing data in a meaningful manner.

Due to its recent discovery, there is limited information about the LPVC. In summary: the Rab5GTPases localise to the compartment (this thesis), it is beyond the PVC in a biosynthetic sense (Foresti et al., 2010), structurally it is multi-vesicular with intralumenal bodies (Haas et al., 2007b) and finally the number of LPVCs increases under ectopic Rab7 dominant negative expression (Bottanelli et al., 2012). As an extension of this, a reasonable assumption would be that the multi-vesicular bodies seen fusing with vacuole like structures in recent electron micrographs are LPVCs fusing with the vacuole (Scheuring et al., 2011). A speculative overall model of LPVC trafficking would start with the maturation mediated biogenesis of the organelle. VSRs would be selectively removed from the PVC, along with specific lipid species. Simultaneously, ubiquitinated proteins would be enveloped into intralumenal bodies. This might happen gradually, but the lack of co-localisation between the organelles implies that there is a critical mass that the PVC needs to reach before VSR recycling is initiated. Perhaps due to the change in lipid contents or the organelle, Rab5 is then recruited, probably providing a hub for interaction with the CORVET complex (Epp et al., 2011). Rab5 is probably activated at this stage, perhaps allowing the recruitment of the SNAREs and the HOPS complex needed for the final fusion event. The final step

is the recruitment of the GTPase Rab7. Rab7 cannot be detected at the LPVC, only the tonoplast, therefore the Rab7GTPase is probably recruited at the final moments. The hydrolysis of the Rab7 probably allows for the final fusion event and the delivery of the contents of the LPVC to the vacuole.

7.1.4 Anterograde Trafficking of the A. thaliana Vacuolar Sorting Receptor occurs in Sequential Signal Mediated Steps

The study of *A. thaliana* VSRs enables understanding of how recycling membrane proteins are sorted (De Marcos Lousa et al., 2012). Unlike their functional analogues in yeast and mammals, the C-termini of all the VSR isoforms in plants are comparatively short and consist of a mere 30 to 40 residues. The anterograde sorting of the receptor is known to be dependent on a Tyr in the canonical YXXϕ motif present in the C-terminus, whilst the recycling is dependent on the Leu in the same motif (Foresti et al., 2010). There were multiple points of controversy, some of which have been clarified in this study. The fundamental thesis presented here is that the VSR traffics in several clear signal mediated steps to allow both 'towards vacuole' and 'from vacuole' traffic.

Chapter 5 and 6 demonstrate that the 9 residues proximal to the lipid-bilayer allow for the inclusion of the VSR in COPII vesicles/tubules that traffic to the Golgi apparatus but lead to mistargeting to the plasma membrane. Downstream of the ER export motif, the IMAQ motif was implicated in the endocytic recycling of the receptor (See Figure 5.7). The final motif, and most characterised in the receptor terminus is the YXXϕ motif, which allows the receptor to avoid mistrafficking to the plasma membrane and allows the receptor to reach the PVC.

The data obtained also provide insight into the role of the clathrin coat complex in VSR trafficking. The highly selective nature of vacuolar sorting observed in our transport assays and the co-purification of VSRs with clathrin-coated vesicles in three independent studies (Hinz et al., 1999; Kirsch et al., 1994; Sauer et al., 2013) clearly demonstrate that a minimum of one selective clathrin mediated transport step occurs in biosynthetic VSR-mediated vacuolar sorting. This is also supported by independent studies indicating a critical role of clathrin adaptors (Happel et al., 2004; Park et al., 2013; Sanderfoot et al., 1998). However, the clathrin mediated step is often debated; Golgi/TGN $\rightarrow$ PVC could be clathrin mediated, or alternatively, the pathway to/from the plasma membrane could be clathrin mediated. The data in this study show that the VSR does not normally traffic via the PM, there is strong support that biosynthetic VSR transport occurs in clathrin-coated vesicles from the Golgi/TGN directly to the PVC. This is supported by a recent publication showing that two clathrin binding proteins (ENTH and ARF-GAP) participate in VSR-cargo trafficking to the vacuole (Sauer et al., 2013).

The motifs within the VSR C-terminus seem to work in temporal succession, but it is unlikely that cycling via the plasma membrane plays a physiological role in biosynthetic hydrolase transport to the vacuole. This work suggests that YMPL-mediated VSR transport to the PVC may occur before the point at which targeting to the plasma membrane is significant. It is possible that AP mediated interactions with the VSR tail mask those regions that involve other AP complexes. There are several mechanisms that might work in concert to explain this: lipid affinity, steric exclusivity and protein association. A lipid affinity mechanism would require that each compartment has a particular lipid constitution and the respective cytosolic machinery have affinity for the particular lipid at their

site of action. There is some experimental evidence to support this claim; the retromer sorting nexins that are thought to interact with the VSR at the PVC have Phox homology (PX) domains that mediate interaction with phosphatidylinositol 3-phosphate (PI3P) (Seaman et al., 2012), accordingly PI3P is enriched in the late endosomal system (Kim et al., 2001). Steric exclusivity would occur when a particular cytosolic factor is bound to the tail of the membrane spanning protein, other signals are masked. This phenomenon is particularly appealing due to the small size of the VSR tail. In addition, other mechanisms could be playing a role such as receptor dimerisation/oligomerisation and association with other membrane spanning proteins.

7.2 MODEL AND OUTLOOK

7.2.1 A Model of Vacuolar Receptor Trafficking

The generation of a coherent model of vacuolar sorting requires balancing all published accounts with the data generated in this thesis. It is important to acknowledge that this model is partially speculative. Due to the complex nature of the pathway the model is also simplified as it will focus on the trafficking of the VSR and its ligand from a biosynthetic perspective only.

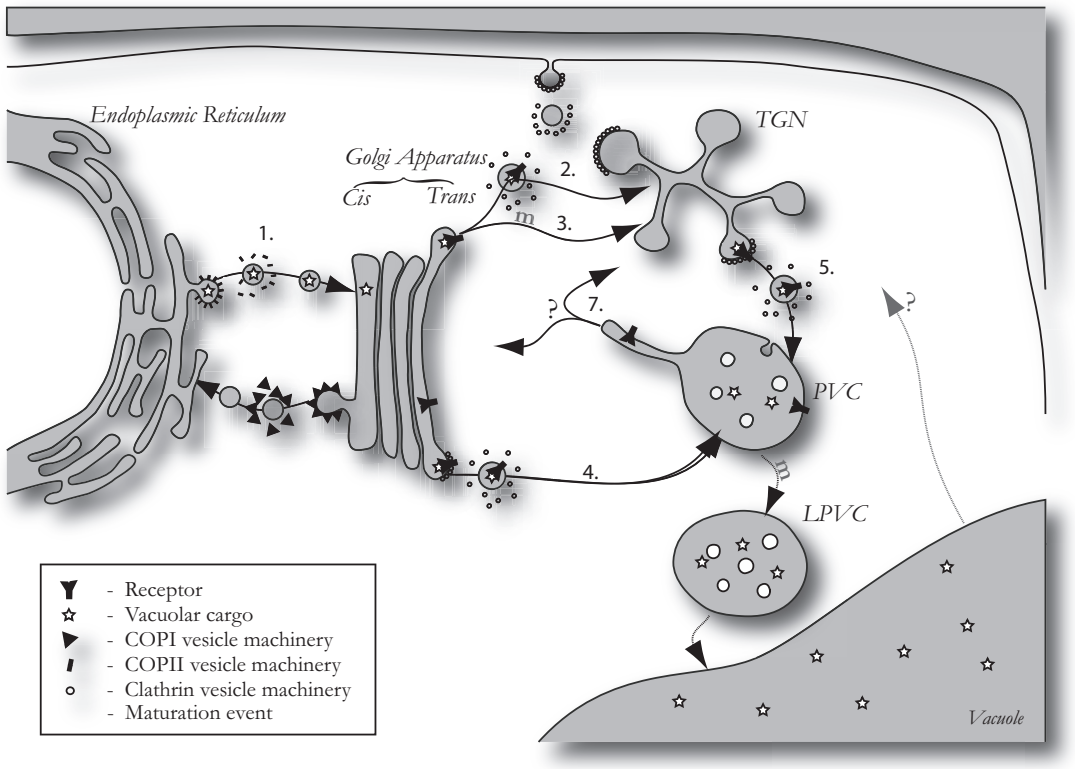

Figure 7.1:

The data from Chapter 5 strongly suggest that after co-translational translocation into the ER the VSR traffics to the Golgi apparatus in COPII vesicles (Figure 7.1, 1.). At the Golgi, the VSR likely traffics to the TGN *or* PVC in clathrin-coated vesicles (CCVs) (Figure 7.1, 2. and 4.), which is strongly supported by the anterograde transport deficiency in Y612A point mutations (DaSilva et al., 2006; Foresti et al., 2010), as well as the recent study on the effects of ENTH and ARF-GAP in VSR-cargo trafficking to the vacuole (Sauer et al., 2013). As discussed above, there has to be at least one CCV mediated step in the trafficking of VSRs (Hinz et al., 1999; Kirsch et al., 1994; Sauer et al., 2013), and it has been demonstrated in this thesis that it is not via the plasma membrane. It is possible that these CCVs containing VSRs bud from the Golgi apparatus, as the clathrin adaptor complexes have been observed at the *trans*-Golgi stack (Happel

et al., 2004). However, it is also possible that the *trans*-Golgi stack matures into the *trans*-Golgi network (TGN) (Figure 7.1,3.). This is supported by recent electron tomography studies (Kang et al., 2011), although these studies were solely qualitative. Clathrin coats have also been seen coating the TGN, it was originally referred to as the partially-coated reticulum for this reason (Pesacreta and Lucas, 1984; Tanchak et al., 1988).

If the VSR does traffic via the TGN, then the export to the PVC might happen by either CCVs or maturation (Figure 7.1, 2. and 3.). Experimental data indicating that a VSR point mutant which does not interact with clathrin adapters (VSR2-Y612A) localises to the TGN suggests that the wild-type VSR exports from the TGN in CCVs (Figure 7.1, 5.). However, this point mutant could be passively trafficking there from the Golgi, because it is unable to follow a signal-mediated Golgi to PVC route. Indeed, in this thesis all Y612A point mutations show strong cargo mis-targeting to the plasma membrane (Figures). Complete deletion of the YMPL motif leads to even stronger mis-sorting effects (compare Δ23 & Δ19 with all Y612A mutants). This result matches with the *in vivo* competition assay where GFP-VSR2 competes for endogenous VSR recycling (DaSilva et al., 2005). The maturation theory (Figure 7.1, 3.) has recently been proposed (Scheuring et al., 2011), however there is a lack of direct evidence to support either argument.

It is highly likely that the PVC is the point of dissociation/recycling of the VSR as a recycling defective VSR(L615A) traffics 'beyond' the PVC to the LPVC (Foresti et al., 2010) and an anterograde trafficking-defective VSR(Y612A) fails to reach PVC (DaSilva et al., 2006). As discussed in the introduction the recycling is probably retromer mediated, although it is still unknown where VSRs end up after they recycle from the PVC. Tubular connections between PVC and TGN membranes observed after drug treatment and partial washout have been

suggested to document TGN to PVC maturation (Scheuring et al., 2011) but may just as well represent retrograde PVC to TGN transport carriers. Whilst it is important to repeat these experiments without drug treatments, to avoid the risk of unspecific merging of organelles (Wang et al., 2009), it remains plausible that VSRs recycling from the PVC are destined to return to the Golgi/TGN (Figure 7.1, 7.), in line with the models in other systems. Regardless of the destination, it is clear that VSR recycling is signal-mediated, requires the core fragment of retromer and occurs from the PVC (Foresti et al., 2010; Kang et al., 2012; Saint-Jean et al., 2010).

7.2.2 Open Questions

The open questions in the field fall into two broad classes– questions regarding the findings in this thesis and questions pertaining to understanding a complete model of vacuolar sorting receptor trafficking.

Within this thesis the VSR paralogue VSR5 has been demonstrated to be functionally different in a number of ways. There are a number of open questions that need to be addressed. Firstly, it needs to be formally shown that these differences are not just due to a pseudogene undergoing genetic drift. As discussed in Chapter 3 the gene is specifically expressed in certain tissue, thus it seems unlikely to be a pseudogene. To rule out this possibility, however, the protein needs to be fully characterised functionally from a physiological perspective. The first functional question to be addressed needs to be on the interacting partner of the lumenal domain. The second question that needs to be addressed is on the functionality of the C-terminus and in particular which cytosolic factors interact.

From Figure 7.1 it is clear that there are two remaining open questions with regards to the trafficking cycle of the VSR. The first of these two is whether the anterograde trafficking route passes through the TGN. This question is difficult to address, as the observed state in live cell microscopy is the steady state distribution of the protein. There are two possible approaches that could be utilised to monitor the trafficking of the receptor, either the use of a VSVGtsO45 temperature sensitive mutant (Kreis and Lodish, 1986; Lafay, 1974) or the recently described retention using selective hooks (RUSH) system (Boncompain et al., 2012). Both systems rely on the same fundamental principle, the receptor is held in a compartment (e.g. the ER) to accumulate. The experimenter then changes the conditions, either by increasing the temperature or by the addition of biotin, which releases the receptor *en masse*, and thus in traceable amounts. The trafficking of the receptor can then be tracked using live cell CLSM over a time series.

The second question relating to the trafficking of the VSR is the recycling mechanism. As discussed above, the receptor likely recycles from the PVC, to the early secretory pathway. The compartment to-which the receptor recycles is unknown and controversial. The experimental basis to answer such a question is difficult as current microscopy techniques are not advanced enough to track the life of individual vesicles in live-cells due to a combination of diffraction limited systems, sensor sensitivity and sensor/laser speed. There could be solutions to these issues on the horizon, with the diffraction limit already overcome in fixed cell microscopy and recent advances in live cell microscopy such as spinning-disk systems.

The final, and as yet, completely experimentally unadressed open question is regarding both the biosynthesis of organelles and the recycling of membranes. The work in this thesis, as well as elsewhere, clearly shows that there is a general

'trend' of protein trafficking from the early secretory pathway towards the late secretory pathway. Along with the proteins trafficking, there are also maturation events in which the lipid membranes follow this flux trend. These lipids are thus depleted from the early secretory pathway. The replenishment of the early secretory pathway lipids, is probably in organelle biogenesis events and is also presumably intrinsically linked to lipid recycling from the late secretory pathway. Whether this happens though vesicular transport, direct lipid contact sites, tubular transport or an uncharacterised mechanism is not yet known.

7.2.3 Outlook

In a long term perspective, experimentally addressing these issues can be considered feasible. At which point, the trafficking route of the VSR will be one of the few fully annotated routes for a recycling membrane protein across all kingdoms. In addition, this platform will generate a good base for a synthetic receptor system. The use of transgenic plants to produce heterologous proteins for either nutritional or pharmacological benefits is a well established principle. To increase the stability of transgenically expressed soluble proteins they need to be targeted to a compartment where they will be stable. This compartment is dependent on the protein, for example a non-catalytically active globular protein might be most stable in the ER, or in the extracellular apoplast, where it will not be degraded, however, a lytic hydrolase might be best targeted to the vacuole, where it cannot degrade essential cellular machinery. In addition, more advanced techniques may attempt to engineer whole synthesis pathways (e.g. lipid metabolism, heterologous protein synthesis/modification), and these techniques will be much more efficient if the enzymes are all expressed in the same compartment. In this thesis, it has been demonstrated that a synthetic receptor can be generated to allow for the

delivery of targeted heterologous cargo to the cell surface. Having knowledge of a complete receptor cycle route, including understanding the overlapping cytosolic sorting motifs, potentially allows for various synthetic targeting receptors to be created that allow the targeting of any ligand to the various compartments that the VSR visits as well as the plasma membrane – possibly allowing for generation of transgenic plants with greater protein stability and therefore yield.

8 MATERIALS AND METHODS

8.1 MOLECULAR BIOLOGY

All DNA and molecular biology manipulations were based on (Sambrook et al., 1987) unless otherwise stated. Reagents were purchased from Sigma-Aldrich (Missouri,USA) unless otherwise stated. Agarose gels were made in 0.5x TBE buffer and pre-stained with ethidium bromide to a final concentration of 0.5μg/ml. DNA was usually prepared, manipulated and stored in 10/1 TE buffer, aside from reactions involving DNA polymerase. Restriction endonucleases were purchased from New England Biolabs (Beverly, USA). The *Escherichia coli* strain used was MC1061 (Casadaban and Cohen, 1980). *E. coli* cultures were grown either on LB-agar plates or in LB culture medium (Bertani, 1951).

10/1 TE buffer: 10mM Tris-HCl pH 8.0; 5mM EDTA. Filter sterilised and stored at 4°C.

5x TBE buffer: 1.1M Tris-HCl pH 8.0; 900mM Borate; 25mM EDTA. Autoclaved and stored at 4°C.

Lysogeny broth (LB): 10g Tryptone, 5g Yeast Extract, 10g NaCl. 15g/l Agar for solid medium. Autoclaved and stored at room temperature.

#	Amplicon Name & Directionality	Primer Sequence
1	VSR5/2 fus VSR5 lum ClaI sense	TTGTCGAAATCGATGTCTCCGAGCAATAAAGGA
2	VSR5/2 fus VSR5 lum BglII anti	CTGCTTCTGGATCCACTTCTTCTCTCGATAC
3	VSR5/2 fus VSR2 C-term BglII sense	CCAAGACGAGATCTCAAGTGAAATCAGCGTGGGCGG
4	VSR5/2 fus VSR2 C-term NOS anti	ATAATTGCGGGACTCTAATCA
5	Gibson GUS Vector TR2' sense	AGTCACGACGTTGTAAAACGACGGCCAGTGTACCCGGCCTGAATTTCGCGGGT
6	Gibson GUS Vector TR2' anti	CATGGATTTGGTGTATCGAGATTGG
7	Gibson GUS Vector GUS sense	CATAACCAATCTCGATACACCAAATCCATGTTACGTCCTGTAGAAACCCC
8	Gibson GUS Vector GUS anti	TCATTGTTTGCCTCCCTGCTGCGG
9	Gibson GUS Vector 3'OCS sense	GGTGAAAAACCGCAGCAGGGAGGCAAACAATGATAGAGTCCTGCTTTAATGAGATATG
10	Gibson GUS Vector 3'OCS-poly anti	CTCGAGCTAGCCATGGATATCGATAGATCTGCAGAATTCCCGGGTCCTGCTGAGCCTCGACATGTTGTCGC
11	Gibson GUS Vector poly-3'NOS sense	CAGATCTATCGATATCCATGGCTAGCTCGAGTCTAGAGGATCCGAAGCAGATCGTTC
12	Gibson GUS Vector 3'NOS-pUC anti	GGAAACAGCTATGACCATGATTACGCCAAGCTTAGGCCTGGGGATCTTCCCGATCTAGTAAC
13	VPS35a ClaI sense	GAGAAGAAATCGATGAGAACGCTCGCCGGAGTAGAAGA
14	VPS35a XbaI anti	TGTCTCGGTCTAGAGTCACAGCTTGATAGGGTCATA
15	VPS29 NcoI sense	CTGTTTTGCCATGGTGCTGGTATTGGCATTGGGGGA
16	VPS29 NheI anti	CTCATTGCGCTAGCCGGACCAGAGCTGGTAGTAGGGGGC
17	RFPClaI	CTCTCTCTATATCGATGGCCTCCTCCGAGGACGTCATC
18	RFPNcoI	CCAGAGCTAGCCATGGATGCTCCTGCGCCGGTGGAGTGGCGGCCCTC
19	*At*FYVE1 BamHI sense	ATTTTTGGATCCATGGCTACTCTCAACGGAAAAGC
20	*At*FYVE1 SalI anti	CTCATTGCGTCGACTTACGGGCGCAAACGAGCATAGAGCTCTC
21	*At*FYVE2 ClaI sense	CTCTAATCGATGGATGAAAGAGATCGAGAAATTCG
22	*At*FYVE2 NheI anti	GGGACGTTAGCTAGCCCTCCCCATCTTCTGATACAG
23	RFP-HDEL-anti	CTGCTTCGGATCCCTAGAGTTCATCATGTGCGCCGGTGGAGTGGCGGCCCTC
24	Δ mutants 35S sense primer	CACTATCCTTCGCAAGACC
25	Δ23 XbaI anti	ATGTACTGTCTAGATTAGGCTCTGATCTCTGAGTCCAT
26	Δ19 XbaI anti	CTGTCCAGTCTAGATTACTGTGCCATTATGGCTCTGAT
27	Δ15 XbaI anti	ACCTCAGGTCTAGATTACAGTGGCATGTACTGTGCCAT

Table 8.1: **Oligonucleotide Primers Used in this Study**
A list of all the primers used in this work for molecular biology. Sequencing primers not included. 'anti' = antisense directionality.

8.1.1 DNA Plasmids

Over 50 recombinant plasmids have been used in this work, with many of them being made over the course of the thesis work. Due to the numbers of plasmids it is impractical to describe the generation of every recombinant construct, therefore a list has been generated that records the plasmids as they appear in this thesis. Any which have been used here, but generated by others, have also been listed and appropriately attributed. The majority of vector backbones are pUC19 origin or C58ClRif^R for *A. tumefaciens* mediated infiltration – indeed many of the effectors are in both vector origins. In addition, the generation of the 'GUS normalisation vector' in Chapter 2 resulted in many effectors being subcloned into this pUC19-GUS vector, they have been annotated in the table below with 'GG'.

Name	Effector	Strategy/Origin	Chapter
pOF128	GFP-VSR1	O. Foresti	2
pLL38	GFP-VSR2	(DaSilva et al., 2005)	2
pOF133	GFP-VSR4	O. Foresti	2
pOF132	GFP-VSR5	O. Foresti	2
pFOX1	GFP-VSR6	S. Fox	2
pFOX2	GFP-VSR7	S. Fox	2
pDCG76	Gus Normalisation Vector	Gibson Assembly	2
pDCG103	GFP-VSR1 GG	EcoRI/HindIII→pDCG76	2
pDCG104	GFP-VSR2 GG	EcoRI/HindIII→pDCG76	2
pDCG105	GFP-VSR4 GG	EcoRI/HindIII→pDCG76	2
pDCG106	GFP-VSR5 GG	EcoRI/HindIII→pDCG76	2
pDCG107	GFP-VSR6 GG	EcoRI/HindIII→pDCG76	2
pDCG108	GFP-VSR7 GG	EcoRI/HindIII→pDCG76	2
pDCG81	FL-VSR2 GG	EcoRI/HindIII→pDCG76	3
pDCG79	FL-VSR2(Y612A) GG	EcoRI/HindIII→pDCG76	3
pDCG96	VSR5/2(Y612A) D&D GG	EcoRI/HindIII→pDCG76	3
pOF100	RFP-VSR2	(Foresti et al., 2010)	3
pSTY	ST-YFP	(Brandizzi et al., 2002)	3
pOF94	RFP-SYP61	(Foresti et al., 2010)	3
pDCG5	VPS35a-YFP	cDNA PCR	4
pDCG11	VPS29-RFP	cDNA PCR	4
pDCG8	VPS29-GFP	cDNA PCR	4
pDCG15	*At*FYVE1-RFP	cDNA PCR	4
pAW7	Aleurain-RFP	A. Watson	4
pDCG21	*At*FYVE2-RFP	cDNA PCR	4
pBBM1	TR2': YFP-VAMP727	ClaI/XbaI→pYSG20 (B. Mughal)	4
pDCG9	TR2': Venus-RhaI	PCR(TR2')+EcoRI/HindIII→pDCG5	4
pDCG7	TR2': Ara6-GFP	NcoI/NheI+NheI/BamHI→pDCG5	4
pOF106	SecRFP	(Samalova et al., 2006)	5
pAL2	Aleurain-RFP-HDEL	EcoRI/PstI+PstI/HindIII→pDCG5 (A. Lee)	5
pOF127	RFP-HDEL	O. Foresti	5
pOF129	Aleurain-α-Amylase	PCR NheI/BamHI→pAW7	5
pDEah	α-Amylase-HDEL	J. Denecke	5
pAL1	Aleurain-α-Amylase-HDEL	SacII/HindIII→pOF129	5
pLL18	SarI(HL)	(Takeuchi et al., 2000)	5
pJNB2	ST-YFP/Sec12	(Bottanelli et al., 2011)	5
pFB62	ST-YFP/PAT	(Bottanelli et al., 2011)	5
pJA1	Aleurain-GFP	J. An	5

Name	Effector	Strategy/Origin	Chapter
pLL53	GFP-VSR2-ΔCT	(DaSilva et al., 2006)	5
pDCG30	GFP-VSR2-Δ23	PCR of pLL38	5
pDCG35	GFP-VSR2-Δ19	PCR of pLL38	5
pDCG34	GFP-VSR2-Δ15	PCR of pLL38	5
pLL54	GFP-VSR2(ASA)	L. L. P. daSilva	5
pLL55	GFP-VSR2(IMAA)	L. L. P. daSilva	6
pLL81	GFP-VSR2(IMAA+Y612A)	L. L. P. daSilva	6
pCM72	pNOS': RFP-RhaI	C. De Marcos Lousa	6
pDCG97	FLVSR2-ΔCT	EcoRI/HindIII→pDCG76	6
pDCG98	FLVSR2-Δ23	EcoRI/HindIII→pDCG76	6
pDCG99	FLVSR2-Δ19	EcoRI/HindIII→pDCG76	6
pDCG100	FLVSR2-Δ15	EcoRI/HindIII→pDCG76	6
pOF35	GFP-VSR2(LoTM)	O. Foresti	6
pOF36	GFP-VSR2(LoTM+Y612A)	O. Foresti	6
pDCG77	FLVSR2(LoTM)	NcoI/HindIII→pDCG76	6
pDCG78	FLVSR2(LoTM+Y612A)	NcoI/HindIII→pDCG76	6

Table 8.2: **DNA Plasmids Used and Assembly Strategies**
A complete list of the recombinant plasmids used in this work, in the order that they appear in the thesis.

8.1.2 Polymerase Chain Reaction

Different DNA template dilutions were made with dH_2O for 10^{-2}, 10^{-3} and 10^{-4} concentrations. A master mix (n+1) was generated with water and made up with template, polymerase buffer, dNTPs, specific primers and DNA Polymerase. The polymerases used were *Hot-start Pfu turbo* (Stratgene, California, USA), *Hot-start KOD polymerase* (Novagen, Darmstadt, Germany) and *Hot-start Q5 polymerase* (New England Biolabs, Beverly, USA). A 2-5 min 94°C-98°C polymerase activation was undertaken 20-45 cycles of the appropriate denaturation, annealing and elongation time and temperature. A typical PCR reaction would be: denaturation of 30 seconds at 94°C, annealing for 1 minute at 50°C and elongation for 1 minute at 72°C, however these condition varied highly dependent on (1) the

polymerase used, (2) the size of the amplicon and (3) the length and calculated annealing temperature of the primers. The products were then separated on an agarose gel to determine the size of the fragment produced and to see if the reaction was successful. The PCR products were precipitated with 10% of the total volume $NaClO_4$ and with 100% of the total volume Isopropanol and mixed at room temperature before being centrifuged for 15 minutes at 18,000g. These products were then resuspended in 41μl 10/1 TE solution and a restriction digest undertaken. Alternatively, the PCR products were mixed with membrane binding buffer and bound to a silica DNA binding column (Quiagen, Venlo, Netherlands) before following the manufacturer's instructions and eluting in 20-50μl of 10/1 TE solution.

8.1.3 Gibson Isothermal Enzymatic Assembly of DNA Fragments

The 'Gibson Assembly' allows for simultaneous assembly of multiple DNA fragments between 150bp and 500kbp in size and up to 12 fragments in one, hour long reaction. DNA fragments were generally produced using *Q5 polymerase* (New England Biolabs, Beverly, USA) before being digested with the methylation sensitive restriction endonuclease *DpnI* which will digest contaminating template plasmid DNA whilst preserving the newly synthesised (non-methylated) PCR amplicon. The DNA was then passed through a Qiaquick DNA purification column (Quiagen, Venlo, Netherlands) according to the manufacturer's instructions. Any larger vector backbone fragments used were generated from restriction digestion followed by DNA purification following agarose gel electrophoresis. The component fragements were then spectrophotometrically quantified for both quantity and quality (260/280 absorbance ratio). The DNA fragments were then adjusted in order to have 50-100ng of vectors with 2-3 fold molar excess of inserts. The

respective fragments were then mixed and made up to a total volume of 25μl. 10μl was then combined with 10μl Gibson Assembly Master Mix (New England Biolabs, Beverly, USA) whilst another 10μl was mixed with 10μl H_2O and used in parallel as a negative control. The samples were then incubated at 50°C for 60 minutes and 1μl of both the sample and its relevant control used to transform chemically competent *E. coli* (see below), that were spread onto Ampicillin$^+$ LB agar plates and left at 37°C. The relative number of colonies on the sample plate compared to the control was used to assess the initial likelihood of a successful reaction. If deemed successful 10-20 colonies were selected, used to inoculate 3ml LB medium and the plasmid purified from the *E. coli* cultures and tested for the presence of the correct plasmid. If the correct plasmid was identified the *E. coli* culture was streaked onto a Ampicillin$^+$ LB agar plate, a single colony picked and a 10ml Ampicillin$^+$ LB culture inoculated. Following culture growth to saturation a 'Promega Wizard Plus^{TM}' (Madison, USA) DNA purification kit was used and then the resulting DNA preparation was sent to be sequenced.

8.1.4 Restriction Endonuclease Digestion

Restriction digests were split into two classes, for diagnostic purposes or for preparative purposes. Preparative digests were used to prepare DNA fragments and vectors before ligation whereas diagnostic digests were used to make qualitative decisions about DNA preparations. Although they are used for different purposes the relative composition of each the reactions was comparable, with different total volumes ($\sim$10μl for diagnostic purposes and $\sim$50μl for preparative purposes). Generally there would be 0.5-1% of a restriction enzyme, 10% of the appropriate NEB buffer, 10-20% DNA and 1% 100x BSA if needed. If the combination of enzymes being used was not compatible then the buffer was either manually

adjusted with the relevant salts or the reaction completed with the first enzyme, stopped, the DNA purified with a phenol-chloroform extraction and isopropanol precipitation (see below), re-suspended in TE 10/1 and the reaction completed with the second enzyme. The progress of 50μl preparative digests was monitored on an agarose gel by a series of 1μl samples taken at the 0, 20 and 40 minute time points.

8.1.5 Dephospohrylation

In order to prevent non-gel purified, restriction cut DNA fragments from self-ligating the DNA preparation was dephosphorylated, removing the 5'PO_4 and thus preventing self-ligation. Usually the starting DNA preparation was at a concentration of $\sim$100ng/μl in a total volume of 50μl and made up to 100μl for the dephophorylation reaction. 40μl of 10/1 TE, 5μl of Calf Intestinal Phosphatsase enzyme (CIP) (1u/μl) and 5μl of CIP buffer (10x) supplied by 'Promega' (Madison, USA). The reagents were added, mixed and incubated for 30 minutes at 37°C.

8.1.6 Phenol-Choloroform 'Clean-Up'

The 'clean-up' stage removes proteins from a sample whilst preserving DNA. The DNA preparation was made up to a volume of 100μl. 50μl of equilibrated phenol were added, then mixed, 100μl of chloroform added, mixed again. The solution was then centrifuged for 5 minutes at 18,000g. The upper, aqueous layer was then removed and added to 100μl chloroform. The solution was then centrifuged for 5 minutes at 18,000g speed. The upper, aqueous layer was then removed. 10μl of 5M $NaClO_4$ was added (and mixed) followed by 110μl of Isopropanol. The solution was centrifuged for 15 minutes at 18,000g in a microfuge. The supernatant was

discarded and the pellet centrifuged for 1 minute at maximum speed. The pellet was dried by using a Pasteur pipette and then left in a vacuum chamber for 5 minutes. The pellet was then resuspended in 10/1 TE buffer on ice. The DNA was stored at -20°C.

8.1.7 DNA Fragment Isolation

In order to isolate a fragment prior to a ligation the restriction digested fragment was loaded onto agarose gel of the appropriate concentration (from 0.5-3 dependent on the fragment). The DNA was then separated on the gel by electrophoresis at 50 volts with a constant current. After band separation the desired fragment was visualised using a transilluminator light-box, excised with a razor blade and deposited into a 1.5ml microfuge tube. The DNA was then isolated from the gel-slice using a Qiaquick DNA purification kit (Quiagen, Venlo, Netherlands) the final elution was usually in a volume of 30μl.

8.1.8 Ligation

Once the appropriate DNA reagents for the reaction were isolated all the reagents were qualitatively compared on an agarose gel. The volumes chosen for the ligation in order to get an approximate molar ratio of 2:1 of vector backbone to the fragment. The ligation was set up in a total volume of 20μl with 1μl T4 DNA Ligase from Invitrogen (California, USA), 4μl of the supplied 5x T4 DNA Ligase buffer, the appropriate amount of fragment or fragments and vector and finally made up to volume with dH_20. As the vector was not usually gel excised there is a risk of the presence of either (1) uncut plasmid or (2) under dephosphorylated vector. Therefore with any ligation two additional controls were used. The first

control contained the vector with all the reagents aside from the T4 DNA Ligase supplied by Invitrogen (California, USA) and the fragment - this will allow for the diagnosis of an improperly cut vector. The second control contains all the reagents aside from the fragment - diagnosing poorly dephosphorylated vector. Both reactions were made up to a total volume of 20μl. The reactions were then incubated for a minimum of either 2 hours at 22°C or overnight at 4°C. After the incubation 5μl of the ligation was used to transform chemically competent *E. coli*. After transformation the bacteria were poured onto a Amp^+ agar plate and incubated overnight at 37°C. The numbers of resulting colonies was used to assess the initial likelihood of a successful reaction. If deemed successful 10-20 colonies were selected, used to inoculate 3ml LB medium and the plasmid purified from the *E. coli* cultures and tested for the presence of the correct plasmid. If the correct plasmid was identified the *E. coli* culture was streaked onto a $Ampicillin^+$ (150μg/μl) LB agar plate, a single colony picked and a 10ml $Ampicillin^+$ LB culture inoculated. Following culture growth to saturation a 'Promega Wizard Plus^{TM}' (Madison, USA) DNA purification kit was used and then the resulting DNA preparation sent to be sequenced.

8.1.9 Generation of Chemically Competent *E. coli*

MC1061 were streaked out on a LB-agar plate and incubated at 37°C for 12-16 hours. 3ml of 2xYT was inoculated with a single colony and incubated at 37°C under constant agitation until slightly turbid. 200ml of 2xYT was inoculated with the pre-culture and incubated at 37°C under constant agitation. When the culture reached an O.D.λ550 of 0.480-0.5 the culture was transferred into four sterile 50ml conical-bottomed centrifuge tubes, which were placed on ice. Further manipulations were carried out at 0-4°C. The cell suspensions were centrifuged

for 20 minutes at 3000g (4°C). The supernatant was discarded and the cell pellets were resuspended in 80ml of TFBI and placed on ice for 5 minutes. The samples were centrifuged for 20 minutes at 3000g (4°C), the supernatant was discarded and the cell pellets were resuspended in 8ml of TFBII and placed on ice for 15 minutes. Using pre-chilled pipette tips, 100μl aliquots of the cell suspension were transferred into pre-chilled 1.5ml microfuge tubes. Aliquots were then frozen at -80°C.

2xYT medium: 16g/l bacto-tryptone; 10g/l bacto-yeast extract; 5g/l NaCl. pH 7.0. Autoclaved.

TFBI solution: 30mM $KC_2H_3O_2$; 100mM RbCl; 10mM $CaCl_2 2H_2O$; 50mM $MnCl_2 4H_2O$; 15% v/v glycerol. pH 5.8 with 0.2M CH_2COOH. Filter sterilised.

TFBII solution: 10mM MOPS, 10mM RbCl, 75mM $CaCl_2 2H_2O$, 15% v/v glycerol. pH 6.6 with 5M KOH. Filter sterilised.

8.1.10 Transformation of Chemically Competent *E. coli*

The desired DNA preparation (1-5μl at $\sim$100ng/μl) was added to 100μl of chemically competent *E. coli* in a 1.5ml microcentrifuge tube, mixed and incubated on ice for 15 minutes. The microcentrifuge tube was incubated in a heating block at 37°C for three minutes. LB was then added (1ml) and the cells were incubated for another 15 minutes at 37°C. The mixture was poured onto an antibiotic containing agar plate, left to dry and incubated at 37°C overnight. Colonies were selected after an overnight incubation at 37°C.

8.1.11 Generation of Chemically Competent *A. tumefaciens*

C58C1rif cells were streaked on a LB-agar plate supplemented with Rifampicin (100μg/ml) and allowed to grow for two days at 25°C. A 3ml Rifampicin MGL medium (at 50μg/ml) culture was then inoculated with a single colony and shaken for 12-16 hours at 25°C. Once turbid a 250ml Rifampicin MGL medium (at 50μg/ml) culture was inoculated and shaken at 25°C for 12-16 hours.The cell suspension was incubated on ice for 5 minutes centrifuged for 30 minutes at 5000g (4°C). The supernatant was discarded and the cell pellet was resuspended in $CaCl_2$ solution (20mM $CaCl_2$ in 15% glycerol). The suspension was then centrifuged for 5 minutes at 5000g (4°C) . The supernatant was once again discarded and the cell pellet resuspended in 15ml of $CaCl_2$ solution. Using pre-chilled pipette tips, 500μl aliquots of cell suspension were transferred into pre-chilled 1.5ml microfuge tubes which were subsequently frozen at -80C.

MGL medium: LB:MG medium 1:1

MG medium: 5.0 g/l mannitol; 1.16 g/l monosodium glutamate; 0.25 g/l KH_2PO_4, 0.1 g/l $MgSO_4.7H_2O$, 1.0 mg/l biotin, pH 7.0)

8.1.12 Transformation of Chemically Competent *A. tumefaciens*

A DNA preparation (1μl at 100ng/μl) was added to 100μl of thawed *A. tumefaciens* competent cells. The sample was then incubated at 0°C for 30 minutes before being heat-shocked at 37°C for 4 minutes after which 1ml of LB medium was added to the cells. The cell suspensions were then transferred in 15ml conical-bottomed tubes and left to incubate for 3-4 hours at 25°C under constant agitation. The LB medium with the transformed competent cells was then poured onto

Streptomycin (300μg/ml), Spectinomycin (100μg/ml), Rifampicin (100μg/ml) containing LB-agar plates, dried and left to incubate for 72 hours at 25°C.

8.1.13 Small Scale Plasmid Purification of DNA from *E. coli*

A colony from a plate incubated overnight was used to inoculate 2ml of LB culture medium. After overnight incubation at 37°C, 1.2ml of the saturated culture was aliquoted into a 1.5ml microcentrifuge tube. The cultures were centrifuged for 1 minute at 18,000g, and then the supernatant discarded preserving the cell pellet. The pellet was resuspended in 150μl of TES solution (see below). 20μl of lysozyme solution (10mg/ml)was added and mixed in the tube. The cell suspension was incubated for 5 minutes at room temperature. 300μl distilled water was pipetted into the microcentrifuge tube, which was then placed into a heating block at 73°C for 15 minutes. After the incubation the sample was centrifuged for 15 minutes at 18,000g. The supernatant was transferred into a new microcentrifuge tube. 5M $NaClO_4$ (approximately 10% of the supernatants volume) was added. 400μl isopropanol was mixed and the sample centrifuged for 15 minutes at 18,000g. The supernatant was discarded and the sample dried at 37°C for 15 minutes. The dry DNA pellet was then re-suspended in 50μl TE. The DNA was stored at -20°C.
TES buffer: 10mM Tris-HCl pH 8.0; 5mM EDTA; 250mM sucrose. Filter sterilised and stored at 4°C.

8.1.14 Large Scale Plasmid Purification of DNA from *E. coli*

A colony from a plate left to incubate overnight from was used to inoculate a 3ml Ampicillin$^+$ (150μg/μl) LB medium. When in exponential growth phase (about 3 hours later O.D. 0.3 λ600) the 3ml LB culture was used to inoculate 500mL of

37°C LB medium. This solution was then left overnight (24h) to grow the *E. coli* culture to saturation. The culture was then centrifuged for 60 minutes, at 5000g in a Mistral Swing-out centrifuge using 500mL buckets. The supernatant was removed and discarded. 8ml of ice-cold TE 50/1 was used to resuspend the cell pellet with occasional vortexing. Once fully resuspended the cell suspension was transferred into pre-cooled 15ml centrifuge tubes. All further manipulations were completed on ice. 2.5ml lysozyme solution (10mg/ml) were added and the tubes inverted 10 times. The suspension was incubated for 5 minutes on ice. 2.0ml of 0.5M EDTA pH 8.0 was added, and the tubes inverted again. 50μl of Ribonuclease was mixed with 150μl Triton X-100 (10% solution) and made up to 1ml with TE 50/1, and was added to each tube. Next the suspension was incubated for 30 minutes on ice and then centrifuged at 38,700g in a Sorvall SS34 rotor for 60 minutes. The supernatant was transferred to a Falcon tube. 20 ml of equilibrated phenol (pH 8.0 with 0.1% 8-hydroxyquinoline) was added then centrifuged at 5000g in a swing out rotor for 20 minutes. The upper aqueous phase was recovered and transferred to a new tube with 20ml chloroform, which was then mixed. This was centrifuged as before for 20 minutes. The upper aqueous phase was, once again, recovered and transferred to a 15ml Corex tube (approx 10ml), 1ml 5M $NaClO_4$ (10% of the water volume) was added, mixed and then 8ml isopropanol (80% of the water volume) was added. The tube was sealed, and inverted 4 times to mix. The glass tube was then centrifuged in a HB6 rotor at 16,000g for 15 minutes to pellet the DNA. The supernatant was discarded, the pellet dried and resuspended in 500μl of TE and transferred to a sterile microcentrifuge tube. The DNA was stored at 4°C.

TE 50/1: 50mM Tris-HCl pH 8.0; 5mM EDTA; 250mM sucrose. Filter sterilised and stored at 4°C.

8.1.15 DNA Sequencing

In order to confirm that DNA sequences amplified by a DNA polymerase did not have any mutations due to the amplification precess, and that fragments isolated from a DNA gel had not mutated after exposure to the mutagens ethidium bromide and UV light, samples were routinely sent to undergo 'Sanger' dideoxynucleotide chain termination sequencing. 'Promega Wizard Plus^{TM}' (Madison, USA) DNA preparations were produced and adjusted to the required DNA concentration before being sent to Source BioScience (Nottingham, UK).

8.2 PLANT TISSUE CULTURE

Nicotiana tabacum seeds were surface sterilised and grown on Murashige and Skoog medium and 2% sucrose at 22deg in a controlled room at 16h day length and light irradiance of 200mE/m^2/s (Murashige and Skoog, 1978)

8.3 PROTOPLAST GENERATION AND TRANSFORMATION

8.3.1 Protoplast Preparation

Leaves were removed from *in vitro* grown tobacco plants and semi-perforated using a needle bed. The leaf midnerve was removed and the two halves were transferred, cut side down, to a Petri dish containing 7ml of Digestion Mix in TEX buffer. The leaves were left overnight for digestion and gently shaken before use. The mix was filtered through a 100μl nylon filter and then washed through with EB buffer. The protoplasts were then centrifuged in 50ml conical centrifuge tubes for 15 minutes at 100g, at room temperature in a swing-out rotor. A Pasteur

pipette connected to a peristaltic pump was used to remove the dead cells and non-protoplast medium (the living protoplasts form a layer on top of the solution). 25ml of EB was added and the protoplasts spun again at 100g for 10 minutes. The above technique was used once again to remove cell debris. The protoplasts were then resuspended in $(500.(n+1)\mu l)$ of EB (where n = the number of samples).

Transient Expression Medium (TEX): B5 salts; 500mg/l MES; 750mg/l $CaCl_2$ $(2H_2O)$; 250mg/l NH_4NO_3; 0.4M sucrose (13.7%). Made to pH 5.7 with KOH and filter sterilised.

Electroporation Buffer (EB): 0.4 M Sucrose; 2.4 g/l HEPES; 6 g/l KCl; 600 mg/l $CaCl_2$; Made to pH 7.2 with KOH and filter sterilised.

Digestion Mix: 2% Macerozyme R10; 4% Cellulase R10 in TEX buffer. Centrifuged to remove insoluble particles and filter sterilised. Stored at -80°C.

8.3.2 Protoplast Electroporation

500μl of protoplasts (as prepared above) were pipetted gently into a disposable 1ml plastic cuvette using a cut volumetric pipette tip to avoid damaging the protoplasts. Plasmid DNA was diluted to a final volume of 100μl with EB and pipetted into the cuvette. DNA/cell mixtures were incubated for 5 minutes. The cuvettes were then electroporated with a pair of stainless steel plate electrodes embedded in a teflon insulator. Between each electroporation, the electrodes were rinsed in distilled sterilized water to remove cell debris and DNA, dipped in 99% ethanol to remove water and briefly passed through a flame to remove the ethanol. The protoplasts were incubated for 15-30 minutes. The mixture was then poured into small Petri dishes and incubated for a minimum of 24 hours at 22°C in the dark.

8.3.3 Protoplast Harvesting

To recover the secreted proteins, each electroporation mixture was transferred to a 15ml round-bottomed centrifuge tube and centrifuged at 100rcf for 5 minutes with 0 braking. A portion of the underlying medium was removed manually with a Pasteur pipette, transferred to a 1.5ml microfuge tube and kept on ice for analysis. If the samples were to be used for an immunoblot assay, in order to reduce background, the dead cells were removed from the bottom of the 15ml centrifuge tube using a Pasteur pippette at this stage. To recover the intracellular proteins, the remaining cell suspension was diluted 10 fold with 250mM NaCl and centrifuged for 3 minutes at 200rcf. The supernatant was completely removed with a Pasteur pippette connected to a peristaltic pump. The cell pellet was immediately placed on ice or stored at -80°C until extraction.

8.4 BIOCHEMICAL ASSAYS

8.4.1 α-Amylase Assay

Culture medium samples were centrifuged at 18,000g at 4°C to remove debris and diluted two-fold in α-amylase extraction buffer. Cell samples were resuspended in 1000μl of buffer and the proteins extracted by sonication (60% of max amplitude) for 5 seconds followed by centrifugation at 18,000g at 4°C. Appropriately diluted extract (30μl) was pre-incubated at 45°C. After 5 minutes of pre-incubation, the reactions for each sample were started at 15 second intervals by adding 30μl of the substrate (blocked P-nitrophenyl maltoheptaoside). After 10-60mins depending on the series, the reaction was stopped by adding 150μl of 1% Trizma base (w/v) at the corresponding 15 second interval. Samples (200μl) were transferred into

the wells of a microtitre plate and the absorbance was read at λ405nm. Negative controls were obtained using medium and cell extracts from mock-electroporated protoplasts, with no DNA. The α-amylase activity was calculated in terms of change in OD compared to negative control, per ml of extract used (taking into account the dilution of extracts) per minute of incubation. The assay was repeated at least three times for each extract, and the average activity was calculated. The secretion index (SI) for each sample was calculated as the ratio between the extracellular and the intracellular activity.

α-amylase extraction buffer: 50 mM malic acid; 50mM sodium chloride; 2M calcium chloride; 0.02% sodium azide and 0.02% BSA.

8.4.2 Beta-Glucuronidase Assay

The quantification of GUS activity allows for the quantitative comparison of different electroporations, using a dual-vector system. From the 2.5ml overnight incubation of the electroporated samples 500μl were taken using a 1ml pipette tip with 1-2mm removed from the end. This was then directly mixed with 500μl of GUS dilution buffer on ice. The remaining 2ml samples were centrifuged as for the α-Amylase Assay (see above). All manipulations of the 1ml samples for the GUS assay were done on ice from this point. These samples were sonicated (40% of max. amplitude for 10s) and vortexed before being centrifuged (4°C) at 18,000g for 10 minutes. The sample (100μl) was then transferred into a microfuge tube and mixed with 100μl of the GUS reaction buffer. These samples were then incubated for 2 hours before being stopped with 80μl of the GUS stop buffer. An aliquot (250μl) of the completed reaction mix was then loaded into a microtitre plate and the optical absorbance at λ405 measured. Controls included a non-electroporated sample as well as a 'zero stop'. Due to the endogenous absorbance of chlorophyll

at λ405 each sample has significant background; in order to control for this, each sample included a duplicate that was stopped, by the addition of 80μl GUS stop buffer, *before* the 2 hour incubation. The individual 'zero stops' were then subtracted from the sample reading. Due to the non-linearity of the reaction a standard curve was constructed (data not shown) and all samples normalised to the factor:

$$y = -0.0003x^2 + 0.0643x + 0.0085$$

y = sample O.D.(λ405)
x = normalised value (0-100)

GUS dilution buffer: 50mM Sodium phosphate buffer pH 7.0; 10mM Na_2EDTA; 0.1% sodium lauryl sarcosine; 0.1% Triton X-100 and 10mM β–Mercaptoethanol (added prior to use).

GUS reaction buffer: 50mM Sodium phosphate buffer pH 7.0; 0.1% Triton; 2mM 4-Nitrophenyl-β-D-glucopyranosiduronic acid and 10mM β–Mercaptoethanol (added prior to use).

GUS stop buffer: 2.5M 2-amino-2methyl propanediol

8.4.3 Protein Extraction from Protoplasts

Cellular proteins were analysed by SDS-PAGE and western blotting in order to either (1) detect protein expression and processing or (2) monitor the expression of a dual-vector. The protein samples were extracted from the cell pellets after protoplast harvesting. The protoplast pellet was resuspened in 250μl α-amylase extraction buffer (see above), sonicated (40-60% 5-10s) and centrifuged at 18,000g for 10 minutes (4°C). The soluble cellular proteins were now in the medium, whilst the membrane bound proteins remained in the pellet. The supernatant

was recovered into a new 1.5ml microcentrifuge tube, and was referred to as the S1 sample. The pellet containing the membrane bound proteins was resuspended in protein extraction buffer in a volume of 250μl, maintaining the volumetric relationship. This sample was sonicated (40-60% of max. amplitude 5-10s) and centrifuged at 18,000g for 10 minutes (4°C). The supernatant was recovered and was referred to as the S2 sample. Equal volumes were subjected to SDS-PAGE after 2x dilution with SDS-PAGE Sample Buffer Mix and boiling at 95°C for 5 minutes. *Protein Extraction Buffer:* 100mM pH 7.8 Tris-HCl; 200mM NaCl; 1mM EDTA; 0.2% Triton X-100 and 1μl/ml β–Mercaptoethanol (added prior to use). *Sample Buffer Concentrate:* 0.1% Bromophenol blue; 5 mM EDTA; 200mM pH 8.8 Tris-HCl; 1M Sucrose. Stored at 4°C.
Sample Buffer Mix: 900μl Sample Buffer Concentrate; 300μl 10% Sodium dodecyl sulphate; 18μl 1M Dithiothreitol (DTT). Prepared freshly.

8.4.4 Protein Immunoblot Assay and Polyacrylamide Gel Electrophoresis

Separation of proteins from cell extracts were performed in SDS-polyacrylamide gels comprising approximately 2.5cm stacking gel followed by a 6cm separation gel. The gels were polymerised in-between glass plates and electrophoresis was performed at 20V constant voltage. After electrophoretic separation, the gel was layered on a piece of nitrocellulose sheet assembled in between two layers of Whatman 3MM paper and soaked sponges. Protein samples were electophoretically transferred onto the nitrocellulose membrane (2 hours at a current of 500 mA). The membrane was washed several times in PBS+0.5% Tween 20. Blocking solution was added and the membrane was rocked for 1 hour. The primary antibody (appropriately diluted) was added and the membrane was rocked for 1 hour. The membrane was then washed for 15 minutes with PBS+0.5% Tween 20. The

secondary anti-rabbit antibodies conjugated to HRP were then added, diluted 1:5000 in blocking solution. This was left rocking for 1 hour. The membrane was then washed for 15 minutes with PBS+0.5% Tween 20 and for 5 minutes with PBS. Samples were then visualised using enhanced chemiluminescence by exposure to X-ray film.

Protogel: 30% w/v acrylamide; 0.8% w/v bisacrylamide.

Stacking Gel: 11.3ml 20% Sucrose; 1ml 1M Tris-HCl pH 6.8; 2.5ml Protogel; 150μm 10% SDS; 30μm TEMED; 50μm 10% APS.

Separating Gel (10%): 23.1ml dH_20; 6.3ml 3M Tris-HCl pH8.8; 15ml Protogel; 450μl 10% SDS; 25μl TEMED; 150μl 10% APS.

Blotting Buffer (2.5l in dH_20: 7.5g Tris; 36g Glycine; 250ml Methanol.

Blocking Solution: 5% milk powder; 0.5% Tween 20, made up to 50 ml in PBS .

10x Phosphate Buffered Saline (PBS): 87g NaCl; 22.5g $Na_2HPO_4.2H_2O$; 2g KH_2PO_4, pH 7.4.

8.5 AGROBACTERIUM TUMEFACIENS MEDIATED TRANSFORMATION OF LEAF EPIDERMAL TISSUE BY INFILTRATION

Soil-grown tobacco plants were infiltrated with overnight cultures of Agrobacterium tumefaciens cultures grown in MGL, diluted to an OD of 0.1 at 600 nm, and infiltrated into leaves of 5 week old soil-grown *N. tabacum* cv Petit Havana (Maliga et al., 1973) as described previously (Sparkes et al., 2006). CLSM analysis was done 48 hours after infiltration, unless otherwise indicated in the figure legends.

8.6 CONFOCAL-LASER SCANNING MICROSCOPY

Infiltrated *N. tabacum* leaves 24-72 hours post infiltration were used as starting material for confocal laser scanning microscopy analysis. A square of ∼0.5-1cm^2 was excised from the infiltrated area and mounted on a glass slide, with the lower epidermal layer towards the coverglass (rectangular, 22mm x 50mm, N.0). A Zeiss LSM 510 META Laser Scanning Microscope or a Zeiss LSM 710 were used for all confocal later scanning microscopy (Zeiss, Germany) with a Plan-Neofluar 40x/1.3 Oil DIC objective on both microscopes. Post acquisition image processing was performed with 'Zeiss LSM 5 Image Browser', Zeiss 'Zen 2011' and 'Image J' (http://rsb.info.gov/ij/). When GFP/CFP and YFP/Venus were co-expressed in the same cell, GFP and CFP excitation was at λ458nm and the YFP flurophores were excited at λ514nm. Emission light was passed through a dichroic beam splitter at λ545nm and the higher energy wavelengths (CFP/GFP) were detected with a filter between the wavelengths λ480-520 and and the lower energy YFP/Venus wavelengths were detected using a filter between 565-615nm. In situations where GFP/YFP and RFP were co-expressed, excitation of the GFP was at λ488nm and at λ543nm for the RFP. Emission light was also passed through a dichroic beam splitter at λ545nm and the higher energy wavelengths (GFP) were detected with a filter between the wavelengths λ500-530 and and the lower energy RFP emission was detected using a filter between 565-615nm.

8.7 IN SILICO ANALYSIS

8.7.1 Pearson-Spearman Correlation Scatterplots

Image analysis was undertaken using the ImageJ analysis program and the PSC co-localization plug-in (French et al., 2008) to calculate co-localization and to produce scatter plots. The degree of correlation is given as the Spearman's rank correlation coefficient, and the PSC co-localization plug-in generates values in the range [-1, 1], where +1 indicates the strongest positive correlation, 0 indicates no correlation and -1 indicates the strongest negative correlation. The shape of the scatterplots indicates more complex scenarios, including a combination of correlating and non- correlating pixel populations, as well as specific shifts in red-green ratios (Bottanelli et al., 2011, 2012). At least 20 images comprising a minimum of 400 independent punctate structures were analysed for each condition, and punctate structures were selected using the 'selection brush' tool as described (Foresti et al., 2010; French et al., 2008). A threshold level of pixel intensity 10 was set, below which pixel values were considered noise and not included in the statistical analysis.

8.7.2 Population Distribution Analysis

Segmented population analysis of scatterplots was carried out to document specific population shifts in a partial co-localisation experiment, as introduced previously (Bottanelli et al., 2012). Scatterplots were subdivided into 16 pie-segments of equal surface, representing data-bins of 16 different categories with progressively increasing red/green ratios (from left to right). The first bin comprises all pixels that have a red/green ratio between 0 and 6.25% red, the second bin includes

ratios from 6.25 to 12.5% red and so on until the 16th and final bin which includes 93.75-100% red. The bar charts obtained show the amount of green and red signals in each bin, progressing from predominantly green (left) to red (right).

9 REFERENCES

Agar, H. D. and Douglas, H. C. (1956). "Studies on the cytological structure of yeast: electron microscopy of thin sections". *Journal of Bacteriology* 73, pp. 365–375

Allan, B. B., Moyer, B. D., and Balch, W. E. (2000). "Rab1 Recruitment of p115 into a cis- SNARE Complex: Programming Budding COPII Vesicles for Fusion". *Science* 289.5478, pp. 444–448

Allison, R., Lumb, J. H., Fassier, C., Connell, J. W., Ten Martin, D., Seaman, M. N. J., Hazan, J., and Reid, E. (2013). "An ESCRT-spastin interaction promotes fission of recycling tubules from the endosome." *The Journal of Cell Biology* 202.3, pp. 527–543

Altschul, S., Gish, W., and Miller, W (1990). "Basic local alignment search tool". *Journal of Molecular Biology*, pp. 403–410

Anderson, D. J., Mostov, K. E., and Blobel, G (1983). "Mechanisms of integration of de novo- synthesized polypeptides into membranes: Signal recognition particle is required for integration into microsomal membranes of calcium ATPase and of lens MP26 but not of cytochrome b5". *Proceedings of the National Academy of Sciences of the United States of America* 80.23, pp. 7249–7253

Anfinsen, C. B. (1973). "Principles that govern the folding of protein chains." *Science* 181.4096, pp. 223–230

Antonny, B and Schekman, R. (2001). "ER export: public transportation by the COPII coach." *Current Opinion in Cell Biology* 13.4, pp. 438–443

Antonny, B, Beraud-Dufour, S, Chardin, P, and Chabre, M (1997). "N-terminal hydrophobic residues of the G-protein ADP-ribosylation factor 1 insert into membrane phospholipids upon GDP to GTP exchange". *Biochemistry* 36.15, pp. 4675–4684

Aridor, M., Bannykh, S. I., Rowe, T, and Balch, W. E. (1995). "Sequential coupling between COPII and COPI vesicle coats in endoplasmic reticulum to Golgi transport." *The Journal of Cell Bology* 131.4, pp. 875–893

Aridor, M., Fish, K. N., Bannykh, S, Weissman, J, Roberts, T. H., Lippincott-Schwartz, J., and Balch, W. E. (2001). "The Sar1 GTPase coordinates biosynthetic cargo selection with endoplasmic reticulum export site assembly." *The Journal of Cell Biology* 152.1, pp. 213–229

Ashford, T. P. and Porter, K. R. (1962). "Cytoplasmic components in hepatic cell lysosomes". *The Journal of Cell Biology* 12, pp. 198–202

Attar, N. and Cullen, P. J. (2010). "The retromer complex." *Advances in Enzyme Regulation* 50.1, pp. 216–236

Auld, K. L., Hitchcock, A. L., Doherty, H. K., Frietze, S., Huang, L. S., and Silver, P. a. (2006). "The conserved ATPase Get3/Arr4 modulates the activity of membrane-associated proteins in Saccharomyces cerevisiae". *Genetics* 174.1, pp. 215–227

Avila, E. L., Brown, M., Pan, S., Desikan, R., Neill, S. J., Girke, T., Surpin, M., and Raikhel, N. V. (2008). "Expression analysis of Arabidopsis vacuolar sorting receptor 3 reveals a putative function in guard cells." *Journal of Experimental Botany* 59.6, pp. 1149–1161

Balch, W. E., McCaffery, J. M., Plutner, H, and Farquhar, M. G. (1994). "Vesicular stomatitis virus glycoprotein is sorted and concentrated during export from the endoplasmic reticulum." *Cell* 76.5, pp. 841–52

Balderhaar, H., Arlt, H., Ostrowicz, C., Bröcker, C., Sündermann, F., Brandt, R., Babst, M., and Ungermann, C. (2010). "The Rab GTPase Ypt7 is linked to retromer mediated receptor recycling and fusion at the yeast late endosome." *Journal of Cell Science* 123.Pt 23, pp. 4085–4094

Banta, L. M., Robinson, J. S., Klionsky, D. J., and Emr, S. D. (1988). "Organelle assembly in yeast: characterization of yeast mutants defective in vacuolar biogenesis and protein sorting." *The Journal of Cell Biology* 107.4, pp. 1369–1383

Barlowe, C. (2003). "Signals for COPII-dependent export from the ER: what's the ticket out?" *Trends in Cell Biology* 13.6, pp. 295–300

Barlowe, C., Orci, L., Yeung, T., Hosobuchi, M., Hamamoto, S., Salama, N., Rexach, M. F., Ravazzola, M., Amherdt, M., and Schekman, R. (1994). "COPII: a membrane coat formed by Sec proteins that drive vesicle budding from the endoplasmic reticulum." *Cell* 77.6, pp. 895–907

Barrieu, F. and Chrispeels, M. J. (1999). "Delivery of a secreted soluble protein to the vacuole via a membrane anchor". *Plant Physiology* 120.August, pp. 961–968

Batoko, H, Zheng, H. Q., Hawes, C, and Moore, I (2000). "A rab1 GTPase is required for transport between the endoplasmic reticulum and golgi apparatus and for normal golgi movement in plants." *The Plant Cell* 12.11, pp. 2201–2218

Bednarek, S. Y., Wilkins, T. a., Dombrowski, J. E., and Raikhel, N. V. (1990). "A carboxyl-terminal propeptide is necessary for proper sorting of barley lectin to vacuoles of tobacco." *The Plant Cell* 2.12, pp. 1145–1155

Bendzko, P, Prehn, S, Pfeil, W, and Rapoport, T. (1982). "Different modes of membrane interactions of the signal sequence of carp preproinsulin and of the insertion sequence of rabbit cytochrome b5." *European Journal of Biochemistry* 123.1, pp. 121–126

Benghezal, M, Wasteneys, G. O., and Jones, D. a. (2000). "The C-terminal dilysine motif confers endoplasmic reticulum localization to type I membrane proteins in plants." *The Plant Cell* 12.7, pp. 1179–1201

Bergmann, L (1960). "Growth and division of single cells of higher plants in vitro." *The Journal of General Physiology* 43, pp. 841–851

Bertani, G. (1951). "Studies on lysogenesis. I. The mode of phage liberation by lysogenic Escherichia coli." *Journal of Bacteriology* 62.3, pp. 293–300

Bertolotti, A, Zhang, Y, Hendershot, L. M., Harding, H. P., and Ron, D (2000). "Dynamic interaction of BiP and ER stress transducers in the unfolded-protein response." *Nature Cell Biology* 2.6, pp. 326–832

Bielli, A., Haney, C. J., Gabreski, G., Watkins, S. C., Bannykh, S. I., and Aridor, M. (2005). "Regulation of Sar1 NH2 terminus by GTP binding and hydrolysis promotes membrane deformation to control COPII vesicle fission." *The Journal of Cell Biology* 171.6, pp. 919–924

Birnstiel, M. L., Chipchase, M. I. H., and Hyde, B. B. (1963). "The nucleolus, a source of ribosomes". *Biochimica et Biophysica Acta* 76, pp. 454–462

Black, V. H., Sanjay, A., Leyen, K. van, Lauring, B., and Kreibich, G. (2005). "Cholesterol and steroid synthesizing smooth endoplasmic reticulum of adrenocortical cells contains high levels of proteins associated with the translocation channel." *Endocrinology* 146.10, pp. 4234–4249

Bliek, A. M. V. D., Redelmeier, T. E., Damke, H., Tisdale, E. J., Meyerowitz, E. M., and Schmid, S. L. (1993). "Mutations in Human Dynamin Block an Intermediate Stage in Coated Vesicle Formation Assay of Tfn Endocytosis". *The Journal of Cell Biology* 122.3, pp. 553–563

Blobel, G and Dobberstein, B (1981). "Presence of Proteolytically Processed and Unprocessed Nascent Immunoglobulin Light Chains On Membrane-Bound Ribosomes of Murine Myeloma". *Annual Review of Biochemistry* 67, pp. 835–851

Blobel, G, Walter, P, and Gilmore, R (1984). "Intracellular protein topogenesis." *Progress in Clinical and Biological Research* 168.3, pp. 3–10

Bock, J. B., Matern, H. T., Peden, a. a., and Scheller, R. H. (2001). "A genomic perspective on membrane compartment organization." *Nature* 409.6822, pp. 839–841

Böcking, T., Aguet, F., Harrison, S. C., and Kirchhausen, T. (2011). "Single-molecule analysis of a molecular disassemblase reveals the mechanism of Hsc70-driven clathrin uncoating." *Nature Structural & Molecular Biology* 18.3, pp. 295–301

Boehm, M. and Bonifacino, J. S. (2001). "Adaptins: the final recount". *Molecular Biology of the Cell* 12.October, pp. 2907–2920

Boevink, P., Oparka, K, Santa Cruz, S, Martin, B, Betteridge, A, and Hawes, C (1998). "Stacks on tracks: the plant Golgi apparatus traffics on an actin/ER network." *The Plant Journal* 15.3, pp. 441–447

Bolte, S., Talbot, C., Boutte, Y., Catrice, O., Read, N. D., and Satiat-Jeunemaitre, B. (2004). "FM-dyes as experimental probes for dissecting vesicle trafficking in living plant cells." *Journal of Microscopy* 214.Pt 2, pp. 159–173

Boncompain, G., Divoux, S., Gareil, N., Forges, H. de, Lescure, A., Latreche, L., Mercanti, V., Jollivet, F., Raposo, G., and Perez, F. (2012). "Synchronization of secretory protein traffic in populations of cells." *Nature Methods* 9.5, pp. 493–498

Bonifacino, J. S. and Glick, B. S. (2004). "The mechanisms of vesicle budding and fusion." *Cell* 116.2, pp. 153–166

Bonifacino, J. S. and Lippincott-Schwartz, J. (1991). "Degradation of proteins within the endoplasmic reticulum." *Current Opinion in Cell Biology* 3.4, pp. 592–600

Bonifacino, J. S. and Lippincott-schwartz, J. (2003). "Coat proteins: shaping membrane transport". *Nature Reviews Molecular Cell Biology* 4, pp. 409–414

Borgese, N., Colombo, S., and Pedrazzini, E. (2003). "The tale of tail-anchored proteins: coming from the cytosol and looking for a membrane." *The Journal of Cell Biology* 161.6, pp. 1013–1019

Bottanelli, F., Foresti, O., Hanton, S., and Denecke, J. (2011). "Vacuolar transport in tobacco leaf epidermis cells involves a single route for soluble cargo and multiple routes for membrane cargo." *The Plant Cell* 23.8, pp. 3007–25

Bottanelli, F., Gershlick, D. C., and Denecke, J. (2012). "Evidence for sequential action of Rab5 and Rab7 GTPases in prevacuolar organelle partitioning." *Traffic* 13.2, pp. 338–354

Bozkurt, G., Stjepanovic, G., Vilardi, F., Amlacher, S., Wild, K., Bange, G., Favaloro, V., Rippe, K., Hurt, E., Dobberstein, B, and Sinning, I. (2009). "Structural insights into tail-anchored protein binding and membrane insertion by Get3." *Proceedings of the National Academy of Sciences of the United States of America* 106.50, pp. 21131–21136

Brandizzi, F. and Barlowe, C. (2013). "Organization of the ERGolgi interface for membrane traffic control". *Nature Reviews Molecular Cell Biology* 14.6, pp. 382–392

Brandizzi, F., Frangne, N., Marc-martin, S., Hawes, C., Neuhaus, J. M., and Paris, N. (2002). "The destination for single-pass membrane proteins is influenced markedly by the length of the hydrophobic domain". *The Plant Cell* 14.May 2002, pp. 1077–1092

Braulke, T. and Bonifacino, J. S. (2009). "Sorting of lysosomal proteins." *Biochimica et Biophysica Acta* 1793.4, pp. 605–614

Brown, D. A. and Rose, J. K. (1992). "Sorting of GPI-Anchored Proteins to Membrane Subdomains during Transport to the Apical Cell Surface". *Cell* 66, pp. 533–544

Brown, W and Farquhar, M (1984). "The mannose-6-phosphate receptor for lysosomal enzymes is concentrated in cis Golgi cisternae." *Cell* 36, pp. 295–307

Campbell, C. H. and Rome, L. H. (1983). "Coated vesicles from rat liver and calf brain contain lysosomal enzymes bound to mannose 6-phosphate receptors." *The Journal of Biological Chemistry* 258.21, pp. 13347–13352

Canuel, M., Lefrancois, S., Zeng, J., and Morales, C. R. (2008). "AP-1 and retromer play opposite roles in the trafficking of sortilin between the Golgi apparatus and the lysosomes." *Biochemical and Biophysical Research Communications* 366.3, pp. 724–730

Cao, X., Rogers, S. W., Butler, J., Beevers, L., and Rogers, J. C. (2000). "Structural requirements for ligand binding by a probable plant vacuolar sorting receptor." *The Plant Cell* 12.4, pp. 493–506

Casadaban, M. J. and Cohen, S. N. (1980). "Analysis of gene control signals by DNA fusion and cloning in Escherichia coli." *Journal of Molecular Biology* 138.2, pp. 179–207

Cereghino, J. L., Marcusson, E. G., and Emr, S. D. (1995). "The cytoplasmic tail domain of the vacuolar protein sorting receptor Vps10p and a subset of VPS gene products regulate receptor stability, function, and localization." *Molecular Biology of the Cell* 6.9, pp. 1089–102

Ceriotti, A., Duranti, M., and Bollini, R. (1998). "Effects of N-glycosylation on the folding and structure of plant proteins". *Journal of Experimental Botany* 49.324, pp. 1091–1103

Chang, Y.-W., Chuang, Y.-C., Ho, Y.-C., Cheng, M.-Y., Sun, Y.-J., Hsiao, C.-D., and Wang, C. (2010). "Crystal structure of Get4-Get5 complex and its interactions with Sgt2, Get3, and Ydj1". *The Journal of Biological Chemistry* 285.13, pp. 9962–9970

Chatre, L., Wattelet-Boyer, V., Melser, S., Maneta-Peyret, L., Brandizzi, F., and Moreau, P. (2009). "A novel di-acidic motif facilitates ER export of the syntaxin SYP31." *Journal of Experimental Botany* 60.11, pp. 3157–3165

Chavrier, P, Parton, R. G., Hauri, H. P., Simons, K., and Zerial, M (1990). "Localization of low molecular weight GTP binding proteins to exocytic and endocytic compartments." *Cell* 62.2, pp. 317–29

Chernomordik, L. V. and Zimmerberg, J (1995). "Bending membranes to the task: structural intermediates in bilayer fusion." *Current Opinion in Structural Biology* 5.4, pp. 541–547

Chou, K. C. and Elrod, D. W. (1999). "Prediction of membrane protein types and subcellular locations." *Proteins: Structure, Function, and Bioinformatics* 34.1, pp. 137–153

Chow, C.-M., Neto, H., Foucart, C., and Moore, I. (2008). "Rab-A2 and Rab-A3 GTPases define a trans-golgi endosomal membrane domain in Arabidopsis that contributes substantially to the cell plate." *The Plant Cell* 20.1, pp. 101–123

Cocucci, E., Aguet, F., Boulant, S., and Kirchhausen, T. (2012). "The first five seconds in the life of a clathrin-coated pit." *Cell* 150.3, pp. 495–507

Collins, B. M. (2008). "The structure and function of the retromer protein complex." *Traffic* 9.11, pp. 1811–1822

Collins, B. M., Skinner, C. F., Watson, P. J., Seaman, M. N. J., and Owen, D. J. (2005). "Vps29 has a phosphoesterase fold that acts as a protein interaction scaffold for retromer assembly." *Nature Structural & Molecular Biology* 12.7, pp. 594–602

Conibear, E and Stevens, T. H. (2000). "Vps52p, Vps53p, and Vps54p form a novel multisubunit complex required for protein sorting at the yeast late Golgi." *Molecular Biology of the Cell* 11.1, pp. 305–323

Conibear, E, Cleck, J. N., and Stevens, T. H. (2003). "Vps51p Mediates the Association of the GARP (Vps52/53/54) Complex with the Late Golgi t-SNARE Tlg1p". *Molecular Biology of the Cell* 14.April, pp. 1610–1623

Connolly, T and Gilmore, R (1989). "The signal recognition particle receptor mediates the GTP-dependent displacement of SRP from the signal sequence of the nascent polypeptide." *Cell* 57.4, pp. 599–610

Connolly, T, Rapiejko, P. J., and Gilmore, R (1991). "Requirement of GTP hydrolysis for dissociation of the signal recognition particle from its receptor." *Science* 252.5009, pp. 1171–1173

Contento, A. L. and Bassham, D. C. (2012). "Structure and function of endosomes in plant cells." *Journal of Cell Science* 125.Pt 15, pp. 3511–3518

Contreras, I., Yang, Y., Robinson, D. G., and Aniento, F. (2004). "Sorting signals in the cytosolic tail of plant p24 proteins involved in the interaction with the COPII coat." *Plant & Cell Physiology* 45.12, pp. 1779–1786

Cooper, A. and Stevens, T. (1996). "Vps10p cycles between the late-Golgi and prevacuolar compartments in its function as the sorting receptor for multiple yeast vacuolar hydrolases." *The Journal of Cell Biology* 133.3, pp. 529–541

Corrigall, V. M., Bodman-Smith, M. D., Fife, M. S., Canas, B, Myers, L. K., Wooley, P, Soh, C, Staines, N. a., Pappin, D. J., Berlo, S. E., Eden, W van, van Der Zee, R, Lanchbury, J. S., and Panayi, G. S. (2001). "The human endoplasmic reticulum molecular chaperone BiP is an autoantigen for rheumatoid arthritis and prevents the induction of experimental arthritis." *Journal of Immunology* 166.3, pp. 1492–1498

Corsi, A and Schekman, R. (1996). "Mechanism of polypeptide translocation into the endoplasmic reticulum." *The Journal of Biological Chemistry* 271.48, pp. 30299–302

Cox, J. S., Shamu, C. E., and Walter, P. (1993). "Transcriptional induction of genes encoding endoplasmic reticulum resident proteins requires a transmembrane protein kinase." *Cell* 73.6, pp. 1197–1206

Craddock, C. P., Hunter, P. R., Szakacs, E., Hinz, G., Robinson, D. G., and Frigerio, L. (2008). "Lack of a vacuolar sorting receptor leads to non-specific missorting of soluble vacuolar proteins in Arabidopsis seeds." *Traffic* 9.3, pp. 408–416

Crofts, A. J., Leborgne-Castel, N., Hillmer, S., Robinson, D. G., Phillipson, B., Carlsson, L. L., Ashford, D., and Denecke, J. (1999). "Saturation of the endoplasmic reticulum retention machinery reveals anterograde bulk flow". *The Plant Cell* 11.11, pp. 2233–2248

Cross, B. C. S., Sinning, I., Luirink, J., and High, S. (2009). "Delivering proteins for export from the cytosol". *Nature Reviews Molecular Cell Biology* 10.4, pp. 255–264

Cullen, B. (2000). "Nuclear RNA export pathways". *Molecular and Cellular Biology* 20.12, pp. 4181–4187

Dannhauser, P. N. and Ungewickell, E. J. (2012). "Reconstitution of clathrin-coated bud and vesicle formation with minimal components." *Nature Cell Biology* 14.6, pp. 634–639

DaSilva, L. L. P., Snapp, E. L., Lippincott-schwartz, J., Hawes, C., Brandizzi, F., and Denecke, J. (2004). "Endoplasmic reticulum export sites and Golgi bodies behave as single mobile secretory units in plant cells". *The Plant Cell* 16.July, pp. 1753–1771

DaSilva, L. L. P., Taylor, J. P., Hadlington, J. L., Hanton, S., Snowden, C. J., Fox, S. J., Foresti, O., Brandizzi, F., Denecke, J., and Luis, L. L. P. L. P. (2005). "Receptor salvage from the prevacuolar compartment is essential for efficient vacuolar protein targeting". *The Plant Cell* 17.January, pp. 132–148

DaSilva, L. L. P., Foresti, O., and Denecke, J. (2006). "Targeting of the plant vacuolar sorting receptor BP80 is dependent on multiple sorting signals in the cytosolic tail". *The Plant Cell* 18.June, pp. 1477–1497

De Marcos Lousa, C., Gershlick, D. C., and Denecke, J. (2012). "Mechanisms and concepts paving the way towards a complete transport cycle of plant vacuolar sorting receptors." *The Plant Cell* 24.5, pp. 1714–1732

Delbarre, A., Muller, P., Imhoff, V., Barbier-Brygoo, H., Maurel, C., Leblanc, N., Perrot-Rechenmann, C., and Guern, J. (1994). "The rolB Gene of Agrobacterium rhizogenes Does Not Increase the Auxin Sensitivity

of Tobacco Protoplasts by Modifying the Intracellular Auxin Concentration." *Plant Physiology* 105.2, pp. 563–569

Dell'Angelica, E. C., Puertollano, R., Mullins, C., Aguilar, R. C., Vargas, J. D., Hartnell, L. M., and Bonifacino, J. S. (2000). "GGAs: a family of ADP ribosylation factor-binding proteins related to adaptors and associated with the Golgi complex." *The Journal of Cell Biology* 149.1, pp. 81–94

Deloche, O., Yeung, B. G., Payne, G. S., and Schekman, R. (2001). "Vps10p transport from the trans-Golgi network to the endosome is mediated by clathrin-coated vesicles." *Molecular Biology of the Cell* 12.2, pp. 475–485

Delprato, A., Merithew, E., and Lambright, D. G. (2004). "Structure, exchange determinants, and family-wide rab specificity of the tandem helical bundle and Vps9 domains of Rabex-5." *Cell* 118.5, pp. 607–617

Dempski, R. E. and Imperiali, B. (2002). "Oligosaccharyl transferase: gatekeeper to the secretory pathway". *Current Opinion in Chemical Biology* 6.6, pp. 844–850

Denecke, J., Botterman, J., and Deblaere, R. (1990). "Protein secretion in plant cells can occur via a default pathway." *The Plant Cell* 2.1, pp. 51–59

Denecke, J., De Rycke, R., and Botterman, J. (1992). "Plant and mammalian sorting signals for protein retention in the endoplasmic reticulum contain a conserved epitope." *The EMBO Journal* 11.6, pp. 2345–2355

Denecke, J., Aniento, F., Frigerio, L., Hawes, C., Hwang, I., Mathur, J., Neuhaus, J. M., and Robinson, D. G. (2012). "Secretory pathway research: the more experimental systems the better." *The Plant Cell* 24.4, pp. 1316–26

Denzer, A. J., Nabholz, C. E., and Spiess, M (1995). "Transmembrane orientation of signal-anchor proteins is affected by the folding state but not the size of the N-terminal domain." *The EMBO Journal* 14.24, pp. 6311–6317

Deshaies, R. J. and Schekman, R. (1987). "A yeast mutant defective at an early stage in import of secretory protein precursors into the endoplasmic reticulum." *The Journal of Cell Biology* 105.2, pp. 633–645

Deshaies, R., Sanders, S., Feldheim, D., and Schekman, R. (1991). "Assembly of yeast Sec proteins involved in translocation into the endoplasmic reticulum into a membrane-bound multisubunit complex". *Nature* 349, pp. 806–808

Dettmer, J., Hong-hermesdorf, A., Stierhof, Y., and Schumacher, K. (2006). "Vacuolar H-ATPase Activity Is Required for Endocytic and Secretory Trafficking in Arabidopsis". *The Plant Cell* 18.March, pp. 715–730

Dobell, C. (1932). *Antony Van Leeuwenhock and His "little Animals"*. New York: Harcourt, Brace and company

Dominguez, M., Dejgaard, K., Füllekrug, J., Dahan, S., Fazel, A., Paccaud, J.-p., Thomas, D. Y., Bergeron, J. J. M., and Nilsson, T.

(1998). “gp25L/emp24/p24 protein family members of the Golgi network bind both COPI and II coatomer”. 140.4, pp. 751–765

Doms, R. W., Ruusala, a, Machamer, C, Helenius, J, Helenius, a, and Rose, J. K. (1988). “Differential effects of mutations in three domains on folding, quaternary structure, and intracellular transport of vesicular stomatitis virus G protein.” *The Journal of Cell Biology* 107.1, pp. 89–99

Donaldson, J. G., Cassel, D, Kahn, R. a., and Klausner, R. D. (1992). “ADP-ribosylation factor, a small GTP-binding protein, is required for binding of the coatomer protein beta-COP to Golgi membranes.” *Proceedings of the National Academy of Sciences of the United States of America* 89.14, pp. 6408–6412

Doray, B., Bruns, K., Ghosh, P., and Kornfeld, S. (2002). “Interaction of the cation-dependent mannose 6-phosphate receptor with GGA proteins.” *The Journal of Biological Chemistry* 277.21, pp. 18477–18482

Duong, F and Wickner, W (1998). “Sec-dependent membrane protein biogenesis: SecYEG, preprotein hydrophobicity and translocation kinetics control the stop-transfer function.” *The EMBO Journal* 17.3, pp. 696–705

Ebine, K., Fujimoto, M., Okatani, Y., Nishiyama, T., Goh, T., Ito, E., Dainobu, T., Nishitani, A., Uemura, T., Sato, H. M., Thordal Christensen, H., Tsutsumi, N., Nakano, A., and Ueda, T. (2011). “A membrane trafficking pathway regulated by the plant-specific RAB GTPase ARA6”. *Nature Cell Biology* 13.7, pp. 853–9

Edidin, M. (2003). “The State Of Lipid Rafts : From Model Membranes to Cells”. *Annual Review of Biophysics and Biomolecular Structure* 32, pp. 257–283

Ehrlich, M., Boll, W., Van Oijen, A., Hariharan, R., Chandran, K., Nibert, M. L., and Kirchhausen, T. (2004). “Endocytosis by random initiation and stabilization of clathrin-coated pits.” *Cell* 118.5, pp. 591–605

Elzenga, J. T. M., Keller, C. P., and Volkenburgh, E. V. (1991). “Patch clamping protoplasts from vascular plants”. *Plant Physiology* 97, pp. 1573–1575

Epp, N., Rethmeier, R., Krämer, L., and Ungermann, C. (2011). “Membrane dynamics and fusion at late endosomes and vacuoles - Rab regulation, multisubunit tethering complexes and SNAREs.” *European Journal of Cell Biology* 90.9, pp. 779–85

Fabene, P. F. and Bentivoglio, M (1998). “1898-1998: Camillo Golgi and ”the Golgi”: one hundred years of terminological clones.” *Brain Research Bulletin* 47.3, pp. 195–198

Fasshauer, D, Sutton, R. B., Brunger, A. T., and Jahn, R (1998). “Conserved structural features of the synaptic fusion complex: SNARE proteins reclassified as Q- and R-SNAREs.” *Proceedings of the National Academy of Sciences of the United States of America* 95.26, pp. 15781–15786

Favaloro, V., Spasic, M., Schwappach, B., and Dobberstein, B (2009). "Europe PMC Funders Group Distinct targeting pathways for the membrane insertion of tail- anchored (TA) proteins". *The Journal of Cell Science* 121.Pt 11, pp. 1832–1840

Ferro-Novick, S, Novick, P. J., Field, C, and Schekman, R. (1984). "Yeast secretory mutants that block the formation of active cell surface enzymes." *The Journal of Cell Biology* 98.1, pp. 35–43

Fiedler, K, Veit, M, Stamnes, M. a., and Rothman, J. E. (1996). "Bimodal interaction of coatomer with the p24 family of putative cargo receptors." *Science* 273.5280, pp. 1396–1399

Fleming, J (1978). "The Nonpolar Peptide Segment of Cytochrome B5". *The Journal of Biological Chemistry* 253.22, pp. 8198–8202

Ford, M. G. J., Mills, I. G., Peter, B. J., Vallis, Y., Praefcke, G. J. K., Evans, P. R., and McMahon, H. T. (2002). "Curvature of clathrin-coated pits driven by epsin." *Nature* 419.6905, pp. 361–366

Foresti, O. and Denecke, J. (2008). "Intermediate organelles of the plant secretory pathway: identity and function." *Traffic* 9.10, pp. 1599–1612

Foresti, O., DaSilva, L. L. P., and Denecke, J. (2006). "Overexpression of the Arabidopsis syntaxin PEP12/SYP21 inhibits transport from the prevacuolar compartment to the lytic vacuole in vivo". *The Plant Cell* 18, pp. 2275–2293

Foresti, O., Gershlick, D. C., Bottanelli, F., Hummel, E., Hawes, C., and Denecke, J. (2010). "A recycling-defective vacuolar sorting receptor reveals an intermediate compartment situated between prevacuoles and vacuoles in tobacco." *The Plant Cell* 22.12, pp. 3992–4008

Frand, A. R., Cuozzo, J. W., and Kaiser, C. A. (2000). "Pathways for protein disulphide bond formation." *Trends in Cell Biology* 10.5, pp. 203–210

Freedman, R. B., Hirst, T. R., and Tuite, M. F. (1994). "Protein disulphide isomerase: building bridges in protein folding." *Trends in Biochemical Sciences* 19.8, pp. 331–6

French, A. P., Mills, S., Swarup, R., Bennett, M. J., and Pridmore, T. P. (2008). "Colocalization of fluorescent markers in confocal microscope images of plant cells." *Nature Protocols* 3.4, pp. 619–628

Fromm, M, Taylor, L. P., and Walbot, V (1985). "Expression of genes transferred into monocot and dicot plant cells by electroporation." *Proceedings of the National Academy of Sciences of the United States of America* 82.17, pp. 5824–5828

Fuji, K., Shimada, T., Takahashi, H., Tamura, K., Koumoto, Y., Utsumi, S., Nishizawa, K., Maruyama, N., and Hara-Nishimura, I. (2007). "Arabidopsis vacuolar sorting mutants (green fluorescent seed) can be identified efficiently by secretion of vacuole-targeted green fluorescent protein in their seeds." *The Plant Cell* 19.2, pp. 597–609

Futter, C. and Ramalho, J. (2004). "The role of Rab27a in the regulation of melanosome distribution within retinal pigment epithelial cells". *Molecular Biology of the Cell* 15.May, pp. 2264–2275

Gibson, D. G., Young, L., and Chuang, R. Y. (2009). "Enzymatic assembly of DNA molecules up to several hundred kilobases". *Nature Methods* 6.5, pp. 12–16

Gill, R., Rashid, A, and Maheshwar, S. C. (1978). "Regeneration of plants from mesophyll protoplasts". *Protoplasma* 379, pp. 375–379

Gillingham, A. K. and Munro, S. (2007). "The small G proteins of the Arf family and their regulators." *Annual Review of Cell and Developmental Biology* 23, pp. 579–611

Gillooly, D. J., Morrow, I. C., Lindsay, M, Gould, R, Bryant, N. J., Gaullier, J. M., Parton, R. G., and Stenmark, H (2000). "Localization of phosphatidylinositol 3-phosphate in yeast and mammalian cells." *The EMBO Journal* 19.17, pp. 4577–4588

Gilmore, R, Walter, P, and Blobel, G (1982). "Protein translocation across the endoplasmic reticulum. II. Isolation and characterization of the signal recognition particle receptor." *The Journal of Cell Biology* 95.2 Pt 1, pp. 470–477

Goldberg, J (1999). "Structural and functional analysis of the ARF1-ARFGAP complex reveals a role for coatomer in GTP hydrolysis." *Cell* 96.6, pp. 893–902

Goloubinoff, P, Mogk, A, Zvi, A. P., Tomoyasu, T, and Bukau, B (1999). "Sequential mechanism of solubilization and refolding of stable protein aggregates by a bichaperone network." *Proceedings of the National Academy of Sciences of the United States of America* 96.24, pp. 13732–13737

Grant, B. D. and Donaldson, J. G. (2011). "Pathways and Mechanisms of Endocytic Recycling". *Nature Reviews Molecular Cell Biology* 10.9, pp. 597–608

Griffiths, G., Doms, R., Mayhew, T., and Lucocq, J. (1995). "The end of bulk flow? The bulk-flow hypothesis: not quite the end". *Trends in Cell Biology*, pp. 9–13

Guan, J. L., Ruusala, a, Cao, H, and Rose, J. K. (1988). "Effects of altered cytoplasmic domains on transport of the vesicular stomatitis virus glycoprotein are transferable to other proteins." *Molecular and Cellular Biology* 8.7, pp. 2869–74

Guermonprez, H., Smertenko, A., Crosnier, M.-T., Durandet, M., Vrielynck, N., Guerche, P., Hussey, P. J., Satiat-Jeunemaitre, B., and Bonhomme, S. (2008). "The POK/AtVPS52 protein localizes to several distinct post-Golgi compartments in sporophytic and gametophytic cells." *Journal of Experimental Botany* 59.11, pp. 3087–3098

Gürkan, C., Stagg, S. M., Lapointe, P., and Balch, W. E. (2006). "The COPII cage: unifying principles of vesicle coat assembly." *Nature Reviews Molecular Cell Biology* 7.10, pp. 727–738

Haas, A. K., Yoshimura, S.-i., Stephens, D. J., Preisinger, C., Fuchs, E., and Barr, F. a. (2007a). "Analysis of GTPase-activating proteins: Rab1 and Rab43 are key Rabs required to maintain a functional Golgi complex in human cells." *Journal of Cell Science* 120.17, pp. 2997–3010

Haas, T. J., Sliwinski, M. K., Martínez, D. E., Preuss, M., Ebine, K., Ueda, T., Nielsen, E., Odorizzi, G., and Otegui, M. S. (2007b). "The Arabidopsis AAA ATPase SKD1 is involved in multivesicular endosome function and interacts with its positive regulator LYST-INTERACTING PROTEIN5." *The Plant Cell* 19.4, pp. 1295–1312

Hadlington, J. L. and Denecke, J. (2000). "Sorting of soluble proteins in the secretory pathway of plants". *Current Opinion in Plant Biology*, pp. 461–468

Hain, R, Stabel, P, Czernilofsky, A., Steinbi, H., Herrera-Estrella, L., and Schell, J (1985). "Uptake, integration, expression and genetic transmission of a selectable chimaeric gene by plant protoplasts". *Molecular Genetics & Genomics*, pp. 161–168

Hamman, B. D., Hendershot, L. M., and Johnson, a. E. (1998). "BiP maintains the permeability barrier of the ER membrane by sealing the lumenal end of the translocon pore before and early in translocation." *Cell* 92.6, pp. 747–758

Hanton, S., Renna, L., Bortolotti, L. E., Chatre, L., Stefano, G., and Brandizzi, F. (2005). "Diacidic Motifs Influence the Export of Transmembrane Proteins from the Endoplasmic Reticulum in Plant Cells". *The Plant Cell* 17.November, pp. 3081–3093

Happel, N., Honing, S., Neuhaus, J. M., Paris, N., Robinson, D. G., and Holstein, S. E. H. (2004). "ArabidopsisuA-adaptin interacts with the tyrosine motif of the vacuolar sorting receptor VSR-PS1". *The Plant Journal* 37.5, pp. 678–693

Hara-Nishimura, I., Shimada, T., Hatano, K, Takeuchi, Y, and Nishimura, M (1998). "Transport of storage proteins to protein storage vacuoles is mediated by large precursor-accumulating vesicles". *The Plant Cell* 10.5, pp. 825–836

Harding, H. P., Zhang, Y., and Ron, D (1999). "Protein translation and folding are coupled by an resident kinase". *Nature* 398.March, pp. 271–274

Harrison, S. C. and Kirchhausen, T. (1983). "Clathrin, cages, and coated vesicles." *Cell* 33.3, pp. 650–652

Hart, W, Brew, K., Lennarzs, J, and Grant, A (1979). "Primary structural requirements bond in glycoproteins for the enzymatic formation of the N-glycosidic bond in glycoproteins". *The Journal of Biological Chemistry* 254.19, pp. 9747–9753

Hartl, F. U. and Martin, J (1995). "Molecular chaperones in cellular protein folding". *Current Opinion in Structural Biology* 381, pp. 571–580

Hartmann, E, Rapoport, T., and Lodish, H. F. (1989). "Predicting the orientation of eukaryotic membrane-spanning proteins." *Proceedings of the National Academy of Sciences of the United States of America* 86.15, pp. 5786–5790

Haucke, V. and Paolo, G. D. (2007). "Lipids and lipid modifications in the regulation of membrane traffic". *Current Opinion in Cell Biology* 19.4, pp. 426–435

Haze, K, Yoshida, H, Yanagi, H, Yura, T, and Mori, K (1999). "Mammalian transcription factor ATF6 is synthesized as a transmembrane protein and activated by proteolysis in response to endoplasmic reticulum stress." *Molecular Biology of the Cell* 10.11, pp. 3787–3799

Hehnly, H. and Stamnes, M. (2007). "Regulating cytoskeleton-based vesicle motility." *FEBS letters* 581.11, pp. 2112–2118

Heijne, G von (1985). "Signal sequences. The limits of variation." *Journal of Molecular Biology* 184.1, pp. 99–105

Heijne, G von and Gavel, Y (1988). "Topogenic signals in integral membrane proteins." *European Journal of Biochemistry* 174.4, pp. 671–678

Heinrich, S. U., Mothes, W, Brunner, J, and Rapoport, T. (2000). "The Sec61p complex mediates the integration of a membrane protein by allowing lipid partitioning of the transmembrane domain." *Cell* 102.2, pp. 233–244

Helenius, J, Ng, D. T. W., Marolda, C. L., Walter, P., Valvano, M. a., and Aebi, M. (2002). "Translocation of lipid-linked oligosaccharides across the ER membrane requires Rft1 protein." *Nature* 415.6870, pp. 447–450

Henne, W. M., Buchkovich, N. J., and Emr, S. D. (2011). "The ESCRT pathway." *Developmental cell* 21.1, pp. 77–91

Hepler, P., Palevitz, B., Lancelle, S. A., McCauley, M. M., and Lichtscheild, I. (1990). "Cortical endoplasmic reticulum in plants". *Journal of Cell Science* 96, pp. 355–373

Herrmann, J. M., Malkus, P, and Schekman, R. (1999). "Out of the ER–outfitters, escorts and guides." *Trends in cell biology* 9.1, pp. 5–7

Hessa, T., Kim, H., Bihlmaier, K., Lundin, C., Boekel, J., Andersson, H., Nilsson, I., White, S. H., and Heijne, G. von (2005). "Recognition of transmembrane helices by the endoplasmic reticulum translocon." *Nature* 433.7024, pp. 377–381

Hicke, L, Yoshihisa, T, and Schekman, R. (1992). "Sec23p and a novel 105-kDa protein function as a multimeric complex to promote vesicle budding and protein transport from the endoplasmic reticulum." *Molecular Biology of the Cell* 3.6, pp. 667–676

Hierro, A., Rojas, A. L., Rojas, R., Murthy, N., Effantin, G., Kajava, A. V., Steven, A. C., Bonifacino, J. S., and Hurley, J. H. (2007). "Functional architecture of the retromer cargo-recognition complex." *Nature* 449.7165, pp. 1063–1067

Hillmer, S, Movafeghi, A, Robinson, D. G., and Hinz, G. (2001). "Vacuolar storage proteins are sorted in the cis-cisternae of the pea cotyledon Golgi apparatus." *The Journal of Cell Biology* 152.1, pp. 41–50

Hinz, G., Hillmer, S., Baumer, M., and Hohl, I. (1999). "Vacuolar storage proteins and the putative vacuolar sorting receptor BP-80 exit the golgi apparatus of developing pea cotyledons in different transport vesicles". *The Plant Cell* 11.8, pp. 1509–1524

Hirst, J, Barlow, L. D., Francisco, G. C., Sahlender, D. a., Seaman, M. N. J., Dacks, J. B., and Robinson, M. S. (2011). "The fifth adaptor protein complex." *PLoS Biology* 9.10, e1001170

Ho, S.-Y., Lorent, K., Pack, M., and Farber, S. a. (2006). "Zebrafish fat-free is required for intestinal lipid absorption and Golgi apparatus structure." *Cell Metabolism* 3.4, pp. 289–300

Hoflack, B. and Kornfeld, S (1985). "Lysosomal enzyme binding to mouse P388D1 macrophage membranes lacking the 215-kDa mannose 6-phosphate receptor: evidence for the existence of a second mannose 6-phosphate receptor." *Proceedings of the National Academy of Sciences of the United States of America* 82.13, pp. 4428–4432

Hofmann, M. W., Höning, S, Rodionov, D, Dobberstein, B, Figura, K von, and Bakke, O (1999). "The leucine-based sorting motifs in the cytoplasmic domain of the invariant chain are recognized by the clathrin adaptors AP1 and AP2 and their medium chains." *The Journal of Biological Chemistry* 274.51, pp. 36153–36158

Höfte, H and Chrispeels, M. (1992). "Protein sorting to the vacuolar membrane." *The Plant Cell* 4.August, pp. 995–1004

Holwerda, B. C., Padgett, H. S., and Rogers, J. C. (1992). "Proaleurain vacuolar targeting is mediated by short contiguous peptide interactions." *The Plant Cell* 4.3, pp. 307–318

Höning, S and Sosa, M (1997). "The 46-kDa mannose 6-phosphate receptor contains multiple binding sites for clathrin adaptors". *Journal of Biological Chemistry* 272.32, pp. 19884–19890

Hooke, R. (1667). *Micrographia: or some physiological descriptions of minute bodies made by magnifying glasses : with observations and inquiries thereupon.* London: J. Martyn and J. Allestry

Horazdovsky, B. F., Davies, B. a., Seaman, M. N. J., McLaughlin, S. a., Yoon, S, and Emr, S. D. (1997). "A sorting nexin-1 homologue,

Vps5p, forms a complex with Vps17p and is required for recycling the vacuolar protein-sorting receptor." *Molecular Biology of the Cell* 8.8, pp. 1529–1541

Hornick, C. A., Hamilton, R. L., Spaziani, E, Enders, G. H., and Havel, R. J. (1985). "Isolation and characterization of multivesicular bodies from rat hepatocytes: an organelle distinct from secretory vesicles of the Golgi apparatus." *The Journal of Cell Biology* 100.5, pp. 1558–1569

Huang, M, Weissman, J. T., Beraud-Dufour, S, Luan, P, Wang, C, Chen, W, Aridor, M., Wilson, I. a., and Balch, W. E. (2001). "Crystal structure of Sar1-GDP at 1.7 A resolution and the role of the NH2 terminus in ER export." *The Journal of Cell Biology* 155.6, pp. 937–948

Hughes, H. and Stephens, D. J. (2008). "Assembly, organization, and function of the COPII coat." *Histochemistry and Cell Biology* 129.2, pp. 129–151

Hummon, M. and Costello, W. (1992). "Cell lineage of flight muscle fibers in Drosophila: a fate map of the induced shibire phenotype in mosaics". *Roux's Archives of Developmental Biology*, pp. 88–94

Hunter, P. R., Craddock, C. P., Di Benedetto, S., Roberts, L. M., and Frigerio, L. (2007). "Fluorescent reporter proteins for the tonoplast and the vacuolar lumen identify a single vacuolar compartment in Arabidopsis cells." *Plant Physiology* 145.4, pp. 1371–1382

Huotari, J. and Helenius, A (2011). "Endosome maturation." *The EMBO Journal* 30.17, pp. 3481–3500

Husnjak, K., Elsasser, S., Zhang, N., Chen, X., Randles, L., Shi, Y., Hofmann, K., Walters, K. J., Finley, D., and Dikic, I. (2008). "Proteasome subunit Rpn13 is a novel ubiquitin receptor." *Nature* 453.7194, pp. 481–488

Ijzendoorn, S. C. D. van (2006). "Recycling endosomes." *Journal of Cell Science* 119.Pt 9, pp. 1679–1681

Jahn, R and Südhof, T. C. (1999). "Membrane fusion and exocytosis." *Annual Review of Biochemistry* 68, pp. 863–911

Jahn, R. and Scheller, R. H. (2006). "SNAREs–engines for membrane fusion." *Nature Reviews Molecular Cell Biology* 7.9, pp. 631–643

Jaillais, Y., Fobis-Loisy, I., Miège, C., Rollin, C., and Gaude, T. (2006). "AtSNX1 defines an endosome for auxin-carrier trafficking in Arabidopsis." *Nature* 443.7107, pp. 106–109

Jaillais, Y., Santambrogio, M., Rozier, F., Fobis-Loisy, I., Miège, C., and Gaude, T. (2007). "The retromer protein VPS29 links cell polarity and organ initiation in plants." *Cell* 130.6, pp. 1057–1070

Jin, J. B., Kim, Y. a., Kim, S. J., Lee, S. H., Kim, D. H., Cheong, G. W., and Hwang, I (2001). "A new dynamin-like protein, ADL6, is involved in trafficking from the trans-Golgi network to the central vacuole in Arabidopsis." *The Plant Cell* 13.7, pp. 1511–1526

Jolliffe, N., Brown, J. C., Neumann, U., Vicré, M., Bachi, A., Hawes, C., Ceriotti, A., Roberts, L. M., and Frigerio, L. (2004). "Transport of ricin and 2S albumin precursors to the storage vacuoles of Ricinus communis endosperm involves the Golgi and VSR-like receptors." *The Plant Journal* 39.6, pp. 821–833

Jones, D. T., Taylor, W. R., and Thornton, J. M. (1992). "The rapid generation of mutation data matrices from protein sequences." *Computer Applications in the Biosciences* 8.3, pp. 275–282

Jonikas, M. C., Collins, S. R., Denic, V., Oh, E., Quan, E. M., Schmid, V., Weibezahn, J., Schwappach, B., Walter, P., Weissman, J. S., and Schuldiner, M. (2009). "Comprehensive characterization of genes required for protein folding in the endoplasmic reticulum." *Science* 323.5922, pp. 1693–7

Jung, C., Lee, G.-J., Jang, M., Lee, M., Lee, J., Kang, H., Sohn, E. J., and Hwang, I. (2011). "Identification of sorting motifs of AtβFruct4 for trafficking from the ER to the vacuole through the Golgi and PVC." *Traffic* 12.12, pp. 1774–1792

Junne, T., Kocik, L., and Spiess, M. (2010). "The hydrophobic core of the Sec61 translocon defines the hydrophobicity threshold for membrane integration". *Molecular Biology of the Cell* 21, pp. 1662–1670

Kahn, R. A. and Gilman, G (1986). "The Protein Cofactor Necessary for ADP-ribosylation of Gs by Cholera Toxin is Itself a GTP Binding Protein". *The Journal of Biological Chemistry* 261.11, pp. 7906–7911

Kaiser, C. A. and Schekman, R. (1990). "Distinct sets of SEC genes govern transport vesicle formation and fusion early in the secretory pathway." *Cell* 61.4, pp. 723–733

Kalies, K. U., Görlich, D, and Rapoport, T. (1994). "Binding of ribosomes to the rough endoplasmic reticulum mediated by the Sec61p-complex." *The Journal of Cell Biology* 126.4, pp. 925–934

Kalies, K.-U., Allan, S., Sergeyenko, T., Kröger, H., and Römisch, K. (2005). "The protein translocation channel binds proteasomes to the endoplasmic reticulum membrane." *The EMBO Journal* 24.13, pp. 2284–2293

Kang, B., Nielsen, E., Preuss, M., Mastronarde, D., and Staehelin, L. (2011). "Electron tomography of RabA4b- and PI-4Kβ1-labeled trans Golgi network compartments in Arabidopsis." *Traffic* 12.3, pp. 313–329

Kang, H., Kim, S. Y., Song, K., Sohn, E. J., Lee, Y., Lee, D. W., Hara-Nishimura, I., and Hwang, I. (2012). "Trafficking of Vacuolar Proteins: The Crucial Role of Arabidopsis Vacuolar Protein Sorting 29 in Recycling Vacuolar Sorting Receptor." *The Plant Cell* 35, pp. 5058–5073

Kaplan, A., Achord, D., and Sly, W. (1977). "Phosphohexosyl components of a lysosomal enzyme are recognized by pinocytosis receptors on human

fibroblasts". *Proceedings of the National Academy of Sciences of the United States of America* 74.5, pp. 2026–2030

Kappeler, F, Klopfenstein, D, Paccaud, J, and Hauri, H (1997). "The recycling of ERGIC-53 in the early secretory pathway". 272.50, pp. 31801–31808

Keenan, R. J., Freymann, D. M., Stroud, R. M., and Walter, P. (2001). "The signal recognition particle". *Annual Review of Biochemistry* 70, pp. 755–775

Kim, D. H., Eu, Y.-j., Yoo, M., Kim, Y.-w., Pih, T., Jin, B., Kim, S. J., Stenmark, H., and Hwang, I. (2001). "Trafficking of Phosphatidylinositol 3-Phosphate from the trans -Golgi Network to the Lumen of the Central Vacuole in Plant Cells". *The Plant Cell* 13.February, pp. 287–301

Kim, H., Kang, H., Jang, M., Chang, J. H., Miao, Y., Jiang, L., and Hwang, I. (2010). "Homomeric interaction of AtVSR1 is essential for its function as a vacuolar sorting receptor." *Plant Physiology* 154.1, pp. 134–148

Kirchhausen, T. (2000a). "Clathrin". *Annual Review of Biochemistry* 69, pp. 699–727

— (2000b). "Three ways to make a vesicle." *Nature Reviews Molecular Cell Biology* 1.3, pp. 187–198

— (2002). "Single-handed recognition of a sorting traffic motif by the GGA proteins." *Nature Structural & Molecular Biology* 9.4, pp. 241–244

— (2012). "Bending membranes." *Nature Cell Biology* 14.9, pp. 906–908

Kirchhausen, T. and Harrison, S. C. (1984). "Structural domains of clathrin heavy chains." *The Journal of Cell Biology* 99.5, pp. 1725–1734

Kirchhausen, T., Bonifacino, J. S., and Riezman, H. (1997). "Linking cargo to vesicle formation: receptor tail interactions with coat proteins." *Current Opinion in Cell Biology* 9, pp. 488–495

Kirsch, T., Paris, N., Butler, J. M., Beevers, L., and Rogers, J. C. (1994). "Purification and initial characterization of a potential plant vacuolar targeting receptor." *Proceedings of the National Academy of Sciences of the United States of America* 91.8, pp. 3403–3407

Kirsch, T., Saalbach, G., Raikhel, N. V., and Beevers, L. (1996). "Interaction of a potential vacuolar targeting receptor with amino- and carboxyl-terminal targeting determinants." *Plant Physiology* 111.2, pp. 469–474

Kleine-Vehn, J, Leitner, J., Zwiewka, M., Sauer, M., Abas, L., Luschnig, C., and Friml, J. (2008). "Differential degradation of PIN2 auxin efflux carrier by retromer-dependent vacuolar targeting." *Proceedings of the National Academy of Sciences of the United States of America* 105.46, pp. 17812–17817

Koch, A. and Silver, S. (2005). "The first cell". *Advances in Microbial Physiology* 50, pp. 227–259

Kocik, L., Junne, T., and Spiess, M. (2012). "Orientation of internal signal-anchor sequences at the Sec61 translocon." *Journal of molecular biology* 424.5, pp. 368–378

Komeili, A, Li, Z, Newman, D., and Jensen, G. (2006). "Magnetosomes are cell membrane invaginations organized by the actin-like protein MamK". *Science* 311.January, pp. 242–245

Kornfeld, S (1992). "Structure and function of the mannose 6-phosphate / insulinlike growth factor II receptors." *Annual Review of Biochemistry* 61, pp. 307–330

Kotzer, A. M., Brandizzi, F., Neumann, U., Paris, N., Moore, I., and Hawes, C. (2004). "AtRabF2b (Ara7) acts on the vacuolar trafficking pathway in tobacco leaf epidermal cells." *Journal of Cell Science* 117.Pt 26, pp. 6377–6389

Kraynack, B. A., Chan, A., Rosenthal, E., Essid, M., Umansky, B., Waters, M. G., and Schmitt, H. D. (2005). "Dsl1p , Tip20p , and the Novel Dsl3 (Sec39) Protein Are Required for the Stability of the Q / t-SNARE Complex at the Endoplasmic Reticulum in Yeast ". *Molecular Biology of the Cell* 16.September, pp. 3963–3977

Kreis, T. E. and Lodish, H. F. (1986). "Oligomerization is essential for transport of vesicular stomatitis viral glycoprotein to the cell surface." *Cell* 46.6, pp. 929–937

Krens, F. A., Molendijk, G. J., Wullems, G. J., and Schilperoot, R. A. (1982). "In vitro transformation of plant protoplasts with Ti-plasmid DNA". *Nature* 296, pp. 72–74

Kutay, U, Hartmann, E, and Rapoport, T. (1993). "A class of membrane proteins with a C-terminal anchor." *Trends in Cell Biology* 3.3, pp. 72–75

Lafay, F (1974). "Envelope proteins of vesicular stomatitis virus: effect of temperature-sensitive mutations in complementation groups III and V." *Journal of Virology* 14.5, pp. 1220–1228

Lam, S. K., Tse, Y. C., Robinson, D. G., and Jiang, L. (2007). "Tracking down the elusive early endosome." *Trends in Plant Science* 12.11, pp. 497–505

Langer, D., Hain, J., Thuriaux, P., and Zillig, W. (1995). "Transcription in archaea: similarity to that in eucarya." *Proceedings of the National Academy of Sciences of the United States of America* 92.13, pp. 5768–5772

Laval, V., Masclaux, F., and Serin, A. (2003). "Seed germination is blocked in Arabidopsis putative vacuolar sorting receptor (atbp80) antisense transformants". *Journal of Experimental Botany* 54.381, pp. 213–221

Lawe, D. C., Patki, V., Heller-Harrison, R., Lambright, D., and Corvera, S (2000). "The FYVE domain of early endosome antigen 1 Is required for both phosphatidylinositol 3-phosphate and Rab5 binding". *Journal of Biological Chemistry* 275.5, pp. 3699–3705

Leborgne-castel, N., Dooren, J., Crofts, A. J., and Denecke, J. (1999). "Overexpression of BiP in tobacco alleviates endoplasmic reticulum stress". *The Plant Cell* 11, pp. 459–470

Lee, A, Frank, D. W., Marks, M. S., and Lemmon, M. a. (1999). "Dominant-negative inhibition of receptor-mediated endocytosis by a dynamin-1 mutant with a defective pleckstrin homology domain." *Current Biology* 9.5, pp. 261–264

Lee, G.-J., Sohn, E. J., Lee, M. H., and Hwang, I. (2004). "The Arabidopsis rab5 homologs rha1 and ara7 localize to the prevacuolar compartment." *Plant & Cell Physiology* 45.9, pp. 1211–1220

Lee, M. C. S., Orci, L., Hamamoto, S., Futai, E., Ravazzola, M., and Schekman, R. (2005). "Sar1p N-terminal helix initiates membrane curvature and completes the fission of a COPII vesicle." *Cell* 122.4, pp. 605–617

Lee, Y., Jang, M., Song, K., Kang, H., Lee, M. C. S., Lee, D. W., Zouhar, J., Rojo, E., Sohn, E., and Hwang, I. (2013). "Functional identification of sorting receptors involved in trafficking of soluble lytic vacuolar proteins in vegetative cells of Arabidopsis." *Plant Physiology* 161.1, pp. 121–133

Lefrancois, S., Zeng, J., and Hassan, A. (2003). "The lysosomal trafficking of sphingolipid activator proteins (SAPs) is mediated by sortilin". *The EMBO Journal* 22.24, pp. 6430–6437

Lerich, A., Hillmer, S., Langhans, M., Scheuring, D., Bentum, P. van, and Robinson, D. G. (2012). "ER Import Sites and Their Relationship to ER Exit Sites: A New Model for Bidirectional ER-Golgi Transport in Higher Plants." *Frontiers in Plant Science* 3.[doi:10.3389], pp. 1–21

Letourneur, F, Gaynor, E. C., Hennecke, S, Démollière, C, Duden, R, Emr, S. D., Riezman, H, and Cosson, P (1994). "Coatomer is essential for retrieval of dilysine-tagged proteins to the endoplasmic reticulum." *Cell* 79.7, pp. 1199–1207

Levine, T. (2004). "Short-range intracellular trafficking of small molecules across endoplasmic reticulum junctions." *Trends in Cell Biology* 14.9, pp. 483–490

Lewis, M. J. and Pelham, H. R. B. (1992). "Ligand-induced redistribution of a human KDEL receptor from the Golgi complex to the endoplasmic reticulum." *Cell* 68.2, pp. 353–364

Lewis, M. J., Sweet, D. J., and Pelham, H. R. B. (1990). "The ERD2 gene determines the specificity of the luminal ER protein retention system." *Cell* 61.7, pp. 1359–1363

Liewen, H., Meinhold Heerlein, I., Oliveira, V., Schwarzenbacher, R., Luo, G., Wadle, A., Jung, M., Pfreundschuh, M., and Stenner Liewen, F. (2005). "Characterization of the human GARP (Golgi associated retrograde protein) complex." *Experimental Cell Research* 306.1, pp. 24–34

Lippincott-Schwartz, J., Bonifacino, J. S., Yuan, L. C., and Klausner, R. D. (1988). "Degradation from the endoplasmic reticulum: disposing of newly synthesized proteins". *Cell* 54, pp. 209–220

Lyko, F, Martoglio, B, Jungnickel, B, Rapoport, T., and Dobberstein, B (1995). "Signal sequence processing in rough microsomes". *Journal of Biological Chemistry* 270.34, pp. 19873–19878

Ma, D, Zerangue, N, Lin, Y. F., Collins, A, Yu, M, Jan, Y. N., and Jan, L. Y. (2001). "Role of ER export signals in controlling surface potassium channel numbers." *Science* 291.5502, pp. 316–319

Malhotra, V, Serafini, T, Orci, L., Shepherd, J. C., and Rothman, J. E. (1989). "Purification of a novel class of coated vesicles mediating biosynthetic protein transport through the Golgi stack." *Cell* 58.2, pp. 329–336

Maliga, P, Sz-Breznovits, A., and Marton, L (1973). "Streptomycin-resistant plants from callus culture of haploid tobacco". *Nature* 244.131, pp. 29–30

Malkus, P, Jiang, F., and Schekman, R. (2002). "Concentrative sorting of secretory cargo proteins into COPII-coated vesicles." *The Journal of Cell Biology* 159.6, pp. 915–921

Marciniak, S. J., Garcia-Bonilla, L., Hu, J., Harding, H. P., and Ron, D (2006). "Activation-dependent substrate recruitment by the eukaryotic translation initiation factor 2 kinase PERK." *The Journal of Cell Biology* 172.2, pp. 201–9

Marcusson, E. G., Horazdovsky, B. F., Cereghino, J. L., Gharakhanian, E, and Emr, S. D. (1994). "The sorting receptor for yeast vacuolar carboxypeptidase Y is encoded by the VPS10 gene." *Cell* 77.4, pp. 579–586

Markin, V. S., Kozlov, M. M., and Borovjagin, V. L. (1984). "On the theory of membrane fusion. The stalk mechanism." *General Physiology and Biophysics* 3.5, pp. 361–377

Martínez, I. and Chrispeels, M. (2003). "Genomic analysis of the unfolded protein response in Arabidopsis shows its connection to important cellular processes". *The Plant Cell* 15.February, pp. 561–576

Marty, F. (1999). "Plant Vacuoles". *The Plant Cell* 11.April, pp. 587–599

Matlack, K. E., Misselwitz, B, Plath, K, and Rapoport, T. (1999). "BiP acts as a molecular ratchet during posttranslational transport of prepro-alpha factor across the ER membrane." *Cell* 97.5, pp. 553–564

Matsui, Y, Kikuchi, A, Araki, S, Hata, Y, Kondo, J, Teranishi, Y, and Takai, Y (1990). "Molecular cloning and characterization of a novel type of regulatory protein (GDI) for smg p25A, a ras p21-like GTP-binding protein." *Molecular and Cellular Biology* 10.8, pp. 4116–4122

Matsuoka, K. and Nakamura, K (1991). "Propeptide of a precursor to a plant vacuolar protein required for vacuolar targeting." *Proceedings of the National Academy of Sciences of the United States of America* 88.3, pp. 834–8

Matsuoka, K. and Neuhaus, J. M. (1999). "Cis-elements of protein transport to the plant vacuoles". *Journal of Experimental Botany* 50.331, pp. 165–174

Maxfield, F. R. and McGraw, T. E. (2004). "Endocytic recycling." *Nature Reviews Molecular Cell Biology* 5.2, pp. 121–132

Mazzarello, P (1999). "A unifying concept: the history of cell theory." *Nature Cell Biology* 1.1, E13–5

Mercanti, V., Marchetti, A., Lelong, E., Perez, F., Orci, L., and Cosson, P. (2010). "Transmembrane domains control exclusion of membrane proteins from clathrin-coated pits." *Journal of Cell Science* 123.Pt 19, pp. 3329–3335

Meusser, B., Hirsch, C., Jarosch, E., and Sommer, T. (2005). "ERAD: the long road to destruction." *Nature Cell Biology* 7.8, pp. 766–772

Miao, Y., Yan, P. K. P., Kim, H., Hwang, I., and Jiang, L. (2006). "Localization of green fluorescent protein fusions with the seven Arabidopsis vacuolar sorting receptors to prevacuolar compartments in tobacco BY-2 cells." *Plant Physiology* 142.3, pp. 945–962

Miller, E., Lee, M. C. S., and Anderson, M. (1999). "Identification and characterization of a prevacuolar compartment in stigmas of nicotiana alata". *The Plant Cell* 11.8, pp. 1499–1508

Miller, J., Wilhelm, H, Gierasch, L, Gilmore, R, and Walter, P (1993). "GTP binding and hydrolysis by the signal recognition particle during initiation of protein translocation". *Nature* 366, pp. 351–366

Mima, J., Hickey, C. M., Xu, H., Jun, Y., and Wickner, W. (2008). "Reconstituted membrane fusion requires regulatory lipids, SNAREs and synergistic SNARE chaperones." *The EMBO Journal* 27.15, pp. 2031–2042

Mizuno, M and Singer, S. (1993). "A soluble secretory protein is first concentrated in the endoplasmic reticulum before transfer to the Golgi apparatus". *Proceedings of the National Academy of Sciences of the United States of America* 90.June, pp. 5732–5736

Mothes, W., Prehn, S., and Rapoport, T. (1994). "Systematic probing of the environment of a translocating secretory protein during translocation through the ER membrane." *The EMBO Journal* 13.17, pp. 3973–3982

Moyer, B. D., Allan, B. B., and Balch, W. E. (2001). "Rab1 interaction with a GM130 effector complex regulates COPII vesicle cis–Golgi tethering." *Traffic* 2.4, pp. 268–276

Munro, S. (2003). "Lipid rafts : elusive or illusive?" *Cell* 115, pp. 377–388

Munro, S. and Pelham, H. R. B. (1987). "A C-terminal signal prevents secretion of luminal ER proteins." *Cell* 48.5, pp. 899–907

Murashige, T and Skoog, F (1978). "A revised medium for rapid growth and bioassays with tobacco tissue cultures". *Physiologia Plantarum* 43, p. 1978

Nakatsu, F. and Ohno, H. (2003). "Adaptor Protein Complexes as the Key Regulators of Protein Sorting in the Post-Golgi Network Identification of AP complexes Recognition of sorting signals by AP complexes". *Cell Structure and Function* 429, pp. 419–429

Natsume, W., Tanabe, K., and Kon, S. (2006). "Novel ARF GTPase-activating Protein, Interacts with Clathrin and Clathrin Assembly Protein and Functions on the AP-1positive Early Endosome/Trans-Golgi Network". *Molecular Biology of the Cell* 17.June, pp. 2592–2603

Nebenführ, A, Gallagher, L. A., Dunahay, T. G., Frohlick, J. A., Mazurkiewicz, A. M., Meehl, J. B., and Staehelin, L. A. (1999). "Stop-and-go movements of plant Golgi stacks are mediated by the acto-myosin system." *Plant Physiology* 121.4, pp. 1127–1142

Nebenführ, A. (2002). "Vesicle traffic in the endomembrane system: a tale of COPs, Rabs and SNAREs". *Current Opinion in Plant Biology* 5.6, pp. 507–512

Negrutiu, I, Shillito, R, Potrykus, I, Biasini, G, and Sala, F (1987). "Hybrid genes in the analysis of transformation conditions". *Plant Molecular Biology* 373, pp. 363–373

Neuhaus, J. M. and Paris, N. (2005). "Plant Vacuoles: from Biogenesis to Function". In: *Plant Endocytosis SE - 5*. Ed. by J. Šamaj, F. Baluška, and D. Menzel. Vol. 1. Plant Cell Monographs. Springer Berlin Heidelberg, pp. 63–82

Neuhaus, J. M., Sticher, L, Meins, F, and Boller, T (1991). "A short C-terminal sequence is necessary and sufficient for the targeting of chitinases to the plant vacuole." *Proceedings of the National Academy of Sciences of the United States of America* 88.22, pp. 10362–10366

Nielsen, M. S., Madsen, P, Christensen, E. I., Nykjaer, A, Gliemann, J, Kasper, D, Pohlmann, R, and Petersen, C. M. (2001). "The sortilin cytoplasmic tail conveys Golgi-endosome transport and binds the VHS domain of the GGA2 sorting protein." *The EMBO Journal* 20.9, pp. 2180–2190

Niemes, S., Langhans, M., Viotti, C., Scheuring, D., San, M., Yan, W., Jiang, L., Hillmer, S., San Wan Yan, M., Robinson, D. G., and Pimpl, P. (2010a). "Retromer recycles vacuolar sorting receptors from the trans-Golgi network." *The Plant Journal* 61.1, pp. 107–121

Niemes, S., Labs, M., Scheuring, D., Krueger, F., Langhans, M., Jesenofsky, B., Robinson, D. G., and Pimpl, P. (2010b). "Sorting of plant vacuolar proteins is initiated in the ER." *The Plant Journal* 62.4, pp. 601–614

Nishikawa, S. I., Fewell, S. W., Kato, Y, Brodsky, J. L., and Endo, T (2001). "Molecular chaperones in the yeast endoplasmic reticulum maintain

the solubility of proteins for retrotranslocation and degradation." *The Journal of Cell Biology* 153.5, pp. 1061–1070

Nishimura, N. (1999). "A di-acidic (DXE) code directs concentration of cargo during export from the endoplasmic reticulum". *Journal of Biological Chemistry* 274.22, pp. 15937–15946

Nishimura, N. and Balch, W. E. (1997). "A Di-Acidic Signal Required for Selective Export from the Endoplasmic Reticulum". *Science* 277.5325, pp. 556–558

Nothwehr, S. F., Ha, S. a., and Bruinsma, P (2000). "Sorting of yeast membrane proteins into an endosome-to-Golgi pathway involves direct interaction of their cytosolic domains with Vps35p." *The Journal of Cell Biology* 151.2, pp. 297–310

Okada, T., Yoshida, H., Akazawa, R., Negishi, M., and Mori, K. (2002). "Distinct roles of activating transcription factor 6 (ATF6) and double-stranded RNA-activated protein kinase-like endoplasmic reticulum kinase (PERK) in transcription during the mammalian unfolded protein response." *The Biochemical Journal* 366.Pt 2, pp. 585–594

Okamura, K, Kimata, Y, Higashio, H, Tsuru, A, and Kohno, K (2000). "Dissociation of Kar2p/BiP from an ER sensory molecule, Ire1p, triggers the unfolded protein response in yeast." *Biochemical and Biophysical Research Communications* 279.2, pp. 445–450

Oliviusson, P., Heinzerling, O., Hillmer, S., Hinz, G., Tse, C., Jiang, L., Robinson, D. G., and Tse, Y. C. (2006). "Plant Retromer, Localized to the Prevacuolar Compartment and Microvesicles in Arabidopsis , May Interact with Vacuolar Sorting Receptors". *The Plant Cell* 18.May, pp. 1239–1252

Orci, L., Glick, B. S., and Rothman, J. E. (1986). "A new type of coated vesicular carrier that appears not to contain clathrin: its possible role in protein transport within the Golgi stack." *Cell* 46.2, pp. 171–184

Ostrowicz, C. W., Bröcker, C., Ahnert, F., Nordmann, M., Lachmann, J., Peplowska, K., Perz, A., Auffarth, K., Engelbrecht-Vandré, S., and Ungermann, C. (2010). "Defined subunit arrangement and rab interactions are required for functionality of the HOPS tethering complex." *Traffic* 11.10, pp. 1334–1346

Palade, G. (1955). "Studies on the endoplasmic reticulum II. Simple dispositions in cells in situ". *The Journal of Biophysical and Biochemical Cytology* 1.6, pp. 567–582

— (1975). "Intracellular aspects of the process of protein synthesis." *Science* 189.4206, pp. 347–358

Paris, N., Stanley, C. M., Jones, R. L., and Rogers, J. C. (1996). "Plant cells contain two functionally distinct vacuolar compartments." *Cell* 85.4, pp. 563–572

Park, E. and Rapoport, T. (2012). "Mechanisms of Sec61/SecY-mediated protein translocation across membranes." *Annual Review of Biophysics and Biomolecular Structure* 41, pp. 21–40

Park, M., Song, K., Reichardt, I., Kim, H., Mayer, U., Stierhof, Y.-D., Hwang, I., and Jürgens, G. (2013). "Arabidopsis μ-adaptin subunit AP1M of adaptor protein complex 1 mediates late secretory and vacuolar traffic and is required for growth." *Proceedings of the National Academy of Sciences of the United States of America* 110.25, pp. 10318–10323

Paszkowski, J, Shillito, R. D., Saul, M, Mandák, V, Hohn, T, Hohn, B, and Potrykus, I (1984). "Direct gene transfer to plants." *The EMBO Journal* 3.12, pp. 2717–2722

Pearse, B. M. (1976). "Clathrin: a unique protein associated with intracellular transfer of membrane by coated vesicles." *Proceedings of the National Academy of Sciences of the United States of America* 73.4, pp. 1255–1259

Pearse, B. M. and Bretscher, M. S. (1981). "Membrane recycling by coated vesicles." *Annual Review of Biochemistry* 50, pp. 85–101

Pelham, H. R. B. (1988). "Evidence that luminal ER proteins are sorted from secreted proteins in a post-ER compartment." *The EMBO Journal* 7.4, pp. 913–918

Pelham, H. R. B. and Rothman, J. E. (2000). "The debate about transport in the Golgi–two sides of the same coin?" *Cell* 102.6, pp. 713–719

Pelham, H. R. B., Hardwick, K. G., and Lewis, M. J. (1988). "Sorting of soluble ER proteins in yeast." *The EMBO Journal* 7.6, pp. 1757–1762

Peplowska, K., Markgraf, D. F., Ostrowicz, C. W., Bange, G., and Ungermann, C. (2007). "The CORVET tethering complex interacts with the yeast Rab5 homolog Vps21 and is involved in endo-lysosomal biogenesis." *Developmental cell* 12.5, pp. 739–750

Perez-Victoria, F., Mardones, G. A., and Bonifacino, J. S. (2008). "Requirement of the human GARP complex for mannose 6-phosphat -receptor dependent sorting of cathepsin D to lysosomes". *Molecular Biology of the Cell* 19.June, pp. 2350–2362

Perez-Victoria, J., Schindler, C., Magadan, J. G., Mardones, G. A., Delevoye, C., Romao, M., Raposo, G., and Bonifacino, J. S. (2010). "Ang2/fat-free is a conserved subunit of the Golgi-associated retrograde protein complex". *Molecular Biology of the Cell* 21, pp. 3386–3395

Pesacreta, T. C. and Lucas, W. J. (1984). "Plasma membrane coat and a coated vesicle-associated reticulum of membranes: their structure and possible interrelationship in Chara corallina." *The Journal of Cell Biology* 98.4, pp. 1537–1545

Peyroche, A, Paris, S, and Jackson, C. (1996). "Nucleotide exchange on ARF mediated by yeast Geal protein". *Nature* 384, pp. 479–481

Pfefffer, S. (2013). "Rab GTPase regulation of membrane identity." *Current Opinion in Cell Biology*, pp. 2–7

Phan, N. Q., Kim, S.-j., and Bassham, D. C. (2008). "Overexpression of Arabidopsis sorting nexin AtSNX2b inhibits endocytic trafficking to the vacuole." *Molecular Plant* 1.6, pp. 961–976

Phillipson, B., Pimpl, P., DaSilva, L. L. P., Crofts, A. J., Taylor, J. P., Movafeghi, A., Robinson, D. G., and Denecke, J. (2001). "Secretory bulk flow of soluble proteins is efficient and COPII dependent." *The Plant Cell* 13.9, pp. 2005–2020

Pimpl, P., Hanton, S., Taylor, J. P., Pinto-dasilva, L. L., and Denecke, J. (2003). "The GTPase ARF1p Controls the Sequence-Specific Vacuolar Sorting Route to the Lytic Vacuole". *The Plant Cell* 15.May, pp. 1242–1256

Pimpl, P., Taylor, J., Snowden, C. J., Hillmer, S., Robinson, D. G., and Denecke, J. (2006). "Golgi-mediated vacuolar sorting of the endoplasmic reticulum chaperone BiP may play an active role in quality control within the secretory pathway". *The Plant Cell* 18, pp. 198–211

Plutner, H, Schwaninger, R, Pind, S, and Balch, W. E. (1990). "Synthetic peptides of the Rab effector domain inhibit vesicular transport through the secretory pathway." *The EMBO Journal* 9.8, pp. 2375–2383

Potter, H, Weir, L, and Leder, P (1984). "Enhancer-dependent expression of human kappa immunoglobulin genes introduced into mouse pre-B lymphocytes by electroporation." *Proceedings of the National Academy of Sciences of the United States of America* 81.22, pp. 7161–7165

Pourcher, M., Santambrogio, M., Thazar, N., Thierry, A., Fobis-Loisy, I., Miège, C., Jaillais, Y., and Gaude, T. (2010). "Analyses of sorting nexins reveal distinct retromer subcomplex functions in development and protein sorting in Arabidopsis thaliana." *The Plant Cell* 22.12, pp. 3980–3991

Rapoport, I., Miyazaki, M, Boll, W, Duckworth, B, Cantley, L. C., Shoelson, S, and Kirchhausen, T. (1997). "Regulatory interactions in the recognition of endocytic sorting signals by AP-2 complexes." *The EMBO Journal* 16.9, pp. 2240–2250

Rapoport, T., Goder, V., Heinrich, S. U., and Matlack, K. E. S. (2004). "Membrane-protein integration and the role of the translocation channel." *Trends in Cell Biology* 14.10, pp. 568–75

Rasband, W. *http://imagej.nih.gov/ij/*

Raymond, C. K., Howald-Stevenson, I., Vater, C., and Stevens, T. (1992). "Morphological classification of the yeast vacuolar protein-sorting mutants: evidence for a prevacuolar compartment in class E vps mutants." *Molecular Biology of the Cell* 3, pp. 1389–1402

Rink, J., Ghigo, E., Kalaidzidis, Y., and Zerial, M. (2005). "Rab conversion as a mechanism of progression from early to late endosomes." *Cell* 122.5, pp. 735–49

Roberts, C., Nothwehr, S., and Stevens, T. (1992). "Membrane protein sorting in the yeast secretory pathway: evidence that the vacuole may be the default compartment." *The Journal of Cell Biology* 119.1, pp. 69–83

Robinson, J. S., Klionsky, D. J., Banta, L. M., and Emr, S. D. (1988). "Protein sorting in Saccharomyces cerevisiae: isolation of mutants defective in the delivery and processing of multiple vacuolar hydrolases." *Molecular and Cellular Biology* 8.11, pp. 4936–4948

Robinson, M. S. (1994). "The role of clathrin, adaptors and dynamin in endocytosis." *Current Opinion in Cell Biology* 6.4, pp. 538–544

Robinson, M. S. and Bonifacino, J. S. (2001). "Adaptor-related proteins." *Current Opinion in Cell Biology* 13.4, pp. 444–53

Rojas, R., Vlijmen, T. van, Mardones, G. a., Prabhu, Y., Rojas, A. L., Mohammed, S., Heck, A. J. R., Raposo, G., Sluijs, P. van der, and Bonifacino, J. S. (2008). "Regulation of retromer recruitment to endosomes by sequential action of Rab5 and Rab7." *The Journal of Cell Biology* 183.3, pp. 513–26

Rojo, E., Gillmor, C. S., Kovaleva, V, Somerville, C. R., and Raikhel, N. V. (2001). "VACUOLELESS1 is an essential gene required for vacuole formation and morphogenesis in Arabidopsis." *Developmental cell* 1.2, pp. 303–310

Rojo, E., Zouhar, J., and Kovaleva, V. (2003). "The AtCVPS protein complex is localized to the tonoplast and the prevacuolar compartment in arabidopsis". *Molecular Biology of the Cell* 14.February, pp. 361–369

Ron, D and Walter, P. (2007). "Signal integration in the endoplasmic reticulum unfolded protein response." *Nature Reviews Molecular Cell Biology* 8.7, pp. 519–529

Rose, M. D., Misra, L. M., and Vogel, J. P. (1989). "KAR2, a karyogamy gene, is the yeast homolog of the mammalian BiP/GRP78 gene." *Cell* 57.7, pp. 1211–1221

Rothman, J. E. and Fine, R. E. (1980). "Coated vesicles transport newly synthesized membrane glycoproteins from endoplasmic reticulum to plasma membrane in two successive stages." *Proceedings of the National Academy of Sciences of the United States of America* 77.2, pp. 780–784

Rothman, J. E. and Wieland, F. T. (1996). "Protein sorting by transport vesicles". *Science* 272.5259, pp. 227–234

Rutherford, S and Moore, I (2002). "The Arabidopsis Rab GTPase family: another enigma variation". *Current Opinion in Plant Biology* 5.6, pp. 518–528

Sacher, M, Barrowman, J, Wang, W, Horecka, J, Zhang, Y, Pypaert, M, and Ferro-Novick, S (2001). "TRAPP I implicated in the specificity of tethering in ER-to-Golgi transport." *Molecular cell* 7.2, pp. 433–442

Saint-Jean, B., Seveno-Carpentier, E., Alcon, C., Neuhaus, J. M., and Paris, N. (2010). "The cytosolic tail dipeptide Ile-Met of the pea receptor BP80 is required for recycling from the prevacuole and for endocytosis." *The Plant Cell* 22.8, pp. 2825–4837

Saitou, N and Nei, M (1987). "The neighbor-joining method: a new method for reconstructing phylogenetic trees." *Molecular Biology and Evolution* 4.4, pp. 406–25

Sakaguchi, M, Tomiyoshi, R, Kuroiwa, T, Mihara, K, and Omura, T (1992). "Functions of signal and signal-anchor sequences are determined by the balance between the hydrophobic segment and the N-terminal charge." *Proceedings of the National Academy of Sciences of the United States of America* 89.1, pp. 16–19

Salama, N. R., Yeung, T, and Schekman, R. (1993). "The Sec13p complex and reconstitution of vesicle budding from the ER with purified cytosolic proteins." *The EMBO Journal* 12.11, pp. 4073–4082

Salminen, A and Novick, P. J. (1987). "A ras-like protein is required for a post-Golgi event in yeast secretion." *Cell* 49.4, pp. 527–538

Samalova, M., Fricker, M., and Moore, I. (2006). "Ratiometric fluorescence imaging assays of plant membrane traffic using polyproteins." *Traffic* 7.12, pp. 1701–23

Sambrook, J., Fritsch, E., and Maniatis, T. (1987). *Molecular Cloning: A Laboratory Manual*. Cold Spring Harbor Laboratory Press,U.S.

Sanderfoot, A. A., Ahmed, S. U., Marty-Mazars, D., Rapoport, I., Kirchhausen, T., Marty, F., and Raikhel, N. V. (1998). "A putative vacuolar cargo receptor partially colocalizes with AtPEP12p on a prevacuolar compartment in Arabidopsis roots." *Proceedings of the National Academy of Sciences of the United States of America* 95.17, pp. 9920–9925

Sapperstein, S. K., Walter, D. M., Grosvenor, a. R., Heuser, J. E., and Waters, M. G. (1995). "p115 is a general vesicular transport factor related to the yeast endoplasmic reticulum to Golgi transport factor Uso1p." *Proceedings of the National Academy of Sciences of the United States of America* 92.2, pp. 522–526

Sato, K. and Nakano, A. (2005). "Dissection of COPII subunit-cargo assembly and disassembly kinetics during Sar1p-GTP hydrolysis." *Nature Structural & Molecular Biology* 12.2, pp. 167–174

Sauer, M., Delgadillo, M. O., Zouhar, J., Reynolds, G. D., Pennington, J. G., Jiang, L., Liljegren, S. J., Stierhof, Y.-D., De Jaeger, G., Otegui, M. S., Bednarek, S. Y., and Rojo, E. (2013). "MTV1 and

MTV4 encode plant-specific ENTH and ARF GAP proteins that mediate clathrin-dependent trafficking of vacuolar cargo from the trans-Golgi network." *The Plant Cell* 25.6, pp. 2217–2235

Scheffzek, K., Ahmadian, M. R., and Wittinghofer, A. (1998). "GTPase activating proteins: helping hands to complement an active site." *Trends in Biochemical Sciences* 23.7, pp. 257–262

Scheuring, D., Viotti, C., Krüger, F., Künzl, F., Sturm, S., Bubeck, J., Hillmer, S., Frigerio, L., Robinson, D. G., Pimpl, P., and Schumacher, K. (2011). "Multivesicular Bodies Mature from the Trans-Golgi Network/Early Endosome in Arabidopsis." *The Plant Cell*, pp. 1–20

Schmitt, H., Wagner, P, Pfaff, E, and Gallwitz, D (1986). "The ras-related YPT1 gene product in yeast: A GTP-binding protein that might be involved in microtubule organization". *Cell* 47, pp. 401–412

Schneider, H., Berthold, J, and Bauer, M. (1994). "Mitochondrial Hsp70/MIM44 complex facilitates protein import". *Nature* 371, pp. 768–774

Schröder, M. and Kaufman, R. J. (2005). "The mammalian unfolded protein response." *Annual Review of Biochemistry* 74, pp. 739–789

Schuldiner, M., Metz, J., Schmid, V., Denic, V., Rakwalska, M., Schmitt, H. D., Schwappach, B., and Weissman, J. S. (2008). "The GET complex mediates insertion of tail-anchored proteins into the ER membrane". *Cell* 134.4, pp. 634–645

Schwientek, T and Ernst, J. F. (1994). "Efficient intra- and extracellular production of human beta-1,4-galactosyltransferase in Saccharomyces cerevisiae is mediated by yeast secretion leaders." *Gene* 145.2, pp. 299–303

Scott, D. C. and Schekman, R. (2008). "Role of Sec61p in the ER-associated degradation of short-lived transmembrane proteins." *The Journal of Cell Biology* 181.7, pp. 1095–1105

Seaman, M. N. J. (2005). "Recycle your receptors with retromer." *Trends in Cell Biology* 15.2, pp. 68–75

Seaman, M. N. J., Marcusson, E. G., Cereghino, J. L., and Emr, S. D. (1997). "Endosome to Golgi retrieval of the vacuolar protein sorting receptor, Vps10p, requires the function of the VPS29, VPS30, and VPS35 gene products". *The Journal of Cell Biology* 137.1, pp. 79–92

Seaman, M. N. J., McCaffery, J. M., and Emr, S. D. (1998). "A membrane coat complex essential for endosome-to-Golgi retrograde transport in yeast." *The Journal of Cell Biology* 142.3, pp. 665–681

Seaman, M. N. J., Harbour, M. E., Tattersall, D., Read, E., and Bright, N. A. (2012). "The retromer complex - endosomal protein recycling and beyond." *Journal of Cell Science* 125.Pt 20, pp. 4693–702

Sevier, C. S., Weisz, O. a., Davis, M, and Machamer, C. E. (2000). "Efficient export of the vesicular stomatitis virus G protein from the endoplasmic

reticulum requires a signal in the cytoplasmic tail that includes both tyrosine-based and di-acidic motifs." *Molecular Biology of the Cell* 11.1, pp. 13–22

Shahriari, M., Keshavaiah, C., Scheuring, D., Sabovljevic, A., Pimpl, P., Häusler, R. E., Hülskamp, M., and Schellmann, S. (2010). "The AAA-type ATPase AtSKD1 contributes to vacuolar maintenance of Arabidopsis thaliana." *The Plant Journal* 64.1, pp. 71–85

Shao, S. and Hegde, R. S. (2011). "Membrane protein insertion at the endoplasmic reticulum." *Annual Review of Cell and Developmental Biology* 27, pp. 25–56

Shaw, A. S., Rottier, P. J., and Rose, J. K. (1988). "Evidence for the loop model of signal-sequence insertion into the endoplasmic reticulum." *Proceedings of the National Academy of Sciences of the United States of America* 85.20, pp. 7592–7596

Sheen, J., Hwang, S., Niwa, Y., Kobayashi, H., and Galbraith, D. (1995). "Green-fluroescent protein as a new vital marker in plant cells". *The Plant Journal* 8.5, pp. 777–784

Shen, J., Chen, X., Hendershot, L., and Prywes, R. (2002). "ER stress regulation of ATF6 localization by dissociation of BiP/GRP78 binding and unmasking of Golgi localization signals." *Developmental Cell* 3.1, pp. 99–111

Shi, Y., Vattem, K. M., Sood, R., An, J., Liang, J., Stramm, L., and Wek, R. C. (1998). "Identification and Characterization of Pancreatic Eukaryotic Initiation Factor 2 α -Subunit Kinase , PEK , Involved in Translational Control". *Molecular and Cellular Biology* 18.12, pp. 7499–7509

Shibata, Y., Shemesh, T., Prinz, W. a., Palazzo, A. F., Kozlov, M. M., and Rapoport, T. (2010). "Mechanisms determining the morphology of the peripheral ER." *Cell* 143.5, pp. 774–788

Shimada, T., Fuji, K., Tamura, K., Kondo, M., Nishimura, M., and Hara-Nishimura, I. (2003). "Vacuolar sorting receptor for seed storage proteins in Arabidopsis thaliana." *Proceedings of the National Academy of Sciences of the United States of America* 100.26, pp. 16095–16100

Shimada, T., Koumoto, Y., Li, L., Yamazaki, M., Kondo, M., Nishimura, M., and Hara-Nishimura, I. (2006). "AtVPS29, a putative component of a retromer complex, is required for the efficient sorting of seed storage proteins". *Plant & Cell Physiology* 47.9, pp. 1187–1194

Shoemaker, R., Polzin, K, and Labate, J (1996). "Genome duplication in soybean (Glycine subgenus soja)". *Genetics* Shoemaker, pp. 329–338

Sidrauski, C and Walter, P (1997). "The transmembrane kinase Ire1p is a site-specific endonuclease that initiates mRNA splicing in the unfolded protein response." *Cell* 90.6, pp. 1031–1039

Simon, S. M. and Blobel, G (1991). "A protein-conducting channel in the endoplasmic reticulum." *Cell* 65.3, pp. 371–380

Simon, S. M., Peskin, C. S., and Oster, G. F. (1992). "What drives the translocation of proteins?" *Proceedings of the National Academy of Sciences of the United States of America* 89.9, pp. 3770–3774

Simons, K. and Ikonen, E. (1997). "Functional rafts in cell membranes". *Nature* 387.6633, pp. 569–572

Simons, K. and Meers, G. (1988). "Perspectives in Biochemistry Lipid Sorting in Epithelial Cells". *Biochemical Society Transactions* 27.17, pp. 6197–6202

Singer, C. (1931). *A Short History of Biology*. Oxford Clarendon

Singer, S. J. and Nicolson, G. L. (1972). "The fluid mosaic model of the structure of cell membranes." *Science* 175.4023, pp. 720–31

Siniossoglou, S and Pelham, H. R. B. (2001). "An effector of Ypt6p binds the SNARE Tlg1p and mediates selective fusion of vesicles with late Golgi membranes." *The EMBO Journal* 20.21, pp. 5991–5998

— (2002). "Vps51p links the VFT complex to the SNARE Tlg1p." *The Journal of Biological Chemistry* 277.50, pp. 48318–48324

Slepenkov, S. V. and Witt, S. N. (2002). "The unfolding story of the Escherichia coli Hsp70 DnaK: is DnaK a holdase or an unfoldase?" *Molecular Microbiology* 45.5, pp. 1197–1206

Snowden, C. J., Leborgne-Castel, N., Wootton, L. J., Hadlington, J. L., and Denecke, J. (2007). "In vivo analysis of the lumenal binding protein (BiP) reveals multiple functions of its ATPase domain." *The Plant Journal* 52.6, pp. 987–1000

Sohn, E. J., Kim, S., Zhao, M., Kim, J., Kim, H., Kim, Y.-w., Lee, J., Hillmer, S., Sohn, U., Jiang, L., and Hwang, I. (2003). "Rha1, an Arabidopsis Rab5 homolog , plays a critical role in the vacuolar trafficking of soluble cargo proteins". *The Plant Cell* 15.May, pp. 1057–1070

Solinger, J and Spang, A (2013). "Tethering complexes in the endocytic pathway: CORVET and HOPS." *The FEBS Journal* 280.12, pp. 2743–2757

Söllner, T, Bennett, M. K., Whiteheart, S. W., Scheller, R. H., and Rothman, J. E. (1993). "A protein assembly-disassembly pathway in vitro that may correspond to sequential steps of synaptic vesicle docking, activation, and fusion." *Cell* 75.3, pp. 409–418

Song, J., Lee, M. H., Lee, G.-J., Yoo, C. M., and Hwang, I. (2006). "Arabidopsis EPSIN1 plays an important role in vacuolar trafficking of soluble cargo proteins in plant cells via interactions with clathrin, AP-1, VTI11, and VSR1." *The Plant Cell* 18.9, pp. 2258–2274

Sorek, N., Bloch, D., and Yalovsky, S. (2009). "Protein lipid modifications in signaling and subcellular targeting." *Current opinion in plant biology* 12.6, pp. 714–720

Sparkes, I., Ketelaar, T., Ruijter, N. de, and Hawes, C. (2009a). "Grab a Golgi: laser trapping of Golgi bodies reveals in vivo interactions with the endoplasmic reticulum". *Traffic*, pp. 567–571

Sparkes, I., Runions, J, Hawes, C, and Griffing, L (2009b). "Movement and remodeling of the endoplasmic reticulum in nondividing cells of tobacco leaves." *The Plant Cell* 21.12, pp. 3937–3949

Sparkes, I. A., Runions, J, Kearns, A, and Hawes, C (2006). "Rapid, transient expression of fluorescent fusion proteins in tobacco plants and generation of stably transformed plants". *Nature Protocols* 1.4, pp. 2019–2025

Stachowiak, J. C., Schmid, E. M., Ryan, C. J., Ann, H. S., Sasaki, D. Y., Sherman, M. B., Geissler, P. L., Fletcher, D. a., and Hayden, C. C. (2012). "Membrane bending by protein-protein crowding." *Nature Cell Biology* 14.9, pp. 944–949

Staehelin, L. and Moore, I. (1995). "The Plant Golgi Apparatus: Structure, Functional Organization and Trafficking Mechanisms". *Annual Review of Plant Physiology and Plant Molecular Biology* 46.1, pp. 261–288

Stefanovic, S. and Hegde, R. S. (2007). "Identification of a targeting factor for posttranslational membrane protein insertion into the ER." *Cell* 128.6, pp. 1147–1159

Steinman, R. M., Mellman, I. R., Muller, W. A., and Cohn, Z. A. (1983). "Endocytosis and the Recycling of Plasma Membrane". *The Journal of Cell Biology* 96, pp. 1–27

Stenmark, H., Aasland, R., Toh, B. H., and DArrigo, A. (1996). "Endosomal Localization of the Autoantigen EEA1 Is Mediated by a Zinc binding FYVE Finger." *The Journal of Biological Chemistry* 271.39, pp. 24048–24054

Stenmark, H. (2009). "Rab GTPases as coordinators of vesicle traffic." *Nature Reviews Molecular Cell Biology* 10.8, pp. 513–525

Storch, S and Braulke, T. (2001). "Multiple C-terminal motifs of the 46-kDa mannose 6-phosphate receptor tail contribute to efficient binding of medium chains of AP-2 and AP-3." *The Journal of Biological Chemistry* 276.6, pp. 4298–303

Strittmatter, P, Rogers, M, and Spatz, L (1972). "The binding of cytochrome b5 to liver microsomes". *The Journal of Biological Chemistry* 247.22, pp. 7188–7194

Stroupe, C., Hickey, C. M., Mima, J., Burfeind, A. S., and Wickner, W. (2009). "Minimal membrane docking requirements revealed by reconstitution of Rab GTPase-dependent membrane fusion from purified components."

Proceedings of the National Academy of Sciences of the United States of America 106.42, pp. 17626–17633

Suen, P. K. K., Shen, J., Sun, S., and Jiang, L. (2010). "Expression and characterization of two functional vacuolar sorting receptor (VSR) proteins, BP-80 and AtVSR4 from culture media of transgenic tobacco BY-2 cells". *Plant Science* 179.1-2, pp. 68–76

Takei, P. K., Schmid, S., and Camilli, P. D. (1995). "Tubular membrane invaginations coated by dynamin rings are induced by GTP-γS in nerve terminals". *Nature* 374, pp. 186–190

Takeuchi, M., Ueda, T., Sato, K., Abe, H., Nagata, T., and Nakano, A. (2000). "A dominant negative mutant of sar1 GTPase inhibits protein transport from the endoplasmic reticulum to the Golgi apparatus in tobacco and Arabidopsis cultured cells." *The Plant Journal* 23.4, pp. 517–525

Tanabe, K. and Torii, T. (2005). "A novel GTPase-activating protein for ARF6 directly interacts with clathrin and regulates clathrin-dependent endocytosis". *Molecular Biology of the Cell* 16.April, pp. 1617–1628

Tanchak, M. a., Rennie, P. J., and Fowke, L. C. (1988). "Ultrastructure of the partially coated reticulum and dictyosomes during endocytosis by soybean protoplasts". *Planta* 175.4, pp. 433–441

Teeri, T. H., Lehvaslaiho, H, Franck, M, Uotila, J, Heino, P, Palva, E. T., and Montagu, M. V. (1989). "Gene fusions to lacZ reveal new expression chimeric genes in transgenic plants patterns of". *The EMBO Journal* 8.2, pp. 343–350

Thor, F., Gautschi, M., Geiger, R., and Helenius, A (2009). "Bulk flow revisited: transport of a soluble protein in the secretory pathway." *Traffic* 10.12, pp. 1819–1830

Thorngren, N., Collins, K. M., Fratti, R. a., Wickner, W., and Merz, A. J. (2004). "A soluble SNARE drives rapid docking, bypassing ATP and Sec17/18p for vacuole fusion." *The EMBO Journal* 23.14, pp. 2765–2776

Tisdale, E. and Bourne, J. (1992). "GTP-binding mutants of rab1 and rab2 are potent inhibitors of vesicular transport from the endoplasmic reticulum to the Golgi complex." *The Journal of Cell Biology* 119.4, pp. 749–761

Travers, K. J., Patil, C. K., Wodicka, L, Lockhart, D. J., Weissman, J. S., and Walter, P (2000). "Functional and genomic analyses reveal an essential coordination between the unfolded protein response and ER-associated degradation." *Cell* 101.3, pp. 249–258

Tse, Y. C., Mo, B., Hillmer, S., Zhao, M., Lo, S. W., Robinson, D. G., and Jiang, L. (2004). "Identification of Multivesicular Bodies as Prevacuolar Compartments in Nicotiana tabacum BY-2 Cells". *The Plant Cell* 16.March, pp. 672–693

Twell, D. and Pelletier, G. (2004). "The putative Arabidopsis homolog of yeast Vps52p is required for pollen tube elongation , localizes to Golgi , and might be involved in vesicle trafficking". *Plant Physiology* 135.July, pp. 1480–1490

Ueda, T., Uemura, T., Sato, M. H., and Nakano, A. (2001). "Ara6, a plant-unique novel type Rab GTPase, functions in the endocytic pathway of Arabidopsis thaliana." *The EMBO Journal* 20.17, pp. 4730–4741

— (2004). "Functional differentiation of endosomes in Arabidopsis cells." *The Plant Journal* 40.5, pp. 783–789

Vanoosthuyse, V., Tichtinsky, G., Dumas, C., Gaude, T., Cock, J. M., Lyon, C. B., and Supe, E. N. (2003). "Interaction of calmodulin , a sorting nexin and kinase-associated protein phosphatase with the Brassica oleracea s locus receptor kinase". *Plant Physiology* 133.October, pp. 919–929

Vembar, S. S. and Brodsky, J. L. (2008). "One step at a time: endoplasmic reticulum-associated degradation." *Nature Reviews Molecular Cell Biology* 9.12, pp. 944–957

Vermeer, J., Leeuwen, W. van, A-Santamaria, R. T., Laxalt, A. M., Jones, D. R., Divecha, N., Jr, T. W. G., and Munnik, T. (2006). "Visualization of PtdIns3P dynamics in living plant cells". *The Plant Journal* 47, pp. 687–700

Vernoud, V., Horton, A. C., Yang, Z., and Nielsen, E. (2003). "Analysis of the Small GTPase Gene Superfamily of Arabidopsis 1". *Plant Physiology* 131.March, pp. 1191–1208

Vitale, A., Ceriotti, A., and Denecke, J. (1993). "The role of the endoplasmicreticulum in protein synthesis, modification and intracellular transport". *Journal of Experimental Botany* 44.9, pp. 1417–1444

Votsmeier, C and Gallwitz, D (2001). "An acidic sequence of a putative yeast Golgi membrane protein binds COPII and facilitates ER export." *The EMBO Journal* 20.23, pp. 6742–6750

Wahlberg, J. M. and Spiess, M (1997). "Multiple determinants direct the orientation of signal-anchor proteins: the topogenic role of the hydrophobic signal domain." *The Journal of Cell Biology* 137.3, pp. 555–62

Walter, J., Urban, J., Volkwein, C., and Sommer, T. (2001). "Sec61p independent degradation of the tail anchored ER membrane protein Ubc6p." *The EMBO Journal* 20.12, pp. 3124–3131

Walter, M., Chaban, C., Schütze, K., Batistic, O., Weckermann, K., Näke, C., Blazevic, D., Grefen, C., Schumacher, K., Oecking, C., Harter, K., and Kudla, J. (2004). "Visualization of protein interactions in living plant cells using bimolecular fluorescence complementation." *The Plant Journal* 40.3, pp. 428–438

Walter, P. and Blobel, G (1980). "Purification of a membrane-associated protein complex required for protein translocation across the endoplasmic reticulum:" *Proceedings of the National Academy of Sciences of the United States of America* 77.12, pp. 7112–7116

Wang, F, Brown, E., Mak, G, Zhuang, J, and Denic, V (2010). "A chaperone cascade sorts proteins for posttranslational membrane insertion into the endoplasmic reticulum". *Molecular Cell* 40.1, pp. 159–171

Wang, F., Whynot, A., Tung, M., and Denic, V. (2011). "The mechanism of tail-anchored protein insertion into the ER membrane." *Molecular Cell* 43.5, pp. 738–750

Wang, H., Tse, Y. C., Law, A. H. Y., Sun, S. S. M., Sun, Y.-b., Xu, Z.-f., Hillmer, S., Robinson, D. G., Jiang, L., Territories, N., and Kong, H. (2009). "Vacuolar sorting receptors (VSRs) and secretory carrier membrane proteins (SCAMPs) are essential for pollen tube growth." *The Plant Journal*, pp. 826–838

Wang, W, Sacher, M, and Ferro-Novick, S (2000). "TRAPP stimulates guanine nucleotide exchange on Ypt1p." *The Journal of Cell Biology* 151.2, pp. 289–296

Watanabe, E., Shimada, T., Kuroyanagi, M., Nishimura, M., and Hara-Nishimura, I. (2002). "Calcium-mediated association of a putative vacuolar sorting receptor PV72 with a propeptide of 2S albumin." *The Journal of Biological Chemistry* 277.10, pp. 8708–8715

Watanabe, E., Shimada, T., Tamura, K., Matsushima, R., Koumoto, Y., Nishimura, M., and Hara-Nishimura, I. (2004). "An ER-localized form of PV72, a seed-specific vacuolar sorting receptor, interferes the transport of an NPIR-containing proteinase in Arabidopsis leaves." *Plant & Cell Physiology* 45.1, pp. 9–17

Waters, M., Serafini, T, and Rothman, J. E. (1991). "'Coatomer': a cytosolic protein complex containing subunits of non-clathrin-coated Golgi transport vesicles". *Nature* 349, pp. 248–251

Wee, E. G. T., Sherrier, D. J., Prime, T. a., and Dupree, P (1998). "Targeting of active sialyltransferase to the plant Golgi apparatus." *The Plant Cell* 10.10, pp. 1759–1768

Weide, T, Bayer, M, Köster, M, Siebrasse, J. P., Peters, R, and Barnekow, a (2001). "The Golgi matrix protein GM130: a specific interacting partner of the small GTPase rab1b." *EMBO reports* 2.4, pp. 336–41

Weihofen, A., Binns, K., Lemberg, M. K., Ashman, K., and Martoglio, B. (2002). "Identification of signal peptide peptidase, a presenilin-type aspartic protease." *Science* 296.5576, pp. 2215–2218

Wickner, W. (2010). "Membrane fusion: five lipids, four SNAREs, three chaperones, two nucleotides, and a Rab, all dancing in a ring on yeast vacuoles." *Annual Review of Cell and Developmental Biology* 26, pp. 115–136

Wieland, F. T., Gleason, M. L., Serafini, T. A., and Rothman, J. E. (1987). "The Rate of Bulk Flow from the Endoplasmic Reticulum to the Cell Surface". *Cell* 50, pp. 289 –300

Wiertz, E, Tortorella, D, Bogyo, M, and Yu, J (1996). "Sec61-mediated transfer of a membrane protein from the endoplasmic reticulum to the proteasome for destruction". *Nature* 384, pp. 432–438

Woese, C. R. (2000). "Interpreting the universal phylogenetic tree." *Proceedings of the National Academy of Sciences of the United States of America* 97.15, pp. 8392–8396

— (2002). "On the evolution of cells." *Proceedings of the National Academy of Sciences of the United States of America* 99.13, pp. 8742–8747

Woese, C. R., Olsen, G. J., Ibba, M., and Soll, D. (2000). "Aminoacyl-tRNA synthetases, the genetic code, and the evolutionary process." *Microbiology and Molecular Biology Reviews* 64.1, pp. 202–236

Wywial, E. and Singh, S. (2010). "Identification and structural characterization of FYVE domain containing proteins of Arabidopsis thaliana." *BMC Plant Biology* 10.doi:10.1186, pp. 1–15

Xing, Y., Böcking, T., Wolf, M., Grigorieff, N., Kirchhausen, T., and Harrison, S. C. (2010). "Structure of clathrin coat with bound Hsc70 and auxilin: mechanism of Hsc70-facilitated disassembly." *The EMBO Journal* 29.3, pp. 655–665

Yabal, M., Brambillasca, S., Soffientini, P., Pedrazzini, E., Borgese, N., and Makarow, M. (2003). "Translocation of the C terminus of a tail-anchored protein across the endoplasmic reticulum membrane in yeast mutants defective in signal peptide-driven translocation." *The Journal of Biological Chemistry* 278.5, pp. 3489–3496

Yamazaki, M., Shimada, T., Takahashi, H., Tamura, K., Kondo, M., Nishimura, M., and Hara-Nishimura, I. (2008). "Arabidopsis VPS35, a retromer component, is required for vacuolar protein sorting and involved in plant growth and leaf senescence." *Plant & Cell Physiology* 49.2, pp. 142–156

Yang, Y. S. and Strittmatter, S. M. (2007). "The reticulons: a family of proteins with diverse functions." *Genome Biology* 8.doi:10.1186, pp. 1–10

Ye, J., Rawson, R. B., Komuro, R., Chen, X., Dave, U. P., Prywes, R., Brown, M. S., and Goldstein, J. L. (2000). "of Membrane-Bound ATF6 by the Same Proteases that Process SREBPs". *Molecular Cell* 6, pp. 1355–1364

Yoshida, H., Matsui, T., Hosokawa, N., Kaufman, R. J., Nagata, K., and Mori, K. (2003). "A time-dependent phase shift in the mammalian unfolded protein response." *Developmental cell* 4.2, pp. 265–271

Yoshihisa, T., Barlowe, C., and Schekman, R. (1993). "Requirement for a GTPase-activating protein in vesicle budding from the endoplasmic reticulum". *Science* 259.5100, pp. 1466–1468

Yu, S., Satoh, A., Pypaert, M., Mullen, K., Hay, J. C., and Ferro-Novick, S. (2006). "mBet3p is required for homotypic COPII vesicle tethering in mammalian cells." *The Journal of Cell Biology* 174.3, pp. 359–368

Zanetti, G., Pahuja, K. B., Studer, S., Shim, S., and Schekman, R. (2012). "COPII and the regulation of protein sorting in mammals." *Nature Cell Biology* 14.1, pp. 20–28

Zhang, D., Vjestica, A., and Oliferenko, S. (2012). "Plasma membrane tethering of the cortical ER necessitates its finely reticulated architecture." *Current Biology* 22.21, pp. 2048–2052

Zhao, L, Helms, J. B., Brügger, B, Harter, C, Martoglio, B, Graf, R, Brunner, J, and Wieland, F. T. (1997). "Direct and GTP-dependent interaction of ADP ribosylation factor 1 with coatomer subunit beta." *Proceedings of the National Academy of Sciences of the United States of America* 94.9, pp. 4418–4423

Zimmer, J., Nam, Y., and Rapoport, T. (2008). "Structure of a complex of the ATPase SecA and the protein-translocation channel." *Nature* 455.7215, pp. 936–943

Zimmerberg, J. and Kozlov, M. M. (2006). "How proteins produce cellular membrane curvature." *Nature Reviews Molecular Cell Biology* 7.1, pp. 9–19

Zink, S., Wenzel, D., Wurm, C. a., and Schmitt, H. D. (2009). "A link between ER tethering and COP-I vesicle uncoating." *Developmental Cell* 17.3, pp. 403–416

Zouhar, J., Muñoz, A., and Rojo, E. (2010). "Functional specialization within the vacuolar sorting receptor family: VSR1, VSR3 and VSR4 sort vacuolar storage cargo in seeds and vegetative tissues." *The Plant Journal* 64.4, pp. 577–588